Dynamical Systems In Biological Modeling: Clustering In the Cell Division Cycle of Yeast

A dissertation presented to

the faculty of

the College of Arts and Sciences of Ohio University

In partial fulfillment

of the requirements for the degree

Doctor of Philosophy

Gregory J. Moses

August 2015

This dissertation titled

Dynamical Systems In Biological Modeling: Clustering In the Cell Division Cycle of Yeast

by

GREGORY J. MOSES

has been approved for

the Department of Mathematics

and the College of Arts and Sciences by

Todd Young

Professor of Mathematics

Robert Frank

Dean, College of Arts and Sciences

Abstract

MOSES, GREGORY J., Ph.D., August 2015, Mathematics

Dynamical Systems In Biological Modeling: Clustering In the Cell Division Cycle of Yeast (218 pp.)

Director of Dissertation: Todd Young

This thesis is devoted to using the techniques of dynamical systems to studying clustering in the cell division cycle of yeast through the medium of a feedback model in which cells in one part of the cell division cycle influence the rate of cells in a different part of the cell division cycle.

In Chapter 1, we introduce the model and see that it causes clustering under both positive and negative feedback.

In Chapter 2 we pass to a clustered submanifold. We factorize a Poincaré map and use this factorization to prove that asymptotically stable cyclic solutions exist under negative feedback. We partition parameter space in a way that allows us to quickly investigate stability of solutions under a wide range of parameter values. In Chapter 3 we prove many of the observations of Chapter 2, in particular that positive feedback gives rise to unstable solutions. We also prove that asymptotic stability in the clustered submanifold implies asymptotic stability in the full phase space.

In Chapter 4, we contrast the effect of adding biologically motivated bounded noise against the effect of zero-mean Gaussian white noise, and see that the various noise models act essentially similarly under a variety of metrics.

In Chapter 5, we consider a modification of the system wherein certain previously disjoint intervals are allowed to overlap. We observe that in the clustered subspace, the dynamics of this system are similar to those of the original system. However, we observe complicated behavior in the full phase space, where solutions that are asymptotically stable in the clustered space are merely stable, or even unstable, in the full phase space.

This thesis is dedicated to my parents for their love and support.

Acknowledgments

I would like to gratefully acknowledge my adviser, Dr. Todd Young.

I would also like to thank my coauthors, Dr. Erik Boczko, Nathan Breitsch, Dr. Richard Buckalew, Dr. Bastien Fernandez, Xue Gong, Dr. Alexander Neiman, and Denise Scalfano. I would like to especially thank Nathan, with whom I worked especially closely of all my coauthors, and who laid the foundation for much of my work.

I am likewise grateful to the following people, who assisted in the writing of the papers that form the basis of this dissertation without attaining the status of co-author. Kara Finley, an Ohio University biology student, helped us tailor the paper [10] that became the major part of Chapter 2 for its target audience. Gabor Balazsi read the paper that forms the basis of Chapter 4 and provided comments. All of the chapters based on published papers were improved by the comments and insight of their various referees.

I further acknowledge the institutional support that I and my coauthors have received. The papers that would become Chapters 2 and 4 were supported by NIH-NIGMS grant R01GM090207.

Finally, I would like to thank my committee, Dr. Winfried Just, Dr. Alexander Neiman, and Dr. Sergiu Aizicovici.

Table of Contents

List of Tables

List of Figures

1 INTRODUCTION*

1.1 Authorship and publication history

This thesis is primarily comprised of material taken from five papers or unpublished manuscripts that I share authorship in †.

The introduction extracts parts of [96]. I am the fourth coauthor, and had the least influence on this paper of all the papers that form this thesis. To limit the chapters of this thesis to material I have personally worked on, I have divided this paper into two, and put work I was not personally involved in into this introduction. The introduction is therefore primarily the work of Dr. Young, Dr. Fernandez, Dr. Buckalew, and Dr. Boczko, although I have edited and expanded when it seemed appropriate. Figure 1.5 and the accompanying discussion (not part of the published paper) is my work.

Chapter 2 extracts the rest of [96]. I contributed to the $k = 2$ section of the published paper, and made the observation that results we had proved under linear feedback could be generalized. In the dissertation, I worked on the $k = M + 1$ case, proving the order of event lemmas that were assumed without proof in the published manuscript. The rest of that chapter is taken from [10] (first author, Nathan Breitsch, other authors, Dr. Young and Erik Boczko; I am the second author). I was part of that paper from its initial conception, writing large parts of the manuscript and working on all the sections of that paper.

Chapter 3 is solo work.

---

* In accordance with ScienceDirect's policy for using previously published articles in an academic dissertation, we here give the DOI number by which the official publication from which this introduction is drawn may be found: 10.1016/j.jtbi.2011.10.002.

† Material published in [10] as Cell cycle dynamics: clustering is universal in negative feedback systems, in the Journal of Mathematical Biology, is reused with kind permission from Springer Science and Business Media. The papers [31] and [96] were published by the Journal of Theoretical Biology, a ScienceDirect journal, which allows academic theses and dissertations to contain embedded published journal articles and be publicly posted by the awarding institution, as long as DOI information is provided.

Chapter 4 is joint work with Xue Gong (first author), Dr. Neiman, and Dr. Young, and was published as [31]. I am the second author. I introduced the variable rate model, met weekly with Xue Gong and Todd Young to discuss the results of the simulations and the programming issues, wrote one of the appendices (Appendix B.2, moved out of the chapter and into the appendix of the dissertation) and edited the paper.

Chapter 5 is joint work with Denise Scalfano. I am the first author; everything but some of the calculations of the appendix (moved into the appendix of the dissertation) and some of the lemmas of Section 5.3.2 is my work (while the calculations and lemmas were collaborative), and I wrote the manuscript.

A full bibliography is included at the conclusion of this document.

1.2 Motivation

Throughout this manuscript, we consider simple dynamical models of the cell division cycle. Specifically, consider a culture of n cells, and visualize the cell division cycle as a circle, $[0, 1]$ where $0 \sim 1$ (0 is identified with 1) and cells move clockwise around the circle as they pass from birth to division. We take the progression of the i-th cell to be governed by the equation

$$\frac{dc_i}{dt} = 1 + a(c_i, \bar{c}) \qquad 1 \leq i \leq n, \tag{1.2.1}$$

where c_i is the position of the cell within the cycle and $\bar{c}$ denotes the state of all the cells in the culture.

Our primary motivation for this model is recent theoretical and experimental work on Yeast Autonomous Oscillations (YAO) [16, 36, 50, 77, 97], the periodic oscillations of physiologically relevant variables that have been reported and studied for over 40 years [16, 26, 45, 52, 59, 64–66, 71, 76, 79, 91] (to name a few that explicitly motivated the research upon which this dissertation is based; a full list would be prohibitively long). Different types of YAO have been called metabolic [97], glycolytic

[5] or respiratory [36] oscillations. The control of oscillation and the regulation of yeast metabolism has been an important theme in the chemical engineering literature devoted to the efficient management of bioprocesses [14, 34, 39, 68, 84]. These phenomena are of basic biological interest because they expose questions regarding the coordination of the cell cycle and metabolism, and interconnectedness of various cellular and genetic processes [7, 50]. A correlation between YAO and the bud index was noted as early as [52, 59]. However, it seems that the link between YAO and the Cell Division Cycle (CDC) was obscured by the fact that the periods of YAO are always shorter than the CDC times (computed from dilution rate) and a relationship between YAO and the CDC seems to have been largely ignored, although in [50], [97], and elsewhere, the correlation between YAO and CDC was again noted in genetic expression data.

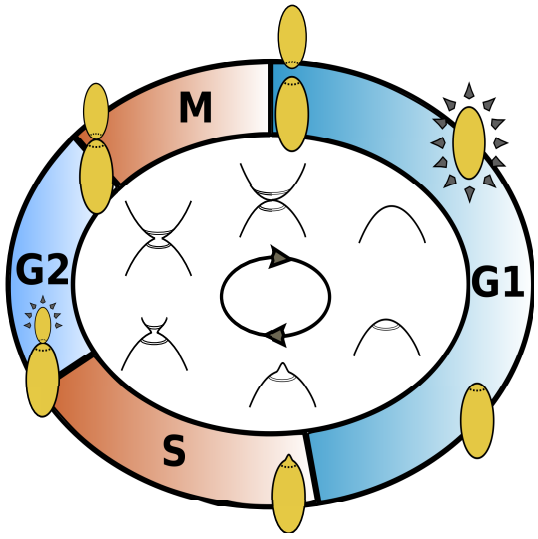

Figure 1.1: Phases of the yeast cell cycle. The G1 phase begins following cell division. The beginning of the DNA synthesis phase, S, coincides with budding. G2 is a second "gap" phase. The M phase is characterized by narrowing or "necking" between the parent and daughter cell; it ends in cell division. The hypothesized *R* region is the later portion of G1 and the signaling region *S* is in the S phase. That is, a large subpopulation of cells in the replicative S phase may promote or inhibit progression of cells approaching the G1-S boundary.

In [6] and [77] the authors proposed *cell cycle clustering* as a possible explanation of the interaction between YAO and the CDC. Figure 1.1 roughly illustrates the arrangement of phases of the cell cycle of yeast. It was hypothesized that subtle feedback effects on CDC progression could cause populations of cells to segregate into approximately CDC-synchronized subpopulations. Experimental bud index data reported in [77] supported this conjecture. In [6] the authors studied a few simple forms of (1.2.1) with the hypothesis that cells in one part of the CDC may influence other cells in different parts of the CDC in different ways through various diffusible chemical products. They hypothesized that a large subpopulation of cells in the critical S-phase might affect metabolism production and the metabolites may in turn inhibit or promote cell growth in the later part of the G1 phase, thus setting up a feedback mechanism in which YAO and CDC clustering are inextricably intertwined, and they showed analytically and numerically that differential CDC feedback such as this can robustly cause CDC clustering in the models. By clustering we do not mean spatial clustering (cultures that exhibit YAO occur in well-mixed bioreactors), but groups of cells that are traversing the CDC in near synchrony.

Guided by these mathematical results, Stowers et. al. verified the existence of clusters in two types of oscillating yeast [83] using both bud index and cell density data. Some of the measurements from those experiments are shown in Figure 1.2. First we note that the cell cycle period, as calculated by the dilution rate, is approximately 400 minutes, and two O_2 oscillations occur during this period, suggesting that there may be two clusters. Next, analyzing the figure, we see that approximately half of the cells are budding at times t = 50 and t = 250, while at t = 170 less than 10% of the cells are budded. Each budding event is accompanied by a decrease in density (no cells are dividing) and followed by a sharp increase in cell density as these budded cells proceed through division. Note that at t = 170 since less than 10% of the cells are budded, most of the cells must be in the G1 phase of the cycle. When the bud index hits its next

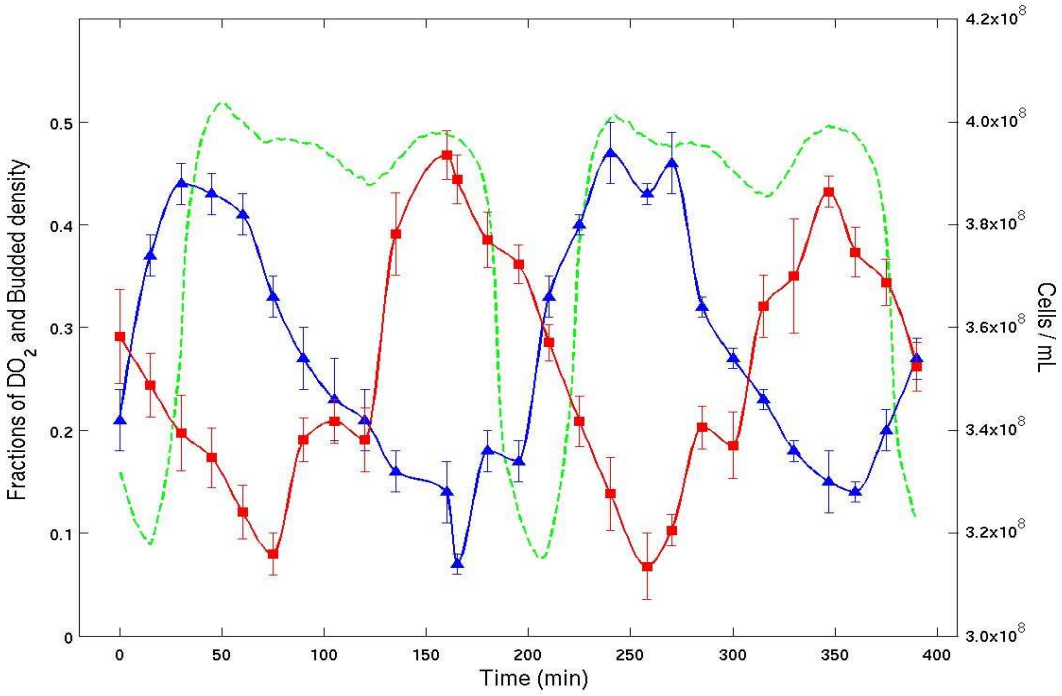

Figure 1.2: Experimental time series from a continuous culture of budding yeast. Dissolved O_2 percentage (green), bud index percentage (blue) and cell density (red) are plotted versus elapsed time. The average cell cycle period as calculated from dilution rate was about 400 minutes. The plot shows clearly that the bud index (percentage of cells with buds from microscopy) and cell density (by flow cytometry) are both synchronized with the oscillation in the level of dissolved O_2.

maximum at t = 250, approximately half of the cells must have budded. The other half of the cells must at that time still be in the G1 phase. As the cells that are budded then divide and the cell density increases, the cells that remained in G1 must still be in G1 since the bud index is again low. When the first group of cells has divided, the second group has been in G1 for at least 200 minutes. The next rise in bud index then must be due to these cells, since they have had time to mature, while the first group of recently divided cells clearly has not had time to reach budding again. Thus, these experiments show conclusively the existence of two clusters and that CDC clustering coexists with YAO.

1.3 Modeling of the cell cycle and feedback

In standard modeling, the cell volume $v_i(t)$ is a proxy for position in the cell cycle. This has justification for yeast in that milestones in the cell cycle, such as the onset of budding, are closely associated with volume milestones and thought to be causally related. Measurements show that the growth of a single cell is roughly exponential [1], so a first order approximation is that the volume of the i-th cell satisfies a linear differential equation

$$\frac{dv_i}{dt} = cv_i. \tag{1.3.1}$$

Growth rate c is often assumed to be independent of v_i, i.e. it is independent of the cell's current state within the cycle and of other cells; it depends instead on the nutrients available and other environmental factors. Applying a logarithmic change of variables the growth law becomes $dc_i/dt = c$, and by further normalizing both the coordinate c and time, the cell cycle can be represented by the unit interval $[0, 1]$, and the equation of motion becomes $dc_i/dt = 1$. In this simple model each cell reaches division (cytokinesis) at 1 when it returns (perhaps with its descendant cell) to 0 and begins the cycle again. Note that a change to normalized coordinates does not depend essentially on the form of (1.3.1). Any model of cell growth where cells do not interact while growing deterministically can be normalized to the form $dc_i/dt = 1$, with $c_i(t) \in [0, 1]$. This model is insufficient in light of the data of [77], as it does not predict clustering behavior.

A much more general model (again using normalized coordinates) is (1.2.1), which we reproduce for convenience:

$$\frac{dc_i}{dt} = 1 + a(c_i, \bar{c}) \qquad 1 \le i \le n, \tag{1.3.2}$$

where c_i is the position of the cell within the cycle and $\bar{c}$ denotes the state of all the cells in the culture.

We propose to consider forms of (1.3.2) where the cells in one region of the cell cycle, S for *signaling*, may influence the growth rate of cells in a preceding portion that we term R for *responsive*. For example the R region may reside in the later portion of the G1 phase and the signaling region S may be the biological S phase (see Figure 1.1). This is philosophically justified by the fact that the S phase is the most critical part of the CDC and the link between YAO and CDC may function to protect the integrity of transcription [16]. It is also known that growing yeast store carbohydrates, then metabolize them in the late G1 phase [28]. The actual positions of the signaling and responsive regions within the biological cell cycle play no role in the mathematical analysis of deterministic models of this form; they will become more relevant in Chapter 4 when noise is introduced to the system, and we will return to the topic at that time. Throughout this manuscript we will use S to denote the signaling region. and on the few occasions when we refer to the yeast's S phase we will do so explicitly.

1.3.1 Definition. *Consider n cells whose coordinates are given by* $c_i \in [0,1]$, 1 *identified with* 0*, and governed by an equation of the form* (1.3.2)*. When a cell reaches* 1 *it continues at* 0*. We call such a system an* RS-feedback system *if:*

(H1) *R is an interval that directly precedes another interval S, i.e. the last endpoint of R is the first endpoint of S,*

(H2) *$a(c_i, \bar{x})$ vanishes except when $c_i \in R$ and there are some c_j in S,*

(H3) *$0 < v_{min} \leq 1 + a(c_i, \bar{c}) \leq v_{max}$ for all c_i and $\bar{c}$,*

(H4) *feedback is monotone, thus adding a cell to S will increase the value $|a(c_i, \bar{c})|$ for $c_i \in R$, and,*

(H5) *$a(c_i, \bar{c})$ is a smooth function for c_i in the interior of R and each c_j in the interior of S, $j \neq i$, and the one sided derivatives exist at the boundaries of R and S.*

The requirements (H2) and (H4) imply that $a(c_i, \bar{x})$ *is either always non-negative or always non-positive. By* positive feedback *we mean a is positive for* $c_i \in R$ *if there are one or more* c_j *in* S*. We define* negative feedback *analogously.*

For the sake of definiteness we will specify:

$$S = [0, s) \quad \text{and} \quad R = [r, 1), \quad 0 < s < r < 1.$$

The final endpoint of R is 1, which corresponds to 0, the initial endpoint of S. See Figure 1.4 below. The regions R and S are thus adjascent but disjoint. See Figure 1.3.

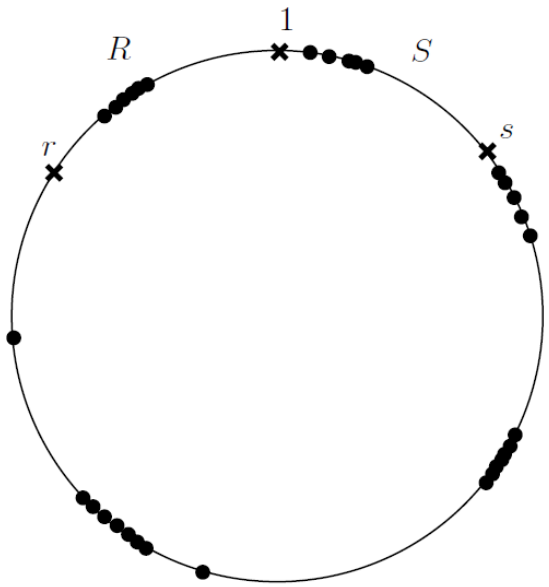

Figure 1.3: The phase diagram of the RS model; cells in S influence the rate of cells in R, causing cells to cluster together. In this example, multiple clusters are forming, which we will see is indicative of negative feedback.

Note that our restriction that R precedes S, while motivated by biological considerations, is not the only possibility. It is worth noting that in the reverse case, when R follows S, many of our results hold with the roles of positive and negative feedback reversed. In particular, this is true for Propositions 1.5.1, 1.5.2, 1.5.4, 1.6.1, 1.6.2, and Corollary 1.6.3. In [30] the authors dropped the requirement (H1) entirely by allowing

S and R to be non-adjacent. We consider in Chapter 5 a similarly-defined model where R and S overlap.

Note that in Definition 1.3.1 the number of cells in the culture is fixed at n. Thus we will consider neither death, harvesting, nor proliferation. In the oscillation experiments we are modeling there are in fact proliferation and harvesting (and an insignificant rate of death), but they approximately balance when averaged over a cell cycle. Thus the expected number of cells descended from a single cell in any future cycle is approximately 1. Further, in the model we are considering, there is no distinction between the two cells resulting from a division and to keep track of both trajectories would be redundant (although in Chapter 4 we will consider modeling the distinction between mother and daughter cells as a natural way to add noise to the system.)

The differential equation in the general model (1.3.2) with RS feedback may have discontinuities, and the standard results of Picard on existence and uniqueness of solutions therefore do not apply. However, note that the equations may be discontinuous only when a variable is at the boundaries of R and S i.e. at the hyper-surfaces given by $\{\bar{x}|x_j = 0, s, \text{ or } r \text{ for some } j\}$. Thus state space consists of open regions of continuity, separated from one another by hyper-surfaces. Because all derivatives are positive and bounded away from 0, any solution can only cross a surface of discontinuity non-tangentially with non-zero speed. In these regions of continuity, unique classical solutions exist, by classical methods; extending these to the hyperplane, we thus have classical solutions joined together continuously at a discrete set of time points. This is a solution in the sense that it satisfies the corresponding integral equation, although the derivative does not exist at the points where the solutions are joined together. More formally, the vector field is directionally continuous, and because solutions can only cross surfaces non-tangentially in zero time, the vector

field has bounded directional variation. Thus solutions exist, are unique, and depend Lipschitz-continuously on initial conditions; see e.g. [11].

We will be primarily concerned with the following special case of the model:

$$\frac{dc_i}{dt} = \begin{cases} 1, & \text{if} \quad c_i \notin R \\ 1 + f(I), & \text{if} \quad c_i \in R \end{cases} \tag{1.3.3}$$

where

$$I(\bar{c}) \equiv \frac{\#\{j : c_j \in S\}}{n} = \frac{\#\{j : c_j \in [0, s)\}}{n}, \tag{1.3.4}$$

i.e. I is the fraction of cells in the signaling region. The "response function" $f(I)$ in (1.3.3) must satisfy $f(0) = 0$ (H2) and be monotone (H4), but can be non-linear, for instance sigmoidal (S-shaped). Models of this form, while fairly general, can be studied in some detail.

Understanding the CDC at the genetic and biochemical level is a topic of intense interest and progress has been made in identifying the agents and the nature of relationships between them [8, 18, 28, 80, 82, 89]. Our approach uses a "caricature" of the cell cycle, rather than detailed modeling, and this simplification demands justification. First, we wish to deal with individual cells in a population-wide phenomenon. If details within each cell are considered, then the dimensions of the phase space would be extremely large and results would be difficult to obtain. Second, our understanding of the details of the cell cycle and its relations with other processes is not complete and even if the general nature of relationships were well-understood, the resulting set of differential equations would contain many parameters, e.g. rate constants, that could only be estimated. With our simplified model which is based on biological insight, we hope to obtain general principles that will inform further detailed investigations.

The approach in part of this work is basically that of "phase oscillator" models, e.g. Kuramoto equations, in which details of each individual actor are projected onto a

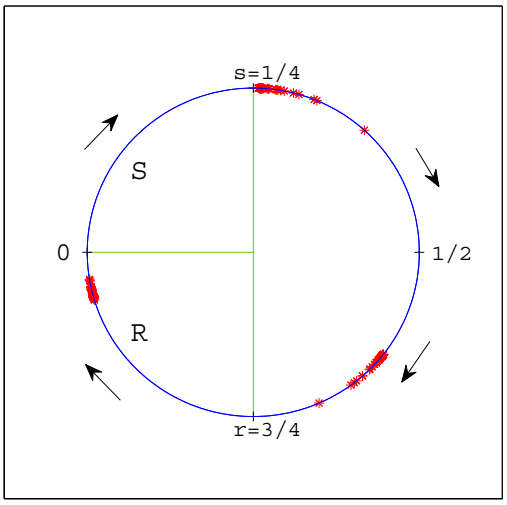

Figure 1.4: Our coordinate representation of the cell cycle and (weakly clustered) groups of cells from a negative feedback simulation with $n = 200$ and parameter values $s = .25$ and $r = .75$. Positions of individual cells are denoted by red asterisks. In this coordinate system the S region is the interval $[0, .25)$ and the R region is $[.75, 1)$, where 1 is identified with 0.

simple phase space and emergent population behaviours are studied. In fact, if $f(I)$ is linear then our model can be put into the Kuramoto form by integrating over the cell cycle for each pair of cells and adding the effects (see [53] p. 65-67). This derivation fails in general for RS models (1.3.2) or (1.3.3), since the effects of cells in general are not additive.

We note here another modeling simplification that we have implicitly made; namely one might more accurately model the feedback term as $a(c_i, z)$ where z is a vector variable representing all substrate factors that contribute to growth rate and z itself is coupled with $\bar{x}$ [38]. Dropping the z variable can be justified if the time-scale of the dynamics of this variable is significantly shorter than the time-scale of the CDC.

1.4 Clusters, gaps, and isolation

In this section we begin to study the existence and stability of periodic "clustered" solutions for both positive and negative RS-feedback systems, and in later sections we point out crucial differences between these two types of feedback. Reducing to the study of clustered solutions is of practical interest since clusters appear in experiments with YAO (and are in fact the motivation for this work). It also limits the dimensions of the problem to a manageable size. This strategy has proven indispensable in many fields; for instance in fluid dynamics, insight is obtained by studying finite dimensional vortex equations rather than the full Navier-Stokes partial differential equations [67].

1.4.1 Definition. *By a* cluster*, we will formally mean a group of cells that are completely synchronized in the CDC. We will denote clusters by x_i rather than c_i to keep them notationally distinct from individual cells.*

The differential equation (1.3.3) can be naturally generalized to the case of clusters,

$$\frac{dx_i}{dt} = \begin{cases} 1, & \text{if} \quad x_i \notin R \\ 1 + h(I), & \text{if} \quad x_i \in R, \end{cases} \tag{1.4.1}$$

where

$$I(\bar{x}) \equiv \frac{\#\{j : x_j \in S\}}{k} = \frac{\#\{j : x_j \in [0, s)\}}{k}, \tag{1.4.2}$$

If the cells that make up the clusters are perturbed, then we pass from (1.4.1) to (1.3.3).

1.4.2 Lemma. *Let k clusters of n/k cells be subject to the dynamical system defined by* (1.4.1)*, with feedback function h. Then $h = f$, where f is the feedback function in* (1.3.3)*.*

In other words, thinking of each cluster moving under the dynamics of (1.4.1) is equivalent to thinking of each cell in each cluster moving under the dynamics of (1.3.3).

Proof. If the clusters are broken into their component cells (which cannot happen under the influence of the stated dynamics, but may, e.g., happen under the influence of noise), then the cells travel under the influence of (1.3.3), with feedback function f.

Now consider (H5) of Definition 1.3.1. By way of contradiction, let q be a rational number between 0 and 1 such that $f(q) \neq h(q)$. Then if q is the fraction of cells in S, (H5) states that moving cells about S (which does not change I), if it causes a to vary at all, will cause it to vary continuously. However, we have just assumed that as the cells pass continuously from an unclustered to a clustered solution, a jumps discontinuously from $f(q)$ to $h(q)$. □

This lemma will be significant in the investigations of stability in Chapter 3.

Note that RS-feedback systems as defined have the symmetry of globally coupled networks with identical nodes; namely, the vector field is equivariant with respect to the group of permutations of coordinates. This symmetry implies that any cells that initially share the same phase keep the same phase as time evolves. The simplest trajectory consists in taking all cells initially in the same phase. We have a single cluster x (synchrony) that generates a periodic solution that runs at velocity 1 around the circle (i.e. $x(t) = x(0) + t \bmod 1$ for all $t > 0$).

1.4.3 Definition. *We call the solution where all cells are initially in the same phase the synchronous solution.*

Note that under the dynamics of the system, cells in the same phase remain in the same phase indefinitely, while cells not in the same phase cannot enter the same phase.

The interval $[0, 1]$, with the endpoints identified, is a circle. On this circle, we can specify a positive direction as associated with the increasing direction on $[0, 1]$. A distance between points x and y on the circle using these coordinates is given by the minimum of $|x - y|$ and $1 - |x - y|$.

1.4.4 Definition. *By the* gap *between two clusters or cells at x_{i-1} and x_i we mean the open interval on the circle from x_{i-1} to x_i, in the direction of the flow that contains no cells and has width $w_i = d(x_i, x_{i-1})$.*

Note that if there are only two clusters x_1 and x_2 in the system, then they define two gaps.

It follows from our assumed coordinates that if two clusters are in $S \cup R$ then the distance between them on the circle is less than $|R| + |S| = 1 - r + s$. Here $|R|$ denotes the length of the interval $R = [r, 1)$, which is $1 - r$ and $|S| = s$ denotes the length of the interval $S = [0, s)$. See Figure 1.4. We say that a cluster of cells is *isolated* if there are gaps between the cluster and any other cells on either side of length at least $|R| + |S|$ and *strictly isolated* if the widths of gaps are more than $|R| + |S|$. This terminology is motivated by the fact that strictly isolated clusters cannot exert feedback on cells outside the cluster, or have feedback exerted upon them from outside. While we consider only clustered solutions in the strictest sense, in real cultures individual cell differences will lead to a weaker form of clustering. For clarity we will refer to such a weakly clustered subset of cells as a *group* of cells. Groups are isolated (strictly isolated) if the distance between any cell in a group and any cell not in that same group is greater than or equal to (strictly greater than) $1 - r + s$.

The following definition will play a large role in the analysis of the model.

1.4.5 Definition. *Define*

$$M := \lfloor (|R| + |S|)^{-1} \rfloor. \tag{1.4.3}$$

M is the maximum number of isolated clusters that can simultaneously exist, given the sizes $|R|$ and $|S|$ of R and S.

Here $\lfloor x \rfloor$ denotes the floor function, that is, the greatest integer less than or equal to x.

1.4.6 Proposition. *For any RS feedback model and any positive integer $k \leq M$ there exist periodic solutions consisting of k isolated clusters that do not interact.*

Proof. For $k \leq M$ consider the solution with initial conditions: $x_1 = 0$, $x_2 = \frac{1}{k}$, ..., $x_k = \frac{k-1}{k}$. We claim that this is such a periodic solution. Notice from the definition of M that

$$M \leq (|R| + |S|)^{-1}$$

and so

$$\frac{1}{k} \geq \frac{1}{M} \geq |R| + |S| = 1 - r + s.$$

Since the distance between any two consecutive clusters x and y is initially $d(x, y) = 1/k$, no two clusters can be in $R \cup S$ simultaneously. Thus no feedback will occur and thus the distance between clusters will not change.

By the same reasoning any initial condition of $k \leq M$ clusters, where all pairs of clusters satisfy $d(x, y) \geq |R| + |S|$, will also lead to a periodic solution where all clusters move indefinitely with speed 1.

Conversely, if more than M clusters exist, then at least two of them are within a distance $|R| + |S|$ of each other, and while the first of these clusters lies in the signaling region, it will exert feedback on the second cluster for a non-empty interval of time. □

Note that a solution consisting of strictly isolated clusters can be at most neutrally stable (not asymptotically stable) since moving a cluster to the left or right still produces an isolated cluster.

In Figure 1.5 we plot the results of numerical simulations which compare the number of clusters that formed with the maximum number M of possible isolated clusters. The number of cells n was 1000, with initial condition $c_i = (i - 1)/1000$; the model used was (1.3.3) with f linear. Specifically, for the positive feedback simulations $f(I) = .6I$, and $f(I) = -.6I$ in the negative feedback simulations. In order to picture r, s, and the number of clusters formed in two dimensions, we set $|S| = |R|$. By letting s run over $[.1, .45]$ in 400 increments, M runs from 1 to 6.

The simulation was performed by selecting a cell c_1 and defining a Poincaré section under the dynamics of the flow, $\{\bar{x}|c_1 = 0\}$. This defines a corresponding Poincaré map, which was iterated 500 times (we will discuss this Poincaré section, together with its map, in far more detail later in this thesis, starting in Chapter 2). In general, sharp clusters formed well before then. We detected clustering automatically by dividing the unit interval into 20 bins; a cluster was a maximal set of adjacent bins each of whom contained a threshhold number of cells. After 200 iterations of the Poincaré map, clustering is observed to be both obvious and tight; for $s = .3$ and $r = .7$, for example, all but 6 cells in the first 500-cell cluster are .517 when rounded to three decimal places (the worst "outlier" is at .495), while all but 4 cells in the second 500-cell cluster lie at 1 when rounded to three decimal places (the worst outlier is a cell at .989). We exclude $0 < s < .1$ because as the size of S and R go concurrently to 0, the number of iterations required for clustering to appear goes to infinity (but we have spot-verified that clustering occurs for these parameter values; for $s = 1 - r = .01$, for example, we clearly observe clustering begin to occur by $40,000$ iterations of the Poincaré map. Note, however, that the number of clusters that appear increases as r and s decrease, so at a critical value, in particular at $s = 1/20000$, clustering will no longer occur; or rather, the "clusters" will contain one cell each. To observe this, note that x_{1000} will enter R at the same time that x_1 leaves S, and the distance between cells will thus never decrease.)

The most striking feature of the plots in Figure 1.5 is that for positive feedback the number of clusters formed is always less than or equal to M, but for negative feedback the number of clusters formed is always greater than M. Notice that clustering is always observed to occur, except when $s \approx 0$, and the nonappearance of clustering in that region is merely an artifact of letting the number of iterations of the Poincaré map run by the algorithm be independent of that parameter, combined with the fact that the number of clusters that form increases as $s \to 0$. Finally, it is worthy

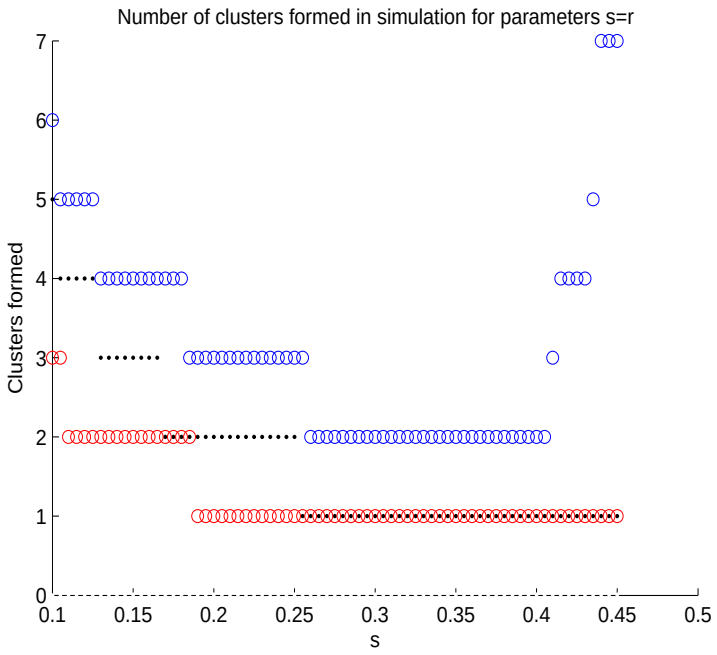

Figure 1.5: The number of clusters that form in simulations compared with $M = \lfloor (|R| + |S|)^{-1} \rfloor$, the maximum number of isolated clusters given R and S, by way of s. Red circles represent positive feedback, blue circles negative feedback, and black dots are placed at M.

of note that for negative feedback, there are no occurrences of one-cluster solutions. Analysis in the next sections will shed light on these observations.

An interesting facet of the diagram is that under negative feedback, the number of clusters formed initially decreases as s increases, but eventually starts to increase with s. This is an artifact of letting $|S| = |R|$; more particularly, as $s \to 1/2$, $s \to r$. We will discuss this phenomon further in Section 2.6.2 of Chapter 2.

Besides solutions consisting of $k \leq M$ isolated clusters, RS-feedback systems have other periodic solutions. One of these consists of all n cells spread along the cycle as uniformly as possible.

1.4.7 Definition. *We will define a* **uniform solution** *to be a trajectory for which the coordinates satisfy the following relation for some time* $d > 0$*:*

$$c_i(d) = c_{i+1}(0) \quad \textit{for all} \quad i = 1, \ldots, n-1, \quad \textit{and} \quad c_n(d) = c_0(0) \mod 1. \tag{1.4.4}$$

Since the velocity of cells in the complement of R is precisely 1, it follows that for such a solution the cells in R^c will be uniformly distributed with inter-cell distance d. The uniform solution represents a completely unclustered state, but the proof of the existence of the uniform solution will also show the existence of stable, clustered solutions.

Suppose that k divides n and k sets of n/k cells are initially synchronized. Then we may greatly reduce the dimensions of the differential equations, from $O(10^{10})$ to $O(k)$, by considering only the positions of the k clusters which we may denote by $\{x_1(t), x_2(t), \ldots, x_k(t)\}$. In particular we will prove that there always exists a solution of k clusters as in the following definition.

1.4.8 Definition. *Let there be some positive number d such that*

$$x_i(d) = x_{i+1}(0) \quad \textit{for all} \quad i = 1, \ldots, k-1, \quad \textit{and} \quad x_k(d) = x_1(0) \mod 1. \tag{1.4.5}$$

We will refer to such solutions as **k-cyclic solutions**.

The uniform solution is thus the n-cyclic solution.

1.4.9 Proposition. *There exists a uniform solution of any RS-feedback system for any n. If k is a divisor of n, then a cyclic k cluster solution exists consisting of n/k cells in each cluster.*

We defer the proof of this proposition until Section 2.1 in Chapter 2.

For n large, as in the application in mind, then we expect k cluster solutions for $k \ll n$ to exist even if k does not exactly divide n. For example hyperbolicity (linear stability or instability) of the k cyclic solutions when k divides n would imply that such solutions exist for all $n' \approx n$.

1.5 Positive feedback systems

In a RS model with positive feedback, a group of cells that is isolated will remain isolated. Such isolated groups will converge to clusters as time goes to infinity.

1.5.1 Proposition. *In a general RS model* (1.3.2) *under positive feedback, suppose that a solution has a gap between two adjacent cells c_{i-1} and c_i of width greater than or equal to $|R|+|S|$. Then the width of this gap will never decrease. In particular, an isolated group or isolated cluster will remain isolated indefinitely.*

If there are only two clusters in the system, then this proposition applies to either of the two gaps that has width at least $|R| + |S|$.

Proof of Proposition 1.5.1. Suppose that two consecutive cells c_{i-1} and c_i are separated by a gap of width $w_i \geq |R|+|S|$. Since feedback is positive, the cell c_i always moves at a speed of at least 1. The cell speed of c_{i-1}, being governed by (1.2.1), will be exactly 1 whenever w_i is greater than or equal to $|R| + |S|$, since there will be no cells in S when x_{i-1} is in R. We then find that the time derivative of w_i is non-negative when $w_i \geq |R| + |S|$. Therefore, the gap can never decrease. It follows immediately that a group or cluster of cells that is isolated will remain isolated. □

1.5.2 Proposition. *In a general RS model* (1.3.2) *with positive feedback, suppose that a group of cells with width w less than $|R| + |S|$ is isolated. Then the width of the group will converge to zero as $t \to +\infty$.*

Proof. By the previous proposition the group will remain isolated for all future time and we may consider this group of cells as a decoupled sub-system. Without loss of generality we may renumber the cells in the group so that they have coordinates: $c_1, c_2, \ldots, c_\ell$, (ordered in the direction of the flow). For $i = 1, \ldots, \ell - 1$, denote by $w_i = c_\ell - c_i$ the width of the interval from c_i to c_ℓ. By assumption $w_{\ell-1} \leq w_i \leq w_1 < |R| + |S|$. Observe that this condition ensures that each c_i, $i = 1, \ldots, \ell - 1$ will experience some acceleration every time it passes through R. This implies that if $w_i(t)$ is non-zero, then $w_i(t)$ will decrease each time the group passes through R and S.

Since the group will remain isolated, the cell c_ℓ will always move with speed 1 and $w_i(t)$ will never increase. Since each $w_i(t)$ is non-increasing and bounded below by

0, it must have a limit w_i^∞. Now consider a solution with an initial condition such that $c_i(0) = c_\ell(0) - w_i^\infty$ for $1 \le i < \ell$, that is to say, we take a solution whose initial condition is the limit of the original solution. By continuous dependence on initial conditions, each $w_i(t)$ will be identically w_i^∞ for all t. This implies that w_i^∞ must be zero, since, from above, a non-zero $w_i(t) < |R| + |S|$ must decrease during each cycle. □

For the case where the RS model has the form of (1.3.3), this proposition is a special case of Lemma 3.2.8 (see Chapter 3).

In the next result we discuss stability, for which we need the concept of distance and neighborhoods in phase space, which for the models we are considering is the n-torus, $\mathbb{T}^n$, where n is the number of cells. We will defer a detailed discussion of this issue until such a time as it will be more useful, in Chapter 3. For the present, we simply note that on $\mathbb{T}^n$ there is a natural metric defined by the maximum of the (mod 1) coordinate differences.

1.5.3 Proposition. *In a RS model* (1.3.2) *with positive feedback, the set of strictly isolated cluster solutions is locally asymptotically stable. A solution consisting of $k \ge 2$ strictly isolated clusters is neutrally stable (stable, but not asymptotically stable) within the set of solutions with k clusters.*

Proof. First observe that an ϵ-neighborhood of a configuration consisting of isolated clusters consists of groups of cells within ϵ of the original clusters. If the original clusters are strictly isolated, then we may make ϵ small enough that the groups are also strictly isolated. By Propositions 1.5.1 and 1.5.2 each of these groups will remain isolated and converge to a cluster. Thus a solution starting at any initial condition within a neighborhood of the set of strictly isolated clusters will asymptotically approach the set.

The second part of the claim follows since, if a strictly isolated cluster is moved a small distance, then it is still strictly isolated. Thus a small perturbation of a solution consisting of k strictly isolated clusters also will be a solution consisting of k strictly

isolated clusters. The distance between the two solutions will remain constant for all future time and thus they are stable, but not asymptotically stable. □

Points near the set of isolated cluster solutions will converge to the set, but individual solutions are only neutrally stable with respect to perturbations inside the set.

Since the set of clustered solutions is locally stable, it must have a basin of attraction and it is natural to ask how big the basin is. In simulations for positive feedback systems, the basin seems to include almost all initial conditions. In the next proposition we see that the basin of attraction extends far beyond a small neighborhood of the set.

1.5.4 Proposition. *Suppose that a solution* $\bar{x}(t)$ *in a RS model* (1.3.2) *with positive feedback has at least one gap of width greater than or equal to* $|R| + |S|$. *Then the solution will converge to a periodic solution consisting entirely of isolated clusters.*

Proof. We will call a gap *large* if its width is greater than or equal to $|R| + |S|$. At time t_0, the cells may be grouped into a minimum number of groups in which there are no large internal gaps. The number of such groups is the same as the number of large gaps. Note that each such group is isolated, and the number of such groups cannot be larger than $M = \lfloor (|R| + |S|)^{-1} \rfloor$. Consider one such group. Since it contains no large internal gaps and it is isolated, during passage through R the last cell must be accelerated by the presence of at least one cell in S and so its speed is sometimes greater than 1. On the other hand, since the group is isolated it will remain isolated by Proposition 3.1, and the lead cell will travel indefinitely with speed 1 by the same argument that appears in the proof of that proposition.

Thus during one passage through R the distance between the lead cell and the final cell in the group must decrease. If this group continues to have no large internal gaps, then it follows that the width of the group will continue to decrease. By an elementary

argument (as in Proposition 1.5.2), the width will converge to zero; in other words the group will converge to a cluster. Otherwise, if a large internal gap develops then the cells that are separated by the gap will be isolated from each other and thus form two isolated groups. When this occurs the number of isolated groups will increase. Since the number of isolated groups is bounded from above, large internal gaps may form only a finite number of times and thus eventually we have a fixed number of groups that never develop large internal gaps and each of these converges to an isolated cluster. □

1.6 Negative feedback systems

The key observation is that for negative feedback, isolated clusters are not stable. This is because as a group of cells crosses the R-S boundary all cells of the group are delayed except the lead cell, which moves with unit velocity, causing the group to spread.

1.6.1 Proposition. *In a RS model* (1.3.2) *with negative feedback, a solution consisting of strictly isolated clusters is locally unstable.*

Proof. Let $c^*(t)$ denote a solution consisting of strictly isolated clusters. First observe that under the condition of strict isolation the gaps between clusters are all larger than $|R| + |S|$, and so any sufficiently small perturbation of the clusters consists of groups that are still isolated. Now let $c(t)$ be a solution with initial condition $c(0)$ that differs from $c^*(0)$ in only the i-th coordinate, i.e. an initial condition such that one cell has been perturbed away from the cluster. When this cluster-cell pair passes through the boundary from R to S the separation between c_i and the cluster to which it formerly belonged will increase. If we further let the perturbation be sufficiently small, then the cluster-cell pair will remain isolated from other clusters.

Now recall the definition of stability: given any $\epsilon > 0$, there exists $\delta > 0$ such that any solution $c(t)$ starting within a δ neighborhood of $c^*(t)$ will remain indefinitely within an ϵ neighborhood of $c^*(t)$. Let ϵ_0 be the largest ϵ so that any $c(0)$ within an ϵ

neighborhood of $c^*(0)$ will consist of isolated groups and let $\epsilon = \epsilon_0/2$. If $c(0)$ is as in the previous paragraph and is arbitrarily close to $c^*(0)$ then the distance between $c(t)$ and $c^*(t)$ will continue to increase on each unit time interval as long as $c(t)$ continues to consist of isolated groups. Therefore it follows that $c(t)$ will eventually be outside of an $\epsilon_0/2$ neighborhood of $c^*(t)$. Thus $c^*(t)$ is not stable. □

For the case where the RS model has the form of (1.3.3), this proposition is a weaker version of Lemma 3.2.7. In fact, Lemma 3.2.7 demonstrates linear instability (i.e. that nearby orbits are exponentially repelled).

It follows that in order for clusters to remain coherent under small perturbations in negative feedback, they must not be isolated, i.e. the gaps between them must be less than $|R| + |S|$, and so the number of stable clusters must be at least $M + 1$. This is clearly confirmed in simulations (see Figure 1.5). We will show in Section 2.3 that a $k = M + 1$ cluster cyclic solution is stable for negative feedback of the form (1.3.3) under certain conditions, and devote all of Chapters 2 and 3 to considering the stability of k-cyclic solutions, under both positive and negative feedback.

In the following proposition we see that interacting clusters tend to spread out from each other as far as possible.

1.6.2 Proposition. *In a RS model* (1.3.2) *with negative feedback suppose that two clusters are within* $|R| + |S|$ *of each other, but are isolated from other cells (non-empty). If they remain isolated from other cells, then the gap between the two clusters will increase and converge to* $|R| + |S|$. *In the case that the two clusters contain all the cells in the system, if one gap has width less than* $|R| + |S|$ *and the second gap has width* $\geq |R| + |S|$, *then as long as the width of the second gap remains greater than* $|R| + |S|$ *the first gap will increase and approach* $|R| + |S|$.

Proof. If the gap width (or smaller gap width in the case of only two clusters) is less than $|R|+|S|$ then each time the second cluster passes through R, the first cluster will be in S for

a non-empty interval of time. During this time interval, the cluster in R will experience deceleration, and the width of the gap will increase during the passage through R. If the cluster pair remains isolated, then the distance will be preserved through the rest of the cycle. Thus the distance between clusters will increase during each cycle. The distance is bounded above by $|R| + |S|$ and so, by a standard argument, the sequence of distances thus generated will converge to $|R| + |S|$. □

1.6.3 Corollary. *Suppose that there are $k \leq M$ clusters in a RS system* (1.3.2) *with negative feedback. Then the solution will converge to a periodic clustered solution with isolated clusters.*

2 The Clustered Subspace[‡]

We have seen that an RS system exhibits, or can exhibit, clustering under either positive or negative feedback. We now turn our attention to the dynamics of a system where clustering has already occurred, i.e. the state space is the k-dimensional simplex $0 \leq x_1 \leq x_2 \leq \ldots \leq x_k \leq 1$, where we recall that we use the notation x_i to denote clusters, differentiating them from cells (denoted by c_i). We assume that clusters are of equal size, although we recall that by the discussion after Proposition 1.4.9, stability results should also hold for clusters of only approximately equal size. The first time clustering was verified in a laboratory setting [85], two clusters were observed, and we are able to consider the 2-cyclic solution in detail. Three clusters have tentatively been observed as well, although the time costs involved in the experiments of [85] did not permit rigorous verification. Even in such low dimensions as $k = 3$, a complete global analysis of the system is prohibitively complicated [25]. Among other complications, the feedback function in the $k = 3$ case may be nonlinear. We can, however, study the k-cyclic solution in the generic case that k is small, in particular where $k = M + 1$.

We will see in the $k = M + 1$ case that the stability of k-cyclic solutions depends on a number of inequalities involving the parameters s and r. Guided by this, we consider how the (s, r)-triangle ($0 \leq s \leq r \leq 1$) may be partitioned into convex regions such that two parameter pairs (s_1, r_1) and (s_2, r_2) in the same region generate k-cyclic solutions of the same stability, and consider a number of such partitions. We observe trends in the stability diagrams so generated; in Chapter 3, we formalize and prove many of those observations.

[‡] In accordance with ScienceDirect's policy for using previously published articles in an academic dissertation, we here give the DOI number by which the official publication from which the first half of this chapter, up to and including Section 2.3, is drawn may be found: 10.1016/j.jtbi.2011.10.002.

2.1 Dynamics in the clustered subspace

2.1.1 The return map for a clustered system

Let us continue to consider the most general model (1.2.1) with RS feedback. Let a population of n cells be organized into k equal clusters and let the clusters be labeled by an index $i \in \{1, \ldots, k\}$ so that $\bar{x} = \{x_i\}_{i=1}^{k}$ represent clusters of n/k cells each. One can assume that all coordinates $x_i(0)$ of the k clusters are initially well-ordered as

$$0 = x_1(0) \leq \ldots \leq x_i(0) \leq \ldots \leq x_k(0) \leq 1, \quad i = 1, \ldots, k-1.$$

This ordering is preserved under the dynamics (this can be well-defined using the orientation of the circle and $x_1(t)$ as a moving reference point). Moreover, the first coordinate x_1 must eventually reach 1, i.e. there exists t_R such that $x_1(t_R) = 1$. Thus the set $\{\bar{x} | x_1 = 0\}$ defines a Poincaré section for the dynamics and the mapping

$$(x_2(0), x_3(0), \ldots, x_k(0)) \mapsto (x_2(t_R), x_2(t_R), \ldots, x_{k-1}(t_R))$$

defines the corresponding return map. However, even in the $k = 2$ case, the Poincaré map is difficult to study directly. Instead, we will consider a factorization of the Poincaré map, as follows.

Starting from $t = 0$, compute the time t_1 that x_k needs to reach 1 and compute the location of the remaining clusters at this time. Define a map F by

$$F : (x_2(0), x_3(0), \ldots, x_k(0)) \mapsto (x_1(t_1), x_2(t_1), \ldots, x_{k-1}(t_1)). \tag{2.1.1}$$

Note that $x_1(t_1) = t_1$, because previous to time t_1, no clusters enter S. Thus, either x_1 does not enter R, and experiences no feedback, or x_1 enters R, but because x_1, the first cluster in S, has already left S, and no cluster has replaced it, S is empty and no feedback occurs. By the method by which F was defined, $x_k(t_1) = 1$. An illustration of F in the case $k = 3$ is given in Figure **??**.

Now the time $t_1 + t_2$ that x_{k-1} needs to reach 1, together with the population configuration at $t = t_1 + t_2$, follow by applying F to the configuration $(x_1(t_1), x_2(t_1), \ldots, x_{k-1}(t_1))$.

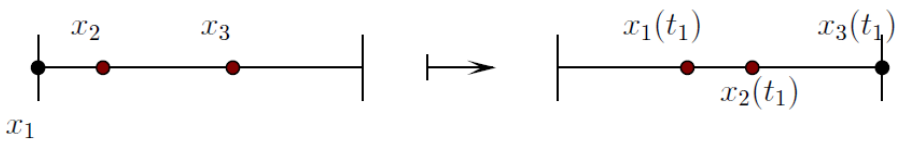

Figure 2.1: The function F for $k = 3$. Note that the domain of F does not include $x_1(0)$, and the range of F does not include $x_3(t_1)$.

By repeating the argument, the return time t_R is given by $t_R = t_1 + t_2 + \cdots + t_k$ and the desired return map is F^k (where F^k is used to denote k compositions of F). Therefore, to study the dynamics one only has to understand the first map F.

We will first consider general properties of the map F and then we will compute and analyze it for feedback of the form (1.3.3) in the simplest case, $k = 2$.

2.1.2 General properties for arbitrary k

We may regard F as a continuous piecewise affine map of the $(k-1)$-dimensional simplex

$$0 \le x_2 \le x_3 \le \cdots \le x_k \le 1$$

into itself. (Although the boundaries 0 and 1 are identified in the original flow, in the analysis here, we consider them as being distinct points for convenience.)

On the edges of the simplex, F has relatively simple dynamics. Indeed, if initially all coordinates are equal, then they must all reach the boundary 1 simultaneously. In other words, on the diagonal ($x_i = x$ for all i), we have $F(x,\ldots,x) = (t_1, 1, \ldots, 1)$ where $t_1 = \min\{t | x_k(t) = 1\}$ depends on r, s and x. Note that during time $0 < t < t_1$, no cluster enters S. Thus even if x_1 enters R during that time interval, it travels at a constant rate of 1 (since if x_1 has left S then all clusters in S have left S, and S is thus empty). This, combined with the assumption that $x_1(0) = 0$, accounts for the fact that $x_1(t_1) = t_1$. Note also that because F has as its domain $(x_2, x_3, ..., x_k)$, the fact that the argument of F in this case is $(x,\ldots,x)$ does not mean that all clusters

are assumed to be synchronized. Clusters $x_2, x_3, ..., x_k$ are synchronized, but this says nothing of x_1. If $x = 0 = x_1$, all k clusters are synchronized and $t_1 = 1$ independently of r and s.

Moreover, starting with $x_k = 1$ implies $t_1 = 0$ which yields

$$F(x_2, \ldots, x_{k-1}, 1) = (0, x_2, \ldots, x_{k-1})$$

whatever the remaining coordinates $x_2, \ldots, x_{k-1}$ are. As a consequence, the edge

$$\{(x, 1, \ldots, 1) \ : \ x \in [0, 1]\}$$

is mapped onto

$$\{(0, x, 1, \ldots, 1) \ : \ x \in [0, 1]\}$$

which is mapped onto $\{(0, 0, x, 1, \ldots, 1) \ : \ x \in [0, 1]\}$ and so on, until it reaches the edge $(0, \ldots, 0, x)$, which is mapped back onto the diagonal (after k iterations; because $x_k(t_1) = 1 = 0$, F may indeed be iterated repeatedly, since it takes configurations with a cluster on 0 to configurations with a cluster on $1 \sim 0$, although it is formally necessary to cyclically relabel the indexes of each cluster after each iteration).

A particular orbit on the edges is the k-periodic orbit passing the vertices, and which corresponds to the single cluster of velocity 1 in the original flow, namely

$$(0, \ldots, 0) \mapsto (1, \ldots, 1) \mapsto (0, 1, \ldots, 1) \mapsto (0, 0, 1, \ldots, 1) \mapsto \cdots \mapsto (0, \ldots, 0, 1) \mapsto (0, \ldots, 0).$$

Geometrically, the corners of the simplex are cyclically permuted by the map F. It follows that the $k - 2$ dimensional simplexes (faces) that make up the boundary of the $k-1$ simplex are also cyclically permuted by F. This implies that F cannot have a fixed point on the boundary.

We now prove that uniform and cyclic solutions exist.

Proposition (Proposition 1.4.9)**.** *There exists a uniform solution of any RS-feedback system for any n. If k is a divisor of n, then a cyclic k cluster solution exists consisting of n/k cells in each cluster.*

Proof of Proposition 1.4.9. The simplex is a convex and compact invariant set under F, and the continuous dependence of the ODE on initial conditions implies that F is continuous. Thus the Brouwer fixed point theorem implies the existence of a fixed point. Since the boundary cannot contain any fixed point, the fixed point is in the interior, i.e. $0 = x_1 < x_2 < x_3 < ... < x_k < 1$. Note that the k-cyclic solutions are fixed points of F and vice versa. Since there exist k-cyclic solutions for any k, there exists an n-cyclic solution, i.e. the uniform solution. □

The proof of Proposition 1.4.9 includes the following important fact about uniform solutions (and hence k-cyclic fixed points), which we extract and isolate.

2.1.1 Corollary. *A configuration of n cells such that no two cells are synchronized, i.e. $c_i \neq c_j$ if $i \neq j$, viewed as a point on the simplex such that $c_1 = 0$, is a point on the uniform solution if and only if it is a fixed point of F. Likewise, a configuration of k clusters is a k-cyclic solution if and only if it is a fixed point of F.*

We further observe that an edge on a simplex is a 1-dimensional k-periodic set, whose coordinates are either 0, 1, or x, $0 \leq x \leq 1$. The boundaries of such a 1-dimensional space, $x = 0$ and $x = 1$, both correspond to the 1-cyclic clustered solution, which Propositions 1.5.2 and 1.6.1 tell us is stable under positive feedback and unstable under negative feedback. Since there are two points of a periodic orbit at each boundary of every edge, and since these points are either both stable or both unstable, there must be at least one other k-periodic orbit on the edges with coordinates between 0 and 1. Whether this orbit is unique might depend on parameters.

2.2 Dynamics for small k

In this section we primarily study the dynamics of 2-cluster systems for the model (1.3.3). Studying the behavior in the cases of a small number of clusters is not just a matter of convenience, but is important from the perspective of applications since presumably only a small number of clusters can form (for fixed n, the presence of more

clusters implies that each cluster contains fewer cells and thus can exert less influence) and be observable (smaller clusters would produce smaller oscillation in metabolites and other chemical agents). In the experiment reported in Figure 1.2 there are two clusters. The dynamics of the 3-cluster system, insofar as they have yielded to analysis, are essentially the same as in the 2-cluster case, and are summarized here as well.

2.2.1 The map F

Consider (1.3.3) where f is a monotone function. In the case $k = 2$, since only one cluster can exert feedback on the other, RS-feedback (1.3.3) simplifies to:

$$\frac{dx_i}{dt} = \begin{cases} 1 + f(\frac{1}{2}) & \text{if} \quad x_i \in [r, 1) \text{ and } x_j \in [0, s), j \neq i \\ 1 & \text{otherwise} \end{cases}$$

Let $\alpha = f(\frac{1}{2})$ for notational simplicity.

For $k = 2$, F is defined on the interval $[0, 1]$ and is determined by $x_1(t_1) = t_1$ where t_1 is the time at which $x_2(t)$ reaches 1. When regarded as a function of x_2 only, its explicit form depends on the parameters r and s. There are two cases depending on the relative sizes of the signaling and responsive regions, specifically on the size of $(1+\alpha)s$ with respect to $1-r$: either $(1+\alpha)s < 1-r$ or $(1+\alpha)s > 1-r$. We have put the details of the computation and analysis of $F(x_2)$ in Appendix A.1.

We observe the meaning of the inequality that differentiates the cases. The first cluster x_1, is in S for a time period of s (as it travels from 0 to s at a rate of 1), and it therefore follows, in the $k = 2$ case, that a cluster can experience feedback for only that length of time over the course of a single Poincaré map. Suppose that $x_2(0) = r$. Then after time s, $x_2(s) = r + (1+\alpha)s$; if $r + (1+\alpha)s > 1$, then x_2 reaches 1 before x_1 reaches s. Since r is the furthest that x_2 can lie from 1 while still being in R, it follows that if $x_2 \in R$ and $r + (1+\alpha)s > 1$, x_2 will reach 1 before x_1 leaves S. It follows that in this case, there can be no fixed point of F such that $x_2 \in R$, since if $x_2 \in R$ and

$T = \min\{t | x_2(t) = 1\}$, $x_1(T) < s < r < x_2(0)$, and a 2-cyclic fixed point is defined by the equality $x_1(T) = x_2(0)$.

Calculating the Poincaré map F^2 is prohibitively complicated, but in Appendix A.1 we use these two possible forms of F to analyze the dynamics. In the next section we summarize the results.

2.2.2 Analysis of the dynamics

In Appendix A.1 we find only four distinct types of dynamics; two for positive feedback and two for negative.

- Positive feedback:

  1. There is a unique unstable fixed point for F^2.
  2. There is an interval of fixed points for F^2.

  All other orbits are asymptotic to the $x_1 = x_2$ boundary of the simplex, i.e. the clusters merge.

- Negative feedback:

  1. There is a unique stable fixed point for F^2.
  2. There is an interval of fixed points for F^2.

  All other orbits, except the boundary points, are asymptotic to the stable fixed point or the interval of fixed points.

These possibilities, for some specific parameter values, are illustrated in Figure 2.2.

An interval of fixed points, we observe in the Appendix A.1, can occur not only because the two clusters may be isolated from each other, but also in certain other situations. Namely if either:

- x_1 is in S for the entire time that x_2 is in R, or,

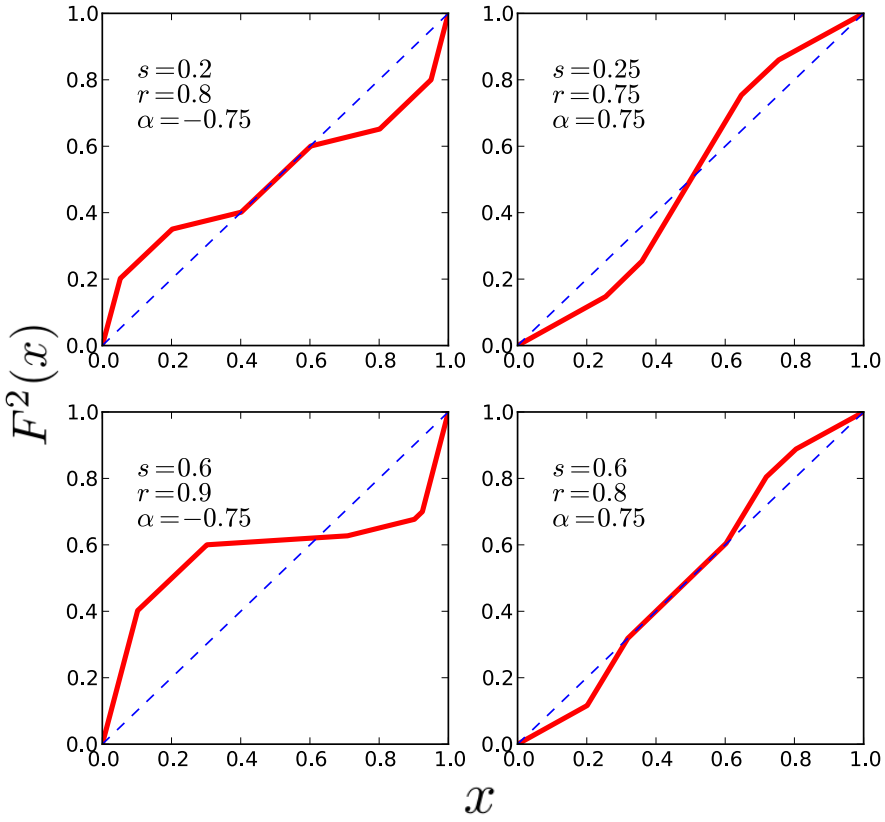

Figure 2.2: Plots of the Poincaré map F^2 in the case $k = 2$ for various parameter values ($\alpha = f(\frac{1}{2})$). Clockwise from top left: interval of fixed points under negative feedback, unstable fixed point under positive feedback, interval of fixed points under positive feedback, stable fixed point under negative feedback.

- x_2 is in R for the entire time that x_1 is in S,

then the unique fixed point of F is neutral and contained in an interval of neutral period 2 points (fixed points of F^2). Both these cases amount to the system decoupling; see Section 3.4 of Chapter 3.

In [25] the authors present similar computations for a subset of parameter values with three clusters and positive linear feedback. The results there are similar to those reported here; for all the cases examined the three cluster cyclic solution is either unstable or in the interior of a set of neutral periodic solutions (period 3

points of F). We will verify in Appendix A.2 that the 3-cyclic solution may never be stable under positive feedback, and comment extensively on instability under positive feedback in Chapter 3. No other periodic orbits were detected in [25], and all other initial conditions tend to two-cluster or one-cluster periodic solutions (on the boundary of the domain of the map F).

For both $k = 2$ and $k = 3$, we find that if the system has positive feedback, then many initial conditions lead to a single cluster, but if the initial condition begins with 2 or 3 clusters, or close to such, then these clusters might persist depending on the parameters and initial conditions, e.g. if the clusters are isolated. If the system has negative feedback, then there may be solutions with 2 or 3 clusters (depending on the parameter values) that are stable within the set of clustered solutions. One cluster is never stable under negative feedback. Biologically, synchrony is likely to appear in systems with positive feedback and clustering in systems that have negative feedback.

2.3 Cyclic $M + 1$ cluster solutions

Again consider the model (1.3.3) of RS feedback. Recall that $M = \lfloor (|R| + |S|)^{-1} \rfloor$ is the maximum number of clusters that can exist without mutual interactions. In this section we consider the cyclic solutions consisting of $k = M + 1$ clusters, with coordinates $x_1, ..., x_k$, in the dynamics corresponding to (1.3.3).

There are a number of reasons for isolating $M + 1$ for special consideration. Biologically, we expect only a small number of clusters to form, but for feedback to occur, the number of clusters cannot be *too* small, or the clusters will be isolated. The $M + 1$ case, being the least number of clusters such that they are not isolated, balances these conflicting requirements. Furthermore, we will see in Chapter 3 that a number of more complicated cases can be understood in terms of the $M + 1$ case (e.g. Theorems 3.4.14 and 3.4.18).

Recall that s is the right endpoint of the signaling region, and r is the left endpoint of the response region. Thus $|S| = s$ and $|R| = 1 - r$.

2.3.1 Proposition. *Consider RS feedback of the form (1.3.3). For any* $0 < s < r < 1$, *there is a cyclic solution consisting of* $k = M + 1$ *equal clusters of the form* $x_1 = 0,\ x_2 = d,\ \ldots,\ x_k = (k-1)d$, *for some* $d > 0$. *If*

$$s < \frac{1}{k}\left(\frac{1+\alpha r}{1+\alpha}\right) \quad \textit{and} \quad r > \frac{k-1}{k}(1 - s\alpha), \tag{2.3.1}$$

where $\alpha = f(\frac{1}{k})$, *then the fixed point is unstable (in the subspace of clustered solutions) for positive* α *and stable for negative* α. *Otherwise, the solution is neutrally stable.*

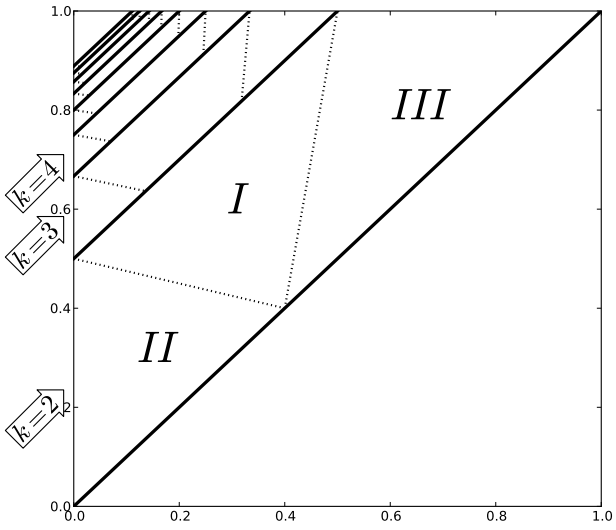

Figure 2.3: Regions of parameter space for the k-cyclic solutions with $k = M + 1$. Each diagonal band contains the parameters for a specific k and is partitioned into three cases. In case I the k-cyclic solution is unstable for positive feedback and stable for negative. In cases II and III the k-cyclic solution is neutral and is contained in a set of neutral period k solutions. In this plot $\alpha = f(\frac{1}{k})$ is taken to be $1/k$.

Note that if the solution is neutrally stable, then the fixed point of F must be contained in the interior of a set of period k points that are also neutrally stable, since

the return map is piece-wise affine. This is consistent with the results for two- and three-cluster systems.

The M-cyclic solution consists of M isolated clusters. This isolation sharply limits the form of the fixed point. When $x_1 = 0$, R must be empty by isolation, and x_k cannot enter R until x_1 has left S. The signaling region S can contain only x_1, since if it included another cluster x_2, $x_1(T) = x_2(0)$ where T is the minimum positive number such that $x_k(T) = 1$, and thus x_k passes through R while x_1 is still in S, i.e. the clusters are not isolated. Adding one additional cluster may cause the $(M+1)$-cyclic solution to have a cluster in R when $x_1 = 0$, or it may cause S to contain the cluster x_2 when $x_1 = 0$, but it may not do both.

2.3.2 Lemma. *When the $(M+1)$-cyclic solution lies on the Poincaré section, either S contains only x_1 and R is empty; or S contains only x_1 and R is nonempty; or S contains clusters other than x_1, and R is empty.*

Proof. By the form of the k-cyclic solutions, all clusters not in R are equally spaced; i.e. there is some positive number d such that $x_{i+1} = x_i + d$ if $x_{i+1} \notin R$. The statement that S contains some cluster other than x_1 when $x_1 = 0$ is equivalent to the inequality $d < s$, and the statement that R is nonempty is equivalent to $r < (k-1)d$. By way of contradiction, suppose that $d < s$ and $r < (k-1)d$. Then in the $k = M+1$ case, where we recall that $M = \lfloor \frac{1}{1-r+s} \rfloor \leq \frac{1}{1-r+s}$, the following string of inequalities holds.

$$\begin{aligned} r &< (k-1)d < (k-1)s = Ms \\ r &< \lfloor \frac{1}{1-r+s} \rfloor s \leq \frac{s}{1-r+s} \\ r - r^2 + rs &< s \\ 0 &< r^2 - r - rs + s \\ 0 &< -r(1-r) + s(1-r) \\ 0 &< (s-r)(1-r) \end{aligned} \tag{2.3.2}$$

This is a contradiction, since $1 - r > 0$ and $s - r < 0$. □

In a neighborhood of the M-cyclic solution, R is empty and S contains one cluster. We have seen that passing to the $M+1$ case can result in either R becoming nonempty, or S containing more than one cluster, but not both. We now prove two additional restrictions. If R is nonempty, it can contain only one cluster. If S contains clusters other than x_1, it contains only one such cluster, which leaves S without exerting feedback on any cluster in R.

2.3.3 Lemma. *On the Poincaré section, if $k = M+1$ then R contains no more than 1 cluster. If R contains a cluster, then x_{k-1} does not enter R until x_1 leaves S, i.e. there is never more than one cluster receiving feedback in the system.*

Proof. Let d be the time it takes for $x_k \in R$ to reach 1. Then d is also the distance between clusters not in R. If there is more than one cluster in R, then $r-(k-2)d < 0 < s$, and

$$\begin{aligned} r-s &< (k-2)d \\ r-s &< \left(\frac{1}{1-r+s}-1\right)d \\ (r-s)(1-r+s) &< (r-s)d \\ 1-r+s &< d. \end{aligned} \tag{2.3.3}$$

If there is 1 cluster in R, $x_{k-1} = (k-2)d$, and $r-(k-2)d < s$ implies that x_{k-1} reaches r before x_1 reaches s. In either event, this is a contradiction. To see this, note that x_k reaches 1 in time $d = 1-r+s+\nu$, where $\nu > 0$. Over the first s time units, x_k moves some distance; it is now strictly within distance $1-r$ of 1. At this point, x_1 has left S, and x_k no longer experiences feedback. The cluster x_k then must travel at rate 1 for time $d' = 1-r+\nu$ before it reaches 1, contradicting the fact that its distance to 1 is less than that.

□

2.3.4 Lemma. *If S contains clusters other than $x_1 = 0$ on the Poincaré section, then it contains only one additional cluster, and that cluster leaves S before x_k reaches r.*

Proof. We prove that $x_1 = d$ must leave S before x_k reaches r. This also proves the first part of the lemma, since if there were more than two clusters in S, then after a single application of F, $x_1(T) = x_2(0) = 2d < s$ would not leave S at all.

By way of contradiction, we suppose $r - (k-1)d < s - d$ and derive

$$\begin{aligned}
&r - (k-1)d < s - d,\\
&r - Md < s - d,\\
&r < s + (M-1)d,\\
&r < s + \left(\lfloor \frac{1}{1-r+s} \rfloor - 1\right) d \le s + \left(\frac{1}{1-r+s} - 1\right) d,\\
&r < s + \frac{r-s}{1-r+s} d,\\
&r - s < \frac{r-s}{1-r+s} d,\\
&1 - r + s < d,\\
&d = 1 - r + s + \nu.
\end{aligned} \tag{2.3.4}$$

As in the previous lemma, this is a contradiction. The cluster x_k is within a distance d of r, or $x_k(d) < r < 1$. Since $d < s$ in this case, by time $t = s$, x_k will have passed into R and S will be empty. Traveling the remaining time $1 - r + \nu$ at a rate of 1, it will pass 1 before time d. But by assumption, $x_k(d) = 1$. □

Proposition (Proposition 2.3.1)**.** *Consider RS feedback of the form* (1.3.3)*. For any* $0 < s < r < 1$*, there is a cyclic solution consisting of* $k = M + 1$ *equal clusters of the form* $x_1 = 0,\ x_2 = d,\ \ldots,\ x_k = (k-1)d$*, for some* $d > 0$*. If*

$$s < \frac{1}{k}\left(\frac{1+\alpha r}{1+\alpha}\right) \quad \textit{and} \quad r > \frac{k-1}{k}(1 - s\alpha), \tag{2.3.5}$$

where $\alpha = f(\frac{1}{k})$*, then the fixed point is unstable (in the subspace of clustered solutions) for positive* α *and stable for negative* α*. Otherwise, the solution is neutrally stable.*

Proof of Proposition 2.3.1. That an $(M+1)$-cyclic solution exists is known from Proposition 1.4.9. We prove that it has the properties claimed of it. Consideration of the

previous lemmas shows that in a neighborhood of the $(M+1)$-cyclic solution, there are never more than 1 clusters in S while R is non-empty, and thus the dynamics of the system are determined entirely by $\alpha = f(\frac{1}{k})$. Those same lemmas demonstrate that the $(M+1)$-cyclic solution can have only a very limited number of forms.

The evolution of the system may be described qualitatively in terms of a sequence of events, e.g. x_1 reaching s, or x_k reaching 1. We first consider a system which evolves via the following sequence of events (which we call Case 1):

$$x_k \mapsto r, \qquad x_1 \mapsto s, \qquad x_k \mapsto 1. \tag{2.3.6}$$

Recall that by definition, a k-cyclic solution is one such that, if $x_k(T) = 1$, then $x_i(T) = x_{i+1}(0)$ for $i = 1, 2, ..., k-1$. Thus, after $x_k \mapsto 1$, after relabeling $x_i := x_{i-1}$ for $i = 2, 3, ..., k$, and $x_1 := x_k = 1 \sim 0$, we have the initial condition again. By calculating the time taken in each step and finding the final value of x_1, one can use the relation $x_k = (k-1)d$ to solve analytically for d, getting:

$$d = \frac{1 + \alpha(r-s)}{k + \alpha(k-1)}\,. \tag{2.3.7}$$

Note that the Case 1 sequence will occur provided that $s < x_2 = d$ and $x_k = (k-1)d < r$. Using (2.3.7) in these relations gives (2.3.5).

Two other sequences of events are possible. Each occurs when one of the constraints in (2.3.5) is dropped (and the other maintained.) Case 2, when we allow $r < x_k$, i.e. $r < (k-1)d$, is characterized by:

$$x_1 \mapsto s, \qquad x_{k-1} \mapsto r \qquad x_k \mapsto 1,$$

and Case 3, when we allow $x_2 < s$, i.e. $s > d$, by:

$$x_2 \mapsto s, \qquad x_k \mapsto r, \qquad x_k \mapsto 1.$$

Following the same procedure as in Case 1, we obtain for Case 2:

$$d = \frac{1 - s\alpha}{k}$$

and for Case 3:

$$d = \frac{1 + r\alpha}{k(1+\alpha)}\,.$$

We have seen in the proceeding lemmas that these three cases are exhaustive. A graphical representation of the regions of parameter space corresponding to these three cases can be seen in Figure 2.3.

The map F is affine in a neighborhood of the fixed point, i.e. $\vec{x} \mapsto A\vec{x} + \vec{b}$ where $\vec{x} = (x_0, ..., x_{k-1})^T$ and A is a matrix. We next analyze A in the three cases.

Case 1:

$$A = \begin{bmatrix} 0 & 0 & 0 & \cdots & 0 & -(1+\alpha) \\ 1 & 0 & 0 & \cdots & 0 & -(1+\alpha) \\ 0 & 1 & 0 & \cdots & 0 & -(1+\alpha) \\ \vdots & & & \ddots & \vdots & \vdots \\ 0 & 0 & 0 & \cdots & 0 & -(1+\alpha) \\ 0 & 0 & 0 & \cdots & 1 & -(1+\alpha) \end{bmatrix} \tag{2.3.8}$$

Thus we may determine the stability of the fixed point by studying the eigenvalues A, which has characteristic equation

$$\lambda^{k-1} + (1+\alpha)(\lambda^{k-2} + \lambda^{k-3} + \cdots + \lambda + 1) = 0. \tag{2.3.9}$$

Observe that if $\alpha > 0$, (2.3.8) has at least one eigenvalue outside of the unit circle. This is because it has determinant of modulus $1 + \alpha > 1$ (the constant term of (2.3.9)), and the modulus of the determinant of a matrix is the product of the moduli of its eigenvalues. Thus the fixed point is unstable in that case; we will in fact demonstrate a stronger result, that all eigenvalues are outside the unit circle.

Now let $\alpha < 0$. Notice that $\lambda = 1$ can easily be ruled out as a root. For $\lambda \neq 1$ we can rewrite (2.3.9) as

$$\frac{1}{1+\alpha}\lambda^k + \sum_{i=0}^{k-1} \lambda^i \;=\; \frac{\lambda^k}{1+\alpha} + \frac{\lambda^k - 1}{\lambda - 1} \;=\; 0.$$

After simplification, we see that $\lambda \neq 1$ is a solution of (2.3.9) if and only if

$$\left(\frac{\lambda+\alpha}{1+\alpha}\right)\lambda^k = 1. \tag{2.3.10}$$

Now, suppose $\alpha > 0$. If $|\lambda| \leq 1$ (and $\lambda \neq 1$), then $|\lambda^k| \leq 1$ and $|\lambda+\alpha| < |1+\alpha|$. Thus

$$\left|\frac{\lambda+\alpha}{1+\alpha}\right|\left|\lambda^k\right| < 1,$$

i.e. λ cannot satisfy (2.3.10). Thus for positive feedback all of the eigenvalues lie outside the unit disk and so the map is unstable at the fixed point. Further, it is not only unstable, but is repelling in all possible perturbation directions.

For the case $\alpha < 0$, suppose $|\lambda| > 1$. Write $\lambda+\alpha$ as $\lambda-(-\alpha)$. Then by the reverse triangle inequality, $|\lambda+\alpha| = |\lambda-(-\alpha)| \geq ||\lambda|-|-\alpha|| = ||\lambda|+\alpha| = |\lambda|+\alpha > 1+\alpha$. Thus we have

$$\left|\frac{\lambda+\alpha}{1+\alpha}\right|\left|\lambda^k\right| > 1,$$

and (2.3.10) is not satisfied. Also, if $|\lambda| = 1$ but $\lambda \neq 1$, then $|\lambda+\alpha| < 1+\alpha$. Therefore if $\alpha < 0$ then all the eigenvalues of A lie on the interior of the unit disc, and the map is stable.

Case 2 and Case 3: In Cases 2 and 3, the linear part of the map at the fixed point is represented by the matrix:

$$A = \begin{bmatrix} 0 & 0 & 0 & \cdots & 0 & -1 \\ 1 & 0 & 0 & \cdots & 0 & -1 \\ 0 & 1 & 0 & \cdots & 0 & -1 \\ & \vdots & & \ddots & \vdots & \vdots \\ 0 & 0 & 0 & \cdots & 0 & -1 \\ 0 & 0 & 0 & \cdots & 1 & -1 \end{bmatrix}.$$

This matrix has characteristic equation $\lambda^{k-1} + \lambda^{k-2} + ... + \lambda + 1 = 0$ whose roots all have modulus 1. Thus the map is linearly neutrally stable in both cases 2 and 3. □

The stability results for case 1 are illustrated in Figure 2.4 for $k = 2, 4, \ldots, 12$ and $\alpha = f(\frac{1}{k}) \in (-0.5, 0.5)$.

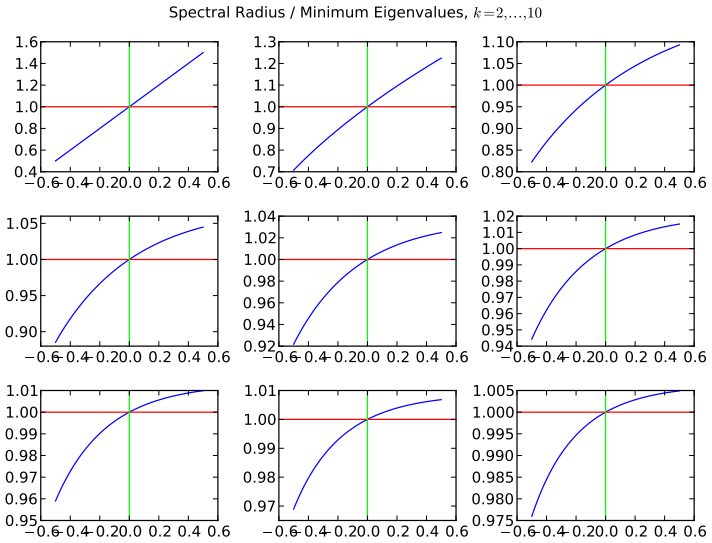

Figure 2.4: Case 1. The spectral radius / smallest eigenvalue modulus for $k = 2, 4, \ldots, 12$. The x-axis is the feedback parameter α. For negative α, the y-axis shows the spectral radius of A. For positive α, the smallest eigenvalue (w.r.t. modulus) is plotted. The plots show that the $k = M + 1$ solution is stable for negative feedback and unstable (in all directions) for positive feedback. Notice that as k grows, the stability/instability becomes weaker.

2.4 The map F near cyclic solutions

2.4.1 Single event maps

We observe in the proof of Proposition 2.3.1 that the form of F hinges on the *order of events* – a cluster's progress through the cell cycle can be described in terms of a sequence of events, such as the cluster entering R or reaching 1. Clusters progress through the cell cycle at rates specified by the equation (1.3.3). These rates remain constant until a cluster reaches s, r, or 1. We denote by e_i the event wherein a cluster reaches the milestone i, i.e. by e_r we mean that a cluster has reached the milestone r. The three events relevant to our needs are thus e_s, e_r, and e_1.

When a k-cyclic solution crosses the Poincaré section (i.e. when $x_1 = 0$), there will be some number of clusters in S and some number of clusters in R. These parameters are fixed, that is they will be the same every time the k-cyclic solution

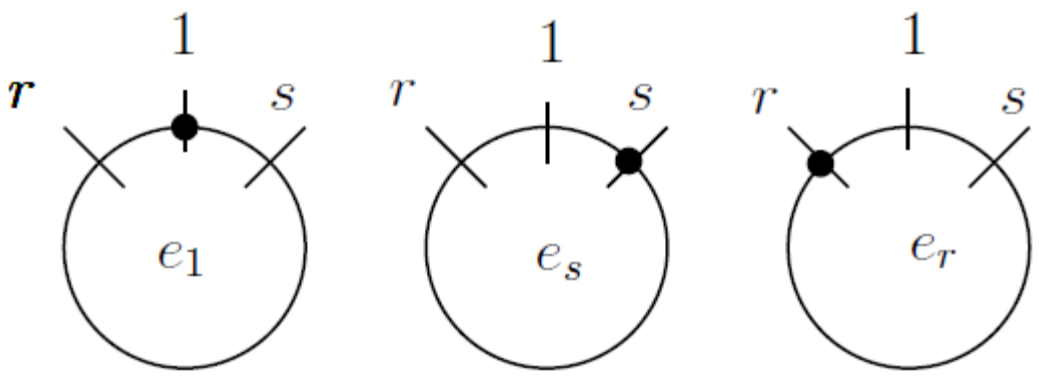

Figure 2.5: Event e_i occurs when a cluster reaches the milestone i, for $i \in \{r, s, 1\}$.

crosses the Poincaré section. We define σ to be the number of clusters in S, and ρ the number of clusters not in R, i.e. $x_\sigma < s \leq x_{\sigma+1}$ and $x_\rho < r \leq x_{\rho+1}$. Thus at the beginning of a time interval on which the map F is applied the initial positions of the k clusters will be:

$$0 = x_1 < \ldots < x_\sigma < s \leq x_{\sigma+1} < \ldots < x_\rho < r \leq x_{\rho+1} < \ldots < x_k < 1.$$

Given the current positions of the clusters, we may calculate the time elapsed until the next event occurs. It is the minimum of

$$t_s = s - x_\sigma, \quad t_r = r - x_\rho, \quad t_1 = \frac{1 - x_k}{1 + f(I)}. \tag{2.4.1}$$

For each event, we define a corresponding function on a subset of the state space:

$$e_i(\mathbf{x}) = e_i(x_1, x_2, ...x_k) = (x_1(t_i), x_2(t_i), ..., x_k(t_i)),$$

where i runs over the symbol space {s,r,1}. The domain of e_i is restricted to those $\mathbf{x}$ such that event i is the first of the three events to occur (or an event such that no other event occurs strictly before it, if events occur concurrently).

Because clusters move at constant speeds between events, $e_i(\mathbf{x})$ can be easily calculated for any $\mathbf{x}$. Each single event map is affine and has the form: $e_i(x_j) = x_j + \text{rate}_{ij} * \text{time}_i$; see Section 2.5 for a more detailed description. Note that when event

e_1 occurs, $x_k = 1 \sim 0$; we therefore introduce a fourth function, e_{re}, that re-indexes the clusters.

If we relabel after each iteration of F, then in a neighborhood of a given k-cyclic solution it is always the same cluster, x_σ, that experiences event e_s. Likewise, x_ρ experiences event e_r and x_k event e_1. If we want to emphasize that a particular cluster undergoes a certain event, we will put it in the superscript, e.g. e_s^σ.

Given parameters (s, r) and an initial condition $\mathbf{x}$ on the Poincaré section, the partial return map F essentially moves the system forward by a discrete time T, where T is the minimum time at which event e_1 occurs. The F-map is thus a composition of the maps e_s and e_r, possibly repeated or empty (for an arbitrary $\bar{x}$ on the Poincaré section; we will see momentarily that in a neighborhood of a k-cyclic solution, each map appears exactly once), followed by e_1, although we note that since the event maps are of the form $A\bar{x}+b$, where A is a $k\times k$ matrix, their composition is of the form $B\bar{x}+c$, where B is a $k \times k$ matrix. However, the first row and column of B will each consist entirely of 0's, and eliminating these gives the expected $(k-1) \times (k-1)$ matrix.

We have assumed above that all k clusters have distinct positions. Clearly we can extend the maps e_j continuously to the boundaries of this region $(x_i = x_{i+1})$. With this extension, the map F (along with reindexing e_{re}) in a continuous mapping of the coordinate simplex:

$$S = \{0 = x_1 \le x_2 \le \ldots \le x_j \le \ldots \le x_k \le 1\} \tag{2.4.2}$$

into itself.

2.4.1 Proposition. *The sequence of events followed by any k-cyclic solution under any feedback is either* $e_s, e_r, e_1, \ldots$ *or* $e_r, e_s, e_1, \ldots$

Proof. Up to relabelling (as per the event map e_{re}), the k-cyclic solution is a fixed point of the map F, and thus the intervals $[0, s)$, $[s, r)$ and $[r, 1)$ must contain the same number of clusters before and after an iteration of F. Exactly one cluster leaves $[r, 1)$ and enters

$[0, s)$ (event e_1) by the way that F is defined. To balance, one cluster must leave $[0, s)$ and one cluster must enter $[r, 1)$. In other words, events e_s and e_r must occur exactly once before or simultaneously with event e_1. □

It was observed in [6], and is reinforced throughout this thesis, that the behavior of k-cyclic solutions seems to be largely independent of the precise form of the feedback function f. From the above proposition we see that, in a neighborhood of a k-cyclic solution in the clustrered subspace, the only relevant values of the feedback function are $f(\sigma/k)$ and $f((\sigma - 1)/k)$. Thus in a neighborhood of a cyclic solution, only two values of the feedback function are relevant.

We wish to consider the map F for arrangements of clusters near the cyclic solutions using a composition of single event maps. Since the form of F will depend upon the order of events, we first partition parameter space into regions for which k-cyclic solutions have a fixed order of events.

2.4.2 Definition. *Fix k. We call a subset τ of the (s, r)-triangle* isosequential *if the k-cyclic solutions corresponding to each parameter pair in the interior of τ has the same σ and ρ and the same order of events.*

For clarity, first consider a system with no feedback. In that case the k-cyclic solution is given by initial condition $x_j = \frac{j-1}{k}$ for $1 \leq j \leq k$, irrespective of σ and ρ. If we move r and s the order of events will change whenever r or s crosses the position of a cluster. This leads to the observation that the order of events partitions the parameter triangle precisely into isosequential, regular sub-triangles. Figure 2.6 shows the simplex partitioned by event order for the cyclic solution with 3 clusters and no feedback. We will call these isosequential sub-triangles *event triangles*.

We first partition parameter space using the values of σ and ρ in the cyclic solution. For $1 \leq i \leq j \leq k$, we may select all values of r and s such that $\sigma = i$ and $\rho = j$; The corresponding subset of parameter space is given by the inequalities $\frac{i-1}{n} < s < \frac{i}{n}$ and

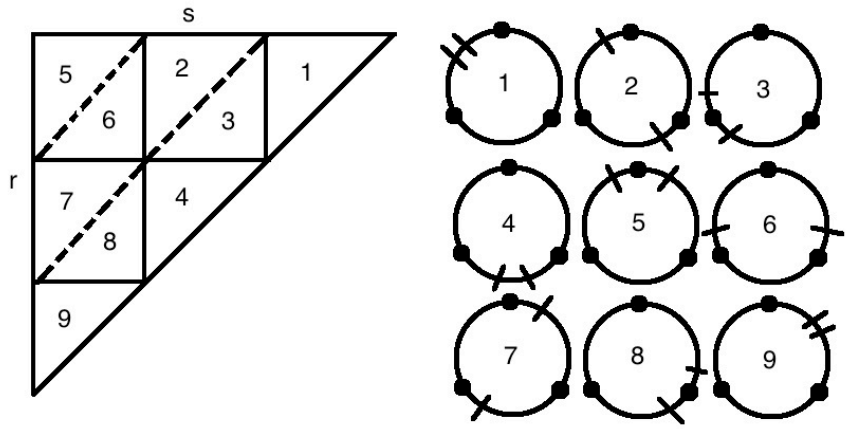

Figure 2.6: Regions of parameter space and appropriate initial conditions for a $k = 3$ cyclic solution. For example, regions 7 and 8 both begin with $x_1 \in [s, r)$ and $x_2 \in R$. In region 7 cluster x_1 reaches s before x_2 reaches r, while in region 8, x_2 reaches r before x_1 reaches s. Boundaries between the regions correspond to simultaneous events (see Section 2.4.2).

$\frac{j-1}{n} < r < \frac{j}{n}$. The two inequalities partition parameter space into quadrilaterals except when $i = j$. In that case the region defined is a triangle with the line $r = s$ forming one of its sides. In Figure 2.6, these correspond to triangles 1, 4, and 9.

Next, we refine the partition by dividing each quadrilateral into two parts depending on which event, e_s or e_r, occurs first. If $(r - x_\rho) < (s - x_\sigma)$, then event e_r happens first. If $(r - x_\rho) > (s - x_\sigma)$, then event e_s happens first. Observe that the line $r = s + (x_\rho - x_\sigma)$ intercepts the corresponding quadrilateral at two of the vertices, and thus each quadrilateral is divided into a pair of triangles. Our partition now matches the one shown in Figure 2.6. Within each triangle, ρ, σ, and the event order are fixed.

For $k = 3$, we observe $3^2 = 9$ event triangles; this reflects the general fact that parameter space will be partitioned into k^2 triangles. There are $k + (k-1) + (k-2) + ... + 1$ ways to select integers $1 \le \sigma \le \rho \le k$; of these ways k (letting $\sigma = \rho$), result in triangles. The remaining $1 + 2 + ... + k - 1$ ways yield quadrilaterals that will be divided into two triangles, and there are thus $2(1 + 2 + ... + (k - 1)) + k = k^2$ triangles in total.

The event triangles constructed in this section (without feedback) are isosequential. We will show that isosequential regions remain triangular under non-zero feedback.

2.4.2 Simultaneous points

Now we return to the model with non-zero feedback. By simultaneous points, we mean points in the (s,r) triangle for which the corresponding k-cyclic solution has events e_s, e_r, and e_1 occurring simultaneously (Thus, when the solution passes the Poincaré section, there is a cluster on s, r, and 1. Note that because 1 and 0 are associated, we do not have to explicitly require a cluster on 1, since there is a cluster on 0 by the way the section is defined. The points where only two of the three events occur simultaniously form the edges of event triangles.) The vertices of each triangular region in Figure 2.6 that fall within the interior of the (s,r)-triangle are simultaneous points. For a k-cyclic solution to lie on a simultaneous point, clusters must initially lie on the milestones r and s. See Figure 2.7.

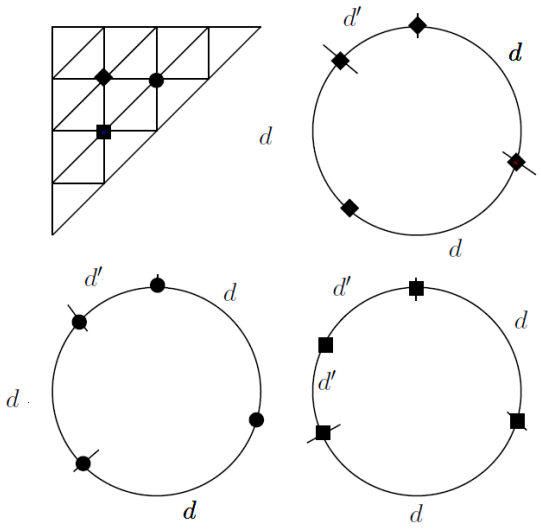

Figure 2.7: The k-cyclic solutions with clusters on all three milestones (s, r, and 1) correspond to vertices of event triangles. We illustrate with with k = 4; the clusters of the 4-cyclic solutions are designated by diamonds, circles, and squares; the corresponding symbol represents the same point on the (s,r)-triangle.

Fix integers σ and ρ with $1 \le \sigma \le \rho \le k$. It is then easy to calculate the exact values of r, s, and $\mathbf{x}$ for a cyclic solution such $x_{\sigma+1} = s$ and $x_{\rho+1} = r$. As shown above, clusters outside the responsive region are spaced by distance d and clusters inside the responsive region by another distance d'. These are the distances clusters move during one iteration of the map F. This is a property shared by arbitrary k-cyclic solutions, but in general, actually calculating the values of d and d' is complicated by the fact that the distance between x_ρ and $x_{\rho+1}$ is neither d nor d'. In this special case where $x_{\rho+1} = r$, however, it is simply d.

Since the distance around the circle is 1, we obtain the equation $\rho d + (k-\rho)d' = 1$. Clusters enter and leave the signaling region at the same time (in particular, x_k enters at the same time that x_σ leaves), and feedback is thus constant, $f(\frac{i}{n}) = \alpha_i$, so $d' = (1+\alpha_\sigma)d$. These equations have a unique solution:

$$d = \frac{1}{\rho + (k-\rho)(1+\alpha_\sigma)}, \qquad d' = \frac{1+\alpha_\sigma}{\rho + (k-\rho)(1+\alpha_\sigma)}.$$

From d we can compute r and s: $r = \rho d$ and $s = \sigma d$.

The simultaneous points on the vertical and horizontal axis are easily computed because on those axis, there is no feedback, and $x_i = (i-1)/k$. Thus the simultanious points on those axes are $(0, i/k)$ and $(i/k, 0)$ for $i = 0, 1, ..., k-1$.

On the diagonal ($r = s$, $\sigma = \rho$), the last cluster lies at $r + (k-\rho-1)e$, and $d = \frac{1-r-(k-\rho-1)e}{1+f(\rho/k)}$. From the equation $\rho d + (k-\rho)d' = 1$, we can then compute d', and hence d.

2.4.3 Convexity of domains

2.4.3 Proposition. *Fix integers σ and ρ with $1 \le \sigma \le \rho \le k$ and parameters r, s. Then the domains of the maps e_s, e_r and e_1 are convex subsets of the coordinate simplex S.*

Proof. First note that for fixed σ, the value of $\alpha_\sigma = f(\frac{\sigma}{k})$ is constant and so it is constant throughout the domain of an event map. The domain of an event map is thus defined by linear constraints and is therefore convex. □

The F-map is the composition of event maps, and event maps are continuous, affine maps with convex domains. Convexity is preserved by affine pre-images, and the following thus holds:

2.4.4 Theorem. *Fix integers σ and ρ with $1 \leq \sigma \leq \rho \leq k$ and parameters r, s. Then the map F is a continuous, piece-wise affine map. On each subdomain on which it is affine it is equal to compositions of event maps e_s and e_r followed by e_1. These affine subdomains are convex.*

For fixed σ and ρ write $E^i_{\sigma\rho}(r, s, \mathbf{x})$ for the map $(r, s, \mathbf{x}) \mapsto (r, s, e_i(\mathbf{x}))$ where $e_i(\mathbf{x})$ is applied with the parameters r and s. We restrict the domains of these functions accordingly:

$$\mathrm{dom}(E^s_{\sigma\rho}) = \{(r, s, \mathbf{x}) \in O_{\sigma\rho} : (s - x_\sigma) \leq (r - x_\rho) \text{ and } (s - x_\rho) \leq \frac{1 - x_k}{1 + \alpha}\}$$

$$\mathrm{dom}(E^r_{\sigma\rho}) = \{(r, s, \mathbf{x}) \in O_{\sigma\rho} : (r - x_\rho) \leq (s - x_\sigma) \text{ and } (r - x_\rho) \leq \frac{1 - x_k}{1 + \alpha}\},$$

$$\mathrm{dom}(E^d_{\sigma\rho}) = \{(r, s, \mathbf{x}) \in O_{\sigma\rho} : \frac{1 - x_k}{1 + \alpha} \leq (s - x_\sigma) \text{ and } \frac{1 - x_k}{1 + \alpha} \leq (r - x_\rho)\},$$

where

$$O_{\sigma\rho} = \{(r, s, \mathbf{x}) : x_j < x_{j+1}, x_\rho < r < x_{\rho+1}, x_\sigma < s < x_{\sigma+1}\}.$$

In the equations above, $O_{\sigma\rho}$ represents basic ordering assumptions.

2.4.5 Proposition. *For a fixed pair of integers σ, ρ, the domain of each $E^i_{\sigma\rho}$ is convex.*

Proof. For a fixed σ, the domain is defined by a set of linear inequalities. □

2.4.6 Definition. *We define a* generalized isosequential region *as a maximal subset I of $\Delta \times S_{k-1}$ such that for any fixed σ and ρ and any $(r, s, \mathbf{x}) \in I$ the map F applied to $\mathbf{x}$ is the same combination of event maps.*

2.4.7 Proposition. *Let $(r_i, s_i, \mathbf{x}_i)_{i=1}^m$ be a set of m points in a generalized isosequential region such that each solution x_i is cyclic. Any weighted average of these points is also cyclic solution which follows the same order of events.*

Proof. Let $\bar{F}$ denote the map $(r, s, \mathbf{x}) \mapsto (r, s, F(\mathbf{x}))$ restricted to the isosequential region. Since each x_i is cyclic $\bar{F}$ is a composition with events in the order $e_s e_r e_1$ or $e_r e_s e_1$. We argue that any weighted average $\sum_{i=1}^{m} \alpha_i (r_i, s_i, \mathbf{x}_i)$ is also a fixed point in the domain of $\bar{F}$. We assume that α_i satisfies $\sum_{i=1}^{m} \alpha_i = 1$ and $(\forall i)(\alpha_i \geq 0)$. Since $\mathrm{dom}(\bar{F})$ is convex, $\sum_{i=1}^{m} \alpha_i (r_i, s_i, \mathbf{x}_i) \in \mathrm{dom}(\bar{F})$. The map $\bar{F}$ is affine, so it can be written in the form $\bar{F} = (r, s, A\mathbf{x}+\mathbf{b})$, where A is constant, depending only on the order of events. The vector b depends on r and s, but can easily be seen from the form of the event maps to be linear in those terms, allowing us to write $\bar{F} = (r, s, A\mathbf{x} + \mathbf{k} + r\mathbf{u} + s\mathbf{v})$, where neither $\mathbf{u}$ nor $\mathbf{v}$ depend on r, s, or $\mathbf{x}$.

Now $(r, s, \mathbf{x})$ is a fixed point of F if and only if $F(\mathbf{x}) = \mathbf{x}$ for parameter values r and s. This condition can be rewritten as $(A - I)\mathbf{x} = \mathbf{b}$. Substituting $(R, S, \mathbf{Y}) = \sum_{i=1}^{m} \alpha_i (r_i, s_i, \mathbf{x}_i)$ yields

$$\begin{aligned}
&(A - I)\mathbf{Y} \\
&= (A - I) \sum_{i=1}^{m} \alpha_i x_j \\
&= \sum_{i=1}^{m} \alpha_i (A - I) x_j \\
&= \sum_{i=1}^{m} \alpha_i (-b_i).
\end{aligned}$$

Factoring the negative sign out of the summand and substituting for b_i, we continue this string of equalities,

$$\begin{aligned}
&(A - I)\mathbf{Y} \\
&= -\sum_{i=1}^{m} \alpha_i (\mathbf{k} + r_i\mathbf{u} + s_i\mathbf{v}) \\
&= -(\mathbf{k} + (\sum_{i=1}^{m} \alpha_i r_i)\mathbf{u} + (\sum_{i=1}^{m} \alpha_i s_i)\mathbf{v}) \\
&= -(\mathbf{k} + R\mathbf{u} + S\mathbf{v}) \\
&= -\mathbf{b}.
\end{aligned}$$

Thus any weighted average of fixed points is a fixed point also. □

2.4.8 Theorem. *For any feedback function and given k, each isosequential region is convex. The parameter triangle Δ is partitioned into k^2 isosequential regions which are triangles with simultaneous points at the corners.*

Proof. By its definition an isosequential region is a set of parameters values in the (s, r)-triangle such that any two parameter points in the same isoequential region define fixed points of F with the same σ and ρ and the same order of event. It follows that it is the projection onto the parameter variables of a cross section of a generalized isosequential region consisting of the fixed points of $\bar{F}$. By the above proposition the cross section is convex and thus its projection is convex.

If we fix $1 \leq \sigma \leq \rho \leq k$ and the order in which events s and r occur, there are three simultaneous points S_1, S_2, and S_3 on the boundary of the domain of the corresponding composite map. At S_1 where $x_\sigma = s$, $x_\rho = r$. At S_2 where $x_\sigma = s$, $x_{\rho+1} = r$ if event s happens first, or, where $x_{\sigma+1} = s$, $x_\rho = r$ if event r happens first. Finally, at S_3, $x_{\sigma+1} = s$, $x_{\rho+1} = r$. By the convexity of the domain of $E^s_{\sigma\rho}$ and $E^r_{\sigma\rho}$ in the parameter triangle, the sub-triangle spanned by these three points defines an order of events for the fixed point associated with any pair (s, r) in its interior. □

Thus generally isosequential regions are triangles and we refer to them as *event triangles*.

2.5 Linear algebra

We have seen that the (s, r) triangle can be partitioned into event triangles, such that if (s_1, r_1) and (s_2, r_s) fall in the same triangle, they share the same values of σ and ρ, and the same order of events. Consider such a triangle. Any k-cyclic solution in that triangle has a known σ, ρ, and order of events, and each event map that makes up F has the form given in Section 2.4.1. The Jacobian of the affine map F can be calculated as the product of the Jacobians of the individual event maps with the first column and row removed (after the product has been taken). Although the Jacobian of the general

F map can also be calculated, the algorithm for generating stability diagrams is based on the event maps; for the sake of completeness, we nevertheless include the Jacobian of F as Appendix A.3

First, we give the explicit functions of the event maps.

$$e_s(\mathbf{x})_j = x_j + \begin{cases} s - x_\sigma & \text{if } j \le \rho \\ (1+\alpha_\sigma)(s - x_\sigma), & \text{if } j > \rho, \end{cases} \qquad e_r(\mathbf{x})_j = x_j + \begin{cases} r - x_\rho & \text{if } j \le \rho \\ (1+\alpha_\sigma)(r - x_\rho), & \text{if } j > \rho, \end{cases}$$

$$e_1(\mathbf{x})_j = x_j + \begin{cases} \frac{1-x_k}{1+\alpha_\sigma} & \text{if } j \le \rho \\ (1 - x_k), & \text{if } j > \rho. \end{cases} \qquad e_{\mathrm{re}}(\mathbf{x})_j = \begin{cases} x_{j-1} & \text{if } j \ne 0 \\ x_k, & \text{if } j = 0. \end{cases}$$

Based on these, each of those Jacobians can be seen to be quite simple; in particular, both De_s and De_r have the same structure.

There are 1's along the diagonal, except for one entry. Let $j = \sigma$ for e_s and $j = \rho$ for e_r. The j-th column has -1's down the first $j-1$ rows, a 0 at the diagonal and $-(1+\alpha_{\sigma+1})$ in the rest of the rows.

$$J_{1,2} = De_{1,2} = \begin{bmatrix} 1 & 0 & \cdots & 0 & -1 & 0 & \cdots & 0 \\ 0 & 1 & \cdots & 0 & -1 & 0 & \cdots & 0 \\ \cdots & \cdots & \cdots & \cdots & \cdots & \cdots & \cdots & \cdots \\ 0 & 0 & \cdots & 1 & -1 & 0 & \cdots & 0 \\ 0 & 0 & \cdots & 0 & 0 & 0 & \cdots & 0 \\ 0 & 0 & \cdots & 0 & -(1+\alpha_\sigma) & 1 & \cdots & 0 \\ \cdots & \cdots & \cdots & \cdots & \cdots & \cdots & \cdots & \cdots \\ 0 & 0 & \cdots & 0 & -(1+\alpha_\sigma) & 0 & \cdots & 1 \end{bmatrix}. \tag{2.5.1}$$

The matrix for e_1 has the following structure:

$$J_3 = De_d = \begin{bmatrix} 1 & 0 & \cdots & 0 & 0 & 0 & \cdots & -\frac{1}{1+\alpha_\sigma} \\ 0 & 1 & \cdots & 0 & 0 & 0 & \cdots & -\frac{1}{1+\alpha_\sigma} \\ \cdots & \cdots & \cdots & \cdots & \cdots & \cdots & \cdots & \cdots \\ 0 & 0 & \cdots & 1 & 0 & 0 & \cdots & -\frac{1}{1+\alpha_\sigma} \\ 0 & 0 & \cdots & 0 & 1 & 0 & \cdots & -\frac{1}{1+\alpha_\sigma} \\ 0 & 0 & \cdots & 0 & 0 & 1 & \cdots & -1 \\ \cdots & \cdots & \cdots & \cdots & \cdots & \cdots & \cdots & \cdots \\ 0 & 0 & \cdots & 0 & 0 & 0 & \cdots & 0 \end{bmatrix}.$$

In the final column, -1 appears for rows $\rho + 1 \leq j \leq k - 1$.

All of these matrices are k by k. The row corresponding to the cluster that will experience an event will consist entirely of 0's, since the corresponding cluster is being moved to either s, r, or 1, regardless of where any of the clusters lie.

Using standard computational software, we may therefore simply calculate the Jacobian and eigenvalues associated with each event triangle.

2.6 Regions of stability and instability

We have outlined a process through which, for a fixed feedback function and a fixed k, we may efficiently and completely characterize the stability of the k-cyclic solution for any parameters s and r. The parameter triangle is partitioned into event triangles for small negative feedback. For each triangle the linear part of F is generated and its eigenvalues are calculated numerically using standard software. Each event triangle is then colored according to the linear stability of cyclic solutions associated with parameter values in its interior. If the eigenvalues of DF are all in the interior of the unit circle in $\mathbb{C}$ then the cyclic solutions are asymptopically stable and the triangle is colored blue. If at least one eigenvalues of DF is on the unit circle and the rest are inside the circle then the cyclic solutions are neutrally stable and the triangle is colored white. If at least one of the eigenvalues of DF has modulus greater than one then the

k-cyclic solutions for those parameter values are unstable and the triangle is colored red.

In this section, we will do this for a number of values of k (we have investigated all values of k between 2 and 100; we reproduce a representative sample). We note the patterns that emerge, some of them open conjectures, others theorems that we will establish in the following chapter.

2.6.1 Instability under positive feedback

The problem of the stability of k-cyclic solutions under positive feedback is largely solved. We reproduce a representative sample of stability diagrams in Figure 2.8.

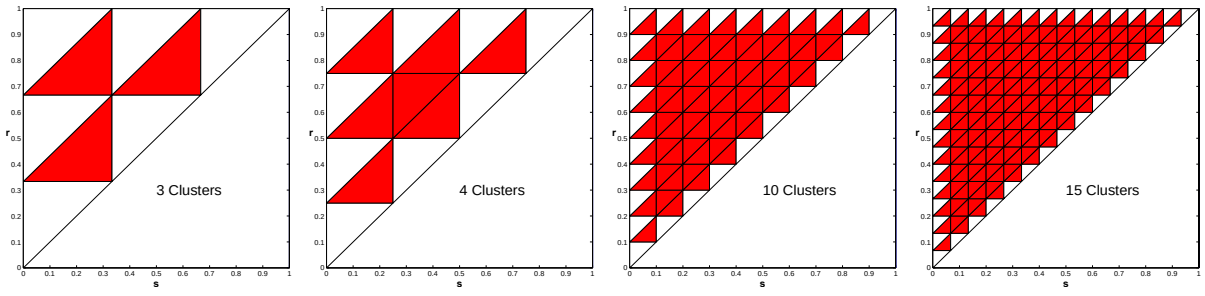

Figure 2.8: Red - Unstable; White - Neutral. Parameter regions of instability for k-cyclic clustered solutions with $k = 3, 4, 10, 15$. The picture is similar for any $k \geq 2$. There are no regions of stability for the clustered solutions with positive feedback.

We observe alternating neutrality along the edges, and instability everywhere else. The instability in the interior of parameter space has been confirmed (Theorems 3.3.3 and 3.3.4), and the neutrality along the vertical and horizontal edges is easily explained (Lemmas 3.4.2 and 3.4.3). The instability of event triangles with a vertex on the vertical or horizontal axes is more intricate, but known (see Section 3.4 of the next chapter for both the theorems and the machinary of the proofs). On the other hand, the behavior on the hypotenuse is a largely open problem. It is known (Theorem 3.4.25) that for

sufficiently strong positive feedback, the observed neutrality will be replaced with instability, but the cause of this remains unknown, and proving that neutrality occurs for weak positive feedback remains open. A detailed discussion of this case is found in Section 3.4.5.

2.6.2 Computation of event triangles and their stability under negative feedback

Under negative feedback, the patterns are more intricate, and theorems harder to come by. Figures 2.9, 2.11, 2.12, and 2.13 illustrate a wide range of k-values.

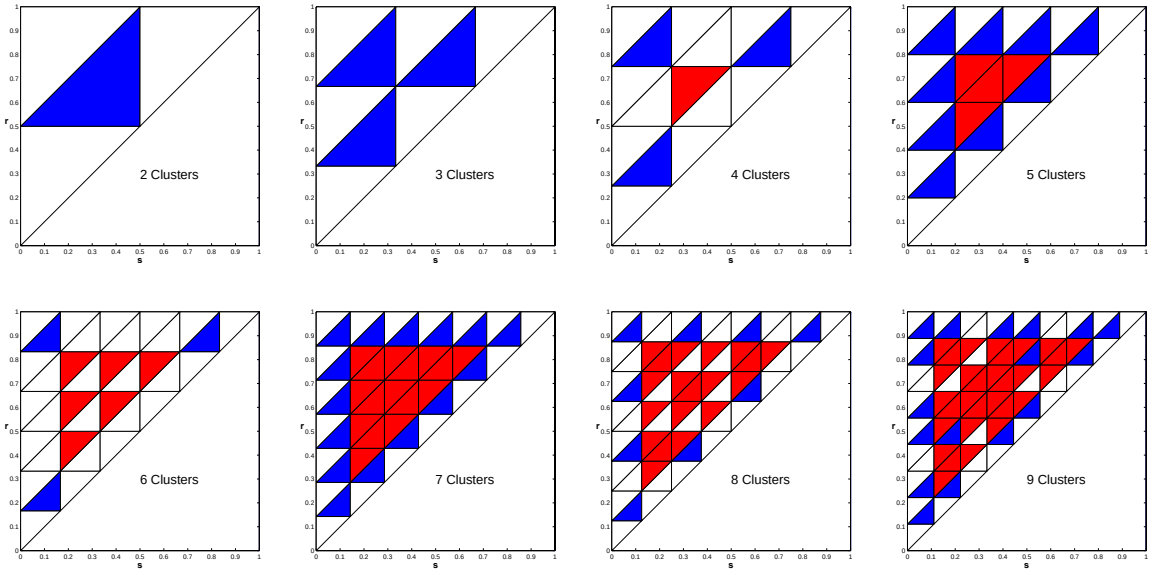

Figure 2.9: Blue - Stable; Red - Unstable; White - Neutral. Parameter regions of stability for cyclic clustered solutions with $k = 2, 3, \ldots, 9$.

In Figure 2.9 we plot the regions of stability, neutrality and instability for the cyclic solution for $k = 2$ to $k = 9$. For $k = 2$ there is a single triangle of parameter values in the triangle for which the 2-cyclic solution is stable, consistent with the analysis in Section 2.2. For $k = 3$ there are three triangles on which the 3-cyclic solution is stable. These calculations are rigorously verified in Appendix A.2. Note that from the two plots for $k = 2$ and $k = 3$ we already observe regions of bi-stability. For these parameters

there exist at least two different stable cyclic solutions and each will have some basin of attraction.

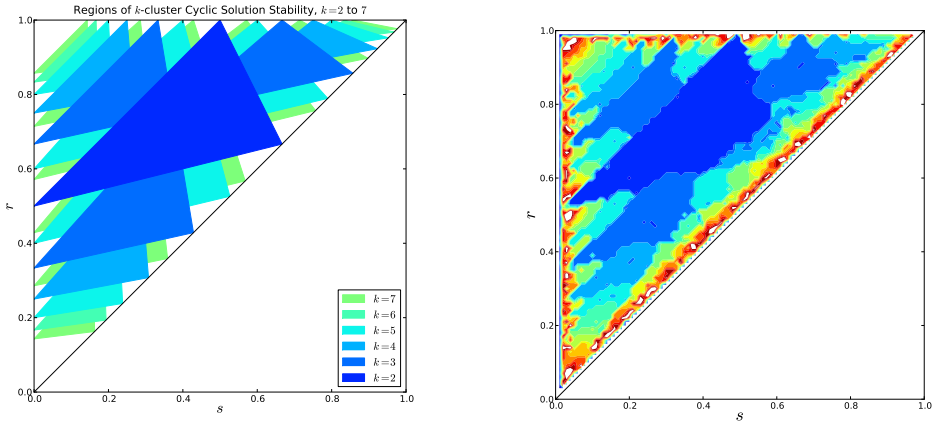

(a) (b)

Figure 2.10: (a) An overlay of regions of stability for $k = 1, \ldots, 7$. Notice that the area not covered by the stability regions are only adjacent to the edges. We conjecture that every parameter pair in the interior of the triangle is eventually covered by a stability region for some k. (b) Numbers of clusters realized in a cell cycle simulation using a mediated feedback. There is strong agreement between the two plots. In both of these plots the feedback function was $f(I) = -.6I$.

If we look at the union of the regions of stability for the first few k, we find that these regions of stability rapidly cover most of the area of the parameter triangle. In Figure 2.10, we plot the union of the regions of stability for $k = 2, \ldots, 7$. We find that the union of these regions account for 82% of the area.

Investigating Figures 2.9 and 2.11, we observe a variety of patterns in the interior space for most values of k. However, for $k = 5, 7, 11, 13$, we observe nothing but instability, with alternating neutrality on the edges. Since those numbers are all the prime numbers between 1 and 15 that have event triangles that do not intersect the boundaries of the simplex, we make the following conjecture.

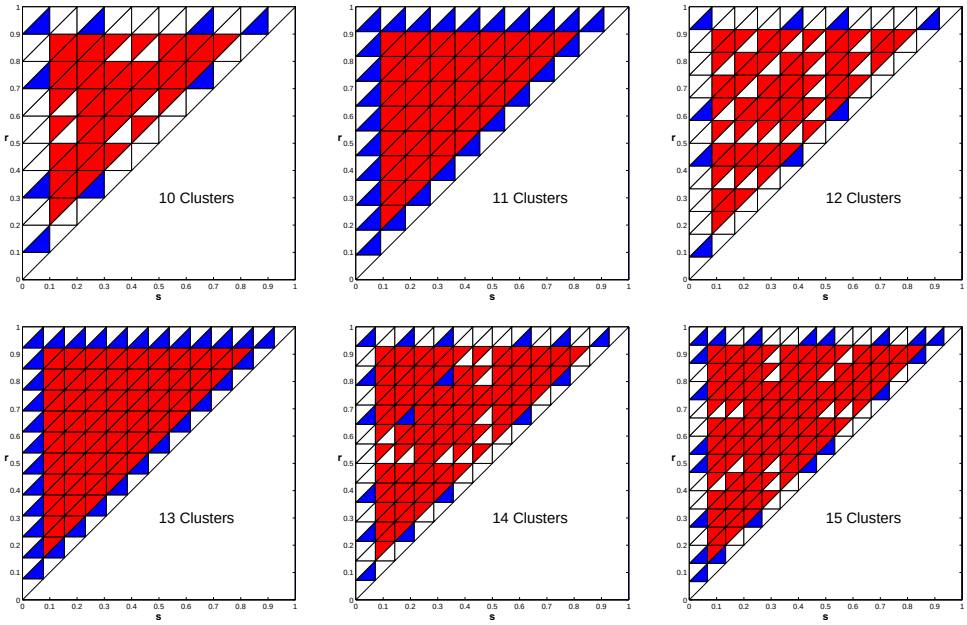

Figure 2.11: Blue - Stable; Red - Unstable; White - Neutral. Parameter regions of stability for cyclic clustered solutions with $k = 10, 11, 12, 13, 14, 15$. We recognize a distinction between prime and composite values of k.

1 Conjecture (Primality conjecture)**.** *For k prime, under negative feedback, the k-cyclic solution in any event triangle strictly in the interior of the* (s,r) *triangle. Triangles with an edge on a boundary of the simplex are neutral, while triangles with a vertex on the boundary of the simplex are stable.*

This conjecture is largely open, although the problem of the horizontal and vertical edges has been solved. We generate the stability diagram for a number of other prime numbers in Figure 2.12, observing the conjectured behavior.

In Figure 2.13 we plot the stability of each event triangles for several composite values of k. The patterns are more complex than for k prime.

From these and similar simulations, we offer the following conjectures.

2 Conjecture. *Given any pair* (s,r) *in the interior of the triangle* $0 < s < r < 1$*, there is some* $k \geq 2$ *such that the k-cyclic solution is stable for* (s,r).

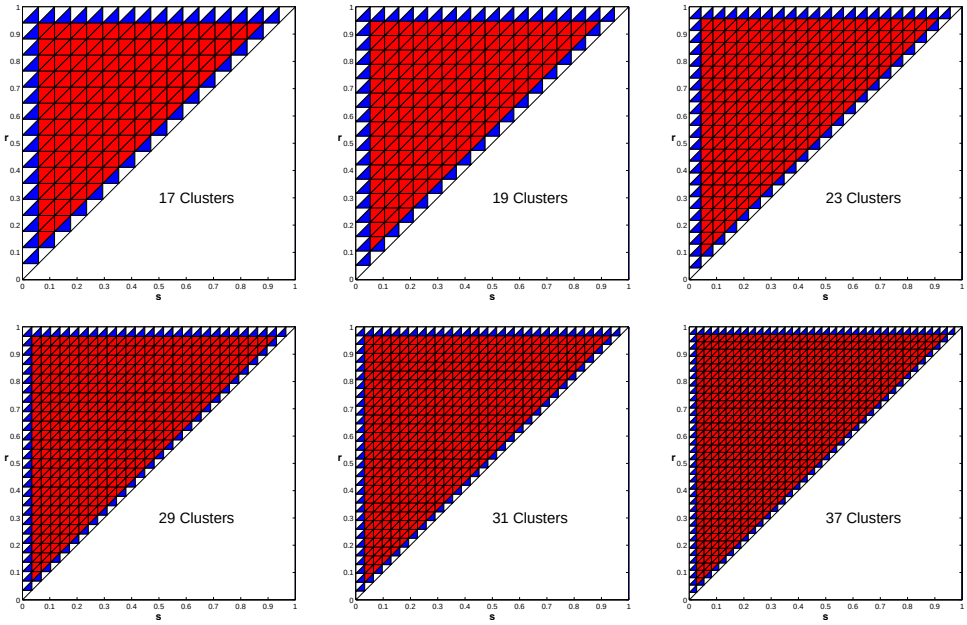

Figure 2.12: Blue - Stable; Red - Unstable; White - Neutral. Parameter regions of stability for cyclic clustered solutions for k prime, $k = 17, 19, 23, 29, 31, 37$. For all prime k we have investigated, the pattern is completely regular.

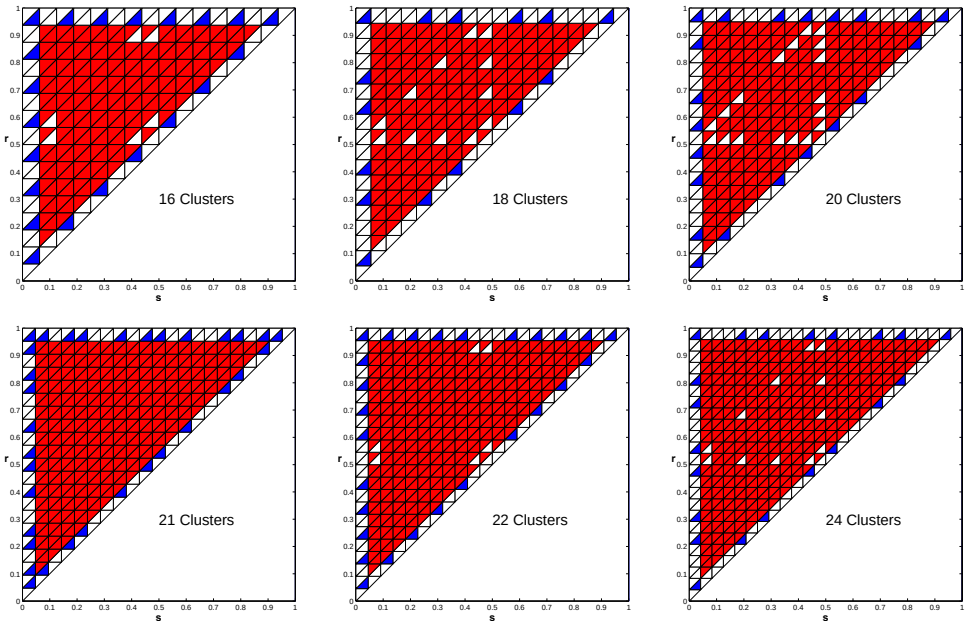

Figure 2.13: Blue - Stable; Red - Unstable; White - Neutral. Parameter regions of stability for cyclic clustered solutions for some k composite, $k = 16, 18, 20, 21, 22, 24$.

3 Conjecture. *If k is composite, triangles in the interior of the simplex are mostly unstable, but some may be neutral along the lines $r = 1/2$, $s = 1/2$ and $1 - r + s = 1/2$. As k grows large the area covered by neutral triangles goes to zero.*

If these conjectures are true, they would imply the following:

4 Conjecture (Instability conjecture)**.** *For k large, the k-cyclic solution is unstable for all except a small set of parameter values with area $O(1/k)$.*

This conjecture is relevant to the uniform solution where $k = n = O(10^{10})$. It would imply the uniform solution, which is the "steady-state" solution is unstable for practically all parameter values and any feedback. This question remains an area of active study.

5 Conjecture. *Stability diagrams are symmetric along the antidiagonal.*

These plots also help explain the seemingly anomalous patterns of Figure 1.5. In the simulation that generated that figure, we let $|S| = |R|$ and considered the number of clusters that formed as $|S| \to 1/2$. We observed that initially, increasing $|S|$ caused the number of clusters that formed to shrink, reflecting the fact that $M + 1$ decreases as $|S|$ increases; but as $|S|$ approached $1/2$, the number of clusters formed began to increase. We may now see that because $|S| = |R|$, as $|S| \to 1/2$, the (s, r)-pair approaches the $s = r$ boundary. Because the stable 2-cyclic triangle has only a vertex on that line, it becomes progressively less likely that a 2-cyclic solution near that boundary will be stable. In general, the number of stable triangles with a vertex on the $r = s$ line increases with k, and as (s, r) approaches that boundary, we observe k-cyclic solutions for larger values of k (in particular for $k = 5$ and $k = 7$, where there are large regions of stability along the $s = r$ line.)

2.7 Simulations

Finally, we consider the formation of clusters in simulation; see Figure 2.14 below. We select parameter values $(.2, .4)$ because, as we have seen from the proceeding diagrams, under negative feedback (Figure 2.9) this is a region of strong multistability. The 3-, 4-, and 5-cyclic solutions ((c), (d), and (e) respectively) are stable under modest feedback, and the 2-cyclic solution (b) is neutrally stable. The synchronous solution (a) is unstable. We also consider an initial condition of 100 equally spaced cells as a loose approxomation of the uniform solution (f), which is unstable under both positive and negative feedback for these parameter values.

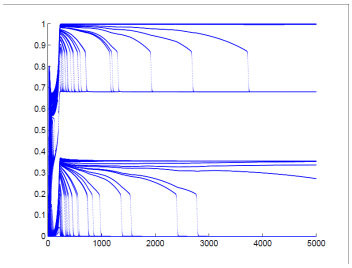

(a) A neighborhood of the 1-cyclic solution.

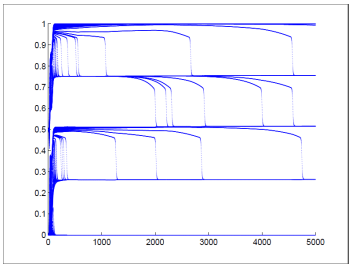

(b) A neighborhood of the 2-cyclic solution.

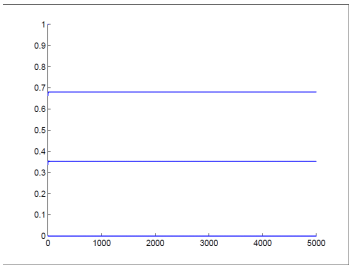

(c) A neighborhood of the 3-cyclic solution.

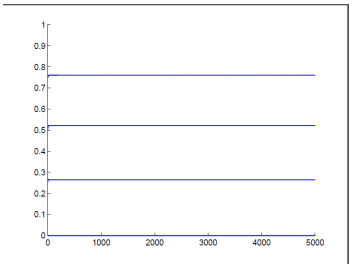

(d) A neighborhood of the 4-cyclic solution.

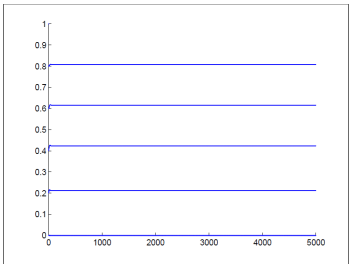

(e) A neighborhood of the 5-cyclic solution.

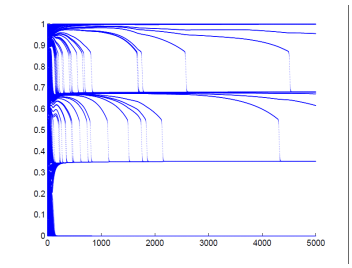

(f) A neighborhood of the uniform solution.

Figure 2.14: Various initial conditions under repeated applications of the Poincaré map with negative feedback. Here $f(I) = -.6I$, $s = .2$, and $r = .4$. For this set of parameter values the 3-, 4-, and 5-cyclic solutions are asymptotically stable. The horizontal axis represents the number of iterations of the Poincaré map, the vertical axis the unit circle.

We see that neighborhoods of the 3-, 4-, and 5-cyclic solutions converge quickly back to the stable fixed point. For an initial condition of two groups near the neutral 2-cyclic solution, each of the two groups breaks fairly neatly into two clusters, while the equally spaced cells converge quickly to a 3-cyclic solution. A neighborhood of the synchronous solution also converges to the 3-cyclic solution; $(.2, .4)$ is solidly in the interior of the stable 3-cyclic event triangle, while it is closer to the boundary of the 4-cyclic triangle, and almost on the boundary of the stable 5-cyclic triangle (observe in Figure 2.14e that x_2 lies practically at $s = .2$; in the zero feedback case, the 5-cyclic solution lies directly on the boundary of the event triangle), so it is not surprising to see initial conditions that are not close to other stable fixed points converge to the 3-cyclic solution.

In the case of positive feedback (Figure 2.15), for the same initial conditions and parameter values ($f(I) = .6I$) as in Figure 2.14, the system converges to the stable 1-cyclic fixed point in five out of six cases. The exception is when the initial condition lies in a neighborhood of the neutrally stable 2-cyclic fixed point, in which case it converges to a 2-clustered solution (although not the 2-cyclic solution).

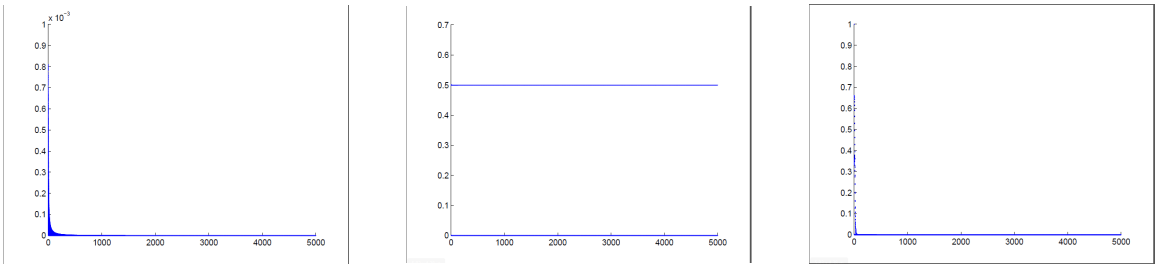

(a) A neighborhood of the 1-cyclic solution.

(b) A neighborhood of the 2-cyclic solution.

(c) A neighborhood of the 3-cyclic solution.

Figure 2.15: Various initial conditions under repeated applications of the Poincaré map with positive feedback. Here $f(I) = .6I$, $s = .2$, and $r = .4$. The vertical axis represents the unit circle, the horizontal axis time.

2.8 Conclusions and discussion

In the first part of this chapter, we showed that under arbitrary negative feedback, cyclic solutions consisting of small (but not small enough to be isolated) numbers of clusters are asymptotically stable. This is consistent with experimental observation, where small numbers of clusters are seen to form.

In the second part, we reduced the study of cyclic solutions to the study of simpler event maps. This has led to the idea of separating parameter space into isosequential regions. Our main result is that isosequential regions are sub-triangles and that the Poincaré map near the cyclic solutions for parameter values in these event triangles all have the same linearization. This has allowed us to conveniently and reliably compute both the event triangles and the stability of k-cyclic solutions for any fixed k.

For negative feedback, we observe that given a small k there are several event triangles for which the k-cyclic solution is stable. Also, given any fixed (s, r) there seems to be at least one, maybe more than one, value of k for which the k-cyclic solution is stable. A surprising observation in the negative feedback case is that the regions of stability depend on whether k is prime or composite.

The computations for positive feedback show that there are no parameter regions on which the k-cyclic solution is stable for any $2 \leq k \leq 100$. The synchronous solution appears to be the only attractor under positive feedback. We will verify this in the following chapter.

The uniform solution ($k = n$ large) appears to be unstable for most parameter values. This is in sharp contrast to previous results on cell cycle models with dispersion and without feedback [21, 22, 33]. In those studies the uniform (steady-state) solution was found to be stable. This shows that feedback is necessary to account for the clustering behavior as observed in yeast experiments. In real systems with both feedback and dispersion we expect a bifurcation curve in the feedback strength vs.

dispersion strength parameter plane. For high dispersion and low feedback, the uniform solution should be stable, whereas for high feedback and low dispersion clustered or synchronous solutions should be stable.

We note that these results are quite general. In particular, all of our results did not assume anything about the feedback function f other than it be either positive or negative. Further, we note that the coupling mechanism modeled here is more general and much closer to biological reality than classical phase oscillator models that have been widely considered.

The main implication of this chapter is that clustering type behavior, such as that in yeast autonomous oscillations require a negative feedback mechanism, whereas synchronous behavior requires a positive feedback. We note that Kilpatrick et al. [46] and Mauroy [58] have found similar results in certain neural network models.

We note that the region of stability for $k = 2$ clusters and the region where 2 clusters are realized is a triangular region with centroid at $s \approx 0.35$ and $r \approx 0.75$. We can hypothesize that since the experiment represented in Figure 1.2 shows the existence of two clusters, then the parameters s and r should be within this region and in particular are likely on the order of $s = 0.35$ and $r = 0.75$. Thus in the search for biological mechanisms involved in the yeast experiments we should expect a signaling mechanism to be active for around 35% of the cell cycle and the response mechanism to be active for around 25% of the CDC.

In the experimental data the time period in which the O_2 dilution drops is relatively narrow. It is $\approx$ 40 minutes or approximately 10% of the cell cycle (see Figure 1.2). If the drop in dissolved oxygen were the signal, then this suggests that $s \approx .1$. We see in Figure 2.10 that the r values corresponding to stability of $k = 2$ and $s = 0.1$ are quite narrow. This suggests that the drop in DO_2 is unlikely to be the primary signaling mechanism involved in the feedback.

3 Stability Results In the Partitioned Parameter Space

3.1 Introduction

In the previous chapter, we considered how we might partition the (s, r)-triangle into isosequential regions, which we saw to be triangles. Each point in a triangle corresponds to a k-cyclic solution of (1.3.3), and points in the same isosequential region share the same stability type (asymptotically stable, linearly neutral, or unstable). We continue our investigation of the stability of k-cyclic fixed points in this chapter. We prove that under positive feedback, k-cyclic solutions are overwhelmingly unstable. We investigate the behavior of stability triangles on the $s = 0$ and $r = 1$ edges of parameter space, and consider triangles on the $s = r$ line. Finally, we prove that stability in the clustered subspace implies stability in the full phase space.

For ease of reference, we reproduce (from Chapter 2) examples of the partitions under consideration (Figure 3.1 and Figure 3.2). For k and f fixed, any pair (s, r) corresponds to a k-cyclic solution with some fixed σ, ρ, and order of events. Likewise, for a fixed feedback function, any k-cyclic solution corresponds uniquely to some pair (s, r) in the parameter space. When convenient, we therefore speak of the k-cyclic solution and its corresponding (s, r) coordinate interchangeably, e.g. when we speak of a solution lying in a certain event triangle.

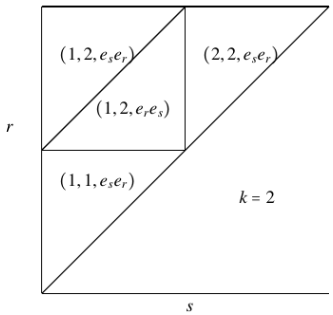

Figure 3.1: When k=2, the (s, r)-triangle is partitioned into four subtriangles. Each triangle is labeled $(\sigma, \rho, \text{order of events})$.

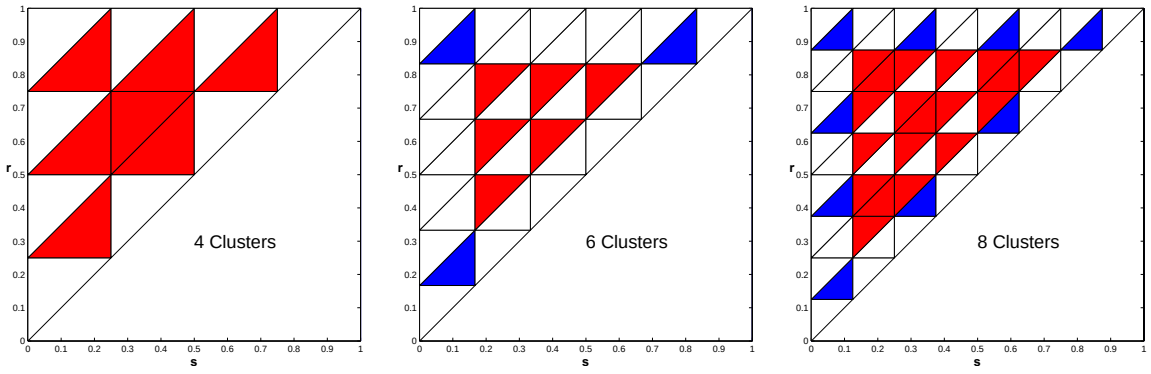

(a) $k = 4$, positive feedback. (b) $k = 6$, negative feedback. (c) $k = 8$, negative feedback.

Figure 3.2: For a fixed k, the parameter space $0 \leq s \leq r \leq 1$ is divided into k^2 triangles. Parameters in the same triangle give rise to k-cyclic solutions with identical Jacobians, and thus identical stability. The figure was generated in the limiting case where f=0, but the triangles were colored according to the stability of k-cyclic solutions in each triangle under weak positive or negative feedback. Red indicates instability of the k-cyclic solution, blue indicates stability, and white neutrality.

3.2 Small perturbations

To answer questions of the stability, we consider small perturbations of k-cyclic solutions, and then investigate the behavior of the perturbed system. We must therefore start any investigation of stability by clarifying what "small" and "perturbation" mean in this context. We consider the second question first.

There are two obvious, but distinct, ways of viewing the k-cyclic solution, where k is the number of clusters and n is the number of cells (and each cluster contains n/k cells). The first is to view it as a point on the k-dimensional simplex $x_1 \leq x_2 \leq ... \leq x_k$, where we know that the k-cyclic solution occurs in the interior of the simplex ($x_i < x_{i+1}$); this is the philosophy of Chapter 2. The second is to view it as a point on the n-dimensional simplex S_n, $c_1 \leq c_2 \leq ... \leq c_{n/k+1} \leq ... \leq c_n$, where

$$c_1 = c_2 = ... = c_{n/k} < c_{n/k+1} = c_{n/k+2} = ... < c_{(k-1)(n/k)+1} = ... = c_n. \tag{3.2.1}$$

Initially synchronized cells cannot de-synchronize under the dynamics of the system, and in the absence of noise, these two viewpoints generate identical systems. In

particular, F defines a discrete dynamical system on each simplex. Let $A \subset S_n$ be the clustered subset of the n-dimensional simplex whose coordinates satisfy (3.2.1). Then $i : S_k \mapsto A \subset S_n$, the "identity" map defined by

$$i(c_1, c_{n/k+1}, ..., c_{(k-1)(n/k)+1}) = (c_1, c_2, ..., c_{n/k+1}, ..., c_{2n/k+1}, ..., c_{(k-1)(n/k)+1}) \tag{3.2.2}$$

is a conjugacy on the maps of the system, that is to say that it is a homeomorphism from S_k to A such that $i(F(x)) = F(i(x))$ (see also Figure 3.3; in this special case, F_1 and F_2 are defined identically). However, the effect of independently perturbing each oscillator will be radically different depending on whether the domain of F is taken to be S_k or the clustered n-dimensional submanifold $A \subset S_n$. In the first case, there will still be k distinct oscillators after a small perturbation. In the second case, perturbing each oscillator will cause the clusters to de-synchronize into loose groups. We refer to the first case as a perturbation in the clustered subspace (for brevity; the "subspace" is actually a submanifold of the simplex S_n, which is itself a manifold with boundary), and to the second as a perturbation in the full phase space.

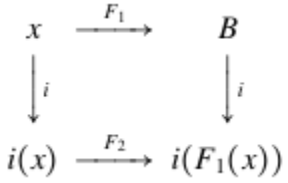

Figure 3.3: Dynamical systems defined by maps F_1 and F_2 are conjugate if there is a homeomorphism i between their state spaces such that this diagram commutes. A seemingly complicated system may sometimes be understood in terms of a more transparent conjugate system, an idea we will exploit several times in this chapter.

We now consider the question of perturbations. Let $\bar{x}$ be a k-cyclic solution on the Poincaré section. We have seen that the Poincaré map (and its factorization F) may be understood purely as a sequence of event maps indexed by symbols e^i_j, where i is a number $1 \leq i \leq k$, and j belongs to the symbol space $\{r, s, 1\}$. The symbol e^i_j encodes the information that x_i has reached j. In a neighborhood of the k-cyclic

solution, each event has a single cluster uniqely associated with it, and the superscript may be dropped. A sequence of these symbols, read left to right, defines the order of events of an F-map and a Poincaré map; we call this the event string of $\bar{x}$. For an event string to be defined in this way, it is necessary to restrict $\bar{x}$ such that distinct events do not occur simultaniously (i.e. to the interior of an event triangle), although the concept of defining F in terms of its order of events can be extended to the boundaries of event triangles. We observe that by definition, the event string of a k-cyclic solution is invariant under the Poincaré map. The event string of a k-cyclic solution is likewise invariant under F if we include in F a cyclic relabeling of coordinates (i.e. if after each iteration of F we relabel clusters in ascending order so that the number σ of clusters in S is also the subscript of the last cluster in S).

3.2.1 Definition. *Let $\bar{x}$ be a configuration of clusters on the Poincaré section. We define the event neighborhood of $\bar{x}$ to be the set of all states lying on the Poincaré section that have the same event string as $\bar{x}$. We call $\bar{y}$ an event-small perturbation of $\bar{x}$ if $\bar{y}$ is in the event neighborhood of $\bar{x}$.*

Since the definition of event strings is restricted to the interiors of event triangles, the definitions of event neighborhoods and event-small perturbations are likewise restricted. Note one motivation of this restriction: event neighborhoods are open sets in the Euclidean metric on the k-dimensional simplex, and thus for all finite-dimensional metrics generated by a p-norm. Event neighborhoods of points on the edges of event triangles, defined in the natural way, are non-open, while the event neighborhoods of vertices of event triangles would be singletons.

We have only defined an event-small perturbation in the clustered subspace. But the notion generalizes naturally to the full phase space. Let $\bar{x}$ be a point as described on the clustered submanifold embedded in the n-dimensional simplex, whose cells are initially synchronized into k clusters. After perturbing the solution in the full phase space, we define k groups, $g_i = \{c_{(i-1)/k+1}, c_{(i-1)/k+2}, ..., c_{i/k}\}$ for $1 \leq i \leq k$. Once the

cells have been perturbed, their order becomes invariant, so relabeling as necessary, we may assume without loss of generality that the cells in a group are listed in ascending order. The first and last cells of a group g_i will be of particular importance, since a group converges to a cluster if and only if the distance between them (defined below) converges to 0. We define symbols

$$\begin{aligned} c_{iF} &= \max\{c_j | c_j \in g_i\} \\ c_{iL} &= \min\{c_j | c_j \in g_i\}, \end{aligned} \tag{3.2.3}$$

where the i will be suppressed unless confusion is likely to occur. We have numbered the cells of a group in ascending order of be consistent with the numbering of clusters. An artifact of this is that c_{iF}, the first cell of g_i to undergo any event, is the last cell in the list $g_i = \{c_{(i-1)/k+1}, c_{(i-1)/k+2}, ..., c_{i/k}\}$.

3.2.2 Definition. *The diameter of a group is* $diam(g_i) = d(c_{iF}, c_{iL}) = \min\{|c_{iF} - c_{iL}|, 1 - |c_{iF} - c_{iL}|\}$.

Once a cluster has been broken into a group, the previously-defined order of events concepts can be applied without modification to the component cells of the groups. We define a group event to be an ordered pair $eg_i^j = \{e_i^{jF}, e_i^{jL}\}$, $i \in \{s, r, 1\}$, $j \in \{1, 2, ..., k\}$, and say that a group event eg_i^j occurs before a group event eg_ℓ^m if both e_i^{jF} and e_i^{jL} occur before e_ℓ^{mF} occurs.

Note that the concept of one group event happening before another can not be used to define a total order on the events; if the diameters of one or more groups is sufficiently large then for some events $i, m \in \{s, r, 1\}$, and distinct groups g_ℓ and g_j, the cells $c_{\ell F}$, c_{jF}, and $c_{\ell L}$ may undergo events $e_i^{\ell F} e_m^{jF} e_i^{\ell L}$. In other words, the first cell of g_ℓ crosses some milestone, and before the last cell of g_ℓ can do the same, the first cell of another group crosses some other milestone. In this case, neither group event is said to happen before the other. However, where group events are comparable, we may define their event string in the natural way.

Let $\bar{x}$ be a k-clustered solution on the n-dimensional simplex, as described by (3.2.1), i.e. $\bar{x} \in A$. Note that the function (3.2.2) is one-to-one. Its inverse takes a clustered configuration in S_n and maps it to a configuration in S_k. Let $\bar{x} \in A$. Define a k-dimensional representative point $\bar{y} = i^{-1}(\bar{x})$. We must do this to speak of the event string of $\bar{x}$ because $\bar{x}$ is not in the interior of the n-dimensional simplex. Then we generalize the concept of event-small perturbations to the full phase space as follows.

3.2.3 Definition. *Let $\bar{x} \in S_n$ have a representative point $\bar{y} \in S_k$, and let the Poincaré map of $\bar{y}$ have an event string $e_{i_1}^{j_1} e_{i_2}^{j_2} \dots e_{i_m}^{j_m}$. Then a perturbation of $\bar{x}$ in the full phase space is said to be event-small if the resultant groups have the same event string $eg_{i_1}^{j_1} eg_{i_2}^{j_2} \dots eg_{i_m}^{j_m}$. The collection of event-small perturbations is the event neighborhood of $\bar{x}$.*

Again, we restrict our attention to those cases where $\bar{x}$ lies in the interior of an event triangle, and the event neighborhood is an open set in any finite-dimensional metric generated by a p-norm. We always consider "small" perturbations to be event-small, in clustered subspace or in the full space, when considering stability.

3.2.1 Divisions of parameter space

Throughout this chapter, we will classify the stability of k-cyclic solutions based on which event triangle they fall into. We consider two natural ways that event triangles may be classified.

We have seen one method of classification. A k-cyclic solution can only have one of two orders of events (Proposition 2.4.1 of Chapter 3): $e_r e_s e_1$ or $e_s e_r e_1$. Every event triangle may thus be classified by its order of events.

Another method of classification comes from the observation that when event triangles have an edge or boundary on the edge of parameter space (i.e. on the lines $r = 1$, $s = 0$, and $s = r$), that sharply restricts the complexity of the k-cyclic solution, since it implies that either $\sigma = 1$ (an edge or vertex on $s = 0$), $\rho = k$ (an edge or vertex on $r = 1$), or $\sigma = \rho$ (an edge or vertex on $s = r$), and thus eliminates one of the two

parameters that control the form of the solution. We therefore define an event triangle to be a boundary triangle if it has an edge or vertex on the lines $s = 0$, $r = 1$, or $s = r$, and an interior triangle otherwise.

These two methods of classification are summarized in Figure 3.4.

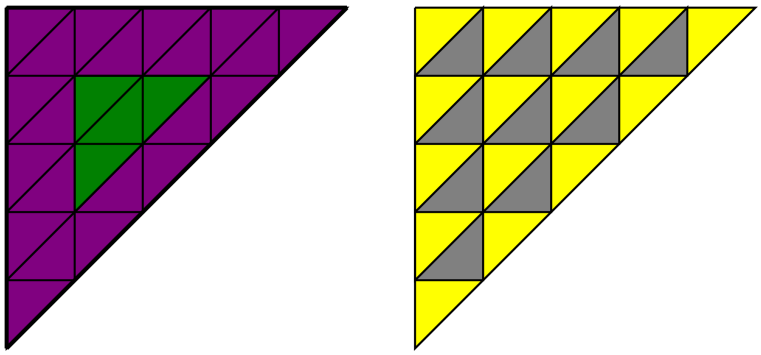

Figure 3.4: We classify each event triangle in two ways. In the left-hand figure, triangles are classified as either interior (green) or boundary (purple). On the right, triangles are classified according to order of events; yellow triangles have event strings $e_s e_r$, while grey triangles have order of events $e_r e_s$.

3.2.2 Order of event results

We start with a number of results that are true for both interior and boundary triangles. We note that if $k = 1$, Lemma 3.2.7 and Corollary 3.2.9 are alternative proofs of the (already known) facts that the synchronous solution is unstable under negative feedback and stable under positive feedback. Having made that observation, we will assume that $k > 1$ for the remainder of the section.

3.2.4 Lemma. *Consider a negative-feedback system. Let $\bar{x}$ be any k-cyclic solution such that x_ρ enters R before x_σ leaves S, i.e. assume $\bar{x}$ has event chain $e_r e_s$. Let $\bar{y}$ be any event-small perturbation of $\bar{x}$ in the full phase space. Then after the application of a single Poincaré map, the diameters of each group of $\bar{y}$ will contract uniformly. In other words,*

for each i, diam$(g_i(T)) \leq c \cdot diam(g_i(0))$ *where T is the Poincaré return time and* $c < 1$ *is independent of i.*

Proof. Let $\bar{x}$ be a k-cyclic solution that has the order of events $e_r e_s$. Let g be a group in the (full phase) event neighborhood of $\bar{x}$. From time $t = 0$ to time $t = T$, where T is the return time of the Poincaré map, the diameter of the group will change twice, when it enters R and when it leaves R.

We select an arbitrary group g of diameter ϵ. Let c_F be its first cell, c_L the final cell of that group. Then from the time c_F enters R until the time c_L enters R, the diameter ϵ is contracted to $(1 + f(\sigma/k))\epsilon$, since there are σ groups in S. The diameter will not change again until c_F reaches 1, before which time one group has left S. As the cells of g begin to enter S, the feedback on the cells of g still in R increases, but the proportion of cells exerting feedback is always strictly less than $\frac{\sigma}{k}$; an explicit upper bound is $\alpha = \frac{(\sigma)(n/k)-1}{n} < \frac{\sigma(n/k)}{n} = \frac{\sigma}{k}$.

Thus, although negative feedback now begins to pull the solution away from the clustered subspace (i.e. the cells spread out as they enter S), by the time g has entirely entered S, its diameter is no more than $\frac{1+f(\sigma/k)}{1+f(\alpha)}\epsilon$. Since feedback is monotone and f is negative, the denominator of the coefficient is less than the numerator, and this is a contraction of the diameter. Since the upper bound of α is uniform, every group experiences a contraction of at least that degree. □

The proof of the following lemma is essentially identical.

3.2.5 Lemma. *Consider a positive-feedback system. Let* $\bar{x}$ *be any k-cyclic solution with order of events* $e_r e_s$*, and let* $\bar{y}$ *be any event-small perturbation of* $\bar{x}$ *in the full phase space. Then the diameters of each group will expand uniformly over the course of a single Poincaré map, i.e. for each i,* $diam(g_i(T)) \geq c \cdot diam(g_i(0))$ *where T is the Poincaré return time and* $c > 1$ *is independent of i.*

Proof. A group of diameter ϵ that enters R while σ cells are in S is expanded to a diameter of $(1 + f(\sigma/k))\epsilon$. Its diameter will then remain constant until it enters S. At this time, it will start to contract, but there are strictly fewer cells in S, no more than $\alpha = \frac{(\sigma)(n/k)-1}{n} < \frac{\sigma}{k}$. Thus after the group has passed completely into S, its diameter is no less than $\frac{1+f(\sigma/k)}{1+f(\alpha)}\epsilon$, and since the feedback function is positive and monotone, the numerator of that fraction is strictly greater than the diameter. □

Note that Lemma 3.2.4, taken by itself, is fairly weak; it gains significance when the k-cyclic fixed point is stable in the submanifold (Theorem 3.5.1). On the other hand, since a necessary condition for stability is that a solution remain in an ϵ-small neighborhood of the fixed point, Lemma 3.2.5 has the following corollary.

3.2.6 Corollary. *Consider a positive-feedback system. Let $\bar{x}$ be any k-cyclic solution with order of events $e_r e_s$ (x_ρ enters R before x_σ leaves S). Then $\bar{x}$ is unstable in the full phase space.*

In the order of events $e_r e_s$ of the previous two lemmas, groups entering R experience the full feedback of σ groups, and groups entering S experience strictly less feedback. If we reverse the order of events, this effect is reversed, and the previous results likewise are reversed.

3.2.7 Lemma. *Consider a negative-feedback system. Let $\bar{x}$ be any k-cyclic solution governed by the event string $e_s e_r$, and let $\bar{y}$ be any event-small perturbation of $\bar{x}$ in the full phase space. Then over the Poincaré return time T, the diameters of each group will expand uniformly, as in Lemma 3.2.5.*

Proof. As a group of diameter ϵ passes into R, there are $\sigma - 1$ clusters in S, and thus $\epsilon \to \frac{\epsilon}{1+f((\sigma-1)/k)}$. The diameter will not change again until the group leaves R. When that happens, there will be $\sigma - 1$ clusters in S, but the first cell of the group will be exerting feedback on the last cell of the group. From the time the first cell of the group enters R to the time the last cell enters R, the last cell will travel a distance of $\frac{\epsilon}{1+f((\sigma-1)/k)}$ at a

(variable) rate bounded above by $1 + \alpha < 1 + f((\sigma - 1)/k)$. Thus the final diameter of the group is greater than $\frac{\frac{\epsilon}{1+f((\sigma-1)/k)}}{1+\alpha}$, which is greater than ϵ. □

3.2.8 Lemma. *Let $\bar{x}$ and $\bar{y}$ be as in Lemma 3.2.7 (with event string $e_s e_r$) in a positive feedback system. Then over the course of a single Poincaré map, the diameters of each group will contract uniformly, in the sense of Lemma 3.2.4.*

Proof. When a group enters R its diameter expands to $\frac{\epsilon}{1+f((\sigma-1)/k)}$. When it leaves S, there are $\sigma - 1$ clusters in S, together with cells of the group, and the rate of the last cell is therefore bounded below by some rate $1 + \alpha > 1 + f((\sigma - 1)/k)$, and the final diameter of the group is bounded above by $\frac{1+f((\sigma-1)/k)}{1+\alpha}\epsilon < \epsilon$. □

3.2.9 Corollary. *Consider a negative-feedback system. Let $\bar{x}$ be any k-cyclic solution such that x_ρ enters R after x_σ leaves S (event string $e_s e_r$). Then $\bar{x}$ is unstable in the full phase space.*

The case of isolated groups (i.e., a configuration of groups such that when any cells of one group lie in R, only cells of that same group can lie in S) are a special case of the $e_s e_r$ order of events, and we demonstrate Lemmas 3.2.7 and 3.2.8 in simulations. If $s = .2$ and $r = .8$, then $x_2 = .5$ (on the Poincaré section) undergoes order of events $e_s e_r$. Under negative feedback, this fixed point is unstable in the full phase space (Corollary 3.2.9). Under positive feedback, on the other hand, event-small perturbations collapse back the the clustered submanifold; it is only when the groups grow large enough in diameter that they begin to influence on another, and Lemma 3.2.7 no longer applies, that the trajectory of the system can exhibit different behavior, in this case converging to the 1-cyclic solution.

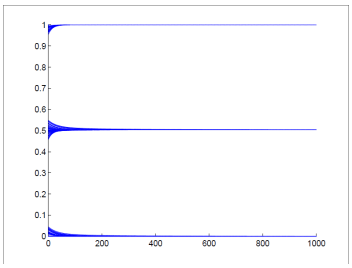

(a) α = .05

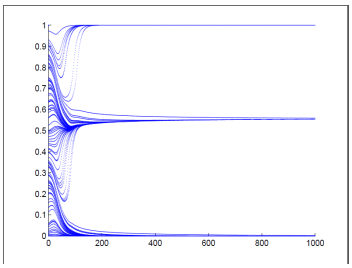

(b) α = .26

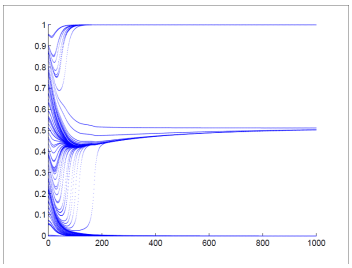

(c) α = .27

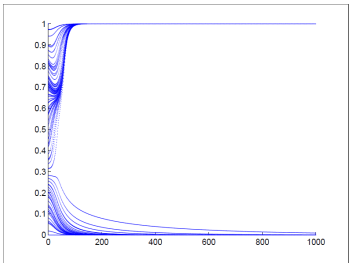

(d) α = .28

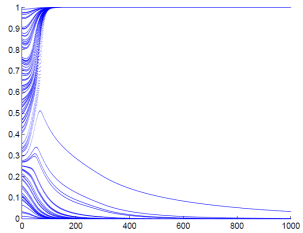

(e) α = .29

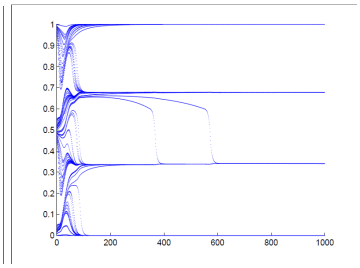

(f) α = .05 under negative feedback.

Figure 3.5: From an initial condition in a neighborhood of the isolated, neutral 2-cyclic solution, we consider the state of the system (i.e. the location of cells on the unit circle, represented by the vertical axis) as a function of the number of iterations of the Poincaré map (the horizontal axis). There are 100 cells in total, spread uniformly in α-balls around x_1=0 and x_2=.5. Figures (a)-(e) represent positive feedback of strength $f(I)$=.2I. We see that the previous lemmas continue to apply outside the realm of the hypothesis, i.e. it does not effect the stability of the system if there is still one cell of g_1 in S when g_2 begins to enter R. Nevertheless, the transition from convergence to isolated, neutral 2-clustered solutions under positive feedback to convergence to the synchronous solution is fairly abrupt. The instability under negative feedback ($f(I) = -.6I$) is seen in (f).

3.3 Results in the interior of parameter space

We now turn our attention to interior event triangles. In all the results of this section, we assume implicitly that the event triangle under consideration is an interior event triangle. A consequence of this is that $k > 2$, since for $k \leq 2$, all event triangles are boundary triangles.

The order of events sharply limits where asymptotic stability can occur in the clustered subspace, for either positive or negative feedback. We have seen

(Corollary 3.2.9) that one order of events implies instability of the k-cyclic solution under negative feedback in the full phase space. We will now see that this order of events always implies instability in the clustered subspace. We start by noting that it cannot imply stability.

3.3.1 Lemma. *For any order of event triangle where x_ρ enters R after x_σ leaves S $(e_s e_r)$, the k-cyclic solution is not exponentially attracting in the clustered submanifold, under either positive or negative feedback, i.e. it cannot have all eigenvalues strictly inside the unit disk.*

We introduce a minor change of variables that will simplify this and later calculations. In a neighborhood of the k-cyclic solution, any cluster in R always experiences feedback from either σ or $\sigma - 1$ clusters. Thus the feedback $f((\sigma - 1)/k)$ is in some sense "background feedback" that can be thought of as existing independently of the location of the clusters. If we rescale the system, in particular by allowing division to occur at some number other than 1 and appropriately increasing or decreasing the size of R so that a cluster, influenced solely by the background feedback, takes R time units to traverse R, we may eliminate that feedback. Thus we can think of a cluster in R as experiencing feedback only when a full set of σ clusters are in S. This change of variables, stated as a function $V : I \to [0, r + \frac{1-r}{1+f((\sigma-1)/k)}]$ is given by the piecewise affine map

$$V(x) = \begin{cases} x & \text{if } 0 \le x \le r \\ r + \frac{x-r}{1+f((\sigma-1)/k)} & \text{if } r < x \le 1. \end{cases} \tag{3.3.1}$$

This function V is a homeomorphism from S^1 onto itself, and when $\bar{x}$ is sufficiently close to the k-cyclic solution,

$$\tilde{V} : (x_1 < x_2 < ... < x_k) \to (V(x_1) < V(x_2) < ... < V(x_k)),$$

defines a topological conjugacy ($\tilde{V}$ serves the role of i in Figure 3.3, where F again serves as the map for both discrete dynamical system). Note that this defines a change

of variables locally, in an event-small neighborhood of $\bar{x}$. Once a solution moves sufficiently far from the k-cyclic solution, clusters may be in R while fewer than $\sigma - 1$ clusters are in S, and the change of variables it is no longer appropriate. However, since we are considering only local stability, a piece-wise smooth coordinate change in a neighborhood of the k-cyclic solution will not alter the dynamics being analyzed. This helps explain the observation, made in [6] and throughout this thesis, that the exact form of the feedback function seems to have a minimal influence on the system, since locally to any cyclic solution, the feedback function can be treated as linear.

Proof of Lemma 3.3.1. Consider the Jacobian of the F-map of the k-cyclic solution, and the characteristic polynomial it defines. The Jacobian is extremely sparse. Scaling away the background feedback as described, we find that the rows corresponding to clusters in R (the $(\rho + 1)$'st row to the $(k - 1)$'st row) have a 1 on the semi-diagonal and -1 in the last column. Rows corresponding to clusters not in R have -1's down the last column as well, and a 1 in the semi-diagonal as well; the only difference is that they also have a $\beta = f(\sigma/k)$ term down the column corresponding to x_σ (which is the $(\sigma - 1)$'st column), and there is a $1 + \beta$ term where the semidiagonal meets that column. The β terms below the $1 + \beta$ entry in the $(\sigma - 1)$'st column extend down to the ρ'th row (thus in the special case that $\sigma = \rho$ they are absent, which will account for the restriction that $\sigma \neq \rho$ in Lemma 3.3.2). The matrix can be derived from the matrix DF_{sr} of Appendix A.3 by letting $f((\sigma - 1)/k) = 0$.

$$J_{sr} = \begin{pmatrix} 0 & 0 & 0 & \dots & \beta & 0 & \dots & 0 & 0 & -1 \\ 1 & 0 & 0 & \dots & \beta & 0 & \dots & 0 & 0 & -1 \\ 0 & 1 & 0 & \dots & \beta & 0 & \dots & 0 & 0 & -1 \\ \dots & \dots & \dots & \dots & \dots & \dots & \dots & \dots & \dots & \dots \\ 0 & 0 & 0 & \dots & 1+\beta & 0 & \dots & 0 & 0 & -1 \\ 0 & 0 & 0 & \dots & \beta & 1 & \dots & 0 & 0 & -1 \\ \dots & \dots & \dots & \dots & \dots & \dots & \dots & \dots & \dots & \dots \\ \dots & \dots & \dots & \dots & \dots & \dots & \dots & \dots & \dots & \dots \\ 0 & 0 & 0 & \dots & 0 & 0 & \dots & 1 & 0 & -1 \\ 0 & 0 & 0 & \dots & 0 & 0 & \dots & 0 & 1 & -1 \end{pmatrix}$$

Because J only has two columns with more than a single non-zero element in them, and all the columns with a single non-zero element have 1 as that element, computing the determinant of J is an elementary exercise. We select a column with a single element, and expand along it to compute $\det J = \pm 1 \det J'$, where J' has the same sparcity properties as J. Repeating this process, we arrive at $\det J = \pm 1 \cdot \begin{vmatrix} \beta & -1 \\ 1+\beta & -1 \end{vmatrix} = \pm 1$. We recall that the constant term of the characteristic polynomial of J is $(-1)^{k-1} \det(J) = \pm 1$, while the leading coefficient is 1.

If all the roots of a discrete system are inside the unit circle, then the constant term of the characteristic polynomial must be less in absolute value than the leading term; this is often stated as part of the Jury Criterion. It is not the case here, as the leading and constants terms are both 1 in absolute value. As an alternative argument, we observe that since the absolute value of the determinant is 1, and the determinant is the product of the eigenvalues, the eigenvalues cannot all have modulus less than 1. □

We now prove that, in fact, these solutions are unstable. We will do this through investigation of the characteristic polynomial.

3.3.2 Lemma. *If $\bar{x}$ is a k-cyclic solution with order of events $e_s e_r$ and $\sigma \neq \rho$, the linear term of the characteristic polynomial of the Jacobian of F is an integer.*

Proof. The linear term of the characteristic polynomial is the sum of the determinants of the submatrices formed by removing row i and column i for $i = 1, 2, ..., k$ (i.e. the sum of the determinants of the principle minors). It is easily seen, from the sparsity of the matrix, that each of these determinants is either ± 1 or 0, and their sum is thus an integer.

The requirement that $\sigma \neq \rho$ is necessary for the determinant of the submatrix formed by removing the σ'th row (and thus the σ'th column) to be ± 1. If $\sigma = \rho$ then by pivoting down the first $\sigma - 2$ (sparse, containing only a single non-zero term) columns, the determinant of that submatrix is calculated to be $\pm 1 \det K$, where K has a column that consists entirely of 0's, except for one nonzero entry of β, introducing this (presumably non-integer) term into the sum. If $\rho > \sigma$, repeatedly pivoting down sparse columns will not cause that column to become sparse, and the determinant of that minor is $\pm 1 \cdot \begin{vmatrix} \beta & -1 \\ 1+\beta & -1 \end{vmatrix} = \pm 1.$ □

This lemma gains it significance from three facts. First, the trace of the Jacobian can be easily seen by studying the matrix to be $-1 + \beta$, which, in general, is not an integer. More formally, we have noted that by scaling away "background" feedback, a feedback function in a neighborhood of a k-cyclic solution may be defined entirely in terms of a single positive number, $f(\sigma/k)$, which takes its values over $(-1, \infty)$. For only a discrete subset of the real numbers (the integers) is $-1 + f(\sigma/k)$ an integer. Thus, for any feedback function f outside of the exceptional set of functions that take integer values on some rational number, $-1 + f(\sigma/k)$ is not an integer. For negative feedback, $-1 + \beta$ is never an integer, since $\beta \in (-1, 0)$.

Second, the trace (up to sign) is the coefficient of the $k - 2$ term of the $(k - 1)$-degree characteristic polynomial of the Jacobian. In other words, outside of a discrete

set, the characteristic polynomial is $p(x) = x^{k-1} + c_{k-2}x^{k-2} + ... + c_1x^1 + c_0$, where (because one of them is an integer, and the other is not) $|c_{k-2}| \neq |c_1|$.

Third, it is necessary (although not sufficient) [17] for polynomials with real coefficients, all of whose roots lie on the unit circle, to be symmetric or anti-symmetric. That is, for either $\alpha_{k-i} = \alpha_i$ for $i = 0, 1, ..., k$, or $\alpha_{k-i} = -\alpha_i$ for $i = 0, 1, ..., k$, where α_i is the coefficient of x^i. We have just seen that in any interior event triangle with order of events e_se_r, the characteristic polynomial of the Jacobian of the fixed point cannot be symmetric or anti-symmetric under negative feedback, and can only be symmetric under positive feedback for some discrete set of values of $f(\sigma/k)$. If the product of the eigenvalues is 1, as we have seen, and all of the eigenvalues do not lie on the unit circle, then some roots lie inside the unit circle, and some roots lie outside the unit circle. We have thus proved the following major result.

3.3.3 Theorem. *Consider a k-cyclic solution $\bar{x}$ in the interior of event space with order of events e_se_r. For any negative feedback function, $\bar{x}$ is unstable in the clustered submanifold. For any given positive feedback function that does not take integer values on rational numbers, $\bar{x}$ is unstable in the interior of event space in the clustered subspace.*

We believe that the conclusion of this theorem is true for all positive feedback functions; the requirement that $-1 + \beta \notin \mathbb{N}$ is a technical requirement that allows the proof to pass through, but we have not found examples where violating that restriction results in neutrality. For a fixed k the restriction that the feedback function does not take integer values on rational arguments could be weakened considerably, to say that the function must not take integer values between $-k$ and k on arguments i/k for $i = 0, 1, ..., k - 1$.

The form of the proof shows that in the interior of event space, under this order of events, some eigenvalues of the Jacobian lie inside the unit circle, and others lie outside of it. Thus the k-cyclic fixed point is a saddle; this is a weaker instability than

the $k = M + 1$ case, where all eigenvalues lie outside the unit circle, and the fixed point is therefore a source.

Every interior event triangle (in fact, every event triangle) has one of two orders of events. We have seen that one order of events, $e_s e_r$, yields instability under both positive and negative feedback. We now consider the other order of events, $e_r e_s$. Under positive feedback, these event triangles are also unstable.

3.3.4 Theorem. *For any order of event triangle where x_ρ enters R before x_σ leaves S, the k-cyclic solution is unstable for positive feedback in the clustered submanifold.*

Proof. Again, the Jacobian is extremely sparse. In fact, the Jacobian in this case is identical to the Jacobian of the last case, with the exception of one entry: $J(\rho, \rho - 1) = 1 + \beta$. That is the only non-zero entry in the $(\rho - 1)$'th column, and if one expands down that column, one finds that $\det J = \pm(1 + \beta) \det J'$, where, since expanding down that column removes the only point of difference, J' has the same form as the Jacobian from the proof of Lemma 3.3.1 (the reader is again referred to Appendix A.3 of the previous chapter for a detailed derivation). Thus the determinant is $\pm(1 + \beta)$. Since the modulus of the determinant is the product of the moduli of the eigenvalues, at least one eigenvalue has modulus at least $1 + \beta > 1$. □

This proof cannot be generalized to negative feedback, and in fact, we do not always observe instability in the interior of event space under negative feedback (e.g. $k = 8$; see Figure 3.1). Note that since the constant term of the characteristic polynomial, $1 + \beta$, is different from the leading term 1, when neutrality occurs under negative feedback, it means that some, perhaps most, of the eigenvalues are inside the unit circle. Thus such neutral fixed points are attracting in some directions. Contrast this to neutral fixed points on the edge of parameter space, all of whose eigenvalues have modulus 1.

Since Theorems 3.3.3 and 3.3.4 cover both possible orders of events, the following result for positive feedback is reached.

3.3.5 Corollary. *For a fixed feedback function that satisfies the technical restrictions outlined in Theorem 3.3.3, the k-cyclic solution is unstable (in the clustered subspace, and thus also in the full phase space) under positive feedback.*

We recall the restriction that $k > 1$. The 1-cyclic (synchronous) solution has already been seen to be stable in the full phase space under positive feedback, and unstable under negative feedback. We will see in the next section that for $k > 1$, event triangles on the edge of parameter space are not asymptotically stable under positive feedback (they may be neutral). This, together with Corollary 3.3.5, implies that the 1-cyclic solution is the only stable k-cyclic solution under positive feedback.

However, one should take care not to read more into this result than it actually implies. Consider the 2-cyclic solution under positive feedback for $s = .2$ and $r = .8$. The 2-cyclic solution is defined by $x_2 = .5$, and it is neutrally stable, due to the isolation of the clusters (see Figure 3.5). Now consider an event-small perturbation of the 2-cyclic solution in the full phase space. The groups will remain isolated from each other (Proposition 1.5.1), and thus the diameters of both groups will converge to 0 (Lemma 3.2.8). Thus although this perturbation need not converge back to the 2-cyclic solution (a fixed point of F), it converges back to a 2-clustered solution ϵ-close to the 2-cyclic solution, where ϵ depends on the size of the initial perturbation. We have seen such clusters form in simulations (Figure 1.5), and know that the set of strictly isolated, clustered solutions is locally asymptotically stable under positive feedback (Proposition 1.5.3).

3.4 Specialized results along the edge of parameter space

3.4.1 Introduction and a summary of previous results

We now turn our attention to the edges of parameter space. We reiterate that by the edge of parameter space we are referring not to the topological boundary of the triangle formed by the lines $s = 0$, $r = 1$, and $r = s$, but to event triangles that have a boundary or vertex on one of those lines. On the other hand, the interior of an event triangle is its topological interior, and all the theorems that follow apply only for k-cyclic solutions in that interior. Context should prevent any confusion.

In this section, we will accomplish two aims. First, we will examine the stability of event triangles that have a vertex, but no edge, on either the vertical ($r = 1$) or horizontal ($s = 0$) edge of parameter space. Under positive feedback, we see only instability, but under negative feedback, more complicated patterns emerge. This is a result of a decoupling mechanism. We explore this decoupling in depth, and state and prove the theorems governing its behavior.

Second, we discuss the "hypotenuse" of parameter space. Although the questions of stability in those event triangles remains more open, we illustrate a signal difference between those and previous cases, that for strong enough positive feedback, neutrality in those event triangles can be broken. This represents the first observed case where the strength of the feedback, rather than its sign, dictates the stability of the k-cyclic solution.

We have previously considered the following event triangle, stated in a different form as part of the $k = M + 1$ case.

3.4.1 Corollary. *A k-cyclic solution in the event triangle defined by S containing only* x_1 *when* $\bar{x}$ *passes the Poincaré section, R being empty, and order of events* $e_r e_s$ *is unstable under positive feedback and stable under negative feedback in the clustered subspace.*

The neutral $k = M + 1$ cases are special cases of the following lemmas.

3.4.2 Lemma. *If S initially contain only x_1 and x_ρ enters R after x_1 leaves S, the k-cyclic solution is neutrally stable in the clustered subspace.*

Proof. In this case, no feedback is ever exerted; for small perturbations, the k-cyclic solution still experiences no feedback. Thus all clusters move at a constant rate of 1, and the distance between them never changes. □

3.4.3 Lemma. *If R is initially empty and x_ρ enters R after x_σ leaves S, the k-cyclic solution is neutrally stable in the clustered subspace.*

Proof. Any time a cluster is in R in a neighborhood of the cyclic solution, it experiences the constant feedback $f(\frac{\sigma-1}{k})$; by rescaling the size of R, as discussed in the proof of Lemma 3.3.1, we may produce a conjugate system that removes that feedback effect (locally to the k-cyclic solution). Thus all clusters travel at a constant rate of 1 without interacting with one another, as in Lemma 3.4.2. Alternatively, we could simply note that since clusters in a neighborhood of the k-cyclic solution experience constant feedback in R, rather than a feedback that changes as clusters enter and leave S, they are not actually coupled to each other, and individual clusters may be perturbed without having any effect on the rest of the system. □

Referring back to Figure 3.2, Corollary 3.4.1 and Lemmas 3.4.3 and 3.4.2 all relate to the edge of parameter space. In particular, the stated theorems fully explain the behavior of the event triangles that have an edge along the $r = 1$ or $s = 1$ axis (Lemmas 3.4.2 and 3.4.3), and the single event triangle that has a vertex on each of those axes (Corollary 3.4.1). See Figure 3.6.

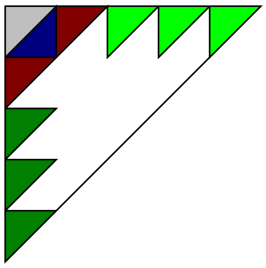

Figure 3.6: For any k (k=5 for this figure), there is an event triangle (blue), corresponding to the $k = M + 1$ proposition, that is stable under negative feedback and unstable under positive feedback. There are two other k=$M + 1$ triangles that are neutral under any feedback (maroon), and an event triangle that is neutral because the clusters of the k-cyclic solution are isolated (grey). We have seen in this section that the other triangles with edges on the r=1 axes (light green, Lemma 3.4.3) and s=0 axes (dark green, Lemma 3.4.2) are neutrally stable under either positive or negative feedback.

3.4.2 Decoupling

Over the course of the next sections, we will finish classifying the dynamics on $s = 0$ and $r = 1$; see Figure 3.7. The event triangles with vertices on these axes have more intricate behavior than the event triangles with edges on $r = 1$ or $s = 0$, both of which cases were disposed of rather easily. This section will lay the necessary groundwork.

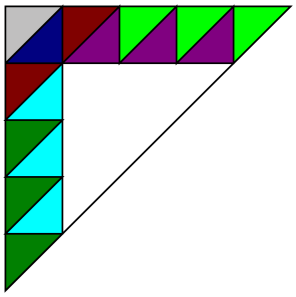

Figure 3.7: We finish classification of the dynamics on the vertical and horizontal edges. This section provides the necessary background; the light blue triangles the subject of Section 3.4.4, while the purple triangles are the subject of Section 3.4.3. The other triangles are as in Figure 3.6.

We consider what effect each cluster has on each other cluster in a neighborhood of a k-cyclic solution. We begin with a concrete example to clarify the results of this subsection.

Consider a k-cyclic solution $\bar{x}$ such that when $\bar{x}$ crosses the Poincaré section, there are σ clusters in S and no clusters in R, and when x_k reaches r, there are still σ clusters in S, i.e. $\bar{x}$ has event string $e_r e_s$. Thus in a neighborhood of the k-cyclic solution, x_k receives feedback first from clusters $x_1, x_2, ..., x_\sigma$, then from $x_1, x_2, ..., x_{\sigma-1}$. Biologically, we would say that cells in cluster x_k are receiving feedback from σ clusters and then from $\sigma - 1$ clusters. Mathematically, however, the derivative of the cluster x_k depends only on its own location (whether or not it is in R), and the cluster x_σ (whether or not it is in S). It travels at a rate of 1 until it reaches r at time $r - x_k$, and then travels at a rate of $1 + f(\sigma/k)$ for time $s - x_\sigma - (r - x_k)$. At this point, x_σ reaches s. The cluster x_k then travels at a rate of $1 + f((\sigma - 1)/k)$ until it reaches 1, and travels at a rate of 1 for the remainder of the Poincaré map. The precise locations of clusters x_1, x_2, ..., $x_{\sigma-1}$, to which it is hypothetically coupled, do not effect x_k at all, beyond the general fact that they are somewhere in S for time $0 \le t \le T$, where T is the return time of F.

Thus, over the course of a single Poincaré map, perturbing one cluster may have no influence on the rate of another cluster, even though they are theoretically coupled. Putting the discussion above into the form of a differential equation, we see that the derivative of x_k over the course of a single Poincaré map, as long as $\bar{x}$ remains in an event neighborhood of the k-cyclic solution, can be understood as

$$\dot{x}_k(\bar{x}, t) = \begin{cases} 1 & \text{if } x_k \notin R \\ 1 + \beta_\sigma & \text{if } x_k \in R \text{ and } x_\sigma \in S \\ 1 + \beta_{\sigma-1} & \text{if } x_k \in R \text{ and } x_\sigma \notin S. \end{cases}$$

Thus in a neighborhood of the k-cyclic solution, $\dot{x}_k(\bar{x},t) = \dot{x}_k(x_k, x_\sigma, t)$, since it is constant with respect to the all other variables.

The mathematical context of the dynamical system has been the torus (original, continuous system) or the k-simplex (the discrete system defined by F). Viewing a cluster as a coordinate of a point on a simplex is not convenient to our current purpose, which is to study subcollections of clusters in isolation, however. In the following discussion, we therefore view $\bar{x}(t) = \{x_1(t), x_2(t), ..., x_k(t)\}$ as a simple set of variables, each changing at a rate that depends on some or all of the other variables. So we may, for example, isolate a subset of clusters, as in Definition 3.4.4.

Preliminarily to that definition, we formalize the notion of a set of clusters being "in the neighborhood" of a point on a simplex (or torus). Define a series of projection maps, one for every combination of indices,

$$p_{i,j,...,\ell}\langle x_1(t), x_2(t), ..., x_i(t), ..., x_j(t), ..., x_\ell(t), ..., x_k(t)\rangle = (x_i(t), x_j(t), ..., x_\ell(t)). \quad (3.4.1)$$

A set of clusters is in a small neighborhood of the k-cyclic solution if it is a projection of a point in a small neighborhood of the solution.

The previous discussion of decoupling motivates the following definition. If a configuration of clusters is in the neighborhood of a k-cyclic solution, then given a cluster x in that configuration, there is a minimum collection of clusters such that knowledge of the location of each cluster in that collection gives complete information of the location and derivative of x at any time.

3.4.4 Definition. *Let k be fixed, $\bar{x}$ be a k-cyclic solution, and let A be a set of clusters. We say a cluster x is S-coupled to A, denoted $x \in_S A$, if A is a minimal set such that in a neighborhood of the k-cyclic solution, $\dot{x}_k(\bar{x},t) = \dot{x}_k(A,t)$. If $x \in_S A$ but $x \notin A$, we redefine $A = A \cup \{x\}$. We say that a cluster x is S-coupled to another cluster y if $x \in_S A$ and $y \in A$.*

If clusters are not isolated then the implication $x \in_S A \rightarrow x \in A$ comes automatically, since the rate of x depends on whether or not it is in R. We will want

to be able to gain complete information of a cluster x, both its position and derivative, from complete information of the clusters it is S-coupled to, which is why when $x \in_S A$, we define A to necessarily include x. The following lemma is obvious, but is only true because any cluster is S-coupled to itself. Otherwise, an isolated cluster would be S-coupled to the empty set.

3.4.5 Lemma. *For any cluster x there exists a nonempty set A such that $x \in_S A$.*

If a cluster x is S-coupled to a set A then given the location of x and the location of all the clusters in A, the derivative of x can be determined. This is *not* equivalent to saying that the cluster is moving about S^1 independently of clusters not in A; if $x_1 \in_S \{x_1, x_2\}$ and $x_2 \in_S \{x_2, x_3\}$ then perturbing x_3 may influence x_2, which may in turn influence x_1. However, at any given time, the rate and position of x_1 can be calculated from the position of x_1 and x_2, without knowledge of the position of x_3.

It is possible that in a neighborhood of a k-cyclic solution, a collection of clusters might be truely self-contained, in the sense that perturbing one cluster of the collection will only effect the rates and locations of other clusters in the collection, while perturbing clusters not in the collection will not effect the clusters in the collection.

3.4.6 Definition. *A set of clusters A is S-isolated if in a neighborhood of a k-cyclic solution,*

1. *for any $x_i \in A$, if $x_i \in_S B$ then $B \subset A$, i.e. in a neighborhood of the k-cyclic solution, the derivatives of clusters in A depend only on the locations of other clusters in A, and*

2. *if $x_i \in_S B$ and $B \cap A \neq \varnothing$ then $x_i \in A$, i.e. the rates of clusters not in A do not depends on the locations of clusters in A.*

One visualization of these definitions would be to define an undirected graph of k nodes, and let an edge connect nodes x and y if either $x \epsilon_S A$ and $y \in A$, or vice

versa; this visualization is suggested by Figure 3.8. In that context, S-isolated sets are the connected components of the graph.

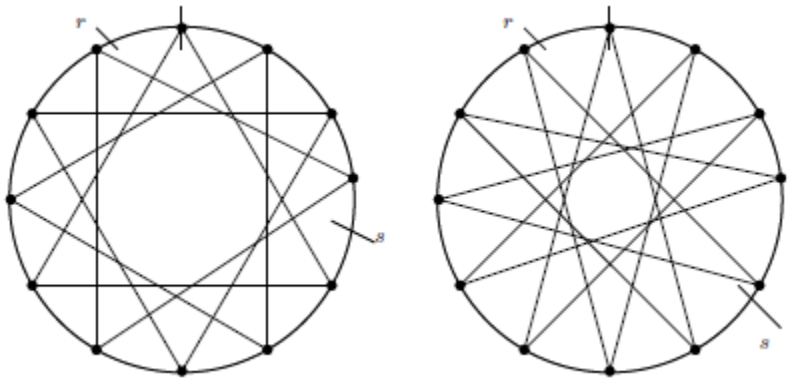

Figure 3.8: Two cyclic solutions. In both figures, $x_k \in_S \{x_k, x_\sigma\}$. In the right-hand diagram, the entire k-cyclic solution is the S-isolated set, reflecting the discussion immediately previous to Definition 3.4.6. In the left-hand figure, however, the k-cyclic solution is the union of four disjoint S-isolated sets.

As long as an S-isolated set remains in a neighborhood of the k-cyclic solution, it exists as a truely isolated object. Perturbing a cluster in an S-isolated set does not effect the position or rate of clusters not in that S-isolated set (if perturbing $x_i \in S$ affects the rate of x_j in a neighborhood of the k-cyclic solution then $x_j \in_S B$, and $B \subset A$ by Condition 1 of Definition 3.4.6), and perturbing a cluster not in an S-isolated set never affects the rate of clusters in the set (Condition 2). We have seen one example of this phenomenon already.

3.4.1 Example. *If $\bar{x}$ is a neutrally stable solution consisting of isolated clusters, as in Lemma 3.4.2, each singleton is an S-isolated set.*

The following example is slightly less trivial.

3.4.2 Example. *Any k-cyclic solution as in Lemma 3.4.3 consists of S-isolated singletons.*

The important point is that when a cluster is in R, it receives constant feedback, so its rate is determined entirely by its position on the unit circle, even though, absent the variable change in the proof, clusters are not isolated in a traditional sense, i.e. feedback is being exerted. The cluster x_k recieves feedback from clusters $x_1, x_2, ..., x_{\sigma-1}$, but perturbing those clusters slightly has no effect on the rate of x_k, which is a constant $1 + f((\sigma - 1)/k)$.

3.4.3 Example. *The above definitions pass through unchanged if clusters are replaced with cells. Consider a (neutrally stable in the clustered subspace) set of isolated clusters, and an event-small perturbation in the full phase space. Then each group is an S-isolated set. In particular, if the cells of a group are numbered in the counterclockwise direction (so that c_1 if the first cell of the group to undergo any order of events) then $c_1 \in_S \{c_1\}$, $c_2 \in_S \{c_1, c_2\}$, $c_3 \in_S \{c_1, c_2, c_3\}$, and so forth.*

Since S-coupling is defined in terms of event neighborhoods, it follows that it is preserved by small perturbations.

3.4.7 Lemma. *Let $\bar{x}$ be a k-cyclic fixed point (viewed as a set), and let $x_i \in_S A$. If $\bar{x}'$ is an event-small perturbation of $\bar{x}$, such that x_i is perturbed to x_i', then $x_i' \in_S A'$, where $A' = \{x_j' | x_j \in A\}$.*

Proof. Consider a cluster x. This cluster moves at a rate of 1 when it is not in R, and when it is in R, its rate changes when a cluster enters S or leaves S. It is therefore S-coupled to the clusters that enter or leave S while x is in R. Since we are always assuming that the k-cyclic solutions are in the interiors of event triangles, small perturbations of x and small perturbations of the clusters x is S-coupled to will not change these orders of events. □

S-isolation is potentially temporary, in the sense that it is defined in terms of behavior in a neighborhood of a k-cyclic solution, but if the k-cyclic solution is unstable, initial conditions near the solution will leave such a neighborhood. In

Example 3.4.3, under positive feedback the groups will be isolated for all time, by Proposition 1.5.1, while under negative feedback, isolated groups will spread out (Lemma 3.2.7) until they are no longer isolated.

We will mostly consider two special cases of S-isolated groups. We make the following observation.

3.4.8 Lemma. *Let $\bar{x}$ be a k-cyclic solution, and let $A \subset \bar{x}$ be a proper S-isolated subset of $\bar{x}$ of cardinality j. Then $\bar{x}$ is the disjoint union of k/j S-isolated sets, which are cyclic permutations of each other in the sense that if $\bar{x}$ and $\bar{y}$ are two such sets, there is a value of T such that $\bar{x}(T) = \bar{y}$.*

Proof. This follows immediately from the symmetry of k-cyclic solutions, and from the fact that S-coupling and S-isolation are spacial properties, i.e. they depend on the location of clusters on the circle. Let $x \in_S A$ and $y \notin_S A$. Then there is some minimum time T such that $y(T) = x(0)$, and y is S-coupled to $B = A(-T)$. □

The above lemma is always true, although in general only trivially, that is, the only S-isolated set is, in most cases, all of $\bar{x}$.

The point of writing a k-cyclic solution $\bar{x}$ as the union of S-isolated sets is that, in a neighborhood of the k-cyclic solution, the behavior of the k-cyclic solution may be understood as, essentially, the union of the behavior of S-isolated sets. We define a special sort of S-isolated set that will be most relevant to our needs. For ease of notation, when a cluster x is S-coupled to the two-element set $\{x, y\}$, we drop set notation and write $x <_S y$.

3.4.9 Definition. *An S-chain is a nonrepeating sequence of clusters $\{x_{bi}\}_{i=1}^{j}$ such that $x_{bi} <_S x_{bi+1}$ for $1 \leq i < j$ and $x_{bj} <_S x_{b1}$. Call j the length of the S-chain.*

If $\bar{x}$ contains an S-chain, one of two things might happen; either the S-chain $x_k <_S x_\sigma <_S \ldots$ might cover $\bar{x}$ (i.e. be of length k), or it does not, in which case it is of length j and $\bar{x}$ is the union of k/j S-chains (Lemma 3.4.8).

If $\mathbf{x} = \wp\{x_1, x_2, ..., x_k\}$, then any point in $\mathbf{x}$ of cardinality C can be naturally ordered and mapped to the C-dimensional simplex. Using this mapping, S-chains of length j of a k-cyclic solution may be studied as points on a j-dimensional simplex. In fact, the S-chains of a k-cyclic solution, viewed in this light, are themselves j-cyclic solutions, after a rescaling of the feedback function.

3.4.10 Theorem. *If $x = \{x_1, x_2, ..., x_k\}$ is a k-cyclic solution containing an S-chain $\bar{y}$ of length j, then $\bar{y}$ is a j-cyclic solution on the j-dimensional simplex, if the feedback function is rescaled appropriately.*

Proof. This follows immediately from the symmetry of the cyclic solution. If $x_i <_S x_j$, and x_j is the m'th cluster after x_i (counting clockwise for definiteness), then $x_j <_S x_\ell$, where x_ℓ is the m'th cluster after x_i, and so on, by the symmetry of the solution. Then if T is minimal such that $x_k(T) = 1$, mT is minimal such that every member of the S-chain, at time mT, passes to the adjacent member of the S-chain. This is true in the original setting, i.e. when all clusters are present.

On the j-dimensional simplex, the feedback function must be rescaled, because removing clusters not in the S-chain changes the parameter σ and the fractions I. On the k-dimensional simplex, clusters in a neighborhood of the k-cyclic solution experience only two feedbacks, $f(\sigma/k)$ and $f((\sigma - 1)/k)$. Removing clusters not in the S-chain produce new values of σ and k, and we define new feedback values $f_{\text{new}}(\sigma_{\text{new}}/j) = f(\sigma/k)$ and $f_{\text{new}}((\sigma - 1)_{\text{new}}/j) = f((\sigma - 1)/k)$. These are the only arguments that the feedback function takes in a neighborhood of the k-cyclic solution, and so the details of f_{new} are not otherwise relevant. □

If a k-cyclic solution is the union of disjoint S-chains, those S-chains control the stability of the k-cyclic solution. Such a k-cyclic solution is never stable.

3.4.11 Lemma. *A k-cyclic solution that is the union of disjoint S-chains of length i, all of which are stable as i-cyclic solutions on the i-simplex, is neutrally stable.*

Proof. For ease of writing we consider a specific k-cyclic solution $\bar{x}$ that is the union of two S-chains, $z_1, z_2, ..., z_i$ and $y_1, y_2, ..., y_i$, where $i = k/2$. The same proof works for any number of S-chains. A perturbation of $\bar{x}$, $\bar{x}'$, can be viewed as a perturbation of $\bar{y}$ and a perturbation of $\bar{z}$, $\bar{y}'$ and $\bar{z}'$

As long as $\bar{y}'$ and $\bar{z}'$ remain in event neighborhoods of $\bar{x}$, they will remain disjoint, non-interacting S-chains. They do remain in such an event neighborhood, since by stability, $\bar{y}'$ and $\bar{z}'$ remain in neighborhoods of $\bar{z}$ and $\bar{y}$, and $\bar{x} = \bar{y} \cup \bar{z}$. Thus $\bar{y}'$ and $\bar{z}'$ do not interact, and $\bar{z}' \to \bar{z}$, while $\bar{z}' \to \bar{z}$.

To understand why this does not imply stability, we consider that although $\bar{x} = \bar{y} \cup \bar{z}$, and $\bar{y}(T)$ and $\bar{y}(T + \epsilon)$ define the same periodic orbit, $\bar{x}(T) \neq \bar{y}(T + \epsilon) \cup \bar{z}(T)$. It may therefore happen that a small perturbation of $\bar{x}$ converges back not to $\bar{x} = \bar{y} \cup \bar{z}$, but to $\bar{y}(T + \epsilon) \cup \bar{z}(T)$. In fact, to produce an explicit example of a neighborhood of $\bar{x}$ that does not converge back to $\bar{x}$, simply take all the clusters of $\bar{y}$ and run time forward by ϵ for those clusters alone. From the point of view of the S-chains, this is no perturbation at all; $\bar{y}$ and $\bar{z}$ are still on their orbits. But it is a perturbation of $\bar{x}$ that will be maintained indefinitely. □

Theoretically, Lemma 3.4.11 could be strengthened to the case where some S-chains are stable and some are neutral, but such a situation cannot occur. By the symmetry of the k-cyclic solutions, all S-chains share the same stability.

We omit the proofs of the following, which are trivial variations of the proof of Lemma 3.4.11.

3.4.12 Lemma. *A k-cyclic solution that is the union of disjoint S-chains of length i, all of which are neutral as i-cyclic solutions on the i-simplex, is neutral.*

3.4.13 Lemma. *A k-cyclic solution that is the union of disjoint S-chains of length i, all of which are unstable as i-cyclic solutions on the i-simplex, is unstable.*

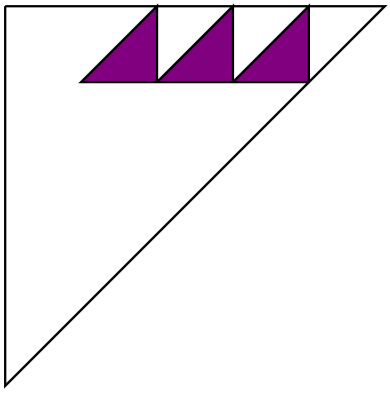

Figure 3.9: In Section 3.4.3, we consider the stability of triangles with a vertex on the $r = 1$ boundary of the simplex, excluding one such triangle whose stability is already known from the $k = M + 1$ case.

3.4.3 Decoupling along the $r = 1$ axes

Although we did not explicitly use the terminology, Lemmas 3.4.2 and 3.4.3 were essentially proven using Lemma 3.4.12, where the S-chains are of length 1. We will now apply the machinery of the last subsection to more complicated cases.

Consider boundary triangles such that, when the k-cyclic solution crosses the Poincaré section, R is empty but S contains more than 1 cluster. We know they are neutrally stable under the order of events $e_s e_r$ (Lemma 3.4.3). We now consider the other order of events. For positive feedback, we will observe instability in all such triangles, as a consequence of Lemma 3.4.13 (we will see this in detail shortly). For negative feedback, the behavior is more complicated, and depends on $\gcd(k, \sigma)$. We first consider the case where $\gcd(k, \sigma) = 1$.

3.4.14 Theorem. *Consider an event triangle such that $\rho = k$, $\sigma > 1$ is fixed, and cyclic solutions have event string $e_r e_s$. Then if $\gcd(k, \sigma) = 1$, the corresponding cyclic solution is asymptotically under negative feedback, and unstable under positive feedback.*

Under the hypothesis of the theorem, when the solution passes the Poincaré section, R is empty. The restriction $\sigma > 1$ is unnecessary for the statement of the

theorem, but the $\sigma = 1$ case has already been proven as Proposition 2.3.1 (and it was necessary to prove it separately, as the proof of Theorem 3.4.14 depends on the $\sigma = 1$ case).

We first observe the following.

3.4.15 Lemma. *If the hypothesis of Theorem 3.4.14 holds, then the k-cyclic solution is itself an S-chain.*

Proof. Let $w = k - \sigma$. Then $x_k <_S x_{k-w} <_S x_{k-2w} <_S x_{k-3w} <_S \ldots <_S x_k$, where the substraction in the subscript is done modulus k. The reason that the cluster x_k $(= x_\rho)$ about to enter R depends only upon itself and the last cluster in S has already been elaborated on. The list $x_k, x_{k-w}, x_{k-2w}, \ldots$ does not terminate early because if $k = k - \alpha(k - \sigma) \mod k$ then $\alpha k = \alpha\sigma \mod k$, and the property of being relatively prime implies $\alpha = k \mod k$. □

Proof of Theorem 3.4.14. First, we replace the system in question with the conjugate system defined by (3.3.1).

Let $s_{\text{new}} = s - x_\sigma$. We renumber the clusters so that $x_1 <_S x_2 <_S x_3 <_S <_S \ldots <_S x_k$. Then the dynamical system is defined by the differential equation

$$\dot{x}_i(\bar{x}, t) = \begin{cases} 1 & \text{if } x_i \notin R \\ 1 + \alpha & \text{if } x_i \in R \text{ and } x_{i+1} \in S \\ 1 + \beta & \text{if } x_i \in R \text{ and } x_{i+1} \notin S, \end{cases}$$

where $|\beta| < |\alpha|$.

Now consider the original system (or rather, the conjugate, rescaled, but not renumbered system). Redefine s to be s_{new}. Then the dynamical system is defined by the differential equation

$$\dot{x}_i(\bar{x},t) = \begin{cases} 1 & \text{if } x_i \notin R \\ 1+\alpha & \text{if } x_i \in R \text{ and } x_{i+1} \in S \\ 1+\beta & \text{if } x_i \in R \text{ and } x_{i+1} \notin S, \end{cases}$$

where $|\beta| < |\alpha|$.

The dynamics of these two systems are identical in a neighborhood of the k-cyclic solution. Each cluster is uniquely coupled with one other cluster; perturbing one cluster will change the amount of time it spends in S, which will perturb the cluster coupled with it, which will change the amount of time it spends in S, and so on, until the "perturbation wave" has passed through the entire cycle, and the last cluster influences the first. More formally, the renumbering of clusters defines a conjugacy map on the two copies of S_k being considered.

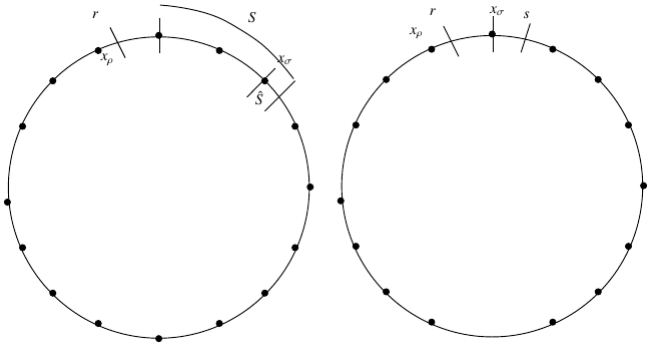

Figure 3.10: We summarize the proof of Theorem 3.4.14 pictorially. In this case, S is theoretically quite large, but when the background feedback is scaled away, there is only signaling when one cluster (x_σ) lies in a small region ($\hat{S}$). We define a conjugate system (right) that shares this behavior, relabeling clusters so that x_ρ remains S-coupled to x_σ under the conjugacy.

We observe that the second system is simply the Corollary 3.4.1 case, and its stability, and thus the stability of the system under consideration, is known. □

When the greatest common denominator of k and σ is greater than 1, the k-cyclic solution decouples into disjoint S-chains, and is therefore neutral (when the S-chains are stable) or unstable (when the S-chains are unstable.)

3.4.16 Lemma. *Consider an event triangle such that $\rho = k$, $\sigma > 1$ is fixed, and cyclic solutions have event string $e_r e_s$. If there exists a maximum integer $a > 1$ such that $a|k$ and $a|\sigma$, then the k-cyclic solution $\bar{x}$ is the union of a disjoint S-chains of length k/a.*

Proof. One explicit S-chain in this case is $x_k <_S x_{k-(k-\sigma)} = x_\sigma <_S x_{k-2(k-\sigma)} = x_{2\sigma-k} <_S x_{k-3(k-\sigma)} = x_{3\sigma-2k} <_S \ldots <_S x_{k-(k/a)(k-\sigma)} = x_0 = x_k$, where the last equality is made clear be letting $k = m_1 a$, $\sigma = m_2 a$, and recalling that we are working modulus k. The other S-chains are cyclic shifts of this by Lemma 3.4.8. □

3.4.17 Lemma. *If the hypotheses of Lemma 3.4.16 holds, then the disjoint S-chains are stable under negative feedback and unstable under positive feedback.*

Proof. An S-chain in this case is itself a (k/a)-cyclic solution that satisfies the hypothesis of Theorem 3.4.14. □

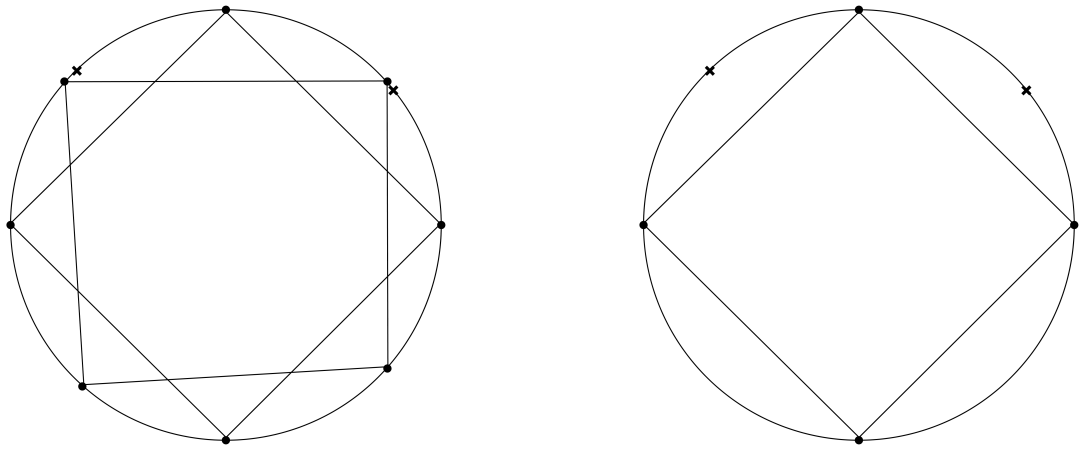

Figure 3.11: When the greatest common denominator of k and σ is greater than 1, the k-cyclic solution under discussion in this section can be decomposed into independent subcollections of clusters, each governed by the $k = M + 1$ theorem.

We now characterize the stability of k-cyclic solutions on the $r = 1$ axis when k and σ have a greatest common denominator greater than 1.

3.4.18 Theorem. *In the order of events triangle such that the hypothesis of Lemma 3.4.16 holds, the corresponding k-cyclic solution is neutrally stable under negative feedback, and unstable under positive feedback.*

Proof. This is immediate from Lemmas 3.4.17, 3.4.12 and 3.4.13. □

3.4.4 Decoupling along the $s = 0$ axes

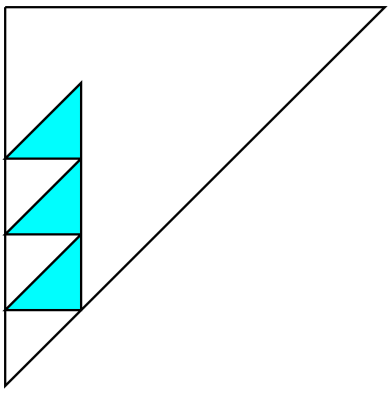

Figure 3.12: In Section 3.4.4 we consider the stability of event triangles with a vertex on the line s=0, excluding one case whose stability is known from previous results.

The results in this section are analogous to those of the previous section, but it is necessary to slightly recast the framework in which we consider them.

Consider event triangles such that, when $\bar{x}$ passes the Poincaré section, S contains only $x_1 = 0$ but R contains multiple clusters. Since we have already considered the order of events $e_s e_r$ (Lemma 3.4.2), we now consider event chain $e_r e_s$.

Consider what happens when x_ρ enters R. It travels at a certain rate $(1 + f(1/k))$, then travels at a rate of 1 until x_k reaches 1. It then travels at a rate of $1 + f(1/k)$ for time s. It then moves at rate 1, until x_{k-1} reaches 1, at which point it travels at rate

$1 + f(1/k)$ for s time units. And so on, until it reaches 1. Thus the only cluster that, when perturbed, affects the time it takes x_ρ to reach 1 is x_1.

We cannot use without modification the concept of S-chains, because in spite of the discussion in the previous paragraph, here clusters are not decoupled in the same sense. The derivative of x_ρ does depend on the location of $x_{\rho+1}, x_{\rho+2}, ..., x_k$. On the other hand, we have largely considered stability in terms of a discrete dynamical system defined by the Poincaré map, rather than in terms of the flow of the original system. In that context, it does not matter if, moment to moment, the rate of each cluster is known; the stability is controlled by DF, the contruction of which does not require such fine detail. We therefore pass to the discrete case. The eigenvalues of F are inside the unit circle (likewise on or outside the unit circle) if and only if the eigenvalues of $F_\rho := F^{k-\rho+1}$ are inside (on, outside) the unit circle, since F is a factorization of F_ρ. We have seen in the previous paragraph that the return time of F_ρ depends directly on only one other cluster.

Let an initial condition $\bar{x}(0)$ be given in the neighborhood of a k-cyclic solution in an event triangle such as we are considering (ρ arbitrary, $\sigma = 1$, event string $e_r e_s$). In a neighborhood of the k-cyclic solution, the time T it takes for x_ρ to reach 1 depends only on the location of x_ρ (and on $x_1 = x_\sigma$, but by assumption on F, and thus F_ρ, we have $x_1 = 0$.) After one iteration of F_ρ, a new cluster, $x_{\rho-(k-\rho+1)}$, takes the place of x_ρ, in the sense that it is the last cluster not in R when $x_\rho = 0$. By symmetry, the return time of this cluster depends only on x_ρ. Proceeding in this manner, we define a list, the discrete equivalent of an S-chain, such that the return time of each cluster under F_ρ depends only on itself and the cluster immediately before it in the list. We will call such a list of clusters an F-chain. Eventually, the F-chain will reach its initial cluster x_ρ, at which time it may or may not cover $\bar{x}$.

Geometrically, S- and F-chains are both formed similarly. Select a cluster x_m; it is coupled with another cluster, x_{m+p} for some p. By symmetry, this cluster is coupled

to x_{m+p+p}, which is coupled to $x_{m+p+p+p}$, and so forth, taking "every p'th cluster."' It is therefore natural that geometrically, F- and S-chains behave in the same way.

3.4.19 Lemma. *If $gcd(k, k-\rho+1) = 1$, $\bar{x}$ is a single F-chain. If $gcd(k, k-\rho+1) > 1$, it is the union of disjoint F-chains.*

Proof. An F-chain is formed by taking every $(k-\rho+1)$'th cluster. An S-chain is formed by taking every σ'th cluster. This lemma therefore is the exact analogue of Lemmas 3.4.15 and 3.4.16, with $k-\rho+1$ in place of σ. □

Because F-chains are self-contained under the discrete dynamics, we obtain the following results.

3.4.20 Theorem. *The i-dimensional F-chains of a fixed point $\bar{x}$ are fixed points of F on the i-dimensional simplex.*

The proof of this theorem is identical to the proof of Theorem 3.4.10, with $x <_S y$ replaced with $x <_F y$, where the $<_F$ relation is defined in the obvious way.

Under the discrete dynamical system, F-chains are self-contained, i.e. the stability of each F-chain depends only on the clusters in the F-chain. A fixed point of a Poincaré map is stable if and only if the corresponding periodic orbit of the continuous dynamical system is stable, so the following three discrete analogues of continuous results follow automatically.

3.4.21 Corollary. *If $\bar{x}$ is the disjoint union of unstable F-chains than $\bar{x}$ is unstable.*

3.4.22 Corollary. *If $\bar{x}$ is the disjoint union of neutral F-chains than $\bar{x}$ is neutral.*

3.4.23 Corollary. *If $\bar{x}$ is the disjoint union of stable F-chains than $\bar{x}$ is neutral.*

Then the stability results, in terms of $\gcd(k, k-\rho+1)$, are parallel to those of the previous section.

3.4.24 Theorem. *If $\bar{x}$ is a k-cyclic solution in an event triangle such that $\sigma = 1$ and the k-cyclic solution has event string $e_r e_s$, and $\gcd(k, k-\rho+1) = 1$, then $\bar{x}$ is unstable under positive feedback and neutrally stable under negative feedback.*

Proof. This theorem is clearly a direct analogue of Theorem 3.4.14, and if instead of replacing s with $s_{\text{new}} = s - x_\sigma$ we replace r with $r_{\text{new}} = r - x_\rho$, the proof passes through without further modification. □

These results apply to the clustered subspace. It is clear, however, that instability in the clustered subspace implies instability in the full phase space, and we will see that the same holds true for aymptotic stability (Theorem 3.5.1). The implications of neutrality in the clustered subspace on the behavior in the full phase space remain a subject for future research.

3.4.5 The hypotenuse

We consider now the hypotenuse of the parameter-space triangle. Event triangles with their edge on the hypotenuse correspond to k-cyclic solutions with every cluster in R or S; there is only one order of events possible in this case, $e_s^\sigma e_r^\sigma$ (as $\sigma = \rho$). Event triangles with a single vertex on the line $s = r$ correspond to k-cyclic solutions where $\rho = \sigma + 1$, and x_ρ enters R before x_σ leaves S; these triangles have no special proporties, e.g. they are unstable under positive feedback.

Consider an event triangle such that σ clusters lie in S and $k - \sigma$ clusters lie in R. The corresponding order of events (necessarily $e_s e_r$) was seen to be unstable in the interior of parameter space, the proof of which rest on the fact that characteristic polynomials are not palindromic (Theorem 3.3.3). On the edge of parameter space, this is not true; we observe palindromic characteristic polynomials, and observe neutrality for weak positive feedback (where we will not formally quantify ”weak” and ”strong’)’. We also observe, however, that neutrality breaks down for sufficiently powerful positive feedback.

3.4.25 Theorem. *Consider a positive feedback system, and let $k > 1$ be fixed. Consider an event triangle such that $\sigma = \rho$ and the order of events is $e_s e_r$. Then there exists some positive number N such that if $f(\sigma/k) \geq N$, then the k-cyclic solution is unstable in the clustered subspace.*

Proof. We cite Theorem 2 of [43], which gives a lower bound on the spectral radius $\boldsymbol{\varrho}(A)$ as $\boldsymbol{\varrho}(A) \geq \frac{1}{\text{rank }(A)}|\text{tr } A|$. The trace of A can easily be calculated as $-1 + f(\sigma/k)$ (see the matrix in the proof of Lemma 3.3.1). The rank, $k - 1$, is fixed and feedback-independent. Therefore, by selecting $f(\sigma/k$ sufficiently large, the spectral radius may be made to be greater than 1, implying instability. □

The characteristic polynomials in this case contain coefficients of the form $(1 - m\beta)$ for integers $m \geq 1$, where β is the feedback exerted by σ clusters once the feedback exerted by $\sigma - 1$ clusters has been scaled from the system. One might expect, therefore, that the change in stability will happen abruptly when coefficients become 0. This, however, is not the case (Figure 3.14a).

We consider in simulation the behavior of the 3-cyclic solution in a neutral (for weak positive feedback) event triangle on the hypotenuse. Using parameter values $s = .5$ and $r = .55$, and an initial condition on the Poincaré section, we iterate the Poincaré map 100 times, plotting the number of iterations (horizontal axis) against the location of cells in the interval $[0, 1]$ (verticall axis). We use feedback functions $f(I) = .2I$ and $f(I) = .6I$ to simulate strong and weak feedback, respectively. We first observe the behavior in a neighborhood of the 3-cyclic solution in a neighborhood of the 3-cyclic solution (i.e. with an initial condition of three clusters, which we place at $x_1 = 0$, $x_2 = 1/3$, and $x_3 = 2/3$) in Figure 3.15a, observing a wave pattern that neither converges to a fixed point (which can be calculated to lie at approxomately $(0, .4273, .7071)$) nor moves too far away from it. The eigenvalues of this system lie at approxomately $\lambda_i = -.4705 \pm .88242i$ and have modulus 1. For strong positive feedback, we use the same initial condition, which is in fact closer to the fixed point (lying at

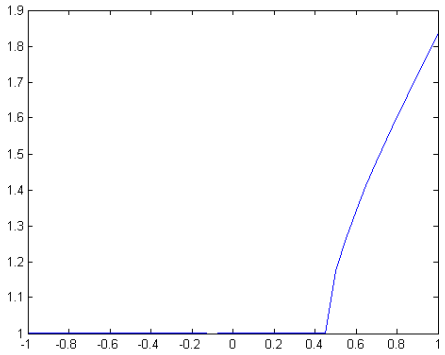

(a) The modulus of the maximum eigenvalue for the 15-cyclic solutions in the event triangle defined by $\sigma = \rho = 4$. A bifurcation occurs at approximately $\beta = .455$.

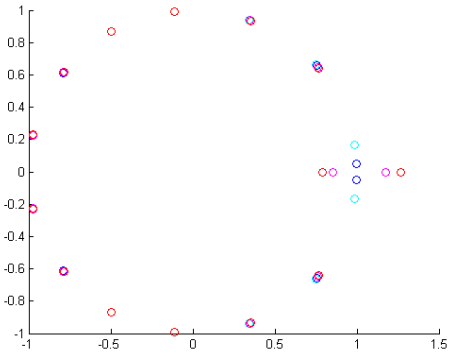

(b) The roots of the polynomial for $\beta = .4$ (cyan), .45 (blue), .50 (magenta), and .55 (red).

Figure 3.14: Two representations of the eigenvalues of the 15-cyclic solutions in the event triangle defined by $\sigma = \rho = 4$. The characteristic polynomial has the form $\lambda^{14} + (1-\beta)\lambda^{13} + (1-2\beta)\lambda^{12} + (1-3\beta)(\lambda^{11} + \lambda^{10} + ... + \lambda^3) + (1-2\beta)\lambda^2 + (1-\beta)\lambda + 1$, where $\beta = f(\sigma/k)$. For any negative and small positive feedback, all the roots of this polynomial are on the unit circle. Referring back to our discussion at the end of Section 3.3, we observe that the characteristic polynomial is symmetric.

approxomately $(0, .4256, .6933)$) then in the previous case. However, the eigenvalues of the strong-feedback case are $\lambda_i = -.609 \pm 1.004$, and have modulus 1.17, causing the initial condition to leave the neighborhood of the fixed point and converge to the synchronous solution (Figure 3.15b).

We also consider the behavior of the initial condition $(0, 1/3, 2/3)$ in the full phase space ($n = 600$). The behavior of the system in the full phase space is substantially similar to the behavior in the clustered subspace. For weak positive feedback (Figure 3.16a), the groups oscillate weakly while their diameters converge to 0; under strong positive feedback (Figure 3.16b), instability in the clustered submanifold is of course inherited.

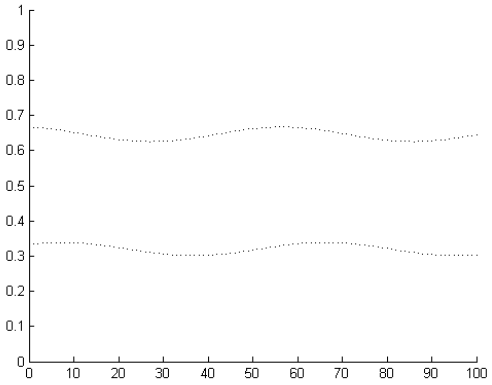

(a) The trajectory of an initial value near the 3-cyclic solution, in the clustered subspace, under weak positive feedback. Three clusters persist, the two visible in the graph and one on the axis.

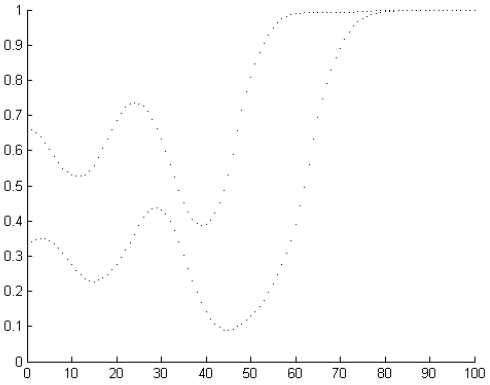

(b) The trajectory of an initial value near the 3-cyclic solution, in the clustered subspace, under strong positive feedback.

Figure 3.15: The trajectory of an initial condition near the 3-cyclic solution with parameters s = .5 and r = .55 in the clustered subspace under weak (a) and strong (b) positive feedback. The horizontal axis represents the number of times the Poincaré map has been interated, while the vertical axis represents the unit circle.

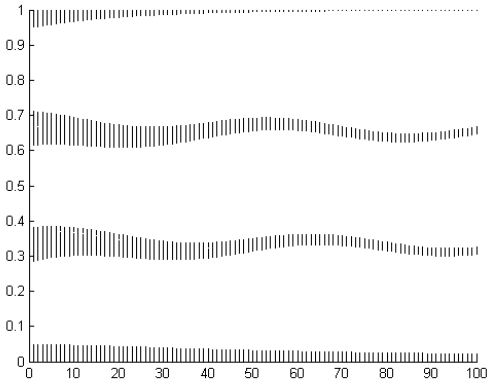

(a) The trajectory of an initial value near the 3-cyclic solution, under weak positive feedback, in the full phase space. The 3-cyclic solution is neutral in the clustered subspace.

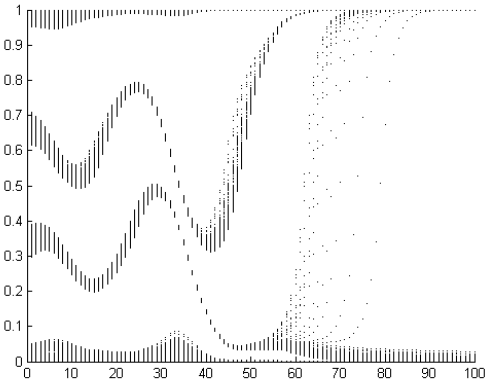

(b) The trajectory of an initial value near the 3-cyclic solution in the full phase space, under strong positive feedback. The 3-cyclic solution is unstable.

Figure 3.16: A trajectory of an initial condition near the 3-cyclic solution for parameters s = .5 and r = .55 in the full phase space (200 cells spread uniformly in a diameter .1 group centered at each of (0, 1/3, and 2/3)) exhibits similar behavior to conditions near the 3-cyclic solution in the clustered subspace.

3.5 Stability in full phase space

We know (Lemma 3.2.4) that in those parts of parameter space where the k-cyclic solution is defined by the order of events $e_r e_s$, the diameters of the groups generated by an event-small perturbation of the k-cyclic solution in the full phase space will shrink uniformly over the course of a single Poincaré map. Thus the Poincaré map, at least initially, moves solutions in the full phase space towards the clustered subspace. If the k-cyclic solution is asymptotically stable in the clustered subspace, then points near the k-cyclic solution are moved towards the k-cyclic solution by the Poincaré map. This combination implies stability in the full phase space

3.5.1 Theorem. *In a negative-feedback system, consider the k-cyclic solution in a stability triangle with order of events $e_r e_s$. If the k-cyclic solution is stable in the clustered subspace, it is stable in the full phase space.*

Proof. Let P be the Poincaré map. By asymptotic stability in the clustered subspace, we may find an arbitrarily small open set U_C in the clustered subspace C containing $\bar{x}$, such that U_C is contained in an event-neighborhood of $\bar{x}$ and Lemma 3.2.4 applies and $P(U_C) \subset U_C$ with $P(\bar{U_C} \backslash U_C) \subset \text{int } U_C$, i.e. U_C is a trapping region in the clustered submanifold.

Now $\bar{U_C} \backslash \text{int } U_C$, and $P(\bar{U_C})$ are disjoint compact sets, so the distance $D = d(\bar{U_c} \backslash U_c, P(\bar{U_C})$ is well-defined. If $w \in P(\bar{U_c})$ and y is an arbitrary point, then for any $z \in C$ such that $z \notin U_C$, we know that $|d(w,z) - d(w,y)| \leq d(y,z)$ by the reverse triangle inequality; if we assume that $d(w,y)$ is sufficiently small, then since $d(w,z)$ is bounded below by D, the argument in the absolute value may be taken to be positive, and we may drop the absolute value to write $d(w,z) - d(w,y) \leq d(y,z)$. Because $D < d(w,z)$, if we assume that $d(w,y) < D$, we may recover a bound on $d(y,z)$: if $d(w,y) < \epsilon_1$, then substituting the appropriate values into the triangle inequality equation yields $D - \epsilon_1 < d(y,z)$. Since D depends only on U_C, which is fixed, whereas ϵ_1 may be

chosen arbitrarily small, we can make such a bound explicit by, for example, proscribing $\epsilon_1 < (1/3)D$, in which case $(2/3)D < d(y,z)$.

Now, because it is definined on a compact space, P is not only continuous, but uniformly continuous. Find $\epsilon_2 < (1/3)D$ such that for any z and y in the full phase space, if $d(z,y) \leq \epsilon_2$, then $d(P(z),P(y)) \leq \epsilon_1$.

Let $\Delta = \{y | d(y,\bar{U_C}) \leq \epsilon_2\}$. We will show that this is a trapping region. First note that $\bar{U_C} \subset \Delta$, and since by construction, $P(\bar{U_C}) \subset U_C$, if $\bar{x} \in \bar{U_C}$, then $P(\bar{x} \in \bar{U_C} \subset \Delta$. Let $y \in \Delta \backslash \bar{U_C}$. Then $0 < d(y,\bar{U_C}) \leq \epsilon_2$. A property of compactness is that if a point is a certain distance from a compact set, it is that same distance from a specific point in that compact set. Thus if $d(y,\bar{U_C}) \leq \epsilon_2$, there exists some point $w \in \bar{U_C}$ such that $d(y,w) \leq \epsilon_2$. Then $d(P(y),P(w)) \leq \epsilon_1$, and $P(w) \in P(\bar{U_C})$. By the above discussion of the reverse triangle inequality, we know that if $v \in C$ but $v \notin U_C$, then $d(P(y),v) > (2/3)D$. However, we also know from the Lemma 3.2.4 that $d(P(y),C) < \epsilon_2 < (1/3)D$, and because the clustered submanifold is compact, there is some realization of this distance, that is, there is some point $W \in C$ such that $d(P(y),W) = d(P(y),C) < \epsilon_2 < (1/3)D$. This W can therefore only be in U_C. Thus $d(P(y),U_C) \leq \epsilon_2$, and $P(y) \in T$.

We may make such trapping regions arbitrarily small by selecting the initial (clustered submanifold) trapping region arbitrarily small. We will show that if $\bar{y}$ is an initial value in such a trapping region, the trajectory of $\bar{y}$ under P has the fixed point $\bar{x}$ as an ω-limit point. These two facts together imply that $\bar{x}$ is a proper limit of the trajectory, since the second fact ensures that the trajectory will get arbitrarily close to $\bar{x}$, and the first fact ensures that, having gotten arbitrarily close, it must stay close.

Let T be any trapping region such as was just constructed, and let $\bar{y} \in T$. Since T is compact, the sequence $\{P^i(\bar{y})\}_{i=1}^{\infty}$ has a limit point $\bar{z}$, which must lie on the clustered submanifold C since any trajectory trapped in T converges exponentially to C. Take a subsequence $\{\bar{z}_i\}$ of $\{P^i(\bar{y})\}_{i=1}^{\infty}$ such that $\bar{z}_i \to \bar{z}$. For all i, $P^i(\bar{z}_n) \to P^i(\bar{z})$, and this,

together with the fact that $P^i(\bar{z}) \to \bar{x}$ as $i \to \infty$ implies that $\bar{x}$ is a limit point of the set $\{P^n\bar{y}|n \in Z\}$, and is thus in the ω-limit set of $\bar{y}$. □

It is now natural to ask, when we have observed stability of the k-cyclic solution, whether it has been in the regions of parameter space such that the hypothesis of Lemma 3.2.4 holds (i.e., where the k-cyclic solution has event string e_re_s). First, we consider what that region looks like. Parameter space is first divided into quadrilaterals by making statements about what clusters lie where when the solution passes the Poincaré section (e.g. "There are 4 clusters in S, 3 clusters between S and R, and 5 clusters in R"), and each quadrilateral is divided into two event triangles by order-of-event restrictions. One half of each quadrilateral, or every other event triangle, satisfies the requirements of Lemma 3.2.4. We consider some concrete examples in Figure 3.17

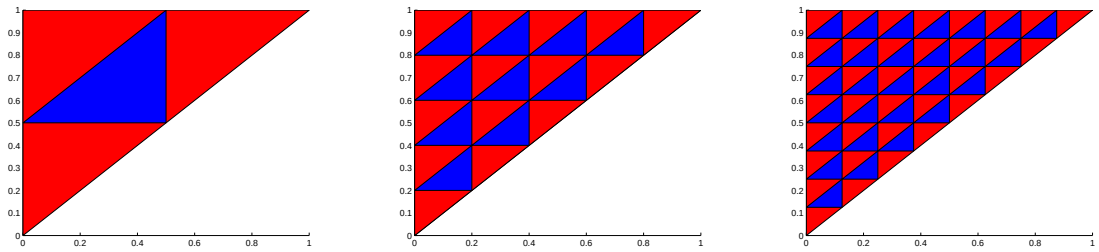

Figure 3.17: We partition parameter space into regions where the hypothesis of Lemma 3.2.4, and thus Theorem 3.5.1, holds (in blue) and regions where it does not (red) for $k = 2, 5,$ and 8.

If we compare regions of observed stability to regions where the lemma holds, we see that the first has always been a subset of the second; thus in all observed cases, stability in the clustered subspace implies stability in the full space. In fact, we have the machinery in place to prove this. Lemma 3.3.1 states that asymptotic stability cannot occur under the order of events e_se_r, under any form of feedback, while Theorem 3.5.1 says that if a k-cyclic solution is asymptotically stable in the clustered

subspace under negative feedback, and has order of events $e_r e_s$, then it is stable in the full phase space. These facts imply the following important theorem.

3.5.2 Theorem. *Every k-cyclic solution that is asymptotically stable in the clustered subspace is asymptotically stable in the full phase space.*

3.6 Conclusions and discussion

In this chapter, we have proven a number of results on the stability of cyclic and uniform solutions. From a biological viewpoint, two of these are paramount.

First, we have proven that cyclic and uniform solutions are unstable under positive feedback in interior triangles, under very minor assumptions. We had suspected positive feedback of being inappropriate for modeling clustering in the cell division cycle of yeast because it facilitates synchrony, which is abiological, and the instability of the $k = M + 1$ case further suggested this; we can now say that positive feedback is appropriate only when synchrony of oscillators is observed. As an example of an application where positive feedback might be an appropriate modeling tool, we cite the work of Buckalew et al. [13], founded on the fact that drosophila embryos divide in synchrony.

Second, we have proven that stability in the clustered subspace implies stability in the full phase space. The significance of this is clear, since in the presence of noise and other neglected biological realities, real configurations of yeast cells cannot occupy the clustered subspace (i.e. go through division in perfect synchrony). We now see that in the study of stability, at least, considering the clustered subspace is a valid simplification.

We have seen in Chapter 2 that s and r may be expected to be on the order of .35 and .75, respectively. Thus, for biologically realistic parameter values, the edges of parameter space are of only mathematical interest. However, we also observed in that chapter that in the negative-feedback case for k prime, stability triangles are

seen to be perfectly regular. On the edges of the (s, r)-triangle this regularity can now be understood, springing from the fact that if k is prime, the greatest common denominator of k and any other number is 1. Although it is possible that the regularity on the boundary and the regularity in the interior are unconnected, it seems more likely that the results on the edge of parameter space are reflections of fundamental number-theoretical properties of the RS model that are still poorly understood. Clarifying this relationship remains an area of open research.

The other major open problem related to this chapter is the stability of the uniform solution. We have proven that the uniform solution (like any k-cyclic solution) is unstable under negative feedback for at least half of parameter space. Based on the observations of the last chapter, we expect a much stronger theorem to be true: as $k \to \infty$, the proportion of parameter space where the k-cyclic solution is unstable should approach 1. This conjecture remains open.

4 Stochastic Noise[§]

4.1 Introduction

In the previous two chapters, we considered the stability of the clustered k-cyclic solutions. We found that the $k = M + 1$ solution, among others, is stable in the clustered subspace, and therefore stable in the full phase space, under negative feedback. We now consider stability in practical terms; what dispersive forces are at work within the biological system, and whether asymptotic stability is powerful enough to counteract them. For example, mother and daughter cells travel through the cell division cycle at slightly different rates, and therefore may tend not to cluster together. Other, less systematic, sources of noise might also tend to cause dispersion. Thus, stability must be strong enough to overcome the specific biological phenomena causing dispersion for clustering to occur. In this chapter we consider the relationship between these two competing tendencies, clustering and dispersion, in the RS model (1.3.3). We reproduce the differential equation below (4.1.1) for ease of reference.

We will consider the two biological mechanisms for dispersion that are known in budding yeast, namely variable growth rate and asymmetric division [95] and contrast them with standard additive Gaussian perturbations in terms of the effect on solutions.

$$\frac{dc_i}{dt} = \begin{cases} 1, & \text{if} \quad c_i \notin R \\ 1 + f(I), & \text{if} \quad c_i \in R. \end{cases} \tag{4.1.1}$$

We recall from the introduction that the signaling region is hypothesized to occur in the S phase of the CDC, and the response region to occur late in the G1 phase, while division occurs at the end of the M phase; see Figure 1.1. Traditionally, division would be taken to occur at time 1 when the CDC is viewed as a unit circle

[§] In accordance with ScienceDirect's policy for using previously published articles in an academic dissertation, we here give the DOI number by which the official publication of which this chapter is an edited version may be found: 10.1007/s00285-014-0786-7.

(satisfying the intuition that a cell should begin its life at 0), while we have also used 1 to be the dividing point between R and S. This conflict, irrelevant to previous chapters, cannot be ignored now that division will be used as a method of adding noise to the system. Throughout this chapter, therefore, we will retain the intuition that cells begin their life at 0 (i.e. that division occurs at 1) and define $R = [0.3, 0.65]$ and $S = [0.65, 0.95]$. Having rescaled the cell division cycle to be of length 1, these intervals are in approxomately the correct location (the end of G1 and the beginning of the biological S-phase), and their length is chosen such that the 2-cyclic solution is in the interior of a stable event triangle.

Throughout this chapter, we will use σ to represent standard deviation, as is standard in probability. We will not have cause to refer to the last cluster not in S on the Poincaré section, and thus there should be no confusion with our previous usage.

4.2 Perturbed models and numerical integration

We summarize three methods of introducing noise into the system. Noise is added on a cell-by-cell basis (i.e. as a method of perturbation in the full phase space). All three of the models in this section will be taken to have the same standard deviation, but in the asymmetric division model (Section 4.2.1), noise is applied once, after which the cell in question travels through the CDC in the normal way (i.e. at a rate governed by (4.1.1)). In the stochastic differential equation (SDE) model (Section 4.2.2) and the variable rate model (Section 4.2.3), noise is applied at each time step, and the effective noise is therefore expected to be higher than in the asymmetric division model; this forms a recurring theme of the simulations, wherein the SDE and variable rate models will frequently exhibit essentially similar behavior, while the asymmetric division model will be phase-shifted to represent the fact that a larger σ is required to produce the same effect. Of the three, asymmetric division is also the only model to make use of a discrete random variable.

4.2.1 Asymmetric division model

Budding yeast divides asymmetrically resulting in distinguishable mother and daughter cells. Because daughter cells are smaller than their mothers at division, they have a longer time to maturity and thus a longer cell cycle. These differences disperse the cell cycle synchrony of an initially synchronous population [86, 95] and complete population synchrony is generally impossible to maintain in the laboratory [9, 45, 93]. We refer to this mechanism of population dispersion as *asymmetric division*. Versions of this mechanism were studied in [21, 33] where, in the absence of coupling, it was shown to lead to a globally attracting steady state.

To model asymmetric division we use equations (4.1.1) for progression through the cell cycle, but we adjust the length of the cell cycle by applying a Bernoulli random variable to each cell when it divides. When a cell arrives at 1, the Bernoulli random variable will determine if the cell begins the next cycle at either 0 or -2σ, with equal probability. Thus each new cell will have equal probability of being either a mother or daughter cell. Note that because if the placement of R and S, such a cell travels at unit rate until it reaches 0. We remind the reader that because the population in a bioreactor is approxomately constant, our model treats the number of cells as fixed, and thus, although biologically division of course produces both a mother and daughter cell, our model does not keep track of both of them.

Let $B_k \sim 2\sigma B(1, 0.5)$ be independent, identically distributed Bernoulli random variables. We apply B_k on the cell c_k when it divides, (i.e. the first time c_k crosses 1 within each cycle). The progression of the k-th cell in each cycle governed by equation (4.1.1) with the addition of this noise can be numerically integrated as

$$c_k^{j+1} = \begin{cases} c_k^j + ha(c_k^j, I_j) - 1 - B_k, & c_k^j + ha(c_k^j, I_j) > 1 \\ c_k^j + ha(c_k^j, I_j), & \text{otherwise.} \end{cases}$$

Thus in the numerics, we do not associate 0 with 1. Rather, we allow the cell c_k to travel for some fixed time step, and subtract 1 during the next time step if the current time step takes it past 1.

The difference between mother and daughter cells is systematic; every time a cell reaches division, it is assigned one of the two roles, but the system is otherwise deterministic. This carries with it the (inaccurate) assumption that any two mother cells or any two daughter cells will be identical at the moment of division. In reality, physical variation and epigenetic differences among the isogenic cells may produce small, non-systematic variations in growth rate. We consider two methods of adding such noise to the system, one biologically motivated, one purely mathematical (but well-understood.) Although it would be biologically realistic to consider a combination of the asymmetric division model with one or both of these methods (thus modeling both the mother/daughter dichotomy and epigenetic differences), we prefer to consider each model separately for now; once each model is well-understood, considering how they interact may form a source of future research.

4.2.2 Stochastic differential equation model

There is an obvious, and mathematically standard, way to add noise to the system.

$$\frac{dc_k}{dt} = a(c_k, I) + \sigma N_k(t) = \left\{ \begin{array}{ll} 1, & \text{if} \quad c_k \notin R, \\ 1 + f(I), & \text{if} \quad c_k \in R \end{array} \right\} + \sigma N_k(t), \tag{4.2.1}$$

where $N_k(t)$ are zero-mean Gaussian white noise sources, uncorrelated among different cells, i.e. $\overline{N_k(t)N_{k'}(t+\tau)} = \delta_{k,k'}\delta(\tau)$.

We used the Euler-Maruyama method to numerically integrate (4.2.1):

$$c_k^{j+1} = c_k^j + h\, a(c_k^j, I_j) + \sigma \sqrt{h} N_k^j,$$

where N_k^j is a normally distributed pseudo-random numbers and h is the integration time step.

The advantage of adding zero-mean Gaussian white noise is that, since it is standard, it is mathematically well-understood. However, this method of adding noise to the system, beyond merely failing to be biologically motivated, is explicitly non-biological, since it may cause cells to travel backwards through the cell division cycle, when in fact cell growth is non-reversible, or cause every cell in the bio-reactor to pass through its cell division cycle in a fraction of a second. We will see in simulation, however, that even if such aberrant events may occur with non-zero probability, they do not have a decisive influence on the system, which acts (under a wide variety of metrics) similarly to more realistic models.

4.2.3 Variable rate model

Considering the epigenetic differences and physiological variations among the isogenic cells which may produce small variations that favors population diffusion [3], we propose the following perturbed coupling model:

$$\frac{dc_k}{dt} = \begin{cases} 1 + U_k(t), & \text{if} \quad c_k \notin R \\ 1 + U_k(t) + f(I), & \text{if} \quad c_k \in R, \end{cases} \tag{4.2.2}$$

where $U_k(t)$ is a uniformly distributed random variable, $U_k(t) \in [-\sigma/\sqrt{3}, \sigma/\sqrt{3}]$. The standard deviation of a continuous, uniformly distributed random variable on an interval $[a, b]$ is $\frac{b-a}{2\sqrt{3}}$, so this interval is chosen to have a standard deviation of σ. Because the noise is being drawn from a closed interval, this model does not suffer from the problems of the SDE model; for appropriately chosen σ, the derivative of (4.2.2) will always be positive, and it is bounded above.

The variables $\{U_k(t), k = 1, \cdots, n\}$ are taken to be independent and identically distributed and satisfy $\overline{U_k U_{k'}} = \delta_{k,k'}\sigma^2$. For the k-th cell, variable $U_k(t)$ remains constant within each cycle and is updated when the k-th cell passes through its division at $1 \sim 0$.

We integrate (4.2.2) numerically by the Euler method,

$$c_k^{j+1} = c_k^j + h\left[a(c_k^j, I_j) + U_k^j\right],$$

where U_k^j is updated when c_k crosses 1. Figure 4.1 shows the distributions of the cells in the variable rate model for several values of the noise's standard deviation, σ.

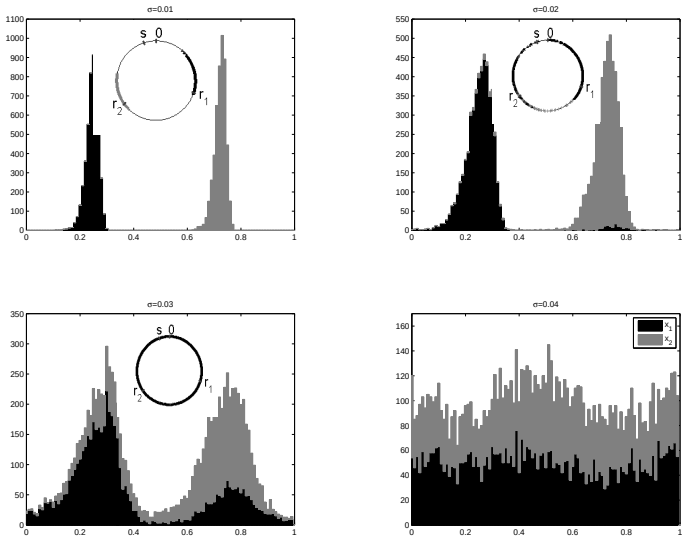

Figure 4.1: Steady-state distributions of two clusters in the variable rate model of noise for the indicated values of σ. Insets show positions of cells on the circle with indicated signaling (S) and responsive (R) regions.

4.2.4 Truncation errors of the method

Note that the vector field given by $a(c_k, I)$ in (1.3.3) is piece-wise constant. On the domains where it is constant a first order Euler method is accurate to machine rounding. A truncation error, δ, may occur when a cell crosses the S boundary, but cells in R cannot increase in rate until the next time step. This error is at most

$$\delta \leq h \left| f\left(\frac{j}{n}\right) - f\left(\frac{j+1}{n}\right) \right| = O(\frac{h}{n}).$$

In the simulations below, we will use $f(I) = -0.5I$ and so the error is precisely bounded by $h/2n$. Furthermore, this error applies to all cells in R equally, thus it does not contribute to the dispersion of a cluster unless the cells in the cluster happen to straddle the boundary of R when a cell crosses the S boundary. For weak noise

($\sigma \ll 1$) these are rare events, since most cells are tightly clustered and the two clusters are expected to cross the S and R boundaries at distinct times (see Appendix B.1). There is also a similarly sized truncation error when a cell steps across the R boundary. In order to make these errors smaller than the applied noise, we used the integration step, $h = 5.0 \times 10^{-3}$, for which local truncation errors are at most 2.5×10^{-7} whereas our smallest non-zero noise σ is 5.0×10^{-4}.

4.3 Simulations and statistical measures

Throughout the simulations we set the coupling term to be linear and negative, $f(I) = -\alpha I$, where the parameter α determines the coupling strength. In the following we fixed $\alpha = 0.5$ and simulated an ensemble of $n = 10^4$ cells which were initially distributed in two clusters at $c_k = \bar{x}_1 = \frac{1}{4}$ for $k = 1, .., \frac{n}{2}$ and $c_k = \bar{x}_2 = \frac{51}{70}$ for $k = \frac{n}{2} + 1, ..., n$, i.e. at the values of the two-cluster periodic solution of the deterministic system (see Appendix B.1).

The collective dynamics of the cell ensemble are conveniently described on a unit circle, so that the probability density function of the ensemble $p(t, x)$ are periodic, i.e. $p(t, x) = p(t, x + 1)$. The second Fourier harmonic of such a distribution is,

$$V_2(t) = \overline{\exp[4\pi i c_k(t)]}, \tag{4.3.1}$$

where $V_2(t)$ is also known as the resultant vector in context of circular statistics [27]. In (4.3.1) the averaging, $\bar{\cdot}$, is taken over the entire ensemble, $\overline{\exp[4\pi i c_k(t)]} \equiv (1/n)\Sigma_{k=1}^{n}[\exp[4\pi i c_k(t)]]$. The magnitude of the second harmonic, $L_2(t) = |V_2(t)|$, which we call the *order parameter* [87],

$$L_2(t) = |\overline{\exp[4\pi i c_k(t)]}|, \tag{4.3.2}$$

serves as a measure of phase coherence of the two-cluster solution. For the deterministic case the probability density is the sum of two delta functions, $p(x) = 0.5[\delta(x - \bar{x}_1) + \delta(x - \bar{x}_2)]$, the order parameter L_2 attains its maximal value near 1 (it

is not exactly 1 since in the periodic solution the phase difference of the clusters is not exactly π). In the opposite limit of a disordered state with a uniform distribution, the order parameter is 0, i.e. $L_2 = 0$.

We comment on our use of the phrase "uniform distribution." Under any type of noise, the system cannot tend to a truely uniform state, because cells in R will always (on average) travel at a slower rate than cells not in R, and thus the probability of a cell being found in R is greater than $|R|$. We retain the phrasology, however, because the disordered state is the continuous analogue of the discrete uniform solution.

Noise-induced spread of a single cluster can be analyzed, with angular deviation defined as follows. We introduce the resultant vector for the first cluster,

$$V_2^1(t) = \overline{\exp[4\pi i c_k(t)]}_1,$$

where the averaging, $\bar{\cdot}_1$, is taken only over the cells which were initially in that cluster, i.e. $\overline{\exp[4\pi i c_k(t)]}_1 \equiv (2/n)\Sigma_{k=1}^{n/2}[\exp[4\pi i c_k(t)]]$. Then, the angular deviation is

$$D_c(t) = \sqrt{2[1 - |V_2^1(t)|]} = \sqrt{2[1 - |\overline{\exp[4\pi i c_k(t)]}_1|]}, \tag{4.3.3}$$

attaining values from 0 (delta-peaked cluster) to $\sqrt{2}$ (uniform distribution).

In addition to circular statistics measures above, the Shannon entropy, which is maximized when a probability density function is uniform [57], is a natural way to measure clustering. We have thus characterized the shape of the steady state probability distribution $p(x)$ using a normalized entropy E. Numerically, we used $M = 100$ equal-sized partitions of the unit interval to estimate $p(x)$ and its Shannon entropy,

$$H = -\sum_{m=1}^{M} p_m \log p_m. \tag{4.3.4}$$

In the absence of noise, the two-cluster solution is characterized by a double delta-peaked distribution and the entropy takes its minimal value, $H_{\min} = \log 2$ for symmetrical clusters with $n/2$ cells in each. In the completely disordered state the distribution $p(x)$ is uniform with the maximal possible entropy $H_{\max} = \log M$. The

normalized entropy defined as,

$$E = \frac{H - H_{\min}}{H_{\max} - H_{\min}} = -\left(\sum_{m=1}^{M} p_m \log p_m + \log 2\right) / \log(M/2), \tag{4.3.5}$$

varies between 0 (noiseless two symmetrical clusters) and 1 (disordered state, cells are distributed uniformly).

We find that increasing σ causes the normalized entropy of the SDE and variable rate models to increase at almost precisely the same rate. The asymmetric division model causes the entropy to increase at a slightly slower rate, since the noise is added only once in that model, as opposed to in every time step, and thus the same σ results in less actual noise being applied to the system. The essential similarity of the models is important; a biologically useful model must be robust under noise, and it would be problematic if two biologically motivated forms of noise gave rise to wildly different behaviors.

For a given value of noise level, σ, the ensemble "thermalizes" – evolving towards a steady state, which we characterized by two methods. The first method was based on comparison of the ensemble distributions at consecutive times when the ensemble was at a given position on the cycle. In particular, snapshots of the ensemble were taken at moment of times when the imaginary part of the ensemble's second harmonic, $\overline{\sin[4\pi i c_k(t)]}$, was crossing zero with a negative slope. A two-sample Kolmogorov-Smirnov (K-S) test was used to probe whether the ensemble distribution settled down to its steady state. In the second method we used convergence to a steady state value of the circular measures, $L_2(t)$ and $D_c(t)$, introduced above. As we show further on, for all the three models, the relaxation time for the ensemble to reach its steady state is less than 100 cycles, as long as σ remains below a critical noise strength at which the clustering effect of the model is destroyed completely. Because of periodicity of the two-cluster solution and finite size fluctuations, the ensemble-averaged measures L_2, D_c and E are time-dependent even in the steady state. We thus

performed additional time averaging of L_2, D_c and E over $T = 100$ after the ensemble reached its steady state, resulting in time-averaged quantities, $\overline{L}_2$, $\overline{D}_c$ and $\overline{E}$.

Representative examples of steady-state distributions for individual clusters are shown in Figure 4.1. For weak noise ($\sigma \in [0.01, 0.02]$) the ensemble converges to the steady state in less than 20 cycles, according to the K-S test. For larger noise, $\sigma > 0.025$, convergence is slower, in about 80 cycles.

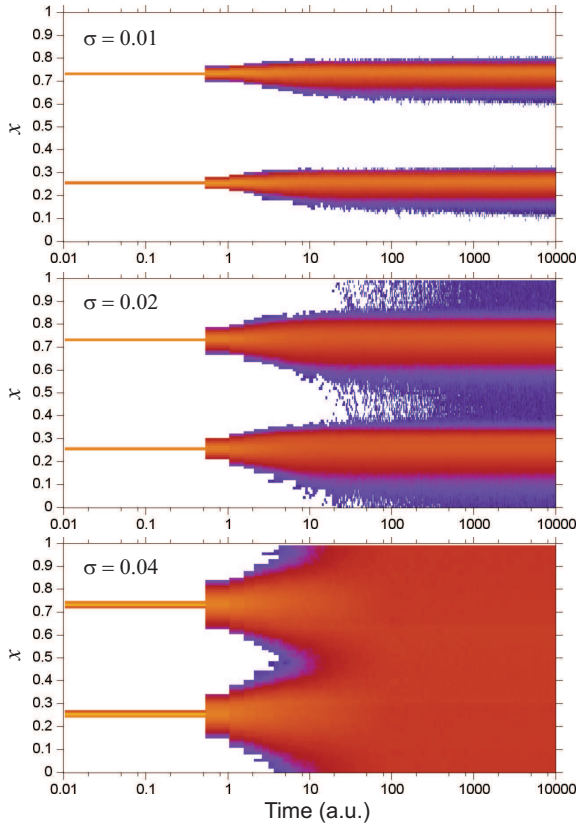

Figure 4.2: Time-dependent probability distributions $p(t, x)$ of the ensemble with Gaussian white noise (SDE model) for the indicated values of noise level σ. Logarithm of the probability distribution, $\log[p(t, x)]$, is shown as filled contours. For weak $\sigma = 0.01$ noise, clusters spread out but remain distinct. For weak-intermediate noise ($\sigma = 0.02$), cells begin to move between clusters, but clustering still occurs. At $\sigma = 0.04$, clustering has been destroyed. The critical point at which clustering fails, about $\sigma = 0.35$, is not shown here, but see Figure 4.3.

4.4 Results

4.4.1 Transitional dynamics

Figure 4.2 shows that the ensemble distributions taken at a fixed position on the cycle (see previous section) evolves towards steady states for the SDE model. Weak noise ($\sigma = 0.01$) results in the spread of cells within each group. Although there is no theoretical minimum level of noise at which cells may transition between groups, exponentially long waiting times for such events to occur in the presence of weak noise make such events profoundly rare. Coherent groups still exist for an intermediate noise ($\sigma = 0.02$), although cells migrate between them, which is indicated by appearance of non-zero probability between peaks in the time-dependent probability map (middle panel of Figure 4.2). For $\sigma > 0.04$ the asymptotic stability of the 2-cyclic solution is no longer sufficient to overcome the dispersive force of the noise, and the ensemble quickly approaches a steady state with a uniform distribution.

The transitional dynamics are characterized further in Figure 4.3. Both the order parameter, $L_2(t)$, and angular displacement of individual clusters, $D_c(t)$, show characteristics approaching the steady state which are similar for all three models of noise. For weak to intermediate noise ($\sigma < 0.03$), the order parameter and angular displacement settle to steady states within 100 cycles as the asymptotic stability of the 2-cyclic solution quickly overwhelms the noise. For large ($\sigma > .04$) noise, the averaging of the expansive effect of the noise and the contractive effect of the stability is expansive, and the parameters again reach steady states within 100 cycles as the system moves to a completely disordered state. However, for a critical noise level ($\sigma \approx 0.035$ for the SDE, $\sigma \approx 0.034$ for the uniform, and $\sigma \approx 0.04$ for the Bernoulli noise model), the relaxation process slows down dramatically and shows larger fluctuations in the steady state. This indicates the occurrence of a phase transition (bifurcation) from the ordered state with two clusters to the completely incoherent disordered state of the

ensemble. We recall again that the noise of the Bernoulli model is applied only once instead of at every time step, explaining why a larger σ is required to achieve the same effect as in the other models. For the SDE model, the cell migration between groups

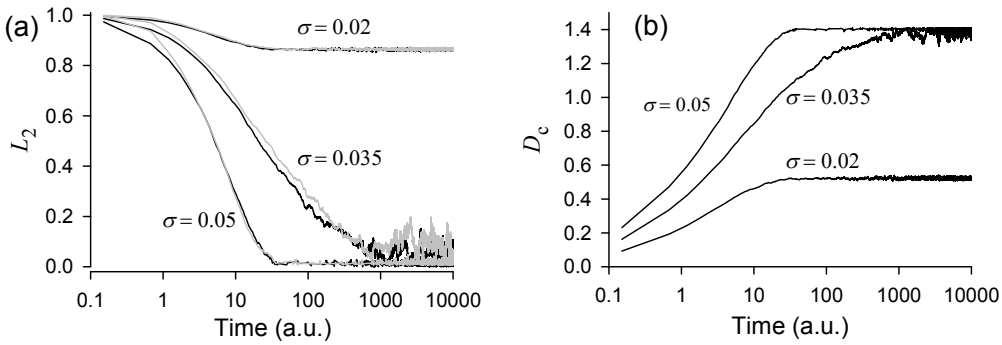

Figure 4.3: Time-dependence of (a) the order parameter, $L_2(t)$, and of (b) the angular deviation, $D_c(t)$, for the indicated values of noise level σ in the SDE model. For a comparison, the corresponding dependencies $L_2(t)$ for the variable rate model are shown by grey lines on panel (a). The values of noise standard deviations are the same as for the SDE model, except for the middle grey curve, where the noise standard deviation is 0.034.

is expected for any non-zero noise intensity with exponentially long waiting time. By contrast, for bounded noise models (variable rate and asymmetric division) there is a critical noise intensity, σ_h at which a "hard" bifurcation occurs [40]. For $\sigma < \sigma_h$ cells are bound to their initial cluster, while for $\sigma > \sigma_h$ cells can migrate between the clusters. Figure 4.4 shows the fraction of migrated cells after the ensemble evolves over 80 cycles, versus noise level. As expected, the fraction of migrated cells grows with σ for all three models, saturating to 1/2 at the disordered state of the ensemble.

Analytic calculations presented in Appendix B.2 show that for the parameter values used, the hard bifurcation occurs at $\sigma_h \leq 1.4 \times 10^{-5}$, which is far below the noise level where cell migration can be observed for a reasonable integration time. We thus conclude that the hard bifurcation plays no essential role in these examples of biologically motivated noise.

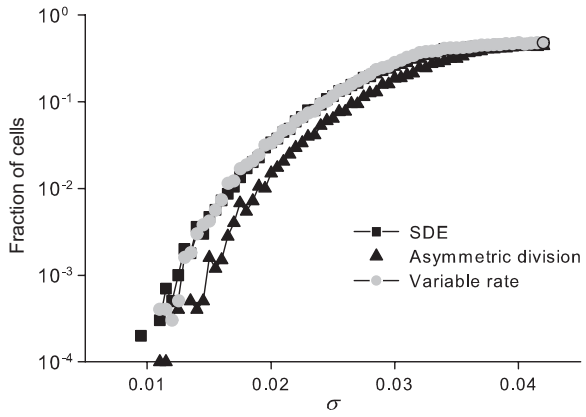

Figure 4.4: Fraction of cells that have escaped from their initial groups after 80 cycles for the three models. For noise levels below $\sigma \approx 0.01$ cells are effectively bound to their cluster by the asymptotic stability of the two-cluster solution.

4.4.2 Sensitivity to noise and order-disorder phase transition

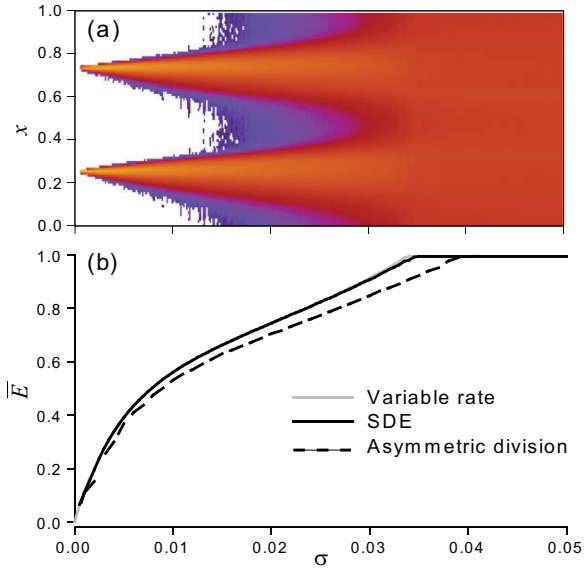

Figure 4.5: (a) Steady-state probability distributions $p(x)$ of the ensemble with Gaussian white noise (SDE model) versus the standard deviation σ of the noise. Logarithm of steady state probability distribution, $\log[p(x)]$, is shown as filled contours. (b) Time averaged normalized entropy $\overline{E}$ of the ensemble in three models versus the standard deviation of the noise σ.

In the absence of noise, groups simply collapse back into clusters (Theorem 3.5.1). As noise is added into the system, such point clustering will cease to occur, but coher-

ent groups will continue to exist. As the strength of the noise increases, grouping will become progressively looser until σ reaches its critical value above which the ensemble assumes a disordered state where no clustering can be distinguishable, as shown in Figure 4.5(a). This change of shape of the steady state distribution is well-reflected by the normalized entropy E, which increases from 0 (no noise) and reaches its maximal value when the ensemble distribution becomes uniform (see Figure 4.5(b)). We can also see from this figure that the three models show qualitatively identical behavior with respect to noise level as to the distribution of the ensemble.

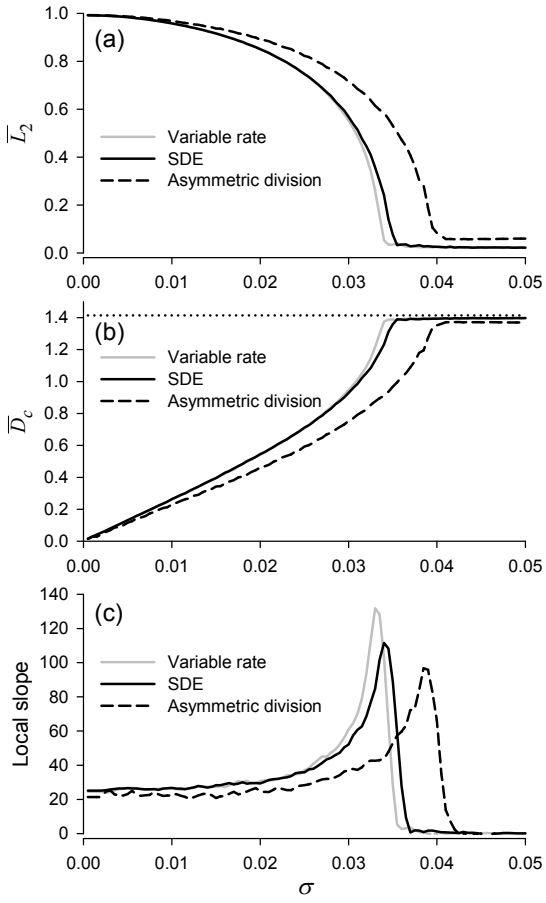

Figure 4.6: Stationary statistical measures of the cell ensemble versus noise level σ for the three noise models. (a) Time averaged order parameter, $\overline{L}_2$, vs noise standard deviation, σ, of the three models. (b) Time averaged angular deviation of the first cluster vs σ. Dotted line shows the maximum possible value of $\sqrt{2}$. (c) Local slopes of angular deviations estimated from the curves in panel (b).

The width of the groups increases along with the strength of the noise, which is characterized by the order parameter and angular deviation shown in Figure 4.6(a,b). This process must eventually terminate, or rather, for any coherent definition of "group," it will cease to be meaningful to talk about multiple groups. The order parameter decreases with the increase of noise until σ reaches a critical effective value σ_c, at which $\overline{L}_2$ vanishes and this occurs.

The spread of the cells in each group is best described by the angular deviation $\overline{D}_c$, which increases with the increase of noise and reaches its maximum value $\sqrt{2}$ at the transition point (i.e. at the point where the uniform distribution is reached and talking about individual groups is no longer meaningful). The dependencies $\overline{D}_c(\sigma)$ in Figure 4.6(b) show three distinct regions of σ. For weak noise, $\sigma < 0.015$, the angular deviation increases linearly with σ, indicating a nearly linear response of the ensemble to noise perturbations. The nearly linear response is broken for intermediate noise whereby $\overline{D}_c$ non-linearly increases with progressively larger slopes. For strong noise, $\sigma > \sigma_c$, the angular deviation $\overline{D}_c$ saturates to its maximum value. This is further illustrated in Figure 4.6(c) by local slopes of $\overline{D}_c$ vs σ dependencies, which clearly shows the regions of linear and non-linear responses. We note that the local slope is a measure of sensitivity of the ensemble to noise perturbations and it shows that this sensitivity is maximal near the transition to the disordered state. This is intuitive, since a small perturbation of noise level where the noise is too small to have significant control over the system will still result in small noise with a small effect. Similarly, for $\sigma > \sigma_c$, i.e. in the disordered state, the ensemble is insensitive to noise perturbations, as indicated by the zero slope of $\overline{D}_c(\sigma)$, since there is a maximum effective noise beyond which the steady state is constant. Only in the border regions can a small change of noise show a significant effect.

Figure 4.6 further indicates that the three noise models show qualitatively identical dependencies on σ. Quantitatively, however, the asymmetric division model

shows consistently lower sensitivity to noise perturbations. We note that while in the SDE and variable rate models noise is applied throughout the whole cycle, the asymmetric division model is perturbed by Bernoulli noise once per cycle only. Hence an effective noise level of the SDE and variable rate model is larger than that of the asymmetric division model. Furthermore, because the distribution of cells in asymmetric division model always has a higher density in the interval $[-2\sigma, 0]$ in phase space the order parameter saturates to a non-zero value for large σ in Figure 4.6(a), although it is functionally uniform.

At the critical value of noise SD, $\sigma = \sigma_c$, the ensemble demonstrates features of an order-disorder phase transition, such as slowdown of transient relaxation to the steady state and large fluctuations (see Figure 4.3). The transition of the distribution of the solution has the characteristics of an Andronov-Hopf bifurcation, as indicated by Figure 4.7. For $\sigma < \sigma_c$ the model possesses a stable limit cycle that bifurcates to a stable focus for $\sigma > \sigma_c$. Here the large noise effectively stabilizes the uniform solution, which otherwise is unstable. Further, in Figure 4.6(a) we observe that the amplitude of the periodic orbit has a square root type dependency on σ, as in a Hopf bifurcation. We note here that this transition is consistent with order-disorder transitions in the Kuramoto model of globally coupled stochastic phase oscillators [74]. There the rotation of the original variables has been discarded by the transformation to phase differences, so the linearization there has zero imaginary part at the bifurcation.

Since the critical noise level, σ_c measures the point at which the noise completely overwhelms the feedback, it is a function of the coupling strength, α. Figure 4.8 shows that a stronger coupling requires stronger noise to destroy the two-cluster ordered state. The white curve in this graph corresponds to a bifurcation line separating ordered and disordered states in the (α, σ) parameter plane. The region below the white curve represents cells in the two-cluster ordered state, possessing a limit cycle. While the region above the white curve represents cells in disordered states,

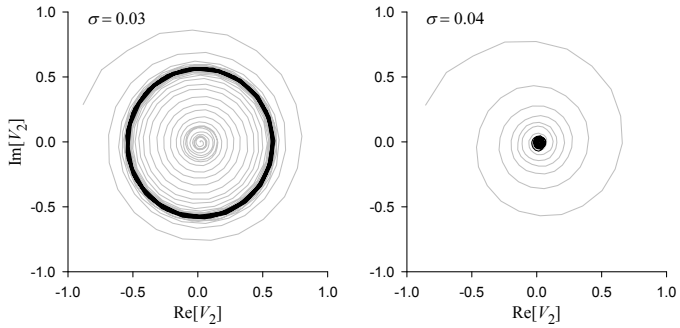

Figure 4.7: Phase portraits of the SDE model projected onto the complex plane of the second Fourier harmonic. Black lines show steady state trajectories; grey lines show transients on both panels. Left: two-cluster ordered state, with a stable periodic orbit, $\sigma = 0.03$. Right: stable equilibrium distribution at the disordered state, $\sigma = 0.04$. The order-disorder transition occurs at $\sigma_c \approx 0.035$.

which is a stable uniform solution. This curve is also consistent with phase transitions observed in globally coupled stochastic phase oscillator systems [74].

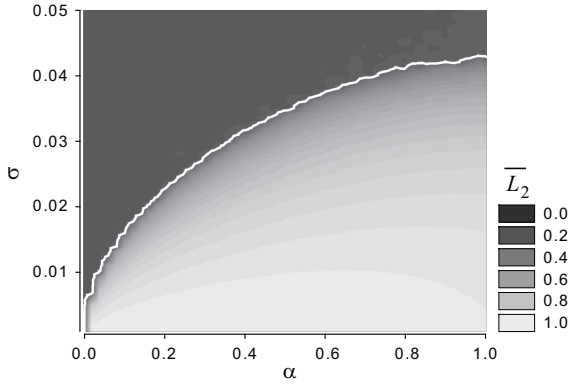

Figure 4.8: Time averaged order parameter, $\overline{L}_2$, as a function of the coupling strength, α, and noise SD, σ.

4.5 Yeast cultures have large coupling mechanisms

In budding yeast, a mother cell carries a scar from the bud and the daughter does not. Replicative age can be determined from the number of scars [75]. A natural

phase space for a model stratified by replicative age is to represent the cell cycle of the daughters by $I_0 = [0, 1]$ and successive generations by $I_m = [a_m, 1]$. In other words, the phase space is: $I_0 \cup I_1 \cup \ldots \cup I_n$ where n is the highest generation considered. In a steady state bioreactor, the fraction of cells in each generation decreases roughly geometrically with age, so n does not need to be large for accurate modeling.

Denote $\tau_m = |I_m| = 1 - a_m$. The age distribution can be measured and is directly related to the relative lengths of the cell cycles τ_m [4]. For one autonomous oscillation experiment in which clustering was detected, our coauthors determined the following population fractions as a function of generation for the first four generations: 0.55, 0.24, 0.11, 0.05 [4]. The corresponding τ_m's are calculated to be: 1.0, 0.93, 0.86, 0.82, so we find:

$$a_0 = 0, \quad a_1 = .07, \quad a_2 = .14, \quad a_3 = .18.$$

In [4, 83] it was shown that simulations using these proportions can accurately reproduce the behavior seen in the YAO experiment [6, 83]. A standard calculation [4] shows that the standard deviation of the generational noise, σ_g, in the experiment is:

$$\sigma_g = 0.0365.$$

This quantity is normalized to a time unit of one cell cycle in the experiment.

In Figure 4.8, we see that for $\sigma \approx 0.036$ a coupling coefficient of $\alpha > 0.6$ is needed for the coupling strength to overcome the dispersive action of the asymmetric division and produce detectable clustering. Consider that the units here are all normalized in terms of one unperturbed cell cycle. We can conclude that for clustering to exist in the autonomous oscillation experiment, as observed, the strength of coupling must be a rather large effect. In a two-cluster state, the clusters as they enter the region where they experience coupling, need to have their rate of progression decreased by a normalized factor of at least 0.3, or, 30%. Such a decrease cannot be considered to be a small perturbation.

4.6 Conclusions and discussion

We have studied the effects of two biologically motivated dispersive mechanisms, as well as standard Gaussian white noise, in an ensemble cell cycle coupling model that successfully predicts clustering behavior observed experimentally.

One conclusion for this simple generic model is that the difference between biologically plausible bounded noise and Gaussian noise mechanisms is insignificant after proper scaling of the noise level. This is observed in both the ensemble statistics of the clusters and in terms of the expected phenomena of bounded noise dynamics. As seen in Figure 4.6, asymmetric division and variable rate perturbations lead to circular statistics measurements that are indistinguishable from the results using Gaussian white noise perturbations. Further, the theory of bounded noise dynamical systems predicts that cells will be unable to escape a stable cluster for noise levels below some threshold. However, we observe in this application that the threshold is far too small to play a role in observed behavior. For such small values of noise, the expected time to escape would be extremely long for the Gaussian noise model and so there is no observable difference.

For all three forms of applied noise perturbations the dispersion of clusters occurs in three distinct phases. First, for small noise there is a linear relationship between the noise level and the dispersion of the clusters measured by the circular angular deviation. In this phase cells do not migrate from their initial groups on the time scales considered. In the second phase cells begin to migrate more frequently between clusters and the slope of the dispersion versus noise increases. Finally, for noise level above a certain threshold the clustering structure is destroyed and the cells assume a nearly uniform distribution. This phase transition between disorder and order exhibits many characteristics of a Hopf bifurcation, e.g.the birth of a stable limit cycle out of a stable equilibrium and a square-root dependence of the amplitude of the periodic orbit on the bifurcation parameter (noise level).

Finally, we conclude that the clustering observed in autonomous oscillation experiments cannot be due to small coupling effects. When we compare experimental data with the transition from clustered to uniform distribution in Figure 4.5, we can see that the expermentally established level of dispersion due to asymmetric division alone is enough to require a coupling strength at least strong enough to produce a 30% relative decrease in rate of progression when a cell enters the responsive region. Although the model is minimal, it is both universal and normalized to the length of the unperturbed cell cycle, so this estimate of relative effects of noise and coupling is reliable. One possible explanation for a coupling strength of this magnitude is that the mechanism actually involves one or more check points in the cycle. We also note an alternative (or complimentary) solution. Xue at al. [30] have shown that modeling even a small delay mechanism into an RS model will strengthen stability, speeding up the rate of convergence significantly. It remains a source of future work to formally investigate how the gap model of [30] and the noise mechanisms of this chapter interact, but intuitively, we expect that modeling a delay will allow groups to remain coherent under weaker feedback. It remains to try to detect such a slow-down in laboratory settings.

5 The Overlap Model

In the previous chapters, we have considered in some depth the RS feedback model defined by regions $R = [r, 1)$, $S = [0, s)$, and differential equation

$$\frac{dx_i}{dt} = \begin{cases} 1, & \text{if} \quad x_i \notin R \\ 1 + f(I), & \text{if} \quad x_i \in R. \end{cases} \tag{5.0.1}$$

In the introduction, we mentioned that a number of theorems continue to hold when positive and negative feedback are reversed, and the position of R and S are also reversed, i.e. $S = [s, 1)$ and $R = [0, r)$. In [30] the authors considered the effect of adding a small gap between R and S.

There remains one natural modification to consider, a converse to adding a gap: that R and S might be allowed to overlap. We consider such a model in this chapter. We analyze the 2-cyclic solutions and the $k = M + 1$ solutions, and find similar behavior to the RS model in the clustered submanifold. In the full phase space, however, we find complex behavior dependent on the form of the feedback function, one of only two known cases where the details of the function, rather than its sign, have a controlling influence on the stability of k-cyclic solutions (see Section 3.4.5 for the other case, where event triangles are neutral under weak positve feedback and unstable under strong positive feedback).

5.1 Background and model

5.1.1 Signaling models

We have considered a feedback model where cells c_i advance around S^1 under the influence of the differential equation

$$\dot{c}_i = \begin{cases} 1 & c_i \notin R \\ 1 + f(I) & c_i \in R, \end{cases} \tag{5.1.1}$$

for $i = 1, 2, ..., n$, where I is the proportion of cells in S and the feedback function f is the mathematical mechanism by which the signaling occurs. The function f may be taken to be quite general, with only a few clearly motivated restrictions:

1. Cells in S cannot produce signaling agents if there are no cells in S. Ergo, $f(0) = 0$.

2. The more cells that are signaling, the stronger the signaling should be. Thus, f should be monotonic.

3. Growth is a non-reversible process. Therefore, $-1 < f(I)$ for all I.

We have assumed in previous chapters that S and R are intervals with an endpoint in common and disjoint interiors, and that a cell not in $R \cup S$, travelling in the direction of the flow, enters R before it enters S. In Chapter 2 and Chapter 3, we defined a specific coordinate system such that $R = [r, 1)$ and $s = [0, s)$. This model is a special case of an RS-feedback system (Definition 1.3.1).

We now consider the behavior of the model under the assumption that the intersection of R and S has non-empty interior, with the following restrictions:

- Both $R \backslash S$ and $S \backslash R$ are nonempty, i.e. neither interval is a proper subset of the other.

- If $c_i \notin S \cup R$ travels clockwise around the circle S^1 with some positive velocity, c_i will enter R before it enters S.

We consider two cases where a cell in R is being influenced by a single cell in S. Intuitively, since the population is so large, a single cell in $S \backslash R$ should have a negligible effect on cells in R (see the discussion after Theorem 5.2.1; also observe that if $f : [0, 1] \to (-1, \infty)$ is a continuous feedback function and n is sufficiently large, then $f(1/n) \approx 0$ by the condition that $f(0) = 0$.)

Now consider the case where S contains only a single cell, but that cell lies in $S \cap R$. This cell is producing a chemical within itself, and immediately responding to the presence of that chemical. This effect need not be trivial, although the cell is still receiving feedback from only one cell, i.e. itself. We modify the differential equation to reflect this. In the following equation, f is a feedback function, i.e. $f(0) = 0$, the function f increases monotonically, and the codomain of f is $(-1, \infty)$:

$$\dot{c}_i = \begin{cases} 1 & c_i \notin R \\ 1 + f(I) & c_i \in R \backslash S \\ 1 + g(I) & c_i \in R \cap S, \end{cases} \tag{5.1.2}$$

where g is a feedback function (i.e. satisfies the requirements (1) - (3) put on f), and has the same sign as f. Since g was explicitly brought into the system to allow for more powerful feedback when a cell influences itself, it should also satisfy the inequality $|f(I)| \leq |g(I)|$ for all I. Viewing g as a function from the unit interval into $(-1, \infty)$, g is presumably discontinuous at 0, since it was explicitly created to allow $|g(1/n)| \gg 0$ when $1/n \approx 0$. The function g should have the same sign as f, and be strictly monotone.

We will define $O := R \cap S = [s_1, r_2)$. It will be necessary to speak of $\widetilde{R} := R \backslash O$; likewise, we will let $\widetilde{S} := S \backslash O$. We now unify our notation for this chapter with that of the previous chapters and [30]. In all three models, we will use r to represent the beginning of the responsive region and s to represent the end of the signaling region. In all three models, we (or the authors of [30]) choose a coordinate system such that the end of the responsive region lies at 1, i.e. $r_2 = 1$. By the definition of the RS model, 1 is thus also the beginning of the signaling region in that model. In [30], ϵ was used to represent the beginning of the signaling region (and, concurrently, the size of the gap); we choose a different representation for the beginning of the signaling region in the overlap model, s_1, to emphasize the fact that the beginning of S happens in a different

part of the circle in each model–to the right of 0 in the gap model, and to the left of 1 in the overlap model.

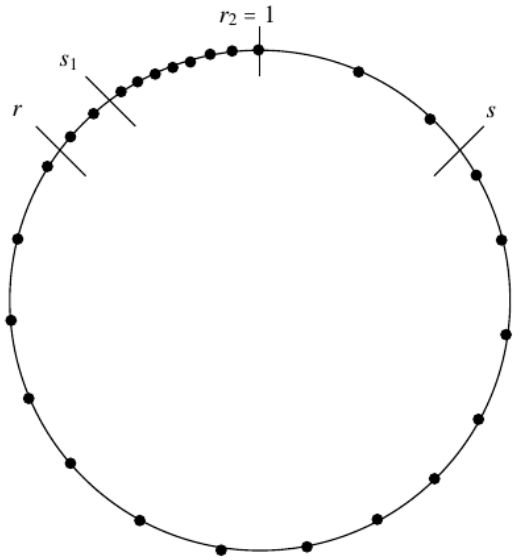

Figure 5.1: The state space of the overlap model is the unit circle S^1 with two overlapping regions, $R = [r, 1)$ and $S = [s_1, s)$. The cells are arranged in the form of a uniform solution under negative feedback. Cells in $\widetilde{R}$ travel at a slower rate than cells in $S^1 \backslash R$, and are therefore closer together, while cells in O are closer together still, by the assumption that $|g| \geq |f|$ ($g < f < 0$ in this example). The overlap region O would normally be assumed to be rather small; it is exaggerated here for emphasis.

5.1.2 Generalizations of previous concepts

The overlap model is similar enough to the RS model that many tools of analyzing the RS model may continue to be used with no or minor modifications. We start by observing that, as in the other models, (5.1.2) can be applied to equally-sized, perfectly synchronized clusters as easily as to cells. Denoting clusters as x_i, we obtain

$$\dot{x}_i = \begin{cases} 1 & x_i \notin R \\ 1 + f(I) & x_i \in \widetilde{R} \\ 1 + g(I) & x_i \in O, \end{cases} \tag{5.1.3}$$

where I is the proportion of clusters in S.

The proof of Lemma 1.4.2 generalizes to the overlap model without modification, and thus the functions f and g for clusters in equation (5.1.3) are the same as in (5.1.2) for cells.

The set $\{\bar{x}|x_1 = 0\}$ still defines a Poincaré section, and the Poincaré map P is still factorized as the composition of k F-maps, where $F(x_2, x_3, ..., x_k) = (x_1(T), x_2(T), ..., x_{k-1}(T))$, $T = \min\{t|x_k(t) = 1\}$. The map F has fixed points in the overlap model, by the same argument as in the RS model, which we term k-cyclic fixed points, and these fixed points correspond to periodic orbits under the flow of the system.

5.2 The synchronized solution

The most basic solution of (5.1.3) occurs when all cells are synchronized into a single cluster that moves around the circle at a rate of 1 when it does not lie in O and a rate of $1 + g(1)$ when it does. In the clustered subspace, it is meaningless to ask questions of stability, since this solution covers the 1-clustered subspace. In the RS model, we have seen that the synchronous solution is unstable in the full phase space under negative feedback, and stable under positive feedback. In the gap model it is neutrally stable. We now show that the overlap model acts similarly to the RS model, with some (seemingly trivial) condition on the feedback function f.

5.2.1 Theorem. *The synchronous solution is unstable in the full phase space under negative feedback provided $|f(\frac{1}{n})|$ is sufficiently small compared to the rate of growth of the function g.*

Proof. We explicitly exhibit a perturbation of the synchronous solution that moves away from the synchronous solution. In particular, consider an arrangement of cells such that each cell lies in one of two clusters, and the clusters are within a distance of ϵ of one another. Let the leading cluster contain p cells and the trailing cluster contain $n - p$ cells.

The distance ϵ between these clusters will change only when the leading cluster is in O and the trailing cluster is in $\widetilde{R}$, or when the leading cluster is in $\widetilde{S}$ and the trailing cluster is in O. We consider both of these cases.

Let the leading cluster lie at s_1. Then the trailing cluster travels a distance ϵ at a rate of $1 + f(p/n)$, and therefore reaches s_1 at time $t = \frac{1}{1+f(p/n)}\epsilon$. During that time the leading cluster has been traveling at a rate of $1 + g(p/n)$, so the distance between the clusters contracts to $\frac{1+g(p/n)}{1+f(p/n)}\epsilon$, since $-1 < g(p/n) \leq f(p/n) < 0$.

Let time run further until the leading cluster reaches 1. Now there are still n cells in S, but only the trailing cluster lies in R to experience feedback. It must travel a distance of $\frac{1+g(p/n)}{1+f(p/n)}\epsilon$ at a rate of $1 + g(1)$, and the time that takes is $\frac{1+g(p/n)}{(1+f(p/n))(1+g(1))}\epsilon$; since the leading cluster has been traveling at rate 1, this is also the new distance between clusters.

For $p = 1$, therefore, $\epsilon \mapsto \frac{1+g(1/n)}{(1+f(1/n))(1+g(1))}\epsilon$. This is an expansion if $1 + f(1/n) < \frac{1+g(1/n)}{1+g(1)}$.

□

For context, we know from Chapter 4 that $f(I) = -.6I$ is strong enough to overcome the noise inherent to the biological system and cause clustering. In a bioreactor of 10^{10} cells, under that feedback, $1 + f(1/n) = 1 - \frac{6}{100{,}000{,}000{,}000}$; if the greatest rate a cell can attain under the effect of g, divided by the smallest rate that such a cell can attain, is greater than this, an expansion will occur. This theorem thus states that the synchronous solution is unstable under negative feedback in an overlap system unless g is almost constant, where the value $f(1/n)$ is used as a measure of what "almost constant" formally means. Note, however, that if g were perfectly constant (which cannot happen, but which we may consider as a limitting case), then it would be true that $\epsilon \mapsto \frac{1}{1+f(1/n)}\epsilon > \epsilon$, which would also represent an expansion. It is therefore not clear whether any restriction is in fact necessary to the theorem, or whether it is an artifact of the method of proof.

The following theorem does not require any additional assumptions.

5.2.2 Theorem. *The synchronous solution is linearly stable under positive feedback.*

Proof. Consider an initial condition in an $\epsilon/2$-neighborhood of the synchronous solution, i.e. all cells lie within an interval of length ϵ. For definiteness, assume that the ϵ-interval has the form $[0, \epsilon]$, and number the cells such that $c_i > c_{i+1}$ for $i = 1, ..., n-1$. If $c_i = c_{i+1}$ for some i, the proof remains valid with only slight modifications. Notice that we have numbered the cells in the reverse order than we have been accustomed to, $0 < c_n < c_{n-1} < ... < c_1$. Assume that $\epsilon << \min\{|S|, |\widetilde{R}|, |O|\}$, in particular small enough that over the course of one iteration of the Poincaré map, once the first cell in the group enters $\widetilde{R}$, S, or O, all of the cells in the group will enter that region before the first cell leaves it.

The cells have been numbered in such a way that when c_i is in O but c_{i+1} is in $\widetilde{R}$, i cells from the group are exerting feedback on themselves (in the form of g) and on the remaining cells in the group (in the form of f.) Let $\epsilon_i = c_i - c_{i+1}$. Let time progress until $c_1 = s_1$; until this time, the distances ϵ_i remain unchanged, since when the group enters $\widetilde{R}$, S is empty.

Consider how a distance ϵ_i changes as c_i passes into O. Once c_i reaches s_1, c_{i+1} starts to experience feedback $1 + f(i/n)$. It therefore takes time $t = \frac{\epsilon_i}{1+f(i/n)}$ for c_{i+1} to reach s_1; during that time c_i is travelling at a constant rate of $1 + g(i/n)$, for a total distance (that is also the new value of ϵ_i) of $\frac{1+g(i/n)}{1+f(i/n)}\epsilon_i$. Once both cells lie in O, they experience the same feedback, and the distance between them does not change again until c_i reaches 1.

When c_i reaches 1, all cells lie in either O or $\widetilde{S}$, so all cells exert feedback. Once c_i reaches 1, its rate slows to 1, while c_{i+1} continues to travel at a rate of $1 + g(1)$. Thus the distance between c_i and c_{i+1}, that initially expanded to $\frac{1+g(i/n)}{1+f(i/n)}\epsilon_i$, is now contracted, and the contraction is powerful enough that the final distance between c_i and c_{i+1} after an iteration of the Poincaré map is strictly less than the initial distance ϵ_i; in particular, to $\frac{[1+g(i/n)]/[1+g(1)]}{1+f(i/n)}\epsilon_i$. This is a contraction, since $1 < g(i/n) \leq g(1)$ for $i = 1, 2, 3, ..., n$ implies that the numerator is at most 1, and it is divided by $1 + f(i/n) > 1$, resulting in a fraction

strictly less than 1. Note that every iteration of the Poincaré map reduces ϵ_i by a constant factor.

□

5.3 Cyclic solutions

5.3.1 General cyclic solutions

Let $\bar{x}$ be a cyclic solution on the Poincaré section. In a neighborhood of a given k-cyclic solution, certain paramaters are fixed. Recalling our previously stated notation, we return to letting σ denote the number of clusters in S on the Poincaré section, i.e.

$$x_\sigma < s < x_{\sigma+1}. \tag{5.3.1}$$

By x_ρ we represent the last cluster not in R,

$$x_\rho < r < x_{\rho+1}, \tag{5.3.2}$$

and introduce x_ζ as the last cluster not in O, so that

$$x_\zeta < s_1 < x_{\zeta+1}. \tag{5.3.3}$$

Since there are k clusters, and we number them in ascending order, we finally let x_k denote the cluster closest to 1. We allow the clusters x_σ, x_ρ, x_ζ, and x_k to coincide (e.g. if O is empty then $x_\zeta = x_k$). Then over the course of a single F-map, x_σ leaves S, x_ρ enters R, x_ζ enters O, and x_k reaches 1. The event "x_k reaches 1" happens last, as it defines the F-map, but the other three events may happen in any order.

We make explicit a lemma that was left implicit in Chapter 2

5.3.1 Lemma. *Let $\sigma \le \rho \le \zeta \le k$ be fixed, and* **o** *be any order of events such that each event occurs exactly once, and the last event is $x_k \to 1$. Then there are nontrivial feedback functions f and g, and an open region of parameter space dependent on f and g, such that in that region of parameter space, the cyclic solution has the prescribed order of events.*

Proof. Let $f = g = 0$. These are not valid assignments of those functions, but we will make our argument under those conditions, then use continuity to glean information about the overlap model with valid feedback functions. Let $x_i = \frac{i-1}{k}$. Then it is certainly possible to move the parameters r, s_1, and s so that x_σ is the last cluster in S, x_ρ is the last cluster not in R, and x_ζ is the last cluster not in O. It is likewise easy to ensure that the desired order of events occur. Both these things may be accomplished while ensuring that no cluster lies on a milestone (s, r, s_1) except for x_1, which is assumed to lie on 0. Then since the cyclic solution depends continuously on the parameters f, g, r, s_1, and s, we may add small but nontrivial feedback, and the k-cyclic solution will retain its desired form. □

The lemma is proven for small feedback, but in numerical simulations, we have observed all orders of events under strong feedback.

5.3.2 The cyclic solution for $k = 2$ clusters

In Appendix C.1 we enumerate every possible order of events that an F-map may experience, 28 in all, and derive F in each of those cases. In order to make the calculations of the appendix less cumbersome, we introduce a change of variables. By the definition of O, any cluster in O experiences a certain amount of feedback regardless of where other clusters lie on the circle. Since this "baseline" feedback of $g(1/k)$ may be thought to exist independently of the state of the system, it may be simply removed by a change of variables that rescales O. We do this in Appendix C.1 for convenience, and thus necessarily do so in this section, whose theorems cite that appendix.

We introduce the notation of the appendix; $\alpha = 1 + f(1/2)$ and $\beta = 1 + g(1)$, and take the opportunity to briefly discuss why, if the change of variables simplifies calculations, we only apply it to this section. In the original system, α and β would have a clear relationship, dictated by the constraints put on f and g. The function g is stronger (or at least not weaker) than the function f, and g is monotonic, so

$|f(1/2)| < |g(1)|$. In the conjugate (rescaled) system, we cannot make any such claim, nor compare α and β. Because so much of its influence has been scaled away (or rather, since we have effectively replaced a strong influence over a short time with a weaker influence over a longer time), g may be weaker or stronger than f.

Any configuration of clusters $\bar{x}$ on the Poincaré section defines an order of events and a corresponding map F. For $\bar{x}$ to be a cyclic solution, $\bar{x}$ and $F^i(\bar{x})$ must have the same order of events for any i. This sharply limits the orders of events that can correspond to a cyclic solution.

5.3.2 Proposition. *For $k = 2$, there are seven possible orders of events that a 2-cyclic solution may exhibit (excluding measure-zero regions of parameter space where multiple events occur concurrently). They are:*

1. *For $x_2 \in \widetilde{R}$*
   - *(a)* $x_1 \to s,\ x_1 \to r,\ x_2 \to s_1,\ x_2 \to 1$
   - *(b)* $x_1 \to s,\ x_2 \to s_1,\ x_1 \to r,\ x_2 \to 1$
   - *(c)* $x_2 \to s_1,\ x_1 \to s,\ x_1 \to r,\ x_2 \to 1$
2. *For $x_2 \in O$*
   - *(a)* $x_1 \to s,\ x_1 \to r,\ x_1 \to s_1,\ x_2 \to 1$
3. *For $x_2 \notin R$*
   - *(a)* $x_1 \to s,\ x_2 \to r,\ x_2 \to s_1,\ x_2 \to 1$
   - *(b)* $x_2 \to r,\ x_2 \to s_1,\ x_1 \to s,\ x_2 \to 1$
   - *(c)* $x_2 \to r, x_1 \to s,\ x_2 \to s_1,\ x_2 \to 1$
   - *(d)* $x_2 \to s,\ x_r \to r,\ x_2 \to s_1,\ x_2 \to 1$

The cyclic solutions in Cases 1b, 1c, 3b, and 3c are asymptotically stable in the clustered subspace under negative feedback and unstable under positive feedback, while

in Cases 1a, 2a, 3a, and 3d, the cyclic solutions are neutrally stable under both positive and negative feedback.

Proof. An exhaustive list of all possible orders of events can be found in the appendix. To be the order of events of a cyclic solution, every "region" of the circle must be left with as many clusters in it after F is applied as before, e.g. if one cluster enters $\tilde{R}$ then one cluster must leave $\tilde{R}$. The seven mentioned are the only ones that satisfy this property. For each order of events, the map $F(x_2)$ is calculated as $F(x_2) = ax_2 + b$; the stability of this dynamical system is governed by the eigenvalue of the Jacobian $[a]$, which is a, the coefficient of x_2 in the function F. Thus the k-cyclic fixed point is asymptotically stable when $|a| < 1$, neutral when $|a| = 1$, and unstable otherwise. □

We assume that $\bar{x}$ is in the interior of an event region, i.e. small perturbations of $\bar{x}$ in the clustered subspace share the order of events of $\bar{x}$, and different events occur at distinct times.

We observe that the neutrally stable cases tend to correspond to "extreme" parameter values. Case 3a occurs when R, S, and O are all sufficiently small that the system decouples, a concept we shall return to in Section 5.4. In Case 2a, O tends to be extremely large compared to $\widetilde{R}$ and $\widetilde{S}$, in Case 1a it is $\widetilde{R}$ that tends to be large, and Case 3d occurs when $\widetilde{S}$ is large compared to other parameters. We do not quantify "largeness," but do observe that for a zero-feedback system, $x_2 = .5$, and therefore, in a system with relatively weak feedback, if x_2 initially lies in O or $\widetilde{S}$, that region must cover almost half of the unit circle. Figure 5.2 depicts each neutral interval in that limitting zero-feedback case.

5.3.3 Proposition. *A neutrally stable* 2*-cyclic fixed point of* F *satisfying one of the orders of events 1a, 2a, 3a, or 3d of Proposition 5.3.2 is contained in a closed interval, invariant under* F*, of* 2*-periodic fixed points of the Poincaré map. The interval is attracting under negative feedback and repelling under positive feedback.*

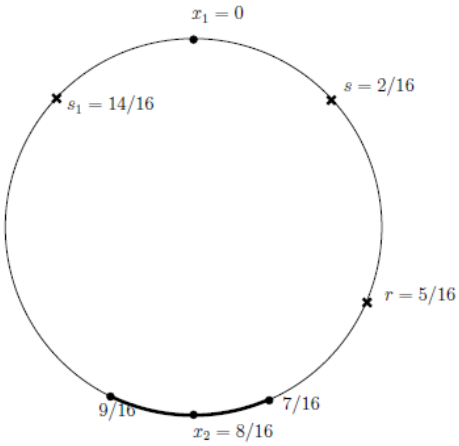

(a) Case 1a

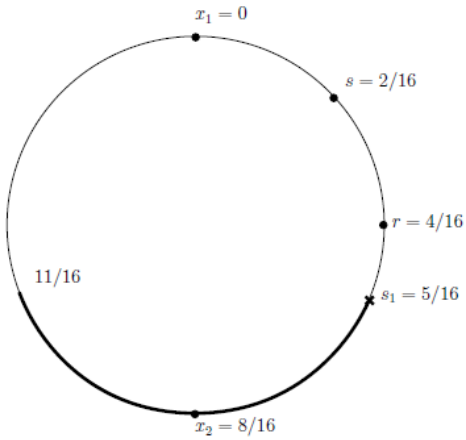

(b) Case 2a

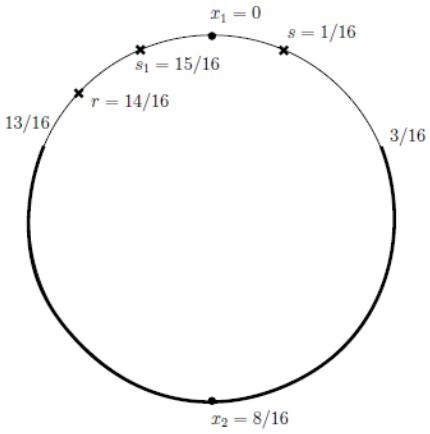

(c) Case 3a

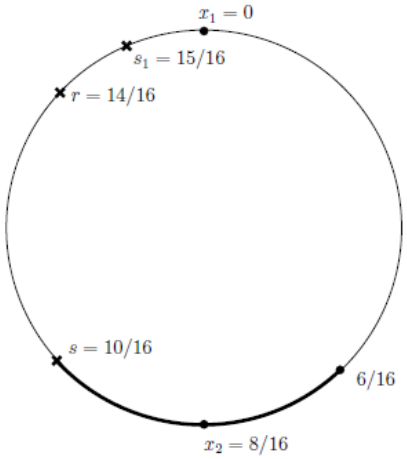

(d) Case 3d

Figure 5.2: Neutrality tends to occur when some interval, either O, $\widetilde{R}$, $\widetilde{S}$, or $(S \cup R)^C$, is much larger than the others.

We prove this proposition in the form of four lemmas, that also explicitly give the endpoints of the intervals. The proofs of these lemmas are essentially similar. First, we determine the endpoints of the interval. We do this by first observing that the dictated orders of events define an interval $[a, b]$, and that $F(x) \in [a, b]$ defines an overlapping interval (non-empty by the assumption that x is in the interior of an event region). The intersection $[a', b']$ of those two intervals is the interval of interest. Having found the interval, $[a', b']$, we explicitly consider values $x_2 = a' - \epsilon$ and $x_2 = b' + \epsilon$

and see what effect the map F has on them. In fact, since the end-points of the neutral intervals lie on the same periodic orbit ($F(a') = b'$, $F(b') = a'$), we need only consider one of the endpoints.

5.3.4 Lemma. *In Case 3a, the neutral fixed point of F is contained in an interval of* 2*-periodic fixed points of the Poincaré map,* $[1-r+s, r-s]$*, whose boundaries are attracting under negative feedback and repelling under positive feedback.*

Proof. The order of events for this case is $x_1 \to s$, $x_2 \to r$, $x_2 \to s_1$, $x_2 \to 1$, with $x_2(0) \notin R$. Let x_2 be an arbitrary point satisfying this order of events.

Both x_1 and x_2 initially move at a rate of 1. For $x_1 = 0$ to reach s before x_2 reaches r is therefore equivalent to $s \leq r - x_2$, or $x_2 \leq r - s$. Thus $x_2 \in (0, r - s]$.

If $\bar{x}$ satisfies the mandated order of events, then x_2 must reach r after x_1 reaches s, but it must also reach 1 before x_1 reaches r. Note that x_1 will reach r at time r. Under the assumption that x_2 reaches 1 before x_1 reaches r, the time T that it takes for x_2 to reach 1 is simply $1 - x_2$, recalling that the effect x_2 has on itself in O has been scaled away by a change of variables. Thus the restriction that x_2 reach 1 before x_1 reaches r is equivalent to the inequality $1 - x_2 \leq r$, i.e. $x_2 \in [1 - r, 1)$.

Thus if x_2 (more formally $(0, x_2)$, but working on the Poincaré section makes 2-cyclic solutions one-dimensional) is to satisfy the given order of events, $x_2 \in (0, r - s] \cap [1 - r, 1)$, which we rewrite as $x_2 \in [1 - r, r - s]$.

For this order of events, $F(x_2) = 1 - x_2$; see Appendix C.1. If $F(x_2)$ also satisfies this order of events, then $F(F(x_2)) = x_2$, and the interval where both x_2 and $F(x_2)$ satisfy the order of events (that is, $(0, x_2)$ and $(0, F(x_2))$ satisfy the order of events) is therefore a neighborhood of fixed points of F^2. Asking that $F(x_2) \in [1 - r, r - s]$ is equivalent to asking that $1 - r \leq 1 - x_2 \leq r - s$, that is to say $x_2 \in [1 - r + s, r]$.

Clearly, $1 - r < 1 - r + s$ and $r - s < r$, so the intersection of the intervals containing x_2 and $F(x_2)$ is $x_2 \in [1 - r + s, r - s]$. It is easily verifiable that $F(1 - r + s) = r - s$ and $F(r - s) = 1 - r + s$.

To determine whether the endpoints of the interval are attracting or repelling we will analyze the F-maps at an arbitrarily small distance, ϵ, outside the interval.

Let $x_2 = r - s + \epsilon$, slightly above the upper endpoint. This value of x_2 gives rise to the order of events $x_2 \to r$, $x_1 \to s$, $x_2 \to s_1$, $x_2 \to 1$, since at $x_2 = r - 2$ the events $x_2 \to r$ and $x_1 \to s$ occur simultaniously, and we now move x_2 slightly closer to r.

Again citing Appendix C.1 (order of events 3(c)), we find that $F(x_2) = 1 - r + s - \alpha(s - r + x_2)$, where α is a rate ($0 < \alpha$). For $x_2 = r - s + \epsilon$, this function is $F(r - s + \epsilon) = 1 - r + s - \alpha\epsilon$, slightly below the lower endpoint.

This places $F(x_2)$ in the original interval $[1 - r, r - s]$, and it therefore has order of events $x_1 \to s$, $x_2 \to r$, $x_2 \to s_1$, $x_2 \to 1$ and F-map $F(x_2) = 1 - x_2$. Thus $F^2(r - s + \epsilon) = 1 - F(r - s + \epsilon) = r - s + \alpha\epsilon$. If the feedback is negative ($0 < \alpha < 1$), then this is a contraction towards the boundary value $r - s$; if the feedback is positive, then the distance to the boundary increases. □

Example 1: After re-scaling, let $s = .2, r = .8$. The parameter s_1 is not relevant here. Then the interval of Theorem 5.3.4 is $[.4, .6]$. We easily calculate $F(.4) = .6$ and $F(.6) = .4$; the 2-periodic fixed point of F is $x_2 = .5$.

5.3.5 Lemma. *For Case 2a the interval of neutrally stable fixed points of the Poincaré map is* $[s_1, 1 - \beta s - r - \frac{s_1 - r}{\alpha} + s]$*, and its boundaries are both attracting under negative feedback and repelling under positive feedback.*

Recall that $\alpha = 1 + f(1/2)$ and $\beta = 1 + g(1)$ after the system has been rescaled.

Proof of Lemma 5.3.5. The order of events is $x_1 \to s$, $x_1 \to r$, $x_1 \to s_1$, $x_2 \to 1$. The cluster x_2 starts in O,

$x_2 \in [s_1, 1]$.

The cluster x_1 must reach s_1 before x_2 reaches 1. It will take x_1 a time of $r + \frac{s_1 - r}{\alpha}$ to reach s_1. At that time, x_2 will have traveled to $x_2 + \beta s + r - s + \frac{s_1 - r}{\alpha}$; in particular, it will travel a distance of βs while $x_1 \in S$, will travel a distance of $r - s$ in the $r - s$ time units it

takes x_1 to travel from s to r, and a distance of $\frac{s_1-r}{\alpha}$ in the time it takes x_2 to traverse $\widetilde{R}$. So any $\bar{x}$ that satisfies the assumptions of the lemma must satisfy $x_2+\beta s+r+\frac{s_1-r}{\alpha}-s\le 1$, i.e.

$x_2 \in \left[0, 1-\beta s-r-\frac{s_1-r}{\alpha}+s\right]$. Thus,

$x_2 \in \left[s_1, 1-\beta s-r-\frac{s_1-r}{\alpha}+s\right]$.

If an invariant interval exists, it must satisfy $F(x_2) \in \left[s_1, 1-\beta s-r-\frac{s_1-r}{\alpha}+s\right]$ for any x_2 in the interval. Appendix C.1 gives the corresponding F-map for every possible order of events; referring to the appendix, we see that for the order of events described by the lemma, F is given by $F(x_2) = s_1 + 1 - x_1 - \beta s - r + s - \frac{s_1-r}{\alpha}$. It is easily observed that $F(F(x_2)) = x_2$. The required inclusion, $F(x_2) \in \left[s_1, 1-\beta s-r-\frac{s_1-r}{\alpha}+s\right]$, simplifies to

$s_1 \le s_1 + 1 - x_2 - \beta s + s - \frac{s_1-r}{\alpha} - r \le 1-\beta s-r-\frac{s_1-r}{\alpha}+s$, or

$x_2 \in \left[s_1, 1-\beta s-r-\frac{s_1-r}{\alpha}+s\right]$,

providing no new restriction. Thus the original restriction that $x_2 \in \left[s_1, 1-\beta s-r-\frac{s_1-r}{\alpha}+s\right]$ is all that is necessary for both x_2 and $F(x_2)$ to satisfy the order of events of the lemma.

Let $x_2 = s_1 - \epsilon$. Then $\bar{x}$ is governed by the order of events $x_2 \to s_1, x_1 \to s$, $x_1 \to r$, $x_1 \to s_1$, $x_2 \to 1$, which is event 1(i) of the appendix, and

$F(x_2) = 1 - \beta s + \frac{\beta s_1}{\alpha} - \frac{\beta}{\alpha}(s_1-\epsilon) - r + s - \frac{s_1-r}{\alpha}$. This is $\frac{\beta}{\alpha}\epsilon$ above the upper bound of the event interval we have calculated. We observe that this is the only part of this section where the ambiguity introduced by the rescaling has the potential to come into play; we do not know whether $\frac{\beta}{\alpha}$ is greater than, less than, or equal to 1. However, the second iteration of F will remove this term.

We note that $F(x_2)$ is in the order of events region $x_1 \to s$, $x_1 \to r$, $x_2 \to 1$, and F in this event region is given by $F(x_2) = r + \alpha(1 - x_1 - \beta s - r + s)$. In particular,

$F\left(1-\beta s+\frac{\beta s_1}{\alpha}-\frac{\beta}{\alpha}(s_1-\epsilon)-r+s-\frac{s_1-r}{\alpha}\right) = r+\alpha\left(1-\left(1-\beta s+\frac{\beta s_1}{\alpha}-\frac{\beta}{\alpha}(s_1-\epsilon)-r+s-\frac{s_1-r}{\alpha}\right)-\beta s-r+s\right) = s_1-\beta\epsilon$. This is a contraction towards the boundary $x_2 = s$ for negative feedback, but repels x_2 away for positive feedback. □

Example 2: Let $s = .1, r = .2, s_1 = .3$. Let $\alpha = \beta = .5$ (remembering that because rescaling the system breaks the assumed relationship between the feedback functions, we are not violating the restrictions on f and g by letting $f(1/2) = g(1)$). Then the interval of fixed points of the Poincaré map is $[.3, .65]$, and we observe, decomposing F into its component event maps, that $\{0, .3\} \to \{.1, .35\} \to \{.2, .45\} \to \{.3, .65\} \to \{0, .65\} \to \{.1, .7\} \to \{.2, .8\} \to \{0, .3\}$. It is easily calculable, using the formula for F, that the fixed point of F is $x_2 = .475$.

5.3.6 Lemma. *For Case 1a the neutrally stable fixed point is located in the interval of* 2*-periodic points* $[r + \alpha(1 - s_1), s_1 - \alpha s - r + s]$*, whose boundaries are attracting for negative feedback and repelling for positive feedback.*

Proof. Here x_2 is initially in R, and the order of events is $x_1 \to s$, $x_1 \to r$, $x_2 \to s_1$, $x_2 \to 1$.

The first and most basic condition that must be met in order to maintain this order of events is that $r \le x_2 \le s_1$, i.e. $x_2 \in [r, s_1]$.

The maintenance of the order of events depends on two further conditions. The first is that x_2 cannot reach s_1 before time $t = r$, when x_1 reaches r. The inequality $x_2 + \alpha s + r - s \le s_1$ ensures this condition and results in the restriction $x_2 \le s_1 - \alpha s - r + s$, i.e.

$$x_2 \in [r, s_1 - \alpha s - r + s].$$

The second constraint needed to maintain the order of events is that x_2 must reach 1 before x_1 reaches s_1, leading to the inequality $r + s_1 - x_2 - \alpha s - r + s + \alpha(1 - s_1) \le s_1$. This gives the restriction $-\alpha s + s + \alpha(1 - s_1) \le x_2$, i.e.

$$x_2 \in [-\alpha s + s + \alpha(1 - s_1), s_1].$$

However, this is a weaker restriction than $r \le x_2$, for reasons that will become apparent. Thus the interval where the desired order of events occurs remains

$$x_2 \in [r, s_1 - \alpha s - r + s].$$

In order for the second iteration of F to also have this order of events, the inequality $r \le s_1 - x_2 - \alpha s + s + \alpha(1 - s_1) \le s_1 - \alpha s - r + s$ must be satisfied, resulting in the inclusion

$$x_2 \in [r + \alpha(1 - s_1), s + s_1 - \alpha s + \alpha(1 - s_1) - r].$$

Taking the intersection of the two intervals results in the final interval of neutrally stable points, $[r+\alpha(1-s_1), s_1-\alpha s-r+s]$. Observe that the upper bound, strictly less than s_1, is obtained from the restriction $r < x_1$. We observe that $-\alpha s + s + \alpha(1 - s_1) \le x_2 \iff F(x_2) < s_1$, a weaker condition than the one implied by $r < x_2$.

To determine whether the endpoints of this interval are attracting or repelling we will analyze the F-maps at an arbitrarily small distance, ϵ, outside the interval. Placing the cluster at an initial point of $r + \alpha(1 - s_1) - \epsilon$ will not change the order of events, and one iteration of F will result in the new position of $x_2 = s + s_1 - \alpha s - r + \epsilon$. This new position changes the order of events to $x_1 \to s$, $x_2 \to s_1$, $x_1 \to r$, $x_2 \to 1$ (Case 1(b)). Applying $F(x_2) = r + \alpha(1 - r + s - x_2 - \alpha s)$ gives a final position of $x_2 = r + \alpha(1 - s_1) - \alpha\epsilon$, which puts the cluster at a point closer to the boundary than it started (negative feedback), or further from the boundary than it started (positive feedback). □

Example 3: Let $s = .2$, $r = .3$, $s_1 = .8$, and $\alpha = \beta = .5$. Then the interval of fixed points of F^2 is $[.4, .6]$, and $\{0, .6\} \to \{.3, .8\} \to \{0, .4\} \to \{.3, .7\} \to \{.4, .8\} \to \{0, .6\}$.

5.3.7 Lemma. *For Case 3d the neutrally stable fixed point is located in the interval of* 2*-periodic points* $[r - s + \frac{s_1 - r}{\alpha} + \frac{1 - s_1}{\beta}, s]$*, whose boundaries are attracting for negative feedback and repelling for positive feedback.*

Proof. Initially, the only restriction on the order of events is $x_2 < s$. For this order of events to occur, x_1 must still be in S when $x_2 \to 1$, i.e. $r - x_2 + \frac{s_1 - r}{\alpha} + \frac{1 - s_1}{\beta} \le s$, or

$$x_2 \in \left[r + \tfrac{s_1 - r}{\alpha} + \tfrac{1 - r}{\beta} - s, s\right].$$

This is the only restriction. A starting condition ϵ above s has order of events $1(h)$ (see appendix), and $F(s + \epsilon) = r - s - \epsilon + \frac{s_1 - r}{\alpha} + \frac{1 - s_1}{\beta}$, a point on the order of ϵ below the

lower endpoint. This has the same order of events of the fixed point (order of events 3(d) in the appendix), and

$$F\left(r - s - \epsilon + \tfrac{s_1 - r}{\alpha} + \tfrac{1 - s_1}{\beta}\right) = s + \beta\epsilon. \qquad \square$$

We observe that this neutrality is consistent with the neutrality of Case 2 in Section 5.4.2, where $x_2 \in S$.

Example 4 Let $s = .7$, $r = .8$, $s_1 = .9$, $\alpha = \beta = .5$. Then the neutral interval is $[.5, .7]$, and it is easily verified that $F(.5) = .7$ and $F(.7) = .5$, while the fixed point lies at $x_2 = .6$.

For $M = 1$ (see Definition 5.4.2), the neutral Case 3d corresponds to the neutral Case 2 of Section 5.4.2; Case 2a to Case 4, Case 1a to Case 3b, while Case 3a cannot occur in the $k = M + 1$ case. Note that in the RS model, there was the potential to have a neutral interval in S, a neutral interval in R, and a neutral interval in $(S \cup R)^c$; adding an additional region O to the system added a corresponding neutral interval. In each of these neutral cases, the system essentially decouples. For example, let O be significantly larger than any other "region" ($\widetilde{R}$, $\widetilde{S}$, or $S^1 \backslash (R \cup S)$) and $x_2(0) \in O$. Then x_2 will travel at a constant rate $(1 + g(1))$ for s time units, at another constant rate $(1 + g(1/2))$ for another constant time unit ($r - s + \frac{s_1 - r}{1 + f(1/2)}$), and then travel at a rate of $1 + g(1)$ until it reaches 1. The exact location of x_1 is never relevant.

5.4 Decoupled and almost-decoupled systems

In this section, we will consider how the concept of isolation extends to the overlap system, and we will investigate the stability of the $k = M + 1$ cyclic solution in the overlap model. All stability results in this section refer to stability in the clustered subspace.

5.4.1 Decoupled systems

A feature unique to the overlap model, as opposed to the RS or gap models, is that any possible configuration of cells must eventually experience feedback; however,

clusters may still be decoupled from one another. We have seen the following definition before; we add a subscript to prevent confusion.

5.4.1 Definition. $M_{RS} := \left\lfloor \frac{1}{|R|+|S|} \right\rfloor = \left\lfloor \frac{1}{1-r+s} \right\rfloor$ *is the maximal number of clusters k in the RS system such that the k-cyclic solution experiences no feedback, i.e. if R is nonempty at any time then S is empty.*

In the RS model, there are an infinite number of non-interacting, neutral solutions of k clusters for $k \leq M$; in particular any sufficiently small perturbation of the k-cyclic solution, that, when it intersects the Poincaré section, has the form $x_i = \frac{i-1}{k}$ for $i = 1, ..., k$. Such a solution experiences no feedback. Thus the lowest value of k guaranteed to be "interesting" in the RS model is $k = M_{RS} + 1$. A system in the overlap model must experience feedback, but the concept of isolation can be naturally defined in the overlap model to produce the following definition.

5.4.2 Definition. *Let M be the maximal number of clusters in the overlap model such that the M-cyclic solution experiences no feedback except that which a cluster exerts upon itself; i.e. if* $\widetilde{R}$ *is nonempty then S is empty, and if O is nonempty then it contains only one cluster and* $\widetilde{S}$ *is empty.*

If we view the RS model as a degenerate case of the overlap model where $O = \varnothing$, then Definitions 5.4.2 and 1.4.5 correspond. The formula for M in the overlap model is more complicated then the formula for M_{RS}, however.

5.4.3 Lemma. *An explicit formula for M is given by*

$$M = \left\lfloor \frac{\frac{1-s_1}{1+g(1/k)} + s_1}{\frac{1-s_1}{1+g(1/k)} + s_1 - r + s} \right\rfloor. \tag{5.4.1}$$

Proof. The form of M_{RS} is easily calculated in the absence of an overlap region; there is no feedback if $r - x_k > s$; in the absence of any feedback, $x_k = \frac{k-1}{k}$, and this inequality can be rewritten as $k < \frac{1}{1-r+s}$. The maximum integer that satisfies this is $M_{RS} = \left\lfloor \frac{1}{1-r+s} \right\rfloor$

We pursue the same line of thought to find the value of M given in the above definition. Because x_k self-influences, it is no longer at a distance of $1/k$ from 1. If T is the time it takes for x_k to reach 1, then since $x_i(T) = x_{i+1}$ by the definition of the cyclic solution, and as all clusters but x_k travel at a constant rate of 1, it follows that $x_k = (k-1)T$, and we therefore calculate

$$\begin{aligned} 1 &= s_1 + (1 + g(1/k))(T - s_1 + (k-1)T), \\ 1 &= s_1 + (1 + g(1/k))(kT - s_1), \\ T &= \frac{\frac{1-s_1}{1+g(1/k)}}{k} + \frac{s_1}{k}. \end{aligned} \tag{5.4.2}$$

Then the inequality $r - (k-1)T \geq s$ can be rewritten as $k \leq \frac{\frac{1-s_1}{1+g(1/k)} + s_1}{\frac{1-s_1}{1+g(1/k)} + s_1 - r + s}$, and the largest integer that satisfies this requirement is

$$M = \left\lfloor \frac{\frac{1-s_1}{1+g(1/k)} + s_1}{\frac{1-s_1}{1+g(1/k)} + s_1 - r + s} \right\rfloor.$$

□

Observe that M_{RS} may be obtained as a special case of M by letting $g(1/k) = 0$.

The presence of the feedback function g in the definition of M is worth observing. In both the original model and the gap model, the actual form of the feedback function has played essentially no part–questions such as stability have depended simply on whether the feedback was positive or negative. The following is obvious.

5.4.4 Lemma. *In the RS model, for any positive integer w, parameters r and s can be chosen so that $M_{RS} = w$ for any feedback function.*

The overlap model gives rise to a slightly weaker lemma.

5.4.5 Lemma. *In the overlap model, for any positive integer w, and any feedback functions f and g, parameters r, s_1 and s can be chosen so that $M = w$ for those fixed feedback functions.*

Proof. By choosing $s_1 \approx r \approx 1$, where the closeness of the required approximation depends on both $g(1/k)$ and the desired M, the fraction $\frac{1-s_1}{1+g(1/k)}$ can be made arbitrarily close to 0, and the argument of the floor function that defines M arbitrarily close to $\frac{1}{s}$. Then s can be chosen freely to give the desired integer. □

We also remark on the recursive elements Definition 5.4.2 brings to the system. In the non-overlap model, we can define parameters r and s; calculate M_{RS}; and if we then wish to investigate $k = M_{RS} + 1$, as in Chapter 4, we may select a feedback function and procede. Such a mode of investigation would lead to difficulties in the overlap model, since the function g depends on the number of clusters in the system, and the number of clusters in the $k = M + 1$ system depends on g. We must then view k and g as defined concurrently; having defined k, g, and the system parameters, an equality such as $k = M$ or $k = M + 1$ is merely a condition, that the system may or may not satisfy. We isolate the following obvious lemma, then turn our attention to the more interesting systems satisfying the equality $k = M + 1$.

5.4.6 Lemma. *If $k \leq M$ for parameters k, g, r, s_1 and s, then the k-cyclic solution is neutrally stable in the clustered subspace.*

Proof. In this case, the clusters do not interact; they each travel at a rate of 1 outside of O, and a rate of $1 + g(1/k)$ inside O, independently of each other. □

5.4.2 The $k = M + 1$ system

If a system satisfies the equality $k = M + 1$, the form it may take is sharply restricted. For $k = M$, when $x_1 = 0$, all other clusters lie in the gap between S and R. Adding another cluster to the system may force another cluster into $\tilde{S}$, or it may force a cluster into $\tilde{R}$; if O is sufficiently large, then a cluster may in fact be forced into O. We consider the possible cases, and the stability of the k-cyclic solution in each case. In all cases, we are referring to the k-cyclic solution when it intersects the Poincaré section.

For each case, we calculate T, the minimum time where $x_k(T) = 1$. We will refer to T as the return time of F. In the case where only x_k experiences feedback, this is sufficient to calculate the Jacobian J in the neighborhood of the k-cyclic fixed point of F. In other cases, we must also calculate $x_{k-1}(T)$. Since F defines a discrete dynamical system and is piecewise affine, a fixed point is stable if and only if all of the eigenvalues of J are strictly in the interior of the unit circle, unstable if and only if at least one eigenvalue is strictly outside the unit circle, and neutrally stable otherwise. In all cases, either the Jacobian itself or the characteristic polynomial is directly comparable to the Jacobian or characteristic polynomial of a case of the RS model, described in Section 2.3 of Chapter 2, and we summarize those cases. The calculations we have described are cumbersome; we put them in Appendix C.2 for reasons of flow.

Case 1 of the RS model:

This case was defined by $\sigma = 1$, $\rho = k$, and event string $e_r e_s$.

The Jacobian J of F in the neighborhood of the $(M+1)$-cyclic solution has the form

$$J = \begin{pmatrix} 0 & 0 & 0 & \dots & 0 & -(1+f(1/k)) \\ 1 & 0 & 0 & \dots & 0 & -(1+f(1/k)) \\ 0 & 1 & 0 & \dots & 0 & -(1+f(1/k)) \\ 0 & 0 & 1 & \dots & 0 & -(1+f(1/k)) \\ \dots & \dots & \dots & \dots & \dots & \dots \\ 0 & 0 & 0 & \dots & 1 & -(1+f(1/k)) \end{pmatrix}. \tag{5.4.3}$$

The characteristic polynomial of J is

$$p(\lambda) = \lambda^{k-1} + (1+f(1/k))(\lambda^{k-2} + \lambda^{k-3} + \cdots + \lambda + 1). \tag{5.4.4}$$

This polynomial has roots strictly within the unit circle (i.e. the fixed point is stable) when $1 + f(1/k) < 1$ (negative feedback), and roots strictly outside the unit

circle (thus, the fixed point is unstable) when $1 + f(1/k) > 1$, that is to say for positive feedback.

Case 2 of the RS model:

There are two other cases in the RS model, but they each give rise to the same Jacobian. One of the cases was defined by $\sigma = 2$, $\rho = k$, and event string $e_s e_r$; the other by $\sigma = 1$, $\rho = k - 1$, and event string $e_s e_r$. In either case, the Jacobian in a neighborhood of an $(M + 1)$-cyclic fixed point has the form

$$J = \begin{pmatrix} 0 & 0 & 0 & \ldots & 0 & -1 \\ 1 & 0 & 0 & \ldots & 0 & -1 \\ 0 & 1 & 0 & \ldots & 0 & -1 \\ 0 & 0 & 1 & \ldots & 0 & -1 \\ \ldots & \ldots & \ldots & \ldots & \ldots & \ldots \\ 0 & 0 & 0 & \ldots & 1 & -1 \end{pmatrix}. \tag{5.4.5}$$

The characteristic polynomial is

$$p(\lambda) = \lambda^{k-1} + \lambda^{k-2} + \lambda^{k-3} + \cdots + \lambda + 1, \tag{5.4.6}$$

all of whose roots lie on the unit circle (i.e. the fixed point is neutral).

Compared to the RS model, where the $(M + 1)$-cyclic solution falls into one of three cases (two of them sharing a Jacobian), the overlap model gives rise to seven cases, categorized based on the initial positions of x_2 and x_k.

5.4.3 $k = M + 1$ cases in the overlap model

Case 1: When $\mathbf{x_1} = 0$, R is empty and S contains no clusters other than x_1

We will see that in this case the k-cyclic solution is stable for negative feedback and unstable for positive feedback. This is identical behavior to that observed in the RS model.

There are two sub-cases; x_k must enter R before x_1 leaves S, or the system is decoupled (violating the fact that $k > M$), but x_2 may or may not enter O before x_1 leaves S.

Case 1a: $\mathbf{x_k \to r, x_1 \to s, x_k \to s_1}$.

The Jacobian in this case is identical to (C.2.1), except that $1 + f(1/k)$ is replaced by $\frac{1+f(2/k)}{1+f(1/k)}$. The question of whether the eigenvalues fall inside or outside of the unit circle in that case is resolved entirely by whether the constant in the last column is between 0 and 1 in absolute value (negative feedback, stable) or greater than 1 (positive feedback, unstable). Since $-\frac{1+f(2/k)}{1+f(1/k)}$ is likewise a constant that is between 0 and 1 for negative feedback, and greater than 1 for positive feedback, this $(M + 1)$-cyclic solution has the same stability as in Case 1 of the RS model, that is to say that it is stable when the feedback is negative, and unstable when the feedback is positive.

Case 2: When $\mathbf{x_1 = 0, x_2 < s}$

The Jacobian near the fixed point is given by (C.2.3). Thus this case shares the stability of Case 2 for the RS model, i.e. the fixed point is neutrally stable.

Case 3: When $\mathbf{x_1 = 0, r \leq x_k < s_1}$

In the RS model, an $(M + 1)$-cyclic solution that has a cluster in R when $x_1 = 0$ is neutrally stable under positive or negative feedback. In the overlap model, there are three subcases, and only one of them is neutrally stable. The key difference is that although x_1 leaves S before x_{k-1} enters R, the cluster x_{k-1} will still experience feedback in this model, since it will be in R while x_k is in O. There are three subcases, corresponding to orders of events.

Case 3a: $\mathbf{x_k \to s_1, x_1 \to s, x_{k-1} \to r}$

For notational simplicity, we let $w = \frac{1+f(2/k)}{(1+f(1/k))(1+f(1/k))} x_k(0)$. The Jacobian of F in this case is given by

$$J = \begin{pmatrix} 0 & 0 & 0 & \dots & 0 & -w \\ 1 & 0 & 0 & \dots & 0 & -w \\ 0 & 1 & 0 & \dots & 0 & -w \\ 0 & 0 & 1 & \dots & 0 & -w \\ \dots & \dots & \dots & \dots & \dots & \dots \\ 0 & 0 & 0 & \dots & (1+f(1/k)) & -(1+f(1/k))w \end{pmatrix}. \tag{5.4.7}$$

Although the Jacobian is different from the RS model, the characteristic polynomial is the same as in Case 1b,

$$p(\lambda) = \lambda^{k-1} + (1+f(1/k))(\lambda^{k-2} + \lambda^{k-3} + \cdots + \lambda + 1), \tag{5.4.8}$$

and is stable for negative feedback and unstable for positive feedback.

Case 3b: $\mathbf{x_1 \to s, x_{k-1} \to r, x_k \to s_1}$

The Jacobian for this case has 1's down the semidiagonal and -1's down the last column, and is neutrally stable for both positive and negative feedback.

Case 3c: $\mathbf{x_1 \to s, x_k \to s_1, x_{k-1} \to r}$

The Jacobian for this case has 1s down the semidiagonal and -1's down the right column, except for the last row: $J(k-1,k-2) = 1+f(1/k)$ and $J(k-1,k-1) = -(1+f(1/k))$. Its characteristic polynomial has leading coefficient 1 and all other coefficients $1 + f(1/k)$, again reducing to Case 1 from Chapter 2, and is thus asymptotically stable under negative feedback, and unstable under positive feedback.

Case 4: When $\mathbf{x_1 = 0, s_1 \le x_k < 1}$

The Jacobian of F near the cyclic solution is

$$J = \begin{pmatrix} 0 & 0 & 0 & ... & 0 & -1/(1+f(2/k)) \\ 1 & 0 & 0 & ... & 0 & -1/(1+f(2/k)) \\ 0 & 1 & 0 & ... & 0 & -1/(1+f(2/k)) \\ 0 & 0 & 1 & ... & 0 & -1/(1+f(2/k)) \\ ... & ... & ... & ... & ... & ... \\ 0 & 0 & 0 & ... & 1+f(2/k) & -1 \end{pmatrix},$$

and it has characteristic polynomial (C.2.4). Thus the fixed point is neutrally stable.

In analysis of the $k = M + 1$ case, the overlap may be seen, in a sense, to strengthen the stability and instability of the RS model. That is to say, that cases that were stable (unstable) under negative (positive) feedback in the RS model retain that stability (instability), but some cases that were previously neutrally stable are promoted to full stability (instability). In particular, although an initial solution with more than one cluster in S can still only be neutrally stable, the overlap region allows for stable solutions to exist where R is not initially empty. We note that the stability-reversal of the gap model, where adding a gap can (in an ϵ-small region of parameter space) cause $k = M + 1$ solutions to be unstable under negative feedback and stable under positive feedback, does not occur in the overlap model.

We summarize the results of this section in Table 5.1.

Table 5.1: Summary of the $k = M + 1$ cases in the overlap model

Case label	σ	ρ	ζ	order of events	Stability
Case 1a	1	k	k	$e_r^k e_s^1 e_\zeta^k e_1^k$	stable/unstable
Case 1b	1	k	k	$e_r^k e_\zeta^k e_s^1 e_k^1$	stable/unstable
Case 2	2	k	k	$e_s^2 e_r^k e_{s_1}^k e_1^k$	neutral
Case 3a	1	k-1	k	$e_{s_1}^k e_s^1 e_r^{k-1} e_1^k$	stable/unstable
Case 3b	1	k-1	k	$e_s^1 e_r^{k-1} e_{s_1}^k e_1^k$	neutral
Case 3c	1	k-1	k	$e_s^1 e_{s_1}^k e_r^{k-1} e_1^k$	stable/unstable
Case 4	1	k-1	k-1	$e_s^1 e_r^{k-1} e_{s_1}^{k-1} e_1^k$	neutral

We summarize the k=M + 1 cases. The "Case label" column refers to the bolded heading by which each case is identified in the text. The columns σ, ρ, and ζ are self-explanatory. Because so many parameters are repeated (e.g. $\rho = \zeta$), superscripts are used in the event chains to prevent confusion. In the final column, "neutral" means that the k-cyclic solution is neutrally stable under either positive or negative feedback, while stable/unstable means that is is stable under negative feedback and unstable under positive feedback.

5.5 The full phase space

Thus far, the results of this chapter have been direct analogues of previous results; the addition of a condition to the synchrony theorem Theorem 5.2.1 seems relativly trivial, and although we observe stability in regions of the parameter space, in the $k = M + 1$ case, where it could not previously occur, we observed no truly unusual behavior, in contrast with [30] where stability can occur under positive feedback. We have conducted our investigation, however, largely in the clustered subspace. We will now see that the overlap model is capable of behavior in the full phase space very different from anything previously observed.

We start by observing that if O is assumed to be sufficiently small, then $x_\zeta \to s_1$ will always be the penultimate event of F, followed by $x_\zeta \to 1$. We conduct our investigation in this context. We first observe a result that is directly parallel to the RS case (in particular, to Corollary 3.2.9).

5.5.1 Theorem. *Let $\bar{x}$ be a k-cyclic solution under negative feedback governed by the order of events $e_s e_r$, such that $\bar{x}$ is not on the boundary of an event region, and let the overlap region O be sufficiently small. Then $\bar{x}$ is unstable in the full phase space.*

The proof of the theorem rests on the observation that small groups (such as the desynchronized collection of cells formerly belonging to a single cluster) increase in diameter under the order of events of the lemma as long they are in a neighborhood of $\bar{x}$.

Proof of Theorem 5.5.1. We mimic the proof of Theorem 5.2.2. Select a group of $m = n/k$ cells and number those cells $c_m < c_{m-1} < ... < c_2 < c_1$. Under this numbering, when the group begins to undergo an event, c_i is the i'th cell of the group to cross that boundary (s, r, s_1, or 1) that defines the event. Let $\epsilon_i = c_i - c_{i+1}$ for $i = 1, 2, ..., m-1$. We consider how ϵ_i changes over the course of a single Poincaré map for a fixed i. First observe that when both c_i and c_{i+1} belong to the same region O, $\widetilde{R}$, or $S^1 \backslash (S \cup R)$, they travel at the same rate, and ϵ_i is unchanging. In fact, ϵ_i can only change during three periods of time: when $c_i \in R, c_{i+1} \notin R$, when $c_i \in O, c_{i+1} \in \widetilde{R}$, and when $c_i \in \widetilde{S}, c_{i+1} \in O$. We consider how ϵ_i changes over these time intervals.

Over the course of a single Poincaré map, we may assume by continuity that entire groups experience the same order of events. That is, the order of events tells us that when the group of interest passes into R, there are $\sigma - 1$ groups in S, or $\frac{\sigma-1}{k}$ of the groups in the system. We now assume that when the group we are interested in passes into R, all of the cells that belonged to those $\sigma - 1$ groups, or $\frac{\sigma-1}{k}$ of the cells in the system, are in S. It takes time ϵ_i for the cells to advance from $c_i = r$ to $c_{i-1} = r$, and over the course of that

period, c_i is traveling at a rate of $(1 + f((\sigma - 1)/k))$. Thus

$$\epsilon_i \to (1 + f((\sigma - 1)/k))\epsilon_i.$$

Now consider how the size of the gap changes as c_i and c_{i+1} enter O. For O sufficiently small, x_k of the k-cyclic solution entered O after x_σ had already left S. For sufficiently small perturbations, group we are considering therefore enter O after k/n cells have left S. We recall that we have taken all ϵ_i to be sufficiently small that the group entirely enters O before any of its cells pass into $\widetilde{S}$. When $x_1 = r$, the fraction of cells in O is $I = \frac{(\sigma-1)(n/k)}{n}$. The cells of the group of interest have been so numbered that when $c_i = s_1$, there are $I = \frac{(\sigma-1)(n/k)+i}{n}$ cells in S, since for O sufficiently small, O may be assumed to be empty except for the i cells of the group that have passed into it.

When $c_i = s_1$, the adjacent cell c_{i+1} lies a distance of $(1 + f((\sigma - 1)/k))\epsilon_i$ behind it. Travelling that distance at a rate of $1 + f(\frac{(\sigma-1)(n/k)+i}{n})$ takes time $t = \frac{(1+f((\sigma-1)/k))}{(1+f(\frac{(\sigma-1)(n/k)+i}{n}))}\epsilon_i$. In the time it takes c_{i+1} to reach s_1, the cell c_i, which is in O and therefore under the influence of a different feedback function g, reaches the point

$$s_1 + \frac{(1 + f((\sigma - 1)/k))}{(1 + f(\frac{(\sigma-1)(n/k)+i}{n}))}(1 + g(\frac{(\sigma - 1)(n/k) + i}{n}))\epsilon_i$$

. Thus

$$\epsilon_i \to (1 + f((\sigma - 1)/k))\epsilon_i \to \frac{(1 + f((\sigma - 1)/k))}{(1 + f(\frac{(\sigma-1)(n/k)+i}{n}))}(1 + g(\frac{(\sigma - 1)(n/k) + i}{n}))\epsilon_i.$$

By the time c_i reaches 1, there are σ/k cells in S, in the form of the cells that formed $\sigma - 1$ of the k clusters lying in $\widetilde{S}$, and the cells that formed another cluster lying in O. Because c_i now moves at unit rate, the final size of ϵ_i is simply the time it takes c_{i+1} to reach 1. And because x_{i+1} is travelling at a constant rate, the time T it takes to traverse distance $\frac{(1+f((\sigma-1)/k))}{(1+f(\frac{(\sigma-1)(n/k)+i}{n}))}(1 + g(\frac{(\sigma-1)(n/k)+i}{n}))\epsilon_i$ at rate $(1 + g(\sigma/k))$ is

$$\frac{(1 + f((\sigma - 1)/k))}{(1 + f(\frac{(\sigma-1)(n/k)+i}{n}))}(1 + g(\frac{(\sigma - 1)(n/k) + i}{n}))\epsilon_i = (1 + g(\sigma/k))T, \text{ so}$$

$$T = \epsilon_{\text{final}} = \frac{(1 + f((\sigma - 1)/k))}{(1 + f(\frac{(\sigma-1)(n/k)+i}{n}))}\frac{(1 + g(\frac{(\sigma-1)(n/k)+i}{n}))}{1 + g(\sigma/k)}\epsilon_i > \epsilon_i.$$

To see the final inequality, note that $((\sigma - 1)/k) = \frac{(\sigma-1)(n/k)}{n} < \frac{(\sigma-1)(n/k)+i}{n}$ and $\sigma/k = \frac{\sigma(n/k)}{n} > \frac{(\sigma-1)(n/k)+i}{n}$ for $0 < i < n/k$. Since f is monotonically decreasing the denominator of the fraction is smaller than the numerator.

Let U be any open neighborhood of $\bar{x}$ small enough that the previous argument holds in U. If an initial condition lies a bounded distance from $\bar{x}$, then there is a uniform bound on the distances between the cells of the clusters, $\epsilon_i \leq \epsilon$. All ϵ_i grow by at least some minimum factor, since there exists a uniform lower bound on that factor; this is because σ and i in the above equation can take on only finitely many values. What that lower bound is depends on the ratios of f and g, and thus on the details of the feedback functions. Repeated applications of the Poincaré map thus take any initial condition in U permanently outside of U, for any sufficiently small neighborhood U of $\bar{x}$, i.e. $\bar{x}$ is unstable. □

If we draw parallels to the results of the RS model, we expect that if we switch the order of events, the expansion we just observed will turn into a compression. That is *not* true in the overlap model, where reversing the order of events can result in a variety of behaviors. We start by the observation that the more unpredictable behavior of the system is a result of it being defined in terms of two different feedback functions. In the special case where $f = g$, the expansion still does not turn into compression, but the behavior of the system is at least straightforward.

5.5.2 Proposition. *Let $f = g$, and let $\bar{x}$ be a k-cyclic solution governed by the order of events $e_r e_s$. Then for $|O|$ sufficiently small, and $\bar{y}$ a sufficiently small perturbation of $\bar{x}$ in the full phase space, as long as $\bar{y}$ remains in a neighborhood of $\bar{x}$, the groups will neither expand nor contract.*

Proof. Mimicking the last proof, we see that $\epsilon_i \mapsto \frac{(1+f(\sigma/k))}{(1+f(\frac{(\sigma-1)(n/k)+i}{n}))} \frac{(1+g(\frac{(\sigma-1)(n/k)+i}{n}))}{1+g(\sigma/k)} \epsilon_i$. For $f = g$, this reduces to $\epsilon_i \to \epsilon_i$. □

We know that in the case of the *RS* system, groups governed by the order of events in Lemma 5.5.2 decrease in diameter under negative feedback (Lemma 3.2.4 of Chapter 3) as long as they are in a neighborhood of the k-cyclic solution. If the k-cyclic solution is stable in the clustered subspace, this implies stability in the full phase space (Theorem 3.5.1). The proof generalizes to the case where solutions in the full phase space do not increase in (component-wise Euclidean) distance from the clustered subspace to yield the following.

5.5.3 Corollary. *If $\bar{x}$ is stable in the clustered subspace of the overlap system, under the restrictions that $|O| << \min\{|\widetilde{S}|, |\widetilde{R}|, r - s\}$ and $f = g$, then $\bar{x}$ is neutrally stable in the full phase space.*

Theoretically, Corollary 5.5.3 applies to either negative or positive feedback. However, in the RS model, asymptotic stability cannot occur under positive feedback, and the behavior of the overlap model in the clustered subspace seems to mimic the behavior of the RS model, suggesting that stability under positive feedback in the clustered subspace in the overlap model does not occur.

For $f \neq g$, no feedback-independent theorem can be stated. For example, if f is approximately constant, and g increases relatively quickly in absolute value, then groups will tend to expand; in the opposite case, with g approximately constant and f quickly changing, groups will tend to contract. Biologically, there may be some justification for assuming g to be approximately constant, if the reaction of a cell to the chemicals it produces within itself is taken to be so overwhelming as to render its reaction to the chemical production of other cells basically irrelevant, but we do not expand this intuition into a restriction on the system.

Consider two graphics (Figure 5.3) illustrating this point. In both cases, fifty cells are initially placed (in a uniform random pattern to remove any systematic bias of the system) within an open ball of radius .01 centered at 0, and fifty cells are likewise placed in a similar open ball centered at .5. In both simulations, we use $s = .3$, $r = .7$,

$s_1 = .98$, and f and g are weak enough that $M = 1$ as in the standard RS model, and the 2-cyclic solution is stable in the clustered subspace. In one case f is almost constant, and in another, g is almost constant. The simulations confirm that this has the predicted results.

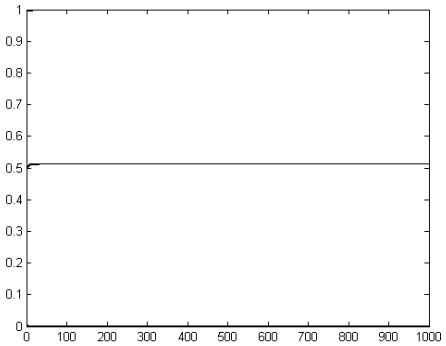

(a) Here, $f(I) = -.3I$ changes rather quickly, while $g(I) = -.01I - .3$ ($g(0) = 0$) is almost constant. As predicted, the groups collapse into clusters almost immediately.

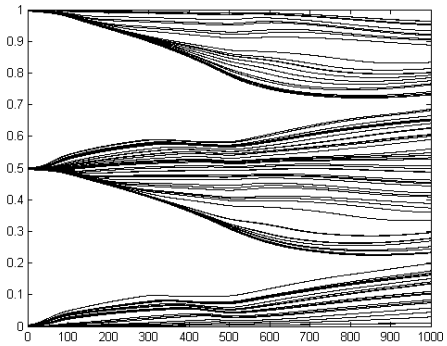

(b) Here, $f(I)$=$-.01I$ and $g(I) = -.1I$. As expected, the groups explode in diameter, and the system moves away from the 2-cyclic solution.

Figure 5.3: In the overlap model (and only in the overlap model, of the three models we have been contrasting), the dynamics of the system in the full phase space can be radically altered by varying the feedback functions. Pictured is a neighborhood of the 2-cyclic solution in a region of parameter space, $s = .3$, $r = .7$, and $s_1 = .98$. The 2-cyclic solution is stable in the clustered subspace in both figures, but different feedback functions yield drastically different behaviors in the full phase space.

In general, from the proof Theorem 5.5.2, we can see that some cells may converge towards one another while other cells remain apart (i.e. $\epsilon_i \to 0$ for some, but not all, i), depending on the feedback functions. In particular, if the feedback functions grow in an erratic fashion, such that adding one cell to S sometimes has a negligable effect on the strength of the feedback, and sometimes causes the strength to change abruptly, then this is likely to occur. We already saw from Lemma 5.4.1 how the strength of the feedback functions can control the behavior of the k-cyclic solutions in the clustered subspace, an idea we shall return to in Section 5.6. We know that the

strength of the feedback functions controls the behavior of the k-cyclic solutions in the full phase space; we consider further the effect of varying the feedback.

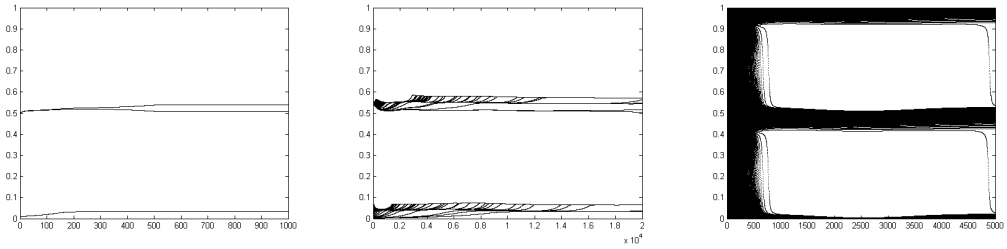

(a) Four clusters are positioned in a neighborhood of the 2-cyclic solution, which is stable in the clustered subspace.

(b) In this figure, we observe 100 cells in a neighborhood of the 2-cyclic solution. They are placed in a sufficiently wide neighborhood that the order of events of Theorem 5.5.2 are not satisfied.

(c) The cells are evenly spread about the circle in an approximation of the uniform solution.

Figure 5.4: The evolution of the system with parameters $s = .3$, $r = .7$, and $s_1 = .98$, with $f(I) = -.1I$ and $g = f - .2$. This is a region of stability for the 2-cyclic solution in the clustered subspace. Intuitively, we expect that since f and g decrease at the same rate, groups near the 2-cyclic solution should neither collapse to points nor expand too far away from the solution. The initial value of (a) results in two pairs of two clusters, something that can happen in the RS and gap model only if the k-cyclic solution is neutrally stable in the clustered subspace. In (b), ϵ_i converges to 0 for some but not all values of i, causing clusters of different sizes to develop. An initial condition of cells spread uniformly around S^1 converges to two groups, which do not contract into clusters.

Figure 5.4c paints a pleasant picture of stability in the full phase space. True, the system is not converging to the 2-cyclic solution in a region of parameter space where, in the clustered subspace, the 2-cyclic solution is stable, but it is clearly self-orgazing into two groups. Unfortunately, no general theorem in that vein can be stated. In Figure 5.3b, we simulate the system for the first several thousand iterations of the Poincaré map, and observe that the groups expand under the effect of the system. We now observe the same system over the course of $15,000$ iterations of P. We observe that although the initial condition was in a neighborhood of the 2-cyclic solution, stable

in the clustered subspace, the system never returns to that neighborhood. Instead, it appears to converge to a 20-clustered solution, although since the size of the clusters are not equal, it is not the 20-cyclic solution.

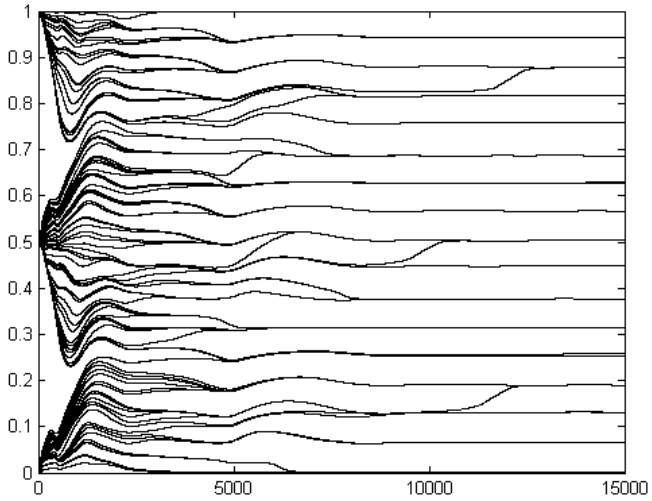

Figure 5.5: For parameter values $s = .3$, $r = .7$, and $s_1 = .98$, and relatively weak feedback functions f and g, the 2-cyclic solution is stable in the clustered subspace, but unstable in the full phase space, behavior unique to the overlap model. We observe this instability in simulation by considering an initial condition of 100 cells placed uniformly in an ϵ-neighborhood of the 2-cyclic solution in the full phase space. Although it is not obvious from the graph, we observe that the clusters that form are not all of the same size, and this solution is therefore not converging to a cyclic solution.

We further consider in simulation what effect varying the strength of g has when the remaining system parameters remain constant. We define the function

$$h(I) = \begin{cases} 0 & I = 0 \\ -1 & \text{otherwise.} \end{cases} \tag{5.5.1}$$

Starting with the feedback function $f(I) = -.6I$, we define a series of weighted averages, $g_i = \frac{ih+f}{i+1}$. Thus $g_0 = f$, and the strength of g_i increases with i. We vary i and observe the effect it has on the model.

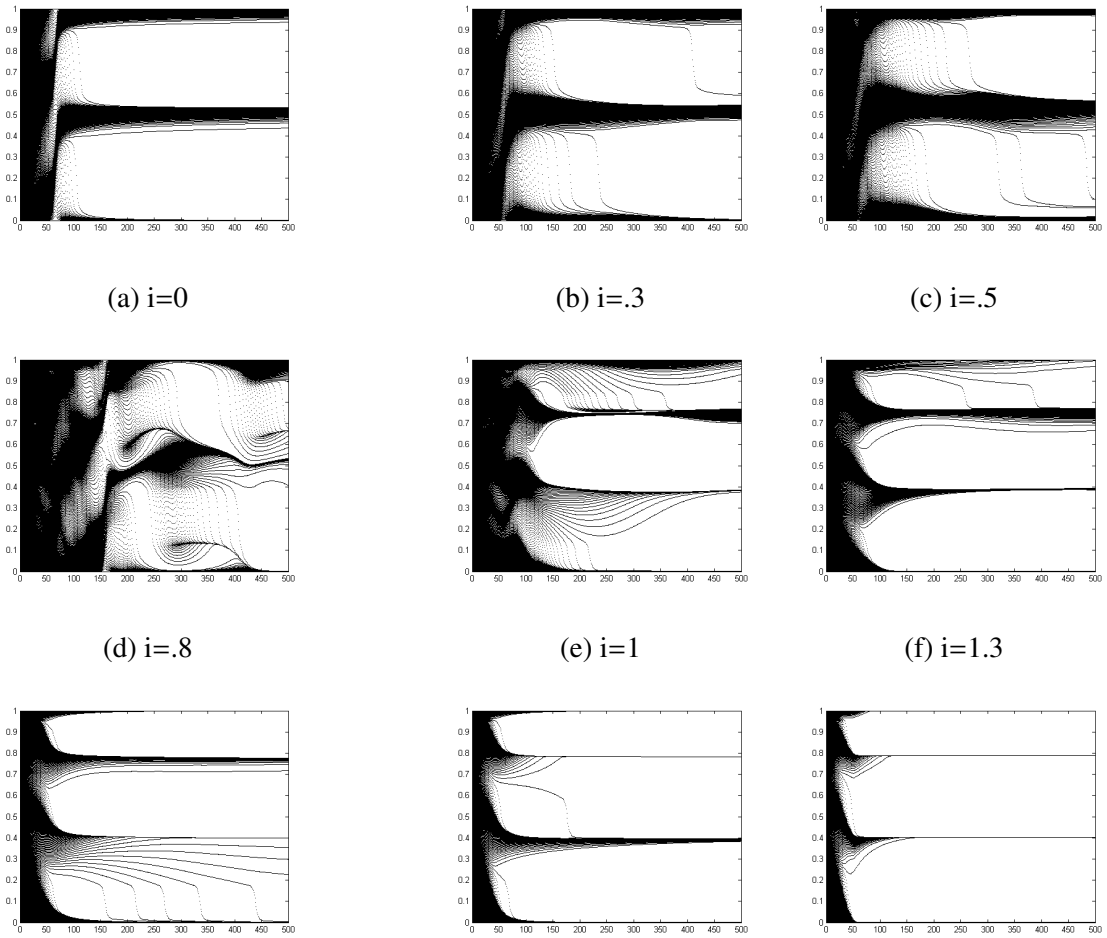

(a) i=0 (b) i=.3 (c) i=.5

(d) i=.8 (e) i=1 (f) i=1.3

(g) i=1.5 (h) i=1.7 (i) i=2

Figure 5.6: Fifty cells are evenly distributed across the interval with $s = .3$, $r = .7$, $s_1 = .95$. The strength of g (in absolute value) increases from top left to lower right.

Here, at least, the behavior of the system is easy to understand in broad terms; as g increases in magnitude, the parameter values move from being in the interior of the (clustered) stability region of the 2-cyclic solution to the interior of the (clustered) stability region of the 3-cyclic solution. Meanwhile, because the strengthening of g is causing it to converge to the constant (zero-slope) function $g = -1$, the diameters of the groups are converging to 0 as discussed after Corollary 5.5.3. Observe that although we have seen that certain feedback functions can cause aberrant behavior, the system here is behaving as one would naively expect, converging to k groups where the k-cyclic

solution is stable in the clustered subspace. We will talk more about this transitioning from one region of stability to another in the next section. Although it is framed in terms of varying s_1, there are obvious similarities between increasing the size of the overlap interval and increasing the strength of the feedback.

5.6 Bifurcations in s_1

Adding a sufficiently small overlap region does not effect the stability of k-cyclic solutions in the clustered subspace.

5.6.1 Theorem. *Consider two systems, an RS system and an overlap system with the same parameters s, r, and f, and k-cyclic solutions $\bar{x}$ and $\tilde{x}$, respectively. There exists an $\epsilon > 0$ such that if $1-\epsilon < s_1 < 1$, then $\bar{x}$ and $\tilde{x}$ share the same stability type (asymptotically stable, unstable, or neutrally stable) in the clustered subspace.*

Proof. Consider $\bar{x}$ in the RS system, and let time run forward until $x_k = s_1$ (a number that has no significance in the RS system). This map, which wil bel denoted by G_{RS}, defines the stability of the system when ϵ is sufficiently small, in the standard sense that the eigenvalues of DG_{RS} are either greater than, less than, or equal to 1. To justify this observation, note that since x_σ has already left S, by the time x_k reaches s_1 (by the assumption that ϵ is sufficiently small), the time for x_k to pass from s_1 to 1 is constant, $t_c = \frac{1-s_1}{1+f((\sigma-1)/k)}$. Thus $F_{RS} = G_{RS} + t_c\mathbf{v} + (1+f((\sigma-1))/k)t_c\mathbf{u}$, where $\mathbf{v}$ and $\mathbf{u}$ are vectors of 1's and 0's carrying the information of which clusters are and are not in R. The map G_{RS} is affine, $G_{RS} = Ax + b$; and $F_{RS} = Ax + c$, where the constant c subsumes b, $t_c\mathbf{v}$, and $t_c\mathbf{u}$. Thus F_{RS} and G_{RS} have the same linear part.

Now consider $\tilde{x}$ in the overlap model. We define G_{RSO} in the analogous way. Because the overlap model acts identically to the RS model until x_k reaches s_1, and the time it takes to travel from s_1 to 1 is a constant that does not affect the Jacobian, $G_{RSO} = G_{RS}$. And for the same reason discussed above, G_{RSO} defines the stability of the overlap system. Thus the stability type of each system is determined by the same matrix. □

As s_1 decreases away from 1, however, the behavior of the overlap model may change from the behavior of the RS model. These changes happen suddenly and discontinuously, and come in two types. In the following definition, and the ensuing discussion, we view M as a function of s_1, with all other parameters fixed.

5.6.2 Definition. *An* **M-Bifurcation** *occurs when reducing s_1 away from 1 causes M to change. More formally, for a fixed f, g, r, and s, a given s_1^* is an M-bifurcation point if $M(s_1^* - \epsilon) \neq M(s_1^*)$ for arbitrarily small ϵ.*

This may happen because the definition of M_{RS}, in the RS model, depends entirely on r and s, while M in the overlap model also depends on s_1 and g.

5.6.1 Example. *Let $s = .2$, $r = .8$, and $f(I) = -\frac{1}{2}I$. Then $M = 2$, and the 2-cyclic solution $(0, 1/2)$ is neutrally stable.*

It can be calculated that in the overlap model, for $f(I) = -.5I$ and $g(1/2) = -.9$, $s_1 = \frac{44}{45}$ is an M-bifurcation value, in the sense that for $s_1 \geq \frac{44}{45}$, $M = 2$, while for $s_1 < \frac{44}{45}$, $M = 1$. The fixed point at $s_1 = \frac{44}{45}$, $x_2 = .6$, lies on the edge of an event triangle (x_2 reaches r at the same time that x_1 reaches s), and is stable.

Since this M-bifurcation causes an interval of neutrally stable points that were 2-periodic under F to converge to a single 1-periodic stable fixed point, this M-bifurcation has parallels to the classic period-doubling bifurcation.

5.6.3 Theorem. *The addition of an overlap region into an RS system, or the increase of the size of O in an existing overlap system, can only cause M to remain constant or decrease, in the case of negative feedback; or remain constant or increase, in the case of positive feedback.*

Proof. Observe that if $s_1 = 1$, $M = M_{RS} = \frac{1}{1-r+s}$. Then if it can be shown that M is increasing on the interval $[r, 1]$, we can conclude that the addition of an overlap to an RS model can only cause M to remain constant or decrease. The derivative of

$\frac{\frac{1-s_1}{1+g(1/k)}+s_1}{\frac{1-s_1}{1+g(1/k)}+s_1-r+s}$ is $\frac{(\frac{-1}{1+g}+1)(-r+s)}{(\frac{1-s_1}{1+g(1/k)}+s_1-r+s)^2}$. Under negative feedback, that is when $g<0$, the derivative is positive. Under positive feedback, the derivative is negative.

□

Because $r < s_1$, there are limits to how large O can be made, and no guarantee that an M-bifurcation will be possible for a given set of parameters (s, r, f, g).

It is possible for M to remain unchanged by the addition of an overlap region into the system, but the order of events, and thus potentially the stability of the system, may change. This may happen, for example, when $M_{RS} = 1$, and thus cannot be reduced further, no matter how powerful and large the overlap region is made.

5.6.4 Definition. *An* **E-Bifurcation** *occurs when M is constant in a neighborhood of* s_1*, but changing* s_1 *changes the order of events, and thus potentially the stability type, of the system.*

5.6.2 Example. *Refer back to Example* 1. *When* s_1 *is slightly less than* $44/45$*, the order of events is* $e_r e_s e_{s_1} e_1$*. This order of events is maintained until* s_1 *is reduced to* $16/17$*, at which point the order of events changes; in particular, this is the point at which events* e_{s_1} *and* e_s *occur concurrently. Since M cannot decrease past* 1*, it is an E-bifurcation. In spite of this language, there is no change in stability, because the new order of events, Item 3b of Proposition 5.3.2, still corresponds to a stable* 2*-periodic fixed point. Although event regions are not triangles (they are convex three-dimensional regions), Chapter 2 still provides enough intuition to see that this is not unexpected; passing from one stability region to another is expected to change the stability in only a minority of cases (for example, in the RS model under positive feedback, transitioning from an interior to a boundary triangle may cause the k-cyclic solution to go from unstable to neutral, but any transition from one interior triangle to another preserves instability.)*

We have seen, however, that M, and the clustered subspace in general, only sporadically and unreliably predict the behavior in the full phase space. Consider again

the parameter values $s = .3$, $r = .7$, and define feedback functions $f(I) = -.2I$ and $g(I) = -.3I - .1$ ($g(0) = 0$). Then $M = 1$ is constant as s_1 runs over R, but the dynamics of the system in the full phase space undergo significant changes. We simulate this behavior for sixteen values of s_1 in Figure 5.7, taken at .02 intervals. Starting with 50 cells spread uniformly around the circle, the Poincaré map is repeatedly applied. The horizontal axes of the graphs represent the number of times the Poincaré map has been applied; once the system comes into a neighborhood of a fixed point the return time becomes approximately constant, so the horizontal axes can also be thought of as roughly representing time. The vertical axes, ranging from 0 to 1, represent the state of the system after that iteration. Although changing s_1 does not change M, it significantly impacts the behavior of the system.

Figure 5.7p is the limiting case where $s_1 = 1$, i.e. the RS model. The 2-cyclic solution is stable for these values of s and r in the clustered subspace, and therefore in the full phase space. As the overlap region widens, the stability in the clustered subspace quickly loses its ability to control the system; for $s_1 = .98$, convergence is radically slowed, and somewhere between $s_1 = .98$ and $s_1 = .94$, the initial condition begins to converge to a very different steady state.

Although a small overlap regions quickly breaks the stability of the 2-cyclic solution in the full phase space, we observe that as $s_1 \to r$, the 2-cyclic solution again begins to appear. For the limiting case $s_1 = r$, the system behaves essentially the same as in the non-overlap case. A cell enters R and starts to experience feedback; the feedback it experiences is piecewise constant, increasing and decreasing as cells enter and leave R according to the effects of a single feedback function. The only difference between this limiting-case overlap model and the RS model is when a cell enters or leaves S. It is therefore unsurprising that for $s_1 = r$ the system behaves similarly to an RS model.

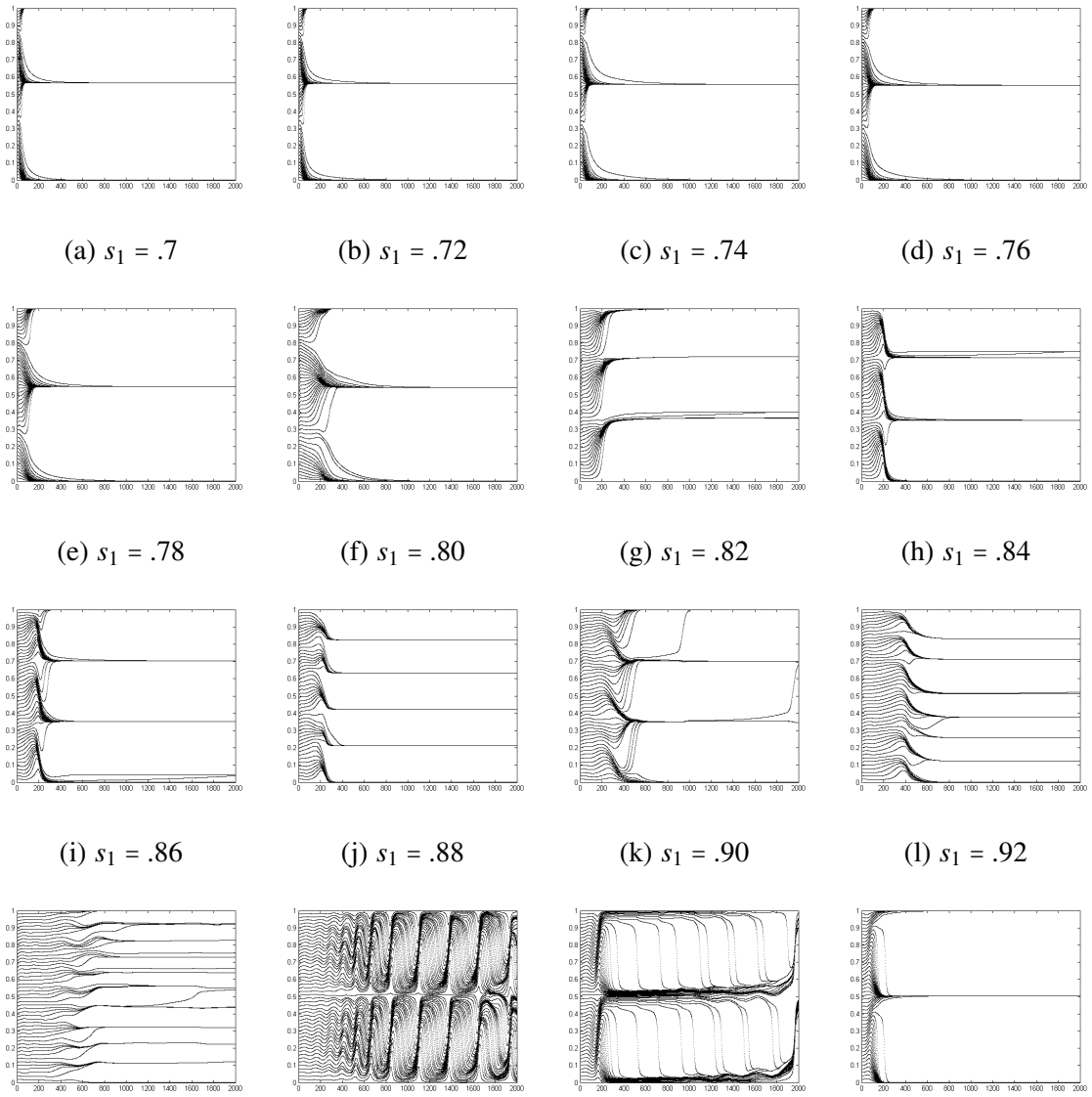

(a) $s_1 = .7$ (b) $s_1 = .72$ (c) $s_1 = .74$ (d) $s_1 = .76$

(e) $s_1 = .78$ (f) $s_1 = .80$ (g) $s_1 = .82$ (h) $s_1 = .84$

(i) $s_1 = .86$ (j) $s_1 = .88$ (k) $s_1 = .90$ (l) $s_1 = .92$

(m) $s_1 = .94$ (n) $s_1 = .96$ (o) $s_1 = .98$ (p) $s_1 = 1$

Figure 5.7: For parameter values $s = .3$, $r = .7$, and feedback functions $f(I) = -.2I$ and $g(I) = -.3I - .1$ ($g(0) = 0$), we consider the effect of changing s_1 on solutions starting from an initial condition of 50 equally spaced cells under 500 iterations of the Poincaré map.

Thus the limiting case where $s_1 = 1$ is the RS model, and the limiting case where $s_1 = r$ is "like the RS model." We have seen that the RS model has the important property that stability in the clustered subspace implies stability in the full phase space, and we have seen that the overlap model lacks this property in general. It is natural to

ask, as an area of future research, whether there are restrictions that can be put on s_1 such that stability in the clustered subspace implies stability in the full phase space in some subset of the (s, r, s_1)-tetrahedron. One might intuitively expect that this behavior will occur when $s_1 \approx 1$, since it occurs when $s_1 = 1$. But it seems in simulation (we include only a representative set of plots, but have performed such simulations with a variety of parameter values) that in fact small perturbations of $s_1 = 1$ cause this property to be lost extremely quickly. On the other hand, the case that is only "like the RS model" preserves the behavior of the RS model extremely well; the endpoint s_1 can increase by a full .10, from $s_1 = .7$ to $s_1 = .8$, before the stability of the 2-cyclic solution in the clustered subspace ceases to result in stability in the full phase space. We are therefore left with the unintuitive suggestion that the wilder behavior of the overlap system is best minimized by increasing rather than decreasing the size of the region that causes that behavior. This suggestion gains support from Section 5.4.2, where cases that imply a large overlap region (Cases 1b and 3a) are seen to correspond to stable solutions.

5.7 Conclusions and discussion

We have seen that the overlap model behaves similarly to the RS model in the clustered subspace. In the full phase space, it acts in somewhat unpredictable ways that require further research and clarification.

When $f = g$, stability in the clustered subspace implies neutrality in the full phase space under one order of events. In the absence of noise, this may be suitable for modeling. However, we have seen in Chapter 4 that even when a solution is asymptotically stable in the full phase space, considerable feedback is required to overcome the dispersive forces inherent to the biological system. When additive noise is added to a system, neutrally stable solutions are likely to be untenable (e.g. [51]).

Thus it is likely that g should be proscribed to be strictly greater than f if noise is to be added to the system.

When $g > f$, we see that asymptotic stability in the clustered subspace may, or may not, imply asymptotic stability in the full phase space. Clarifying the relationship between stability in the clustered and full spaces is a subject of interest as of the time of writing.

References

[1] L. Alberghina, C. Smeraldi, B. M. Ranzi, and D. Porro, Control by nutrients of growth and cell cycle progression in budding yeast, analyzed by double-tag flow cytometry, *Journal of Bacteriology* **180 (15)** (1998), 3864-3872.

[2] F. Antoneli, A.P. Dias, M. Golubitsky, and Y. Wang, Patterns of synchrony in lattice dynamical systems, *Nonlinearity* **18** (2005), 2193-2209.

[3] G. Balázsi, A. van Oudenaarden, and J.J. Collins, Cellular decision making and biological noise: from microbes to mammals, *Cell* **144(6)** (2011), 910-925.

[4] H. Ban and E. Boczko, Age distribution formulas for budding yeast, Vanderbilt Technical Report, http://hdl.handle.net/1803/1166

[5] M. Bier, B.M. Bakker, and H.V. Westerhoff, How yeast cells synchronize their glycolytic oscillations: a perturbation analytic treatment, *Biophys J.* **78(3)** (2000), 1087-1093.

[6] E. Boczko, C. Stowers, T. Gedeon, and T. Young, ODE, RDE and SDE Models of Cell Cycle Dynamics and Clustering in Yeast, *J. Biolog. Dynamics* **4** (2010), 328-345. ArXiv: math.young.16113.

[7] E. M. Boczko, T. G. Cooper, T. Gedeon, K. Mischaikow, D. G. Murdock, S. Pratap, and K.S. Wells, Structure theorems and the dynamics of nitrogen cataboliter repression in yeast, *Proc. Natl. Acad. Sci.* **102** (2005), 5647-5652.

[8] E. Boye, T. Stokke, N. Kleckner, and K. Skarstad, Coordinating DNA replication initiation with cell growth: differential roles for DnaA and SeqA proteins, *Proc. Natl. Acad. Sci.* **93** (1996), 12206-12211.

[9] L.L. Breeden, α-Factor synchronization of budding yeast, *Methods in Enzymology* **283** (1997), 332-342.

[10] N. Breitsch, G. Moses, T. Young, and E. Boczko, Cell cycle dynamics: clustering is universal in negative feedback systems, *J. Math. Biology* **70(5)** (2015) DOI: 10.1007\s00285-014-0786-7

[11] A. Bressan, Unique solutions for a class of discontinuous differential equations, *Proceedings of the American Mathematical Society* **104**:3, 1988, 772 - 778.

[12] R. Buckalew, Cell cycle clustering in a nonlinear mediated feedback model, *DCDS B* **19(4)** (2014), 867-881.

[13] R. Buckalew, S Tanda, K. Finley, and T. Young, Statistical evidence for internuclear feedback in early Drosophila embryogenesis. Submitted.

[14] M. Buese, A. Kopmann, H. Diekmann, and M. Thoma, Oxygen, pH value, and carbon source induced changes of the mode of oscillation in synchronous continuous culture of *Saccharomyces cervisiae*, *Biotechno. Bioeng.* **63** (1998), 410-417.

[15] H. Chen, M. Fujita, Q. Feng, J. Clardy, and G.R. Fink, Tyrosol is a quorum sensing molecule in *Candida albicans*, *Proc. Natl. Acad. Sci.* **101** (2004), 5048-5052.

[16] Z. Chen, E.A. Odstrcil, B.P. Tu, and S.L. McKnight, Restriction of DNA replication to the reductive phase of the metabolic cycle protects genome integrity, *Science* **316** (2007), 1916-1919.

[17] A. Cohn, Über die Anzahl der Wurzeln einer algebraischen Gleichung in einem Kreise, *Math. Zeit.* **14** (1922), 110-148.

[18] J. Collier, H.H. McAdams, and L. Shapiro, A DNA methylation ratchet governs cell cycle progression through a bacterial cell cycle, *Proc. Natl. Acad. Sci.* **104** (2007), 17111-17116.

[19] L. Conlon, *Differentiable Manifolds*, Birkhauser, New York, 2008.

[20] T. Danino, O. Mondragón-Palomino, L. Tsimring, and J. Hasty, A synchronized quorum of genetic clocks, *Nature* **463** (2010) DOI:10.1038/nature08753

[21] O. Diekmann, H. Heijmans, and H. Thieme, On the stability of the cell size distribution, *J. Math. Biol.* **19** (1984), 227–248.

[22] O. Diekmann, M. Gyllenberg, H. Thieme, and S. V. Lunel, A cell-cycle model revisited, *CWI. Depart. Analysis, Algebra and Geometry [AM]*, (1995) No. R9305:1–18.

[23] G. M. Dunny and B. A. B. Leonard, Cell cell communication in Gram Positive bacteria, *Annu. Rev. Microbiol.* **51** (1997), 527-564.

[24] B. Ermentrout, An adaptive model for synchrony in the firefly Pteroptyx malaccae, *J. Math. Biol.* **29** (1991) , 571-585.

[25] B. Fernandez and T. Young, Dynamics of three clusters in a linear, positive feedback cell cycle model, Technical report (2011). Arxiv:1105.2803.

[26] R. K. Finn, R. E. Wilson, Population dynamic behavior of the Chemostat system, *Agric. Food Chem.* **2** (1954), 66-69.

[27] N. Fisher, *Statistical Analysis of Circular Data* (1995), Cambridge University Press.

[28] B. Futcher, Metabolic cycle, cell cycle and the finishing kick to start, *Genome Biology* **7** (2006), 107-111.

[29] T.B. Gage, F.M. Williams, and J.B. Horton, Division synchrony and the dynamics of microbial populations: a size-specific model, *Theoret. Population Biol.* **26** (1984), 296–314.

[30] X. Gong, R. Buckalew, T. Young, and E. Boczko, Cell cycle feedback model with a gap, *J. Biol. Dynamics* **8(1)**(2014), 79-98.

[31] X. Gong, G. Moses, A. Neiman, T. Young, Noise-induced dispersion and breakup of clusters in cell cycle dynamics, *J. Theor. Biology*, **355**, (2014) 160-169.

[32] J. K. Hale, Synchronization by diffusive coupling, Proceedings of *Topological Methods in Differential Equations and Dynamical Systems* (Krakow-Przegorzay, 1996). *Univ. Iagel. Acta Math.* **36** (1998), 17-31.

[33] K. Hannsgen and J. Tyson, Stability of the steady-state size distribution in a model of cell growth and division, *J. Math. Biology* **22** (1985), 293-301.

[34] E. Heinzle, I.J. Dunn, K. Furakawa, R.D. Tanner RD, Modeling of sustained oscillations observed in continuous culture of *Saccharomyces Cerevisiae*, *Modeling and control of biotechnical processes* 1st IFAC Workshop (1982), 57-65.

[35] B. A. Hense, C. Kuttler, J. Muller, M. Rothballer, A. Hartmann, and J. Kreft, Does efficiency sensing unify diffusion and quorum sensing?, *Nat. Rev. Microbiol.* **5** (2007), 230-239.

[36] M. A. Henson, Modeling the synchronization of yeast respiratory oscillations, *Journal of Theoretical Biology* **231** (2004), 443-458.

[37] M. A. Henson, Cell ensemble modeling of metabolic oscillations in continuous yeast cultures, *Comput. Chem. Enginer.* **29** (2005), 645-661.

[38] M. Hjortsø and J. Nielsen, A conceptual model of autonomous oscillations in microbial cultures, *Chemical Engineering Science*, **49** (1994), 1083-1095.

[39] M. A. Hjortsø, Population balance models of autonomous periodic dynamics in microbial cultures. Their use in process optimization, *Can. J. Chem. Engin.*, **74** (1996), 612-620.

[40] A. J. Homburg and T. Young, Hard bifurcations in dynamical systems with bounded random perturbations, *Regular & Chaotic Dynamics*, **11** (2006), 247–258.

[41] A. J. Homburg, T. R. Young, and M. Gharaei, Bifurcations of random differential equations with bounded noise, *Bounded Stochastic Processes in Physics, Biology and Engineering*, A. d'Onofrio ed., Birkhauser-Springer (2013).

[42] J. M. Hornby, E. C. Jensen, A. D. Lisec, J. J. Tasto, B. Jahnke, R. Shoemaker, P. Dussault, and K. W. Nickeron, Quorum sensing in the dimorphic fungus *Candida albacans* is mediated by farnesol, *Appl. Environ. Microbiol.* **67** (2001), 2982-2992.

[43] B. Horne, Lower bounds for the spectral radius of a matrix, *Linear Algebra and Its Applications* **263** (1997), 261-273.

[44] L. M. Jones, A. Fontanini, B. F. Sadacca, P. Miller, and P. B. Katz, Natural stimuli evoke dynamic sequences of states in sensory cortical ensembles, *Proc. Natl. Acad. Sci. USA* **104** (2007),18772-7.

[45] M. Keulers, A. D. Satroutdinov, T. Sazuki, and H. Kuriyama, Synchronization affector of autonomous short period sustained oscillation of *Saccharomyces cerevisiae*, *Yeast* **12** (1996), 673-682.

[46] Z. Kilpatrick and B. Ermentrout, Sparse gamma rhythms arising through clustering in adapting neuronal networks, *PLoS Comput. Biology***7** (2011).

[47] T. Kjeldsen, S. Ludvigsen, I. Diers, P. Balshmidt, A. Sorensen, and N. Kaarshold, Engineering-enhanced protein secretory expression in yeast with applications to insulin, *J. Biol. Chem.***277**(2002), 18245–18248.

[48] R. R. Klevecz, Quantized generation time in mammalian cells as an expression of the cellular clock, *Proc. Natl. Acad. Sci.* **73** (1976), 4012-4016.

[49] R.R. Klevecz, S.A. Kaufman, and R.M. Shymko, Cellular clocks and oscillators, *Inter. Rev. Cytol.* **86** (1984), 97-128.

[50] R. R. Klevecz and D. Murray, Genome wide oscillations in expression, *Molecular Biology Reports* **28** (2001), 73-82.

[51] E. Knobloch and J. Weiss, Effect of noise on discrete dynamical systems, *Noise in Nonlinear Dynamical Systems v. 2: Theory of Noise Induced Processes in Special Applications*, ed. F. Moss and P. V. E. McClintock (1989).

[52] M.T. Kuenzi and A. Fiechter, Changes in carbohydrate composition and trehalose activity during the budding cycle of Saccharomyces cerevisiae, *Arch. Microbiol.* **64** (1969), 396-407.

[53] Y. Kuramoto, *Chemical oscillations, waves, and turbulence*, Springer, New York, 1984.

[54] A. Kuznetsov, M. Korn, and N. Kopell, Synchrony in a population of hysteresis-based genetic oscillators, *SIAM J. Appl. Math.* **65** (2004/05), 392-425.

[55] J. S. W. Lamb, M. Rasmussen, and C. S. Rodrigues, Topological bifurcations of minimal invariant sets for set-valued dynamical systems, ArXiv:1105.5018v1 [math.DS] (2011) (unpublished).

[56] G. J. Lyon and R. P. Novick, Peptide signaling in *Staphylococcus aureus* and other Gram positive bacteria, *Peptides* **25** (2004), 1389-1403.

[57] A. Majda and X. Wang, *Nonlinear Dynamics and Statistical Theores for Basic Geophysical Flows,*

[58] A. Mauroy and R. Sepulchre, Clustering behaviors in networks of integrate-and-fire oscillators, *Chaos* **18** (2008) 037122. doi:10.1063/1.2967806

[59] H. K. von Meyenburg, Energetics of the budding cycle of Saccharomyces cerevisiae during glucose limited aerobic growth, *Arch. Microbiol.* **66** (1969), 289-303.

[60] R. E. Mirollo and S. H. Strogatz, Synchronization of pulse-coupled biological oscillators, *SIAM Journal on Applied Mathematics* **50**, No. 6 (1990), 1645-1662.

[61] Monte, S. D., d'Ovidio, F., Danø, S., and Sørensen, P. (2007), Dynamical quorum sensing: Population density encoded in cellular dynamics, *PNAS*, 104:18377–18381.

[62] G. J. Moses, Stability results in a system of coupled oscillators. Unpublished

[63] G. Moses, D. Scalfino, Cell cycle dynamics in a response/signaling feedback system with overlap. In submission.

[64] D. Muller, S. Exler, L. Aguilera-Vazquez, E. Guerrero-Martin, M. Reuss, Cyclic AMP mediates the cell cycle dynamics of energy metabolism in *Saccharomyces cervisiae*, *Yeast* **20** (2003), 351-367.

[65] T. Munch, B. Sonnleitner, A. Fiechter, The decisive role of the *Saccharomyces cervisiae* cell cycle behavior for dynamic growth characterization, *J. Biotechnol.* **22** (1992), 329-352.

[66] D. Murray, R. Klevecz, and D. Lloyd, Generation and maintenance of synchrony in *Saccharomyces cerevisiae* continuous culture, *Experimental Cell Research* **287** (2003), 10-15.

[67] P. K. Newton, *The N-vortex problem - Analytical techniques*, *Applied Mathematical Sciences***145**, Springer-Verlag, New York, 2001.

[68] G. Zhu, A. Zamamiri, M. A. Henson, and M. A. Hjortsø, Model predictive control of continuous yeast bioreactors using cell population balance models, *Chemical Engineering Science* **55** (2000), 6155-6167.

[69] G. Orosz, P. Ashwin, J. Wordsworth, and S. Townley, Cluster synchronization, switching and spatiotemporal coding in a phase oscillator network, *Proc. Appl. Math. Mech.* **7** (2007), 1030703-1030704.

[70] R. Otnes and L. Enochson, *Digital time series analysis*, Wiley, New York, 1972.

[71] Z. Palkova and L. Vachova, Life within a community: benefits to yeast long term survival, *FEMS. Microbiol. Rev.* **30** (2006), 806-824.

[72] P. R. Patnaik, Oscillatory metabolism of *saccharomyces cerevisiae*: an overview of mechanisms and models, *Biotech. Advances*, **21** (2003), 183–192.

[73] A. Pikovsky, M. Zaks, M. Rosenblum, G. Osipov, and J. Kurths, Phase synchronization of chaotic oscillations in terms of periodic orbits, *Chaos* **7** (1997), 680-687.

[74] A. Pikovsky, M. Rosenblum, and J. Kurths, *Synchronization: A Universal Concept in Nonlinear Sciences* Cambridge Nonlinear Science Series, Cambridge, 2003.

[75] J. R. Pringle, Staining of bud scars and other cell wall chitin with calcoflour, *Methods In Enzymology* **194** (1991), 732-735.

[76] P. Richard, The rhythm of yeast, *FEMS Microbiol. Rev.* **27** (2003), 547-557.

[77] J.B. Robertson, C.C. Stowers, E.M. Boczko, and C.H. Johnson, Real-time luminescence monitoring of cell-cycle and respiratory oscillations in yeast, *Proc Natl Acad Sci U S A*, **105**(46) (2008), 17988-93. PMCID:2584751.

[78] M. Rotenberg, Selective synchrony of cells of differing cycle times, *J. Theoret. Biol.* **66** (1977), 389-398.

[79] A. D. Satroutdinov, H. Kuriyama, and H. Kobayashi, Oscillatory metabolism of *Saccharomyces cerevisiae* in continuous culture, *FEMS Microbiology Lett.* **98** (1992), 261-268.

[80] R. A. Singer and C. C. Johnston, Nature of the G_1 phase of the yeast *Saccharomyces cerevisiae*, *Proc. Natl. Acad. Sci* **78** (1981), 3030-3033.

[81] N. Slavov and D. Botstein, Coupling among growth rate response, metabolic cycle, and cell division cycle in yeast, *Molecular Biology Cell*, **22** (2011), 1999–2009.

[82] P. T. Spellman, G. Sherlock, M. Q. Zhang, and B. Futcher, Comprehensive identification of cell cycle-regulated genes of the yeast *Saccharomyces cerevisiae* by microarray hybridization, *Mol. Cell. Biol.* **9** (1998), 3273-3297.

[83] C. Stowers, T. Young, and E. Boczko, The structure of populations of budding yeast in response to feedback, *Hypoth. Life Sciences* **1** (2011), 71-84.

[84] C. C. Stowers, J. B. Robertson, H. Ban, R. D. Tanner, and E. M. Boczko, Periodic fermentor yield and enhanced product enrichment from autonomous oscillations, *Appl Biochem Biotechnol*, **156** (2009), (1-3), 59-75. DOI: 10.1007/s12010-008-8486-7.

[85] C. C. Stowers, J. B. Robertson, H. Ban, C. H. Johnson, T. R. Young, and E. M. Boczko, Clustering, communication and environmental oscillations in populations of budding yeast (2008). Preprint.

[86] C. Stowers and E.M. Boczko, Extending cell cycle synchrony and deconvolving population effects in budding yeast through an analysis of volume growth with a structured Leslie model, *JBiSE* **3** (2011), 987-1001.

[87] S. H. Strogatz, From Kuramoto to Crawford: exploring the onset of synchronization in populations of coupled oscillators, *Physica D* **143** (2000), 1-20.

[88] B. Tu, A. Kudlicki, M. Rowicka, and S. McKnight, Logic of the yeast metabolic cycle: temporal compartmentation of cellular processes, *Science*, **310** (2005), 1152–1158.

[89] T. Tvegard, H. Soltani, H. C. Skjolberg, M. Krohn, E. A. Nilssen, et al, A novel checkpoint mechanism regulating the G1/S transition, *Genes and Development* **21** (2007), 649-654.

[90] K. Uchiyama, M. Morimoto, Y. Yokoyama, and S. Shioya, Cell cycle dependency of rice α-amylase production in a recombinant yeast, *Biotech. Bioeng.* **54** (1996), 262–271.

[91] K. Von Meyenburg, Stable synchronous oscillations in continuous cultures of s. cerevisiae under glucose limitation, *Biological Biochemical Oscillators* (1973).

[92] C. van Vreeswijk, Partial synchronization in populations of pulsecoupled oscillators, *Phys. Rev. E* **54** (1996), 5522-5537.

[93] G. Walker, Synchronization of yeast cell populations, *Methods Cell Sci.* **21** (1999), 87-93.

[94] Z. Xu and K. Tsurugi, A potential mechanism of energy metabolism oscillation in an aerobic chemostat culture of the yeast *Saccharomyces cervisiae*, *FEBS Journal* **273** (2006), 1696-1709.

[95] C. L. Woldringh, P. G. Huls, N. O. E. Vischer, Volume growth of daughter and parent cells during the cell cycle of *Saccharomyces cerevisiae* a/α as determined by image cytometry, *J. Bacteriology* **175** (2003), 3174-3181.

[96] T. Young, B. Fernandez, R. Buckalew, G. Moses, and E. Boczko, Clustering in cell cycle dynamics with general responsive/signaling feedback, *J. Theor. Biol.*, **292** (2012), 103–115.

[97] B. P. Tu, A. Kudlicki, M. Rowicka, S. L. McKnight, Logic of the yeast metabolic cycle: temporal compartmentation of cellular processes, *Science* **310** (2005), 1152-1158.

[98] G. Zhu, A. Zamamiri, M. Henson, and M. Hjortsø, Model predictive control of continuous yeast bioreactors using cell population balance models, *Chem. Engin. Sci.*, **55** (200), 6155–6167.

[99] H. Zmarrou and A. J. Homburg, Bifurcations of stationary measures of random diffeomorphisms, *Ergod. Th. Dyn. Systems*, **27** (2007), 1651–1692.

Appendix A: Calculations In the RS model

In this appendix, we include such calculations as are necessary for the discussion of the RS model in this thesis but, due to length, cannot be included in the body of the thesis without disruption.

A.1 Analysis for $k = 2$

In this appendix, we completely quantify the possible behaviors of a two-cluster system under the RS model.

Recall the notation $\alpha = f(\frac{1}{2})$.

In the case where $r + (1+\alpha)s < 1$, we obtain that F is a continuous decreasing map:

$$F(x_2) = \begin{cases} 1 - x_2 & \text{if} \quad 0 \le x_2 \le r - s \\ 1 - (1+\alpha)x_2 + \alpha(r-s) & \text{if} \quad r - s < x_2 < r \\ 1 - x_2 - \alpha s & \text{if} \quad r \le x_2 < 1 - (1+\alpha)s \\ \frac{1}{\alpha+1}(1 - x_2) & \text{if} \quad 1 - (1+\alpha)s < x_2 \le 1. \end{cases}$$

In the case where $r + (1+\alpha)s \ge 1$, we calculate F to be

$$F(x_2) = \begin{cases} 1 - x_2 & \text{if} \quad 0 \le x_2 < r - s \\ 1 - (1+\alpha)x_2 + \alpha(r-s) & \text{if} \quad r - s < x_2 \le \frac{1}{\alpha+1} + \frac{\alpha}{\alpha+1}r - s \\ r - x_2 + \frac{1}{\alpha+1}(1-r) & \text{if} \quad \frac{1}{\alpha+1} + \frac{\alpha}{\alpha+1}r - s < x_2 \le r \\ \frac{1}{\alpha+1}(1 - x_2) & \text{if} \quad r < x_2 \le 1. \end{cases}$$

We report the details of computations in the case where $(1+\alpha)s < 1 - r$. The other case can be treated similarly and we only give below the resulting expression of F. When $(1+\alpha)s < 1 - r$, there are 4 situations depending on the location of x_1:

- $x_1 \le r - s$. In this case, x_0 leaves S before x_1 enters R. The point x_1 is not submitted to any feedback and hence $x_1(t) = x_1 + t$ for all t which implies $F(x_1) = t_1 = 1 - x_1$. (The occurrence of this case is independent of $r + (1+\alpha)s < 1$.)

- $r - s < x_1 \leq r$. Here x_1 is influenced, but not during the entire responsive region since x_0 gets out of S before x_1 reaches 1. More precisely, we have[¶]

$$x_1(t) = \begin{cases} x_1 + t & \text{if} \quad 0 < t < r - x_1 \\ r + (1+\alpha)(t - r + x_1) & \text{if} \quad r - x_1 < t < s \\ r + (1+\alpha)(s - r + x_1) + t - s & \text{if} \quad s \leq t \end{cases}$$

  It follows that $F(x_1) = 1 - (1+\alpha)x_1 + \alpha(r - s)$.

- $r < x_1 \leq 1 - (1+\alpha)s$. Then

$$x_1(t) = \begin{cases} x_1 + (1+\alpha)t & \text{if} \quad 0 < t < s \\ x_1 + (1+\alpha)s + t - s & \text{if} \quad s \leq t \end{cases}$$

  from which we obtain $F(x_1) = 1 - x_1 - \alpha s$.

- $1 - (1+\alpha)s < x_1 \leq 1$. In this case, x_1 starts sufficiently close to 1 to have velocity $1 + \alpha$ when reaching the boundary. We have $F(x_1) = \frac{1}{\alpha+1}(1 - x_1)$.

As argued for arbitrary k, the map F has a k-periodic orbit which, for $k = 2$, is composed of the boundaries 0 and 1. By the Intermediate Value Theorem, it must also have a fixed point on the diagonal.

The graph of F coincides with the anti-diagonal $(1 - x_1)$ for $x_1 \leq r - s$. For $\alpha = f(\frac{1}{2}) > 0$ it is strictly lower than this line if $r - s < x_1 < 1$; but if $\alpha < 0$, then it is strictly greater than $1 - x_1$ for $r - s < x_1 < 1$. The dynamics can be characterized completely for arbitrary parameters when $k = 2$. The following conclusions hold:

- If $r - s > \frac{1}{2}$, each point of the interval $[1 - r + s, r - s]$ is part of a 2-periodic orbit $x \mapsto 1 - x \mapsto x$, except for the point $x = \frac{1}{2}$ which is fixed. The return map F^2 thus has an interval of neutrally stable fixed points centered around $x_1 = \frac{1}{2}$.

  - If $\alpha > 0$, if x_1 is above (resp. below) this neutral interval, we have $F^2(x_1) > x_1$ (resp. $F^2(x_1) < x_1$) and so any initial point converges to 1 (resp. 0).

[¶] The occurrence of the late phase where x_1, although being in R, moves with velocity 1, is because $r + (1+\alpha)s < 1$; at time $t = s$, when x_1 has left S, the cluster x_2 is still in R.

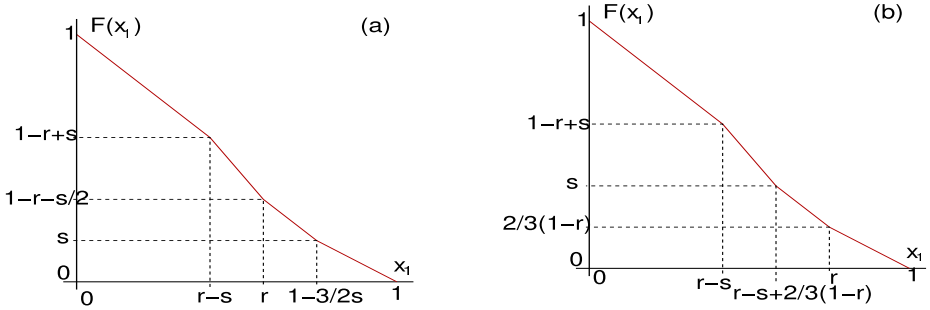

Figure A.1: Plots of the mapping F for $k = 2$ and $\alpha = f\left(\frac{1}{2}\right) = \frac{1}{2}$. (a) $r + \frac{3}{2}s < 1$. (b) $r + \frac{3}{2}s \geq 1$. If $r - s > 1/2$ (which implies $M \geq 2$) then there is a neutral fixed point at $1/2$ that represents an isolated 2 cluster cyclic solution. If the second segment intersects the diagonal, then there is an isolated 2 cluster cyclic solutions that is stable for $\alpha < 0$ and unstable for $\alpha > 0$. There also may exist neutral fixed points for $r - s < 1/2$ ($M = 1$) and certain conditions on the parameters where the third piecewise segment of F intersects the diagonal line. These fixed points represent 2 cluster cyclic solutions that are not isolated, but yet are neutrally stable.

    - If $\alpha < 0$, if x_1 is above (resp. below) this neutral interval, we have $F^2(x_1) < x_1$ (resp. $F^2(x_1) > x_1$) and so any initial point converges to the boundary of the neutral interval.

- If $r - s = \frac{1}{2}$, there is a unique fixed point. It is stable for negative α and unstable for positive α.

- If $r - s < \frac{1}{2}$ there are three possibilities depending on where the diagonal line $x = y$ intersects the graph of F (see Figure A.1).

    - If the diagonal intersects the second segment then there is a unique fixed point which is stable if $\alpha < 0$ and unstable if α is positive.

    - If the diagonal intersects the third segment of F, then there is again an interval of neutral period 2 points. The edge of the interval is stable for negative α and unstable for positive α.

- If the diagonal hits the boundary between segments 2 and 3 of F then there is a unique fixed point which is stable for negative α and unstable for positive α.

All of these possibilities are summarized in just four distinct types of behaviour in Section 2.2 and Figure 2.2.

The condition $r - s > 1/2$ corresponds to $M \geq 2$. In such a case the cyclic 2 cluster solution consists of isolated clusters and it is contained in an interval of neutral period two points. This interval is an attractor for negative feedback and a repeller for positive feedback.

Note that the condition $r - s < 1/2$ corresponds to $|R| + |S| > 1/2$ which implies that $M = \lfloor (|R|+|S|)^{-1} \rfloor = 1$. Thus when the 2 clusters cannot be isolated, there is a cyclic 2 cluster solution which is a fixed point of F. This solution may be unique and stable (under negative feedback), unique and unstable (under positive feedback), or neutral, depending on the parameters.

One can easily calculate that the diagonal line cannot intersect the fourth segment of the graph of F in either case (A.1) or (A.1).

In case A.1 it is seen that the third segment can be intersected by the diagonal by making r sufficiently small. This corresponds to the x_1 coordinate of the fixed point being greater than r so that the second cluster begins in the responsive region R. From the conditions, it is still in R when x_0 leaves S. There is an interval of fixed points for F^2 even though the clusters are not isolated.

The diagonal also can intersect the third segment for case A.1 if x_1 is in S when x_2 enters R, and remains in S until x_2 reaches 1. Thus we have another case of interacting clusters that still leads to a neutral fixed point. Note, however, that in a sufficiently small neighborhood of these fixed points, clusters can be meaningfully

thought of as not interacting; each cluster moves at a rate of

$$\dot{x}_i = \begin{cases} 1 & \text{if} \quad 0 \le x_i < r \\ 1 + f(1/2) & \text{if} \quad r \le x_i < 1, \end{cases} \tag{A.1.1}$$

regardless of the precise location of the other cluster.

A.2 The dynamics of the 3-cyclic solution

In this appendix, we rigorously investigate the stability of the 3-cyclic solution in each of the nine stability triangles (see Chapter 2 that $k = 3$ defines.

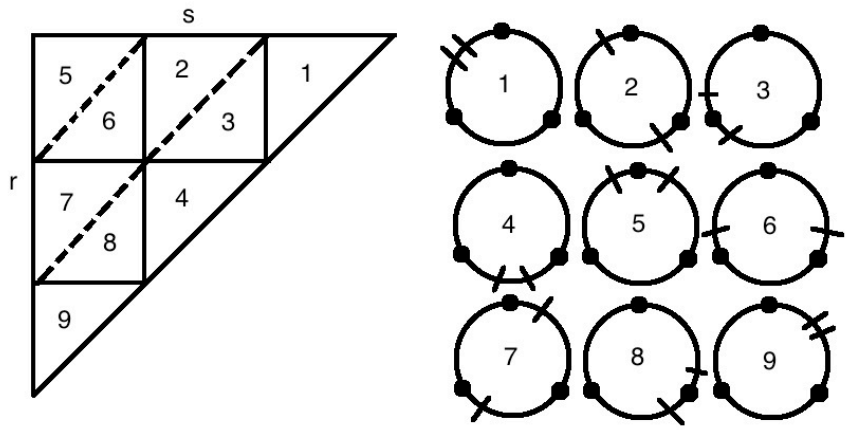

Figure A.2: Regions of parameter space and appropriate initial conditions for a $k = 3$ cyclic solution. For example, regions 7 and 8 both begin with $x_1 \in [s, r)$ and $x_2 \in R$. In region 7 cluster x_1 reaches s before x_2 reaches r, while in region 8, x_2 reaches r before x_1 reaches s. Boundaries between the regions correspond to simultaneous events.

Referring to the labeling in Figure 2.6 (reproduced as Figure A.2), we present calculations verifying rigorously the conclusions of the numerically generated plot in Figure 2.9 for the case $k = 3$ under negative feedback. We also consider positive feedback; the reader may want to focus attention on Region 4, which is of the greatest interest.

Regions 2, 6, 7:

In Figure 2.9 for the case $k = 3$ we see that regions 2 and 7 have neutral stability of the 3-clustered cyclic solution and in region 6 it is stable. These three regions are covered by Proposition 2.3.1.

Region 1:

We wish to confirm that for all parameter values in this region, the 3-cluster cyclic solution is neutrally stable.

For parameter values in this region, all three clusters lie in S when $x_1 = 0$. After the application of a single F-map, x_3 leaves S, enters R, and thereafter travels at a constant rate of $1 + f(2/3)$. Thus in a neighborhood of the 3-cyclic solution, the system is decoupled, i.e. a cluster's rate depends only on whether or not it is in R. Alternatively, we can calculate DF.

For parameter values in region 1 both x_2 and x_3 are initially in S. The order of events is that first x_3 reaches s, then it reaches r and finally it reaches 1. The rate of x_3 will be 1 until it reaches r. While in R the cluster x_2 will experience feedback due to x_1 and x_2, which remain in S until after x_3 reaches 1, and so it's rate will be $1+f(2/3)$. The time required for x_2 to reach 1 is thus:

$$t^* = r - x_2 + \frac{1}{1 + f(2/3)}(1 - r).$$

The positions of x_1 and x_2 at this time will be:

$$x_1(t^*) = t^* \quad x_2(t^*) = x_2 + t^*.$$

We observe that this map is affine in the variables x_1 and x_2. Thus the derivative of the map F in a neighborhood of the initial condition of the cyclic solution is:

$$DF = \begin{pmatrix} 0 & -1 \\ 1 & -1 \end{pmatrix}. \tag{A.2.1}$$

The eigenvalues of this matrix are $-\frac{1}{2} \pm i\frac{\sqrt{3}}{2}$, which have magnitude 1. This implies that the solution is linearly neutrally stable. Since the map is affine in a neighborhood of the initial condition, the cyclic solution is neutrally stable.

Region 3:

In this region we wish to confirm that the 3 cyclic solution is stable under negative feedback, and unstable under positive feedback. The 3-cyclic regions in this region have two clusters in S when $x_1 = 0$, and none in R. The cluster x_3 enters R before x_2 leaves S.

Thus x_3 will experience feedback of $f(2/3)$ for the times $r - x_3 < t < s - x_2$. For $t > s - x_2$ it will be subject to feedback $f(1/3)$. The trajectory of x_3 is thus:

$$x_3(t) = \begin{cases} x_3 + t & \text{for } 0 \le t \le r - x_3, \\ r + (1 + f(2/3))(t - r + x_3) & \text{for } r - x_3 \le t \le s - x_2, \\ r + (1 + f(2/3))(s - x_2 - r + x_3) + (1 + f(1/3))(t - s + x_2) & \text{for } s - x_1 \le t \le t^*. \end{cases}$$

It follows that the return time t^* satisfies:

$$1 = r + (1 + f(2/3))(s - x_2 - r + x_3) + (1 + f(1/3))(t - s + x_2),$$

and so

$$t^* = \frac{f(2/3) - f(1/3)}{1 + f(1/3)} x_1 - \frac{1 + f(2/3)}{1 + f(1/3)} x_2 + C.$$

The local affine map is given by:

$$x_1(t^*) = t^*, \qquad x_2(t^*) = x_2 + t^*,$$

which gives us:

$$DF = \begin{pmatrix} \frac{f(2/3)-f(1/3)}{1+f(1/3)} & -\frac{1+f(2/3)}{1+f(1/3)} \\ 1 + \frac{f(2/3)-f(1/3)}{1+f(1/3)} & -\frac{1+f(2/3)}{1+f(1/3)} \end{pmatrix} = \begin{pmatrix} \frac{f(2/3)-f(1/3)}{1+f(1/3)} & -\frac{1+f(2/3)}{1+f(1/3)} \\ \frac{1+f(2/3)}{1+f(1/3)} & -\frac{1+f(2/3)}{1+f(1/3)} \end{pmatrix}. \qquad \text{(A.2.2)}$$

The characteristic polynomial for this matrix simplifies to:

$$\lambda^2 + \lambda + \frac{1 + f(2/3)}{1 + f(1/3)} = 0.$$

One can verify that the roots of this polynomial are less than 1 in modulus if and only if $f(2/3) < f(1/3)$, and greater than 1 in modulus if and only if $f(1/3) < f(2/3)$.

Those restrictions correspond to monotonicity of positive and negative feedback, respectively.

Region 4:

We confirm that the 3-cyclic solution is neutrally stable in this region under negative feedback, and discuss the positive-feedback case. We first compute the time it takes x_3 to reach 1; x_3 travels with speed $(1 + f(1/3))$ until time $t = s - x_2$, then travels at speed $(1 + f(1/3))$, allowing us to set up the equation:

$$1 = x_3 + (1 + f(2/3))(s - x_2) + (1 + f(2/3))(t^* - s + x_2).$$

Solving, we find $t^* = \dfrac{1 + (f(1/3) - f(2/3))s}{1 + f(1/3)} - \dfrac{1}{1 + f(1/3)}x_3 + \dfrac{f(2/3) - f(1/3)}{1 + f(1/3)}x_2$.

Cluster x_2 travels at speed 1; x_2 travels at speed 1 until $t = r - x_2$, then at speed $(1 + f(1/3))$:

$$x_2(t^*) = t^* \quad x_2(t^*) = r + (1 + f(1/3))(t^* - r + x_2)$$

Gathering for convenience the constant terms as a single C, $x_2(t^*) = (1 + f(1/3))x_2 + (f(2/3) - f(1/3))x_2 - x_3 + C = (1 + f(2/3))x_2 - x_3 + C$; thus

$$DF = \begin{pmatrix} \frac{f(2/3)-f(1/3)}{1+f(1/3)} & -\frac{1}{1+f(1/3)} \\ 1 + f(2/3) & -1 \end{pmatrix}.$$

The characteristic polynomial of DF is given by $\lambda^2 + \lambda(\frac{f(1/3)-f(2/3)}{1+f(1/3)} + 1) + 1$. To simplify the following expressions, we denote $w = \frac{f(1/3)-f(2/3)}{1+f(1/3)}$. The roots of the polynomial are then $\lambda_\pm = \frac{-w-1\pm\sqrt{(w+1)^2-4}}{2} = \frac{-w-1}{2} \pm \sqrt{\frac{(w+1)^2}{4} - 1}$. We remark that for negative feedback, $0 < w$, and the restriction that $-1 < f(2/3)$ implies that $w < 1$. Thus for negative feedback, the roots are complex, and we compute the norm of λ_+ as $|\frac{(-w+1)}{2} + (\sqrt{1 - \frac{(w+1)^2}{4} - 1})i| = 1$

We will see that this is the only one of the nine cases where the strength of the positive feedback, rather than the mere property of being positive, influences the stability of the 3-cyclic solution. We will have more to say about this in Section 3.4.5

of Chapter 3. For now, we observe that $w < 0$ in the case of positive feedback, but unlike in the negative feedback case, w is not bounded in absolute value. For a fixed $f(1/3)$, the value $f(2/3)$ can be made arbitrarily large without violating the conditions of a feedback function. For modest feedback values (in particular, for $2f(1/3) - f(2/3) > -3$, or $w < -3$), the roots are complex and the previous argument shows that they lie on the unit circle. But as $w \to -\infty$, both the summands of λ_+ go to $+\infty$, and the maximum root thus increases past 1, i.e. neutrality is transformed into instability.

Region 5:

In this event triangle, S is always empty when R is nonempty (S contains only x_1 when the cyclic solution passes the Poincaré section, while R is empty, and x_3 enters R only after x_1 has left S). Thus in a neighborhood of the 3-cyclic solution, all clusters move at a constant rate of 1 for all time, and the 3-cyclic solution is a neutral solution contained in a neighborhood of neutral 3-periodic solutions.

Region 8:

For parameter values in this region x_3 is initially in R (while S contains only x_1), and travels with speed $1 + f(1/3)$ until time $t = s$, then at speed 1. The time it takes to reach 1 can thus be calculated:

$$1 = x_3 + (1 + f(1/3))s + t^* - s \to 1 - x_2 - f(1/3)s = t^*.$$

Clearly $x_1(t^*) = t^*$; bearing in mind that x_2 enters R before x_1 leaves S, we calculate:

$$x_2(t^*) = r + (1 + f(1/3))(s - r + x_2) + t^* - s.$$

This gives rise to the matrix

$$DF = \begin{pmatrix} 0 & -1 \\ 1 + f(1/3) & -1 \end{pmatrix},$$

yielding a characteristic polynomial of $\lambda^2 + \lambda + (1 + f(1/3))$ and roots of $\lambda_\pm = \frac{-1 \pm \sqrt{-3-4f(1/3)}}{2}$. If the roots are real, which implies that $f(1/3) < 0$, the maximum root (in absolute value), λ_-, is contained in the interval $(-1, -\frac{1}{2})$; its upper bound from the fact that it has the form $-\frac{1}{2}$ minus a positive number, its lower bound from the fact that it increases monotonically in absolute value as $f(1/3)$ decreases, and takes on the value of -1 when $f(1/3) = -1$. If the roots are complex, their norm can be explicitly calculated as $\sqrt{1 + f(1/3)}$, which is clearly greater than 1 if and only if $f(1/3) > 0$, and less than 1 if and only if $f(1/3) < 0$. There is thus stability under negative feedback, and instability under positive feedback.

Region 9:

In this case, when $x_1 = 0$, both x_2 and x_3 lie in R.

Cluster x_3 travels at rate $(1 + \alpha_1)$ until time $t = s$, whereafter it travels with speed 1. Its rate is thus independent of the exact location of the other clusters, and the system is decoupled, hence neutral. Alternatively, we can calculate the time it takes x_3 to reach 1:

$$1 = x_3 + (1 + f(1/3))s + t^* - s,$$

yielding $t^* = 1 - x_3 - f(1/3)s$.

Cluster x_2 experiences feedback exactly when x_3 does, and thus travels the same distance, $x_2(t^*) = x_2 + 1 - x_3$. The local affine map is given by:

$$x_1(t^*) = t^* \quad x_2(t^*) = x_2 + 1 - x_3.$$

The resultant characteristic polynomial, $\lambda^2 + \lambda + 1$, has roots strictly on the unit circle.

A.3 The Jacobian of F near a k-cyclic solution

We compute the general Jacobian of F in the RS model in a neighborhood of the cyclic solution under either possible order of events, for any triangle in the interior of event space (in particular, such that R is nonempty when $x_1 = 0$). We start

by computing the return time, which is independent of the order of events. We define $\alpha_i = f(i/k)$.

$$\begin{aligned} 1 &= x_k + (1+\alpha_\sigma)(s - x_\sigma) + (1+\alpha_{\sigma-1})(T - s + x_\sigma) \\ 0 &= x_k - (1+\alpha_\sigma)x_\sigma + (1+\alpha_{\sigma-1})T + (1+\alpha_{\sigma-1})x_\sigma + C \\ 0 &= x_k + (\alpha_{\sigma-1} - \alpha_\sigma)x_\sigma + (1+\alpha_{\sigma-1})T + C \\ T &= \frac{\alpha_\sigma - \alpha_{\sigma-1}}{1+\alpha_{\sigma-1}}x_\sigma - \frac{1}{1+\alpha_{\sigma-1}}x_k + C \end{aligned} \tag{A.3.1}$$

Then, again independent of the order of events, the following equation is satisfied:

$$x_i(T) = x_i + \frac{\alpha_\sigma - \alpha_{\sigma-1}}{1+\alpha_{\sigma-1}}x_\sigma - \frac{x_k}{1+\alpha_{\sigma-1}}x_k + C, \text{ for } i = 1, 2, ..., x_{\rho-1}. \tag{A.3.2}$$

.

A special case of the above equation is that

$$x_\sigma(T) = (1 + \frac{\alpha_\sigma - \alpha_{\sigma-1}}{1+\alpha_{\sigma-1}})x_\sigma - \frac{x_k}{1+\alpha_{\sigma-1}}x_k + C. \tag{A.3.3}$$

Any two clusters that start in R travel the same distance (and the last cluster in R travels a distance $1 - x_k$) over the course of the F-map, and thus, independently of the order of events,

$$x_i(T) = x_i - x_k + C \text{ for } i = \rho + 1, ...k. \tag{A.3.4}$$

Case 1: $\mathbf{e_s e_r}$

If x_ρ does not enter R until after x_σ leaves S, we calculate

$$\begin{aligned} x_\rho(T) &= r + (1+\alpha_{\sigma-1})(T - r + x_\rho) \\ x_\rho(T) &= (\alpha_\sigma - \alpha_{\sigma-1})x_\sigma - x_k + (1+\alpha_{\sigma-1})\rho. \end{aligned} \tag{A.3.5}$$

Thus, in this case, we calculate the following matrix, the Jacobian of F.

$$DF_{sr} = \begin{bmatrix} 0 & 0 & \cdots & 0 & \frac{\alpha_\sigma - \alpha_{\sigma-1}}{1+\alpha_{\sigma-1}} & 0 & \cdots & 0 & 0 & 0 & \cdots & 0 & -\frac{1}{1+\alpha_{\sigma-1}} \\ 1 & 0 & \cdots & 0 & \frac{\alpha_\sigma - \alpha_{\sigma-1}}{1+\alpha_{\sigma-1}} & 0 & \cdots & 0 & 0 & 0 & \cdots & 0 & -\frac{1}{1+\alpha_{\sigma-1}} \\ \cdots & \cdots & \cdots & \cdots & \cdots & \cdots & \cdots & . & \cdots & \cdots & \cdots & \cdots & \cdots \\ 0 & 0 & \cdots & 1 & \frac{\alpha_\sigma - \alpha_{\sigma-1}}{1+\alpha_{\sigma-1}} & 0 & \cdots & 0 & 0 & 0 & \cdots & 0 & -\frac{1}{1+\alpha_{\sigma-1}} \\ 0 & 0 & \cdots & 0 & 1 + \frac{\alpha_\sigma - \alpha_{\sigma-1}}{1+\alpha_{\sigma-1}} & 0 & \cdots & 0 & 0 & 0 & \cdots & 0 & -\frac{1}{1+\alpha_{\sigma-1}} \\ 0 & 0 & \cdots & 0 & \frac{\alpha_\sigma - \alpha_{\sigma-1}}{1+\alpha_{\sigma-1}} & 1 & \cdots & 0 & 0 & 0 & \cdots & 0 & -\frac{1}{1+\alpha_{\sigma-1}} \\ \cdots & \cdots & \cdots & \cdots & \cdots & \cdots & \cdots & . & \cdots & \cdots & \cdots & \cdots & \cdots \\ 0 & 0 & \cdots & 0 & \frac{\alpha_\sigma - \alpha_{\sigma-1}}{1+\alpha_{\sigma-1}} & 0 & \cdots & 1 & 0 & 0 & \cdots & 0 & -\frac{1}{1+\alpha_{\sigma-1}} \\ 0 & 0 & \cdots & 0 & \frac{\alpha_\sigma - \alpha_{\sigma-1}}{1+\alpha_{\sigma-1}} & 0 & \cdots & 0 & 1 + \alpha_{\sigma-1} & 0 & \cdots & 0 & -1 \\ 0 & 0 & \cdots & 0 & 0 & 0 & \cdots & 0 & 0 & 1 & \cdots & 0 & -1 \\ \cdots & \cdots & \cdots & \cdots & \cdots & \cdots & \cdots & . & \cdots & \cdots & \cdots & \cdots & \cdots \\ 0 & 0 & \cdots & 0 & 0 & 0 & \cdots & 0 & 0 & 0 & \cdots & 1 & -1 \end{bmatrix}.$$

We clarify the matrix. The i'th row corresponds to the location of x_i at time T; on the other hand, the i'th column corresponds to the coefficient of x_{i+1}. So, for example, assuming that $\rho > 2$, $x_2(T) = x_2 + \frac{\alpha_\sigma - \alpha_{\sigma-1}}{1+\alpha_{\sigma-1}} x_\sigma - \frac{x_k}{1+\alpha_{\sigma-1}} x_k + C$. This corresponds to the second row; the coefficient 1 of x_2 appears in the first column, the coefficient $\frac{\alpha_\sigma - \alpha_{\sigma-1}}{1+\alpha_{\sigma-1}}$ of x_σ appears in the $(\sigma - 1)$'st column, and the coefficient $\frac{x_k}{1+\alpha_{\sigma-1}}$ of x_k appears in the $(k-1)$'st colum.

In summary:

- There are 1's down the semidiagonal, except that $DF_{sr}(\sigma, \sigma - 1) = 1 + \frac{\alpha_\sigma - \alpha_{\sigma-1}}{1+\alpha_{\sigma-1}}$ and $DF_{sr}(\rho, \rho - 1) = 1 + \alpha_{\sigma-1}$.
- In the column corresponding to x_σ (the $(\sigma - 1)$'st column), the constant $\frac{\alpha_\sigma - \alpha_{\sigma-1}}{1+\alpha_{\sigma-1}}$ appears in the first through ρ'th rows, except the σ'th row (see the previous bullet point for the behavior in the σ'th row). From the ρ'th row downwards, a 0 appears.

- In the last colum, the constant $-\frac{1}{1+\alpha_{\sigma-1}}$ appears in the first to ρ'th rows; from the ρ'th to $(k-1)$'st row, -1 appears.

Case 2: $\mathbf{e_r e_s}$

All of the calculations in the previous discussion hold except for that of $x_\rho(T)$. We calculate instead

$$\begin{aligned} x_\rho(T) &= r + (1+\alpha_\sigma)(s - x_\sigma - r + x_\rho) + (1+\alpha_{\sigma-1})(T - s + x_\sigma) \\ x_\rho(T) &= (1+\alpha_\sigma)x_\rho - x_k + C, \end{aligned} \tag{A.3.6}$$

which gives rise to the matrix

$$DF_{rs} = \begin{bmatrix} 0 & 0 & \cdots & 0 & \frac{\alpha_\sigma - \alpha_{\sigma-1}}{1+\alpha_{\sigma-1}} & 0 & \cdots & 0 & 0 & 0 & \cdots & 0 & -\frac{1}{1+\alpha_{\sigma-1}} \\ 1 & 0 & \cdots & 0 & \frac{\alpha_\sigma - \alpha_{\sigma-1}}{1+\alpha_{\sigma-1}} & 0 & \cdots & 0 & 0 & 0 & \cdots & 0 & -\frac{1}{1+\alpha_{\sigma-1}} \\ \cdots & \cdots & \cdots & \cdots & \cdots & \cdots & \cdots & . & \cdots & \cdots & \cdots & \cdots & \cdots \\ 0 & 0 & \cdots & 1 & \frac{\alpha_\sigma - \alpha_{\sigma-1}}{1+\alpha_{\sigma-1}} & 0 & \cdots & 0 & 0 & 0 & \cdots & 0 & -\frac{1}{1+\alpha_{\sigma-1}} \\ 0 & 0 & \cdots & 0 & 1 + \frac{\alpha_\sigma - \alpha_{\sigma-1}}{1+\alpha_{\sigma-1}} & 0 & \cdots & 0 & 0 & 0 & \cdots & 0 & -\frac{1}{1+\alpha_{\sigma-1}} \\ 0 & 0 & \cdots & 0 & \frac{\alpha_\sigma - \alpha_{\sigma-1}}{1+\alpha_{\sigma-1}} & 1 & \cdots & 0 & 0 & 0 & \cdots & 0 & -\frac{1}{1+\alpha_{\sigma-1}} \\ \cdots & \cdots & \cdots & \cdots & \cdots & \cdots & \cdots & . & \cdots & \cdots & \cdots & \cdots & \cdots \\ 0 & 0 & \cdots & 0 & \frac{\alpha_\sigma - \alpha_{\sigma-1}}{1+\alpha_{\sigma-1}} & 0 & \cdots & 1 & 0 & 0 & \cdots & 0 & -\frac{1}{1+\alpha_{\sigma-1}} \\ 0 & 0 & \cdots & 0 & 0 & 0 & \cdots & 0 & 1+\alpha_\sigma & 0 & \cdots & 0 & -1 \\ 0 & 0 & \cdots & 0 & 0 & 0 & \cdots & 0 & 0 & 1 & \cdots & 0 & -1 \\ \cdots & \cdots & \cdots & \cdots & \cdots & \cdots & \cdots & . & \cdots & \cdots & \cdots & \cdots & \cdots \\ 0 & 0 & \cdots & 0 & 0 & 0 & \cdots & 0 & 0 & 0 & \cdots & 1 & -1 \end{bmatrix}.$$

This is identical to the previous matrix, except that $DF_{rs}(\rho, \sigma - 1) = 0$ and $DF_{rs}(\rho, \rho - 1) = 1 + \alpha_\sigma$.

Although we did not use these matrices to generate stability plots, we will make extensive use of them in the next chapter, in particular in the proofs of Theorems 3.3.3 and 3.3.4.

Appendix B: Calculations In the Noise Models

In this appendix, we include two series of calculations necessary for Chapter 4: the location of x_2, and a bound on the strength of the asymptotic stability of the model.

B.1 Calculation of the two-cluster periodic solution

In this appendix we derive the exact initial conditions for the periodic two-cluster solution of the unperturbed (no noise) model.

Recall that the responsive region has coordinates $R = [0.3, 0.65]$ and the signaling region is $S = [0.65, 0.95]$. The coupling function is $f(I) = -\alpha I$, with $\alpha = 0.5$ in our computations. We know from [96] that a periodic two-cluster solution exists and that for these parameter values it must be stable.

Let the initial condition of the first cluster be $x_1(0) = \frac{1}{4}$ and the initial condition of second cluster be denoted as $x_2(0)$ which is near (but not exactly) 0.75 and inside S. The calculation of the solution depends on the "order of events." Namely, from [10] we know that $x_1(t)$ must enter R while $x_2(t)$ is still in S and then $x_2(t)$ must leave S while $x_1(t)$ is still in R. With these facts in mind we may calculate exactly the trajectory of the clusters starting from our initial condition $(1/4, x_2(0))$ as follows.

- x_1 enters the responsive region, i.e. $x_1 = 0.3$. When x_1 reaches 0.3, we have $x_1(t_1) = 0.3$. It is then easy to solve for

  $$t_1 = x_1(t_1) - x_1(0) = \frac{1}{20}.$$

  Since x_2 is progressing with rate 1 during this phase, $x_2(t_1) = x_2(0) + t_1 = x_2(0) + \frac{1}{20}$.

- x_1 experiences feedback before x_2 leaves the signaling region, i.e. until $x_2 = 0.95$.

  Assume t_2 is the time when x_2 leaves the signaling region, then $x_2(t_2) = 0.95$. Since x_2 travels at a constant rate 1, we have

  $$t_2 = x_2(t_2) - x_2(0) = \frac{19}{20} - x_2(0).$$

However, x_1 is slowed by the coupling function $f(\frac{1}{2}) = -\frac{1}{4}$, so

$$x_1(t_2) = x_1(t_1) + \left(1 + f\left(\frac{1}{2}\right)\right)(t_2 - t_1) = \frac{3}{10} + \frac{3}{4}(\frac{9}{10} - x_2(0)) = \frac{39}{40} - \frac{3}{4}x_2(0).$$

- x_2 arrives at $x_1(0) = \frac{1}{4}$ and because this is the periodic solution, x_1 reaches $x_2(0)$.

  During this phase, there is no feedback exerted. Thus the time t_3 for $x_2(t_3) = \frac{1}{4}$ can be found by:

$$t_3 = t_2 + (x_2(t_3) + 1 - x_2(t_2)) = \frac{19}{20} - x_2(0) + \frac{1}{4} + 1 - 0.95 = \frac{5}{4} - x_2(0).$$

  At this time,

$$x_1(t_3) = x_1(t_2) + (t_3 - t_2) = \frac{39}{40} - \frac{3}{4}x_2(0) + \frac{3}{10} = x_2(0).$$

We may solve the above equation to find that $x_2(0) = \frac{51}{70}$.

We can also obtain from the above calculations that $t_3 = \frac{5}{4} - x_2(0) = \frac{73}{140}$. Thus the period for this two-cluster periodic solution is $T_2 = 2t_3 = \frac{73}{70} > 1$. This is slightly larger than 1 as should be expected for negative feedback.

B.2 Hard bifurcation for the bounded noise system

We will derive an upper bound on the noise level σ at which a hard bifurcation must occur. We first observe that in our negative coupling model "back stability" is much weaker than front stability; that is to say a perturbation where one cell is pulled behind the rest of the cluster converges back to the clustered solution very weakly. The reason for this is that when a nearly synchronized group of cells crosses the boundary from R to S the cells in the front of the group begin to add to the negative feedback in R before the trailing cells leave R.

We will now quantify that statement for the parameters under consideration. Consider the variable rate model and first set the noise equal to 0. Now consider the two-cluster periodic solution (i.e. with $x_1(0) = 1/4$ and $x_2(0) = 51/70$), but perturb the

solution by removing one cell from the cluster at $1/4$, and placing it at $1/4 - \epsilon$. Denote the state of this cell by $x_{1\epsilon}$. We may calculate the trajectory in the noiseless system, starting at this initial condition exactly, using the same procedure as in the previous section.

1. x_1 reaches R before x_2 leaves S, i.e. $x_1 = 0.3$.

   At this time, $x_2 = 109/140$ and $x_{1\epsilon} = 0.3 - \epsilon$.

2. $x_{1\epsilon}$ reaches at R before x_2 leaves S, i.e. $x_{1\epsilon} = 0.3$.

   During this period, only x_1 is experiencing coupling $f(I) = -0.5I = -1/4$ because x_2 is in the signaling region. So $x_1 = 0.3 + 0.75\epsilon$ and $x_2 = 109/140 + \epsilon$.

3. x_2 leaves S while x_1 and $x_{1\epsilon}$ are still in R, i.e. $s_2 = 0.95$.

   During this phase, both x_1 and $x_{1\epsilon}$ are affected by the couping. The time for x_2 to reach at 0.95 is $6/35 - \epsilon$. Thus at this time, $x_1 = 0.3 + 0.75\epsilon + (6/35 - \epsilon)0.75 = 3/7$ and $x_{1\epsilon} = 0.3 + (6/35 - \epsilon)0.75 = 3/7 - 0.75\epsilon$.

4. x_1 leaves R and arrives at S while $x_{1\epsilon}$ is still in R, i.e. $x_1 = 0.65$.

   No feedback is exerted. So we have when x_1 reaches 0.65, $x_2 = 0.95 + 31/140 \mod 1 = 6/35$ and $x_{1\epsilon} = 0.65 - 0.75\epsilon$.

5. $x_{1\epsilon}$ reaches at S as well, i.e. $x_{1\epsilon} = 0.65$.

   In this case, x_1 is in S and $x_{1\epsilon}$ is in R. Thus the coupling function is $f(I) = -0.5\frac{4990}{10000} = -0.24995$. The time for $x_{1\epsilon}$ to arrive at 0.65 is $0.75\epsilon/(1 - 0.24995) = \frac{15000}{15001}\epsilon$. So we have $x_1 = 0.65 + \frac{15000}{15001}\epsilon$.

After the first cluster and the cell both get out of R, we find the distance between them is $\frac{15000}{15001}\epsilon$, which was initially ϵ. This spacing will persist as the cluster x_1 returns to $1/4$, so the distance is decreased by a factor of $15000/15001$. Thus we see that the stability of the solution is very weak with respect to this particular perturbation.

To consider how noise breaks this stability, perform the following perturbations which are a possible realization of the variable rate model. Let x_1 progress at a constant rate of $1+\sigma$, the single cell at a rate of $1-\sigma$, and x_2 progress at rate 1. Denote $\beta = f(\frac{1}{2})$ and $\hat{\beta} = f(\frac{4{,}999}{10{,}000})$ where $f(I) = -0.5I$. The cell at $x_{1\epsilon}$ and the cluster x_1 are progressing at different rates and therefore constantly drifting apart, except while the coupling strength is pulling them together. We will make a simplifying assumption here that we consider the drift only during the periods when x_1 and $x_{1\epsilon}$ are experiencing different strength of coupling; we will see that even under such a strong assumption, the derived upper bound on the bifurcation value is extremely small.

Considering a complete cell cycle of the cluster and the cell, there are three stages when they experience different coupling:

1. When the $4,999$-cell cluster $x_1(t)$ enters R, but $x_{1\epsilon}$ has not yet entered R, the second cluster $x_2(t)$ is still in S, so the coupling β only affects x_1. It takes the cell $x_{1\epsilon}$ time $\frac{\epsilon}{1-\sigma}$ to enter R. At this time, the distance between $x_{1\epsilon}$ and $x_1(t)$ is $\frac{1+\sigma-\beta}{1-\sigma}\epsilon$.

2. When the $x_1(t)$ and the cell $x_{1\epsilon}$ both lie in R and the second cluster is still in S, both of the broken cluster and the cell experience the coupling β. We neglect the changing of the distance between the cell and the cluster during this time by our simplifying assumption.

3. When the cell $x_{1\epsilon}$ lies in R and x_1 enters S, we know the second cluster is not in S. Hence the coupling strength the cell experiences is $\hat{\beta}$. The time from the cluster enters S to the cell enters S is $\frac{1}{1-\sigma+\hat{\beta}}\frac{1+\sigma-\beta}{1-\sigma}\epsilon$, thus the distance between the cell and the cluster after the cell enters S is $\frac{1+\sigma}{1-\sigma+\hat{\beta}}\frac{1+\sigma-\beta}{1-\sigma}\epsilon$.

Setting the coefficient $\frac{1+\sigma}{1-\sigma+\hat{\beta}}\frac{1+\sigma-\beta}{1-\sigma}$ equal to 1, we calculate $\sigma = .000014$. For this amount of noise, the original distance between cell and the broken cluster will stay the same. Any more noise will increase the initial distance.

The calculations above assume that we are near the cyclic solution. In our calculations during stage 1, we assumed that when the cluster entered R, the second (unbroken) cluster was in S, and remained there until after the isolated cell entered R. In the calculations in stage 3, we assumed that the single cell reached 1 before the broken cluster entered S again. When the cell is pulled sufficiently far from the cluster to which it used to belong due to the noise, the assumption in stage 1 breaks down. We next calculate the distance if this happens.

Consider the unperturbed model again. The threshold occurs when the broken cluster lies at .65, the nonbroken cluster lies at .12858, and the cell lies at .47858. Move the cell back to $.47858 - \epsilon$, and let $\hat{\epsilon}$ denote the distance between cluster and cell. Then initially, $\hat{\epsilon} = .17142 + \epsilon$. Run time until the first cluster lies at $C_1 = .3$, the second (broken) clutester lies at $C_2 = .77857$, and the cell that was broken away lies at $c = .64 - \epsilon$; now $\hat{\epsilon} = .12857 + \epsilon$. Advance time further so that $C_2 = 1$ and $c = .87143 - \epsilon$; at this time $\hat{\epsilon} = .12857 + \epsilon$. Running time until $c = 1$, we obtain $\hat{\epsilon} = .17142 + 1.3332\epsilon$.

So even in the non-perturbed model, once the cell has achieved a sufficient separation from the cluster, the distance will widen; we do not need noise beyond $\sigma = .000014$ that we initially obtained. The hard bifurcation, below which cells have no possibility to escape their initial groups, is below the value .000014. While this rigorous upper bound on the bifurcation is quite rough, we see in Figure 4.4 that it is already far lower than noise levels for which an escape can actually be observed.

Appendix C: Calculations In the Overlap Model

In this appendix, we isolate calculations from Chapter 5 that would be disruptive if included in the main text. These include all the possible order of events of F for a two-cluster configuration, together with the map F, and the calculations of the Jacobians for the $k = M + 1$ case.

C.1 Calculations relating to the 2-clustered system in the overlap model

This section contains all possible orders of events that a 2-cluster solution might experience in the overlap model, and the corresponding map F.

For $k = 2$, and placement of x_1 such that the clusters lie on the Poincaré section (e.g. $x_1 = 0$) defines a corresponding F map, which is the composition of a number of order-of-event maps. We exhaustively list every possible order of events, and, for every order of events, we calculate the F-map $F(x_2)$. We give the details for the derivation of F in the first case after the list; all others are similar.

Throughout the appendix, we work not in the overlap system (5.1.2), but in a conjugate model. In particular, we observe that any time a cluster is in O, it experiences some feedback as a result of the self-influence of the system. Since the feedback $g(1/2)$ is really independent of the state of the system, we may rescale O such that a cluster travelling through O and experiencing only the feedback it exerts on itself takes time $|O|$ to pass through it, i.e. $[s_1, 1] \to [s_1, s_1 + \frac{1-s_1}{1+g(1/2)}]$. Under this change of variables, a cluster in O when S is otherwise empty travels at a rate of 1. We perform this change of variables, letting $\tilde{1}$ denote the end of O.

We define our shorthand:

$x_1^s : x_1 \to s$

$x_1^r : x_1 \to r$

$x_1^{s_1} : x_1 \to s_1$

$x_2^r : x_2 \to r$

$x_2^{s_1} : x_2 \to s_1$

$x_2^1 : x_2 \to \tilde{1}$

$\alpha = 1 + f(1/2)$

$\beta = 1 + g(1)$

Orders of events that correspond to a cyclic F-map (see Section 5.3) are given in bold.

1. $x_2 \in \widetilde{R}$

   (a) $\mathbf{x_1^s x_1^r x_2^{s_1} x_2^1}$

   $F(x_2) = s_1 - x_2 - \alpha s + s + \alpha(\tilde{1} - s_1)$

   (b) $\mathbf{x_1^s x_2^{s_1} x_1^r x_2^1}$

   $F(x_2) = r + \alpha(\tilde{1} - r + s - x_2 - \alpha s)$

   (c) $\mathbf{x_2^{s_1} x_1^s x_1^r x_2^1}$

   $F(x_2) = r + \alpha(\tilde{1} - s_1 - \beta s - r + s) + \beta(s_1 - x_2)$

   (d) $x_1^s x_1^r x_2^{s_1} x_1^{s_1} x_2^1$

   $F(x_2) = \tilde{1} - (\tilde{1}/\alpha)(x_2 + \alpha s - s)$

   (e) $x_1^s x_2^{s_1} x_2^1$

   $F(x_2) = s - x_2 - \alpha s + 1$

   (f) $x_1^s x_2^{s_1} x_1^r x_1^{s_1} x_2^1$

   $F(x_2) = s_1 + \tilde{1} - r + s - x_2 - \alpha s - \frac{s_1 - r}{\alpha}$

   (g) $x_2^{s_1} x_2^1$

   $F(x_2) = \frac{s_1 - x_2}{\alpha} + \frac{\tilde{1} - s_1}{\beta}$

   (h) $x_2^{s_1} x_1^s x_2^1$

   $F(x_2) = s + \tilde{1} - s_1 - \beta(s - \frac{s_1 - x_2}{\alpha})$

   (i) $x_2^{s_1} x_1^s x_1^r x_1^{s_1} x_2^1$

   $F(x_2) = \tilde{1} - \beta s + \frac{\beta s_1}{\alpha} - \frac{\beta}{\alpha} x_2 - r + s - \frac{s_1 - r}{\alpha}$

2. $x_2 \in O$

   (a) $\mathbf{x_1^s x_1^r x_1^{s_1} x_2^1}$

   $F(x_2) = s_1 + \tilde{1} - x_1 - \beta s - r + s - \frac{s_1 - r}{\alpha}$

   (b) x_2^1

   $F(x_2) = \frac{\tilde{1} - x_2}{\beta}$

   (c) $x_1^s x_2^1$

   $F(x_2) = s + \tilde{1} - x_2 - \beta s$

   (d) $x_1^s x_1^r x_2^1$

   $F(x_2) = r + \alpha(\tilde{1} - x_1 - \beta s - r + s)$

3. $x_2 \notin R$

   (a) $\mathbf{x_1^s x_2^r x_2^{s_1} x_2^1}$

   $F(x_2) = \tilde{1} - x_2$

   (b) $\mathbf{x_2^r x_2^{s_1} x_1^s x_2^1}$

   $F(x_2) = s + \tilde{1} - s_1 - \beta(s - r + x_2 - \frac{s_1 - r}{\alpha})$

   (c) $\mathbf{x_2^r x_1^s x_2^{s_1} x_2^1}$

   $F(x_2) = \tilde{1} - r + s - \alpha(s - r + x_2)$

   (d) $\mathbf{x_2^r x_2^{s_1} x_2^1}$

   $F(x_2) = r - x_2 + \frac{s_1 - r}{\alpha} + \frac{\tilde{1} - s_1}{\beta}$

   (e) $x_1^s x_2^r x_2^{s_1} x_1^r x_2^1$

   $F(x_2) = r + \alpha(\tilde{1} - x_2 - r)$

   (f) $x_1^s x_2^r x_2^{s_1} x_1^r x_1^{s_1} x_2^1$

   $F(x_2) = s_1 + \tilde{1} - x_2 - r - \frac{s_1 - r}{\alpha}$

   (g) $x_1^s x_2^r x_1^r x_2^{s_1} x_2^1$

   $F(x_2) = s_1 - x_2 + \alpha(\tilde{1} - s_1)$

(h) $x_1^s x_2^r x_1^r x_2^{s_1} x_1^{s_1} x_2^1$

$F(x_2) = \tilde{1} - \frac{x_2}{\alpha}$

(i) $x_2^r x_2^{s_1} x_1^s x_1^r x_2^1$

$F(x_2) = r + \alpha(\tilde{1} - s_1 - r + s) - \alpha\beta(s - r + x_2 - \frac{s_1 - r}{\alpha})$

(j) $x_2^r x_2^{s_1} x_1^s x_1^r x_1^{s_1} x_2^1$

$F(x_2) = \tilde{1} - r + s - \frac{s_1 - r}{\alpha} - \beta(s - r + x_2 - \frac{s_1 - r}{\alpha})$

(k) $x_2^r x_1^s x_2^{s_1} x_1^r x_2^1$

$F(x_2) = r + \alpha(\tilde{1} - 2r + s) - \alpha^2(s - r + x_2)$

(l) $x_2^r x_1^s x_2^{s_1} x_1^r x_1^{s_1} x_2^1$

$F(x_2) = \tilde{1} + s_1 - 2r + s - \frac{s_1 - r}{\alpha} - \alpha(s - r + x_2)$

(m) $x_2^r x_1^s x_1^r x_2^{s_1} x_2^1$

$F(x_2) = s_1 - r - \alpha(s - r + x_2) + s + \alpha(\tilde{1} - s_1)$

(n) $x_2^r x_1^s x_1^r x_2^{s_1} x_1^{s_1} x_2^1$

$F(x_2) = \tilde{1} - s + r - x_2 - \frac{r - s}{\alpha}$

Sample Calculation: We derive the F-map for case 1a. Initially, $x_1 = 0$ and x_2 is arbitrary, such that the required order of events occurs. We consider where each cluster lies after each event map.

Event	Location of x_1 after event	Location of x_2 after event
$t = 0$	$x_1 = 0$	$x_2 = x_2$
x_1^s	$x_1 = s$	$x_2 = x_2 + \alpha s$
x_1^r	$x_1 = r$	$x_2 = x_2 + \alpha s + r - s$
$x_2^{s_1}$	$x_1 = s_1 - x_2 - \alpha s + s$	$x_2 = s_1$
x_2^1	$x_1 = s_1 - x_2 - \alpha s + s + \alpha(1 - s_1)$	$x_2 = 1$

By definition, $F(x_2)$ is the location of x_1 when $x_2 = 1$, so $F(x_2) = x_1 = s_1 - x_2 - \alpha s + s + \alpha(1 - s_1)$

C.2 Calculations relating to the 2-clustered system in the overlap model

We derive the Jacobians and characteristic polynomials of Section 5.4.2.

Case 1 of the RS model:

This case was defined by $\sigma = 1$, $\rho = k$, and event string $e_r e_s$.

The Jacobian J of F in the neighborhood of the $(M+1)$-cyclic solution has the form

$$J = \begin{pmatrix} 0 & 0 & 0 & \dots & 0 & -(1+f(1/k)) \\ 1 & 0 & 0 & \dots & 0 & -(1+f(1/k)) \\ 0 & 1 & 0 & \dots & 0 & -(1+f(1/k)) \\ 0 & 0 & 1 & \dots & 0 & -(1+f(1/k)) \\ \dots & \dots & \dots & \dots & \dots & \dots \\ 0 & 0 & 0 & \dots & 1 & -(1+f(1/k)) \end{pmatrix}. \tag{C.2.1}$$

The characteristic polynomial of J is

$$p(\lambda) = \lambda^{k-1} + (1+f(1/k))(\lambda^{k-2} + \lambda^{k-3} + \cdots + \lambda + 1). \tag{C.2.2}$$

This polynomial has roots strictly within the unit circle (i.e. the fixed point is stable) when $1 + f(1/k) < 1$ (negative feedback), and roots strictly outside the unit circle (thus, the fixed point is unstable) when $1 + f(1/k) > 1$, that is to say for positive feedback.

Case 2 of the RS model:

There are two other cases in the RS model, but they each give rise to the same Jacobian. They are $\sigma = 2$, $\rho = k$, and event string $e_s e_r$; and $\sigma = 1$, $\rho = k - 1$, and event string $e_s e_r$. In either case, the Jacobian in a neighborhood of an $(M+1)$-cyclic fixed

point has the form

$$J = \begin{pmatrix} 0 & 0 & 0 & \dots & 0 & -1 \\ 1 & 0 & 0 & \dots & 0 & -1 \\ 0 & 1 & 0 & \dots & 0 & -1 \\ 0 & 0 & 1 & \dots & 0 & -1 \\ \dots & \dots & \dots & \dots & \dots & \dots \\ 0 & 0 & 0 & \dots & 1 & -1 \end{pmatrix}. \tag{C.2.3}$$

The characteristic polynomial is

$$p(\lambda) = \lambda^{k-1} + \lambda^{k-2} + \lambda^{k-3} + \cdots + \lambda + 1, \tag{C.2.4}$$

all of whose roots lie on the unit circle (i.e. the fixed point is neutral).

Compared to the RS model, where the $(M + 1)$-cyclic solution falls into one of three cases (two of them sharing a Jacobian), the overlap model gives rise to seven cases, categorized based on the initial positions of x_2 and x_k.

C.2.1 $k = M + 1$ cases in the overlap model

Case 1: When $\mathbf{x_1} = 0$, R is empty and S contains no clusters other than x_1

We will see that in this case the k-cyclic solution is stable for negative feedback and unstable for positive feedback. This is identical behavior to that observed in the RS model.

There are two sub-cases; x_k must enter R before x_1 leaves S, or the system is decoupled (violating the fact that $k > M$), but x_2 may or may not enter O before x_1 leaves S.

Case 1a: $\mathbf{x_k \to r, x_1 \to s, x_k \to s_1}$.

All clusters but x_k move at a constant rate of 1 for the time it takes x_k to reach 1.

The first event occurs when x_k reaches r. The time this takes is $t_1 = r - x_k$, and $x_1(t_1) = r - x_k$.

The second event occurs when x_1 reaches s. This takes time $t_2 = s - r + x_k(0)$. Over the time interval $[t_1, t_1 + t_2]$, the cluster x_k travels at a constant rate of $1 + f(1/k)$, and $x_k(t_1) = r$. Thus $x_k(t_1 + t_2) = r + (1 + f(1/k))(s - r + x_k(0))$.

At time $t_1 + t_2$, S is empty, and thus although $x_k \in R$, it moves at a rate of 1. We therefore calculate t_3, the time it now takes x_k to reach s_1, as $t_3 = s_1 - r - (1 + f(1/k))(s - r + x_k(0))$. During the time it then takes x_k to reach 1, the cluster x_k will experience only the feedback it exerts upon itself. Since it must traverse an interval of length $1 - s_1$ at a rate of $1 + g(1/k)$, we calculate the time this takes as $t_4 = \frac{1-s_1}{1+g(1/k)}$.

The total return time is

$$T = t_1 + t_2 + t_3 + t_4 =$$
$$r - x_k(0) + s - r + x_k(0) + s_1 - r - (1 + f(1/k))(s - r + x_k(0)) + \frac{1 - s_1}{1 + g(1/k)} =$$
$$- (1 + f(1/k)(x_k(0)) + \alpha,$$

where α is a constant.

Since all clusters except for x_k move at unit rate,

$x_i(T) = x_i(0) - (1 + f(1/k))x_k(0) + \alpha$ for all $1 \le i \le k - 1$, and the Jacobian of F in a neighborhood of the fixed point is identical to (C.2.1), and it therefore has the same stability. It follows that the k-cyclic solution is stable when the feedback is negative, and unstable when the feedback is positive.

Case 1b: $\mathbf{x_k \to r, x_k \to s_1, x_1 \to s}$

It takes a total time of $t_1 = r - x_k(0) + \frac{s_1 - r}{1 + f(1/k)}$ for x_k to reach s_1, at which time x_1 is still in S. It will take a further time $t_2 = s - r + x_k - \frac{s_1 - r}{1 + f(1/k)}$ for x_1 to reachy s (for a total time of s), at which point $x_k(t_1 + t_2) = x_k(s) = s_1 + (1 + g(2/k))(s - r + x_k(0) - \frac{s_1 - r}{1 + f(1/k)})$.

The time it takes x_k to traverse O is $t_3 = \frac{1 - s_1 - (1 + g(2/k))(s - r + x_k(0) - \frac{s_1 - r}{1 + f(1/k)}}{1 + g(1/k)}$. Absorbing together various constants, $t_3 = -\frac{1 + g(2/k)}{1 + g(1/k)} x_k(0) + \alpha$, and the return time is $T = t_1 + t_2 + t_3 = -\frac{1 + g(2/k)}{1 + g(1/k)} x_k(0) + \alpha + s$.

The resultant Jacobian is identical to (C.2.1), except that $1 + f(1/k)$ is replaced by $\frac{1+g(2/k)}{1+g(1/k)}$. The question of whether the eigenvalues fall inside or outside of the unit circle in that case is resolved entirely by whether the constant in the last column is between 0 and 1 in absolute value (negative feedback, stable) or greater than 1 (positive feedback, unstable). Since $-\frac{1+g(2/k)}{1+g(1/k)}$ is likewise a constant that is between 0 and 1 for negative feedback, and greater than 1 for positive feedback, this $(M+1)$-cyclic solution has the same stability as in Case 1 of the RS model, that is to say that it is stable when the feedback is negative, and unstable when the feedback is positive.

Case 2: When $\mathbf{x_1 = 0, x_2 < s}$

In this case, x_2 leaves S before x_k enters R, and there are no subcases. Having entered R at time $t_1 = r - x_k(0)$, the last cluster x_k passes from r to s_1 in time $t_2 = \frac{s_1 - r}{1+f(1/k)}$, and from s_1 to 1, at time $t_3 = \frac{1-s_1}{1+f(2/k)}$. The return time is $T = t_1+t_2+t_3 = -x_k(0)+\alpha$, and the linear system is defined by the system of equations $x_i(T) = x_i(0) - x_k(0)$ for $1 \le i \le k-1$. The Jacobian near the fixed point is given by (C.2.3). Thus this case shares the stability of Case 2 for the RS model, i.e. the fixed point is neutrally stable.

Case 3: When $\mathbf{x_1 = 0, r \le x_k < s_1}$

In the RS model, an $(M+1)$-cyclic solution that has a cluster in R when $x_1 = 0$ is neutrally stable under positive or negative feedback. In the overlap model, there are three subcases, and only one of them is neutrally stable. The key difference is that although x_1 leaves S before x_{k-1} enters R, the cluster x_{k-1} will still experience feedback in this model, since it will be in R while x_k is in O. There are three subcases, corresponding to orders of events.

Case 3a: $\mathbf{x_k \to s_1, x_1 \to s, x_{k-1} \to r}$

We first calculate the F-return time T. We will concurrently keep track of the position of x_{k-1}, since that cluster now experiences feedback and will not simply travel a distance of T, as the other clusters do.

The first event occurs when x_k reaches s_1 at time $t_1 = \frac{s_1 - x_k(0)}{1+f(1/k)}$. At that time, $x_1(t_1) = t_1$, $x_k(t_1) = s_1$, and $x_{k-1}(t_1) = x_{k-1}(0) + t_1$.

At time $t_2 = s - t_1$, x_1 reaches s. During that time, x_{k-1} travels at unit rate, and thus $x_{k-1}(t_1 + t_2) = x_{k-1}(0) + s$. The final cluster x_k is in O and travels at a rate of $1 + g(2/k)$. Thus $x_k(t_1 + t_2) = s_1 + (1 + g(2/k))(s - t_1)$.

The next event occurs when x_{k-1} reaches r at time $t_3 = r - x_{k-1}(0) - s$. At that time, $x_k(t_1 + t_2 + t_3) = s_1 + (1 + g(2/k))(s - t_1) + (1 + g(1/k)(r - x_{k-1}(0) - s)$. Grouping constants together, this simplifies to $x_k(t_1+t_2+t_3) = \frac{1+g(2/k)}{1+f(1/k)}x_k(0) - (1+g(1/k))x_{k-1}(0) + \alpha$.

The final event occurs when x_k reaches 1. The cluster travels at a constant rate of $1 + g(1/k)$ over a distance of $1 - \frac{1+g(2/k)}{1+f(1/k)}x_k(0) + (1 + g(1/k))x_{k-1}(0) - \alpha$. The time this takes is $t_4 = -\frac{1+g(2/k)}{(1+f(1/k))(1+g(1/k))}x_k(0) + x_{k-1}(0) + \alpha_2$. The total return time is thus $T = t_1 + t_2 + t_3 + t_4 = -\frac{1+g(2/k)}{(1+f(1/k))(1+g(1/k))}x_k(0) + \alpha_3$. Because $x_{k-1}(t_1 + t_2 + t_3) = r$, we calculate $x_{k-1}(T) = r + (1 + f(1/k))t_4 = -\frac{1+g(2/k)}{1+g(1/k)}x_k + (1 + f(1/k)x_{k-1} + (1 + f(1/k))\alpha_2$.

For notational simplicity, we let $w = \frac{1+g(2/k)}{(1+f(1/k))(1+g(1/k))}x_k(0)$.

The Jacobian is given by

$$J = \begin{pmatrix} 0 & 0 & 0 & ... & 0 & -w \\ 1 & 0 & 0 & ... & 0 & -w \\ 0 & 1 & 0 & ... & 0 & -w \\ 0 & 0 & 1 & ... & 0 & -w \\ ... & ... & ... & ... & ... & ... \\ 0 & 0 & 0 & ... & (1 + f(1/k)) & -(1 + f(1/k))w \end{pmatrix}. \tag{C.2.5}$$

Although the Jacobian is different from either of the Jacobians associated with the RS model, the characteristic polynomial is the same as in Case 1b of the overlap model, and is asymptotically stable for negative feedback and unstable for positive feedback.

We note that we may perform a change of variables such as is described in Section 5.3.2. In fact, we may perform two such changes of variables. Any time a cluster is in O it experiences a certain background feedback, that we may scale away.

In addition, any time a cluster is in $\widetilde{R}$ it experiences feedback from one cluster, and we may also scale that feedback away (since, in a neighborhood of the k-cyclic solution, that level of feedback is always present, independent of the state of the system). Although we have tended against such changes of variables, for reasons already discussed, it greatly simplifies the calculations, and the modified system has a Jacobian, (C.2.6), that is directly comparable to Case 1 of the RS model. This is an advantage, since proving that (C.2.5) has the characteristic polynomial claimed of it is somewhat cumbersome.

$$J = \begin{pmatrix} 0 & 0 & 0 & \dots & 0 & -(1+f(2/k)) \\ 1 & 0 & 0 & \dots & 0 & -(1+f(2/k)) \\ 0 & 1 & 0 & \dots & 0 & -(1+f(2/k)) \\ 0 & 0 & 1 & \dots & 0 & -(1+f(2/k)) \\ \dots & \dots & \dots & \dots & \dots & \dots \\ 0 & 0 & 0 & \dots & 1 & -(1+f(2/k)) \end{pmatrix}. \tag{C.2.6}$$

Case 3b: $\mathbf{x_1 \to s, x_{k-1} \to r, x_k \to s_1}$

The first event occurs when x_1 leaves s. At time $t_1 = s$, $x_k(s) = x_k(0) + (1 + f(1/k))s$ and $x_{k-1}(s) = x_{k-1}(0) + s$. Although the next event technically occurs when x_{k-1} enters R, S is empty, and thus even when x_{k-1} enters R, its rate does not change. Rather, the next significant event occurs when x_k reaches s_1, at time $t_2 = s_1 - x_k(0) - (1 + f(1/k))s$. Because it travels at a unit rate, $x_k(t_1 + t_2) = x_{k-1} + s + s_1 - x_k - (1 + f(1/k))s$.

The next event occurs when x_k reaches 1, at time $t_2 = \frac{1-s_1}{1+g(1/k)}$. The total return time is $T = t_1 + t_2 + t_3 = -x_k(0) + \alpha$, and although it experiences feedback, $x_{k-1}(t_1 + t_2 + t_3) = x_{k-1} - x_k + \alpha_2$.

The Jacobian for this case thus has 1's down the semidiagonal and -1's down the last column, and is neutrally stable for both positive and negative feedback.

Case 3c: $\mathbf{x_1 \to s, x_k \to s_1, x_{k-1} \to r}$.

First, observe that x_k moves entirely independently of other clusters in a neighborhood of this solution; it travels at a rate of $1 + f(1/k)$ for time s, then at a rate

of 1 until it reaches s_1, then at a rate of $1 + g(1/k)$ until it reaches 1. Thus the return time T can be easily calculated as $T = -x_k(0) + \alpha$.

At time $t_1 = s$, $x_{k-1}(t_1) = x_{k-1}(0) + s$ and $x_k(t_1) = x_k(0) + (1 + f(1/k))s$. At time $t_2 = s_1 - x_k - (1+f(1/k))s$, $x_k(t_1+t_2) = s_1$ and $x_{k-1}(t_1+t_2) = x_{k-1}(0)+s+s_1-x_k-(1+f(1/k))s$.

At time $t_3 = r - x_{k-1} - s - s_1 + x_k(0) + (1 + f(1/k))s$, $x_{k-1}(t_1 + t_2 + t_3) = r$ and $x_k(t_1 + t_2 + t_3) = s_1 + (1 + g(1/k))(r - x_{k-1} - s + s_1 + x_k + (1 + f(1/k))s)$.

The time t_4 it now takes x_k to reach 1 is calculable as $\frac{1-s_1-(1+g(1/k)(r-x_{k-1}-s+s_1+x_k+(1+f(1/k)s))}{1+g(1/k)}$. Combining constants, we write $t_4 = x_{k-1} - x_k + \alpha$. Thus $x_{k-1}(t_1 + t_2 + t_3 + t_4) = (1 + f(1/k))x_{k-1} - (1 + f(1/k))x_k + (1 + f(1/k))\alpha$.

The Jacobian for this case therefore has 1s down the semidiagonal and −1's down the right column, except for the last row: $J(k - 1, k - 2) = 1 + f(1/k)$ and $J(k - 1, k - 1) = -(1 + f(1/k))$. Its characteristic polynomial has leading coefficient 1 and all other coefficients $1 + f(1/k)$, again reducing to Case 1 from Chapter 2. To see this, observe that if we write

$$J(k-1) = \begin{pmatrix} -\lambda & 0 & 0 & \dots & 0 & -1 \\ 1 & -\lambda & 0 & \dots & 0 & -1 \\ 0 & 1 & -\lambda & \dots & 0 & -1 \\ 0 & 0 & 1 & \dots & 0 & -1 \\ \dots & \dots & \dots & \dots & \dots & \dots \\ 0 & 0 & 0 & \dots & 1 + f(1/k) & -(1 + f(1/k)) - \lambda \end{pmatrix}, \qquad \text{(C.2.7)}$$

then by expanding across the first row, we find $\det(J(k)) = -\lambda \det J(k-2) + 1 + f(1/k)) = -\lambda \det(k - 3) + \lambda(1 + f(1/k)) + (1 + f(1/k)) = \lambda \det(k - 4) + \lambda^2(1 + f(1/k)) + \lambda(1 + f(1/k)) + (1 + f(1/k))$.... This characteristic polynomial is the same as (C.2.4), and the k-cyclic solution is unstable when the feedback is positive and stable when the feedback is negative.

Case 4: When $\mathbf{x_1} = \mathbf{0}$, $\mathbf{s_1} \leq \mathbf{x_k} < \mathbf{1}$

We calculate T and $x_{k-1}(T)$ concurrently. The order of events is $x_1 \to s, x_{k-1} \to r, x_{k-1} \to s_1, x_k \to 1$.

At $t_1 = s$, $x_k(t_1) = x_k(0) + (1 + g(2/k))s$ and $x_{k-1}(t_1) = x_{k-1}(0) + s$.

At time $t_2 = r - x_{k-1}(0) - s$, the cluster $x_{k-1}(0)$ reaches r. At this time, $x_k(t_1 + t_2) = x_k(0) + (1 + g(2/k))s + (1 + g(1/k))(r - x_{k-1}(0) - s) = x_k(0) - (1 + g(2/k))x_{k-1}(0) + \alpha$.

The time it takes x_{k-1} to traverse R is a constant, $t_3 = \frac{s_1 - r}{1 + f(1/k)}$. Thus $x_k(t_1 + t_2 + t_3) = x_k - (1 + g(2/k))x_{k-1}(0) + \alpha_2$.

The time it takes x_k to reach 1 is $t_4 = \frac{1 - x_k + (1 + g(2/k))x_{k-1}(0) - \alpha_2}{1 + g(2/k)}$. Because $x_{k-1}(t_1 + t_2 + t_3) = s_1$, $x_{k-1}(t_1 + t_2 + t_3 + t_4) = s_1 + (1 + g(2/k))t_4 = -x_k(0) + (1 + g(2/k))x_{k-1}(0) - \alpha_2 + 1$. The total return time, $T = t_1 + t_2 + t_3 + t_4$, can be seen to be $T = -\frac{1}{1 + g(2/k)} + \alpha_3$.

The Jacobian near the cyclic solution is thus

$$J = \begin{pmatrix} 0 & 0 & 0 & \dots & 0 & -1/(1 + g(2/k)) \\ 1 & 0 & 0 & \dots & 0 & -1/(1 + g(2/k)) \\ 0 & 1 & 0 & \dots & 0 & -1/(1 + g(2/k)) \\ 0 & 0 & 1 & \dots & 0 & -1/(1 + g(2/k)) \\ \dots & \dots & \dots & \dots & \dots & \dots \\ 0 & 0 & 0 & \dots & 1 + g(2/k) & -1 \end{pmatrix}, \tag{C.2.8}$$

and using the same method as in Case 3c, where $\det(J(k)) = -\lambda \det J(k-2) - 1$, we see that it has characteristic polynomial (C.2.4). Thus the fixed point is neutrally stable.

Thesis and Dissertation Services